

**FOLDAMERS AND MACROCYCLES BASED ON  
FORMAMIDOXIME SUBUNITS**

BY

WEIWEN ZHAO

A thesis submitted to the Department of Chemistry  
in conformity with the requirements for  
the degree of Master of Science

Queen's University

Kingston, Ontario, Canada

July 2011

Copyright © Weiwen Zhao, 2011

## ABSTRACT

The objective of this thesis is the study of the control of the shape of formamidine motifs and application to folding open-ended structures and more elaborate macrocycles.

The multi-step synthesis of macrocycles **M1** and **M2**, which are analogs of 18-crown ether-6, have been successfully achieved. Macrocycles **M1** and **M2** have been fully characterized. The study of the crystal structures of **M1** and **M2** gave interesting information about their packing and molecular recognition properties.

Moreover, analysis of some by-products formed in macrocyclizations gave intriguing results. The existence of a four-pyridine-unit interlocked catenane which was isolated from the synthesis of **M1** has been confirmed by MS-MS. A surprisingly large 54-membered macrocycle “**Maxi-M2**” was isolated from the synthetic crude product of **M2** and confirmed by X-ray crystallography.

Driven by the desire to understand the formation of catenane and “**Maxi-M2**”, a systematic study of the corresponding condensation reaction was performed. The E isomers derived from N-acyl-N’-substituted formamidoximes were, for the first time, reported and isolated. The protons can facilitate E to Z isomerization. The best conditions to selectively generate either the E or Z isomers have been fully studied and applied to the synthesis.

The unexpected formation of the E isomers may promote polymerization and limit the yield improvement of macrocyclization. Therefore, a new synthetic method for the target macrocycle **M2** was investigated, trying to avoid the formation of E isomers and thus cyclize more efficiently.

## **ACKNOWLEDGEMENT**

I would like to express my deepest gratitude to my supervisor, Dr. Anne Petitjean. Without her endless support, kindest advices and encouragement, it's not possible for me to complete my thesis. As my supervisor, she has not only patiently passed on knowledge and skills to me, but also set herself as an example to show me how to be a good chemist. I am deeply inspired by her great passion to work and wariness on research. It is my fortune to meet such a nice mentor who always helps me overcome difficulties in a foreign country.

Special acknowledgements are given to Dr. François Sauriol for her sincerely help on solving NMR problems and beneficial discussions, and to Dr. Ruiyao Wang for his kindly assistance with x-ray crystallography. Dr. Jiaxi Wang and James Wei are acknowledged for their support in MS spectroscopy. Prof. Richard Oleschuk and Dr. Graham Gibson are also appreciated for helpful discussions on MS technology applied to catenane issues.

I would like to acknowledge Prof. Donal Macartney, Prof. Gang Wu and Prof. Jean-Michel Nunzi for being my supervisor committee members to give invaluable suggestions and help.

I would like to express my gratitude to all the group members who have accompanied with me in the past two years: Cyndy Cruze, Catlin Miron, Scott Strum, Nan Wu, Caroline Melan and Alexandre Faurie. Special thanks are given to Dr. Olivier Fleischel and Dr. Ganga Subhash for their guidance and friendly support when I was a freshman in the lab. Moreover, I would like to thank 4<sup>th</sup> undergraduate student Sarah Smart who has been great of help on my research.

I would like to acknowledge Dr.Yingdong Lu for providing helpful advice on purification of macrocycles,Qian Cui for tutoring me how to use HPLC.

Special thanks are given to my friends Xue Li, Jingwei Luo, Jianxian Yang and Qingxiang song for their great support on my research and daily life.

Moreover, I would like to thank my family. Without their endless support, encouragement and love, I could not walk so far. I sincerely wish them live a happy and healthy life forever.

Last but not least, the financial support from Queen's University, Department of

Chemistry, Ontario Ministry of Research and Innovation and NSERC Canada is greatly acknowledged.

## **STATEMENT OF ORIGINALITY**

All the work presented in the thesis was performed by the author under supervision of Prof. Anne Petitjean at Queen's University, except for the X-ray crystallography data which were collected by Dr. Ruiyao Wang; MS spectroscopy data which were provided by Dr. Jiaxi Wang and James Wei; NOESY NMR experiment of suspected catenane in  $\text{CDCl}_3$  was conducted with the assistance of Dr. Françoise Sauriol.

## TABLE OF CONTENT

ABSTRACT .....	ii
ACKNOWLEDGEMENT .....	iii
STATEMENT OF ORIGINALITY .....	v
TABLE OF CONTENT .....	vi
LIST OF ABBREVIATION .....	xii
LIST OF FIGURES AND TABLES.....	xiv
Chapter 1 .....	1
Shape control using formamidine and pyridine-amide derivatives.....	1
1.1      Amidines and Formamidines .....	1
1.1.1 Isomerisms within the formamidine unit .....	1
1.1.2 Shape control on formamidine unit.....	2
1.2 Design of folding motifs .....	3
1.2.1 Conformational control based on aryl-amide bonds .....	4
1.2.2 Pyridine-2,6-dicarboxamide derivatives leading to helical structures .....	5
1.2.3 Pyridine-2,6-dicarboxamide derivatives: folded to macrocycles and knot	8
1.3 New formamidoxime folding motifs.....	10
1.3.1 Foldamers based on 2,6-pyridine-dicarboxamide and formamidoxime...	10
1.3.2 Macrocycles M1 and M3.....	11
Chapter 2 .....	14
Macrocycle M1 .....	14
2.1 Synthetic route to macrocycle M1 .....	14
2.1.1 Synthesis of pyridine-2,6-dimethylalcohol (2.2).....	15
2.1.2 Synthesis of 2,6-bis(bromomethyl) pyridine (2.3).....	15
2.1.3 Synthesis of pyridine-2,6-diylmethanamine (2.4).....	16
2.1.4 Synthesis of pyridine-2,6-bis-(N,N-dimethylformamidine) (2.6).....	17
2.1.5 Synthesis of O,O'-(pyridine-2,6-diylbis(methylene))bis(hydroxylamine) (2.5) .....	18
2.1.6 Synthesis of Macrocycle M1 .....	19

2.2 Results and Discussion.....	19
2.2.1 Characterization of macrocycle M1 .....	19
2.2.1.1 $^1\text{H}$ NMR of macrocycle M1 .....	20
2.2.1.2 Mass spectrometry study of Macrocycle M1 .....	21
2.2.1.3 Single crystal X-ray structure of M1 .....	21
2.2.2 Other isolated products.....	22
2.2.2.1 Introduction of interlocked molecules: Catenanes .....	22
2.2.2.2 Larger structures made of four pyridine units: large macrocycles or catenane? .....	24
2.3 Conclusion of Chapter 2.....	25
2.4 Experimental details .....	25
Pyridine-2,6-dimethylester (2.1) .....	25
Pyridine-2,6-dimethylalcohol (2.2).....	26
2,6-Bis(bromomethyl) pyridine (2.3) .....	26
Pyridine-2,6-diylidemethanammonium bromide (2.4a).....	27
Pyridine-2,6-diylidemethanamine (2.4) .....	27
Pyridine-2,6-diylbis(methylene)bis(N,N-dimethylformamidamide) (2.6).....	27
O,O'-(pyridine-2,6-diylbis(methylene))bis(hydroxylamine) (2.5) .....	28
Macrocycle M1 .....	29
References .....	30
Chapter 3 .....	31
Macrocycle M2 .....	31
3.1 Synthesis of macrocycle M2 .....	31
3.1.1 Synthesis of pyridine-2,6-dicarboxamide (3.1).....	31
3.1.2 Synthesis of (N <sub>2</sub> E,N <sub>6</sub> E)-N <sub>2</sub> ,N <sub>6</sub> -bis((dimethylamino)methylene)-pyridine-2,6-dicarboxamide (3.2) .....	32
3.1.3 Synthesis of Macrocycle M2.....	34
Method A: in the presence of a Lewis Acid catalyst.....	34
Method B: in the presence of Brønsted acids as catalysts.....	34
3.2 Results and Discussions .....	35

3.2.1 Characterization of macrocycle M2 .....	35
3.2.1.1 $^1\text{H}$ NMR of macrocycle M2 .....	35
3.2.1.2 Mass spectrometry study of macrocycle M2.....	36
3.2.1.3 Crystal structure of macrocycle M2 .....	37
3.2.2 Incredibly large macrocycle: “Maxi-M2” .....	39
3.3 Conclusion of Chapter 3.....	42
3.4 Experiment details.....	42
2,6-Pyridine dicarboxamide (3.1).....	42
(N <sub>2</sub> E,N <sub>6</sub> E)-N <sub>2</sub> ,N <sub>6</sub> -bis((dimethylamino)methylene)pyridine-2,6-dicarboxamide (3.2) .....	42
Macrocycle M2 and Maxi-M2 .....	43
Chapter 4 .....	45
Configurational control in alkoxyamine-derived formamidines.....	45
4.1 Reflections on the macrocyclization to M2.....	45
4.2 First evidence of the existence of the E isomer.....	46
4.2.1 ZE isomer .....	46
4.2.2 E/Z isomeric mixtures and isomerization.....	48
4.2.3 Relationship between yield of E/Z isomers and acidity of reaction mixture .....	49
4.2.4 Isolation condition for E mono-pyridyl-acyl-formamidoximes .....	50
4.2.5 X-ray crystallographic analysis of Z and E mono-pyridyl-acyl-formamidoximes .....	51
4.2.6 Short Summary.....	52
4.2.7 E isomers of acetyl formamidoxime .....	53
4.3 Conditions for isolation of the E isomer .....	55
4.3.1 Kinetic study of E/Z isomerization promoted by acid .....	55
4.3.2 Kinetic study of the condensation and isomerization reactions .....	57
4.3.3 Reversible Z to E isomerization .....	62
4.4 Conclusion.....	62
4.5 Experimental details .....	63

(E)-N-((Dimethylamino)methylene)picolinamide (4.3).....	63
(E)-N-((Dimethylamino)methylene)acetamide (4.6) .....	63
(E)-N,N-Dimethyl-N'-p-tolylformamidamide (4.9) .....	64
(E)-N-((Dimethylamino)methylene)-4-methylbenzamide (4.13) .....	64
(E)-N'-Benzyl-N,N-dimethylformimidamide (4.10) .....	65
N <sub>2</sub> ,N <sub>6</sub> -Bis((Z)-(benzyloxyimino)methyl)pyridine-2,6-dicarboxamide (4.2ZZ)	
.....	65
N <sub>2</sub> -((E)-(Benzyloxyimino)methyl)-N <sub>6</sub> -((Z)-(benzyloxyimino)methyl)pyridine-2,6-dicarboxamide (4.2ZE) .....	66
(Z)-N-((Benzyloxyimino)methyl)picolinamide (4.4Z) .....	67
(Z)-N-((Methoxyimino)methyl)picolinamide (4.5Z)	
and (E)-N-((methoxyimino)methyl)picolinamide (4.5E).....	67
(Z)-N-((Benzyloxyimino)methyl)acetamide (4.7Z) .....	and
(E)-N-((benzyloxyimino)methyl)acetamide (4.7E) .....	69
(Z)-N-((Methoxyimino)methyl)acetamide(4.11Z) .....	and
(E)-N-((methoxyimino)methyl)acetamide(4.11E) .....	70
(Z)-N'-((Benzyloxy)-N-p-tolylformimidamide (4.12).....	70
(E)-N-((Benzyloxyimino)methyl)-4-methylbenzamide (4.8E)	
and (Z)-N-((benzyloxyimino)methyl)-4-methylbenzamide (4.8Z).....	71
References .....	72
Chapter 5 .....	74
Conclusion and perspectives .....	74
5.1 Summary and conclusion .....	74
5.2 Future directions.....	75
Appendix A: NMR and MS spectra .....	77
Pyridine-2,6-dimethylester (2.1) .....	77
Pyridine-2,6-dimethylalcohol (2.2) .....	77
2,6-Bis(bromomethyl)-pyridine (2.3).....	78
Pyridine-2,6-diyldimethan ammonium bromide (2.4a).....	78
Pyridine-2,6-diyldimethanamine (2.4) .....	79

Pyridine-2,6-diylbis(methylene)bis(N,N-dimethylformamidamide) (2.6).....	79
O,O'-(pyridine-2,6-diylbis(methylene))bis(hydroxylamine) (2.5).....	80
Intermediate (precursor for compound 2.5) .....	80
Macrocycle M1- COSY (400 MHz; CDCl <sub>3</sub> ; 25 °C).....	81
2,6-Pyridine dicarboxamide (3.1).....	81
(N2E,N6E)-N2,N6-bis((dimethylamino)methylene)pyridine-2,6-dicarboxamide (3.2) .....	82
Macrocycle M2-HMBC (500 MHz; CDCl <sub>3</sub> ; 25 °C).....	83
Maxi-M2.....	84
(E)-N-((dimethylamino)methylene)picolinamide (4.3) .....	84
(E)-N-((dimethylamino)methylene)acetamide (4.6) .....	86
(E)-N,N-dimethyl-N'-p-tolylformamidamide (4.9) .....	87
(E)-N-((dimethylamino)methylene)-4-methylbenzamide (4.13) .....	88
(E)-N'-benzyl-N,N-dimethylformimidamide (4.10).....	89
N2,N6-bis((Z)-(benzyloxyimino)methyl)pyridine-2,6-dicarboxamide (4.2ZZ).....	89
N2-((E)-(benzyloxyimino)methyl)-N6-((Z)-(benzyloxyimino)methyl)pyridine- 2,6-dicarboxamide (4.2ZE) .....	91
Z)-N-((benzyloxyimino)methyl)picolinamide (4.4Z) .....	91
(Z)-N-((methoxyimino)methyl)picolinamide (4.5Z) .....	93
(E)-N-((methoxyimino)methyl)picolinamide (4.5E) .....	94
E and Z isomeric mixtures of acetyl-formamidoxime (4.7E+4.7Z).....	95
(Z)-N-((benzyloxyimino)methyl)acetamide (4.7Z) .....	95
(E)-N-((benzyloxyimino)methyl)acetamide (4.7E) .....	97
(Z)-N-((methoxyimino)methyl)acetamide (4.11Z) .....	98
(E)-N-((methoxyimino)methyl)acetamide (4.11E) .....	99
(Z)-N'-(benzyloxy)-N-p-tolylformimidamide (4.12) .....	100
(E)-N-((benzyloxyimino)methyl)-4-methylbenzamide (4.8E).....	101
(Z)-N-((benzyloxyimino)methyl)-4-methylbenzamide (4.8Z).....	102
ESI-MS of Catenane (in CH <sub>2</sub> Cl <sub>2</sub> ).....	104
ESI-MS of Maxi-M2 (in CH <sub>2</sub> Cl <sub>2</sub> ) .....	104

Appendix B: Crystallography Data .....	105
1) Macrocycle M2 dimer ((M2) <sub>2</sub> .H <sub>2</sub> O.(CH <sub>3</sub> ) <sub>2</sub> NH <sub>2</sub> <sup>+</sup> .OTf)) .....	105
2) Macrocycle M2-MeOH adduct .....	123
3) Maxi-M2 .....	132
4) Macrocycle M1 .....	148
5) 4.2 ZE .....	156
6) 4.4Z .....	177
7) 4.7E .....	184
8) 4.5E-room temperature-monoclinic .....	191
9) 4.5E-low temperature, non-merohedrally twinned triclinic.....	197

## LIST OF ABBREVIATION

Ar	aromatic
Bn	benzyl
COSY	correlation spectroscopy
Conc.	concentration
°C	degree Celsius
d	doublet
dd	doublet of doublet
TFA	trifluoroacetic acid
DMF	dimethyl formamide
DMSO	dimethylsulfoxide
DCM	dichloromethane
ESI	electrospray ionization
ESI-MS	electrospray ionization mass spectrometry
EA	elemental analysis
EI	electron impact
g	gram
H <sub>F</sub>	formamidine hydrogen
Hz	hertz
h	hour(s)
HRMS	high resolution mass spectrometry
HPLC	High Performance Liquid Chromatography
HMBC	Heteronuclear Multiple Bond Correlation
J	vicinal coupling constant
K	Kelvin
L	liter(s)
LRMS	low resolution mass spectrometry
m	multiplet
MS	mass spectroscopy

m/z	mass to charge ratio
mg	milligram
min	minute(s)
mL	milliliter(s)
mmol	millimole(s)
mol	mole
M	moles per liter
MHz	Megahertz
mM	millimoles per liter
NMR	nuclear magnetic resonance
NOESY	Nuclear Overhauser Effect Spectroscopy
nm	nanometer
Ph	phenyl
Py	pyridine
ppm	part(s) per million
q	quartet
rt	room temperature
t	time
t	triplet
s	singlet or second(s)
UV	Ultraviolet
$\delta$	chemical shift
$\Delta G$	Gibbs free energy
$\Delta H$	enthalpy
$\text{\AA}$	Angstrom

## LIST OF FIGURES AND TABLES

<b>Figure 1.1</b> Configurational equilibrium within the formamidine motif .....	3
<b>Figure 1.2</b> Hydrogen bond within the alkoxyformamidine unit.....	3
<b>Figure 1.3</b> Favorable conformations of different NHCO-aryl linkages. ....	4
<b>Figure 1.4 a)</b> Pyridine-2,6-dicarboxamide derivatives .....	5
<b>Figure 1.5 a)</b> Crystal structure of a single helix, grown from DMSO/CH <sub>3</sub> CN .....	6
<b>Figure 1.6</b> Double helices formed in CDCl <sub>3</sub> at various concentrations at 25 °C, 400 MHz <sup>1</sup> H NMR.....	7
<b>Figure 1.7</b> Crystal structure of the double helical dimer, grown from nitrobenzene/heptane.....	7
<b>Figure 1.8</b> Intramolecular hydrogen bonds lead to the folding of a tetrameric macrocycle. ....	8
<b>Figure 1.9</b> Macrocycle bearing pyridine-2,6-dicarboxamide units as quinone receptor.	9
<b>Figure 1.10 a)</b> Synthetic schemes targeting at macrocycles <b>b)</b> crystal structure of the trefoil molecule knot obtained by Vogtle. ....	9
<b>Figure 1.11 a)</b> Folded open-ended structure; <b>b)</b> macrocycle <b>M2</b> ; <b>c)</b> deprotonated form of macrocycle <b>M2</b> ; <b>d)</b> crystal structure of 18-C-6 crown ether coordinating to a potassium.....	10
<b>Figure 1.12</b> Shapes of different macrocycles: flexible, not planar <b>M1</b> ; less flexible, mostly planar <b>M2</b> ; rigid, almost planar <b>M3</b> . ....	11
<b>Figure 2.1</b> <sup>1</sup> H NMR spectrum of macrocyle <b>M1</b> in CDCl <sub>3</sub> (300 MHz, 25 °C). ....	20
<b>Figure 2.2</b> ESI-mass spectrum of macrocycle <b>M1</b> .....	21
<b>Figure 2.3</b> Crystal structure of macrocycle <b>M1</b> .....	22
<b>Figure 2.4</b> Cartoon representation of a [2]catenane. ....	23
<b>Figure 2.5</b> Mechanically interlocked architectures as components for molecular machines.....	24
<b>Figure 2.6</b> MS evidence for existing catenane, and catenane crude model.....	25

<b>Figure 3.1</b> $^1\text{H}$ NMR spectrum of macrocycle M2 in $\text{CDCl}_3$ (500 MHz, 25 °C).....	36
<b>Figure 3.2</b> Mass spectrum of macrocycle <b>M2</b> .....	37
<b>Figure 3.3</b> Crystal structure of macrocycle <b>M2</b> for two different crystals.....	38
<b>Figure 3.4</b> $^1\text{H}$ NMR spectrum of “ <b>Maxi-M2</b> ” in $\text{CDCl}_3$ (500 MHz, 25 °C). ....	39
<b>Figure 3.5 a)</b> Trefoil molecular knot obtained by Vogtle; <b>b)</b> knot enantiomers.....	40
<b>Figure 3.6</b> Crystal structure of “ <b>Maxi-M2</b> ” and molecule structure.....	40
<b>Figure 3.7</b> Stacking of “ <b>Maxi-M2</b> ”.....	41
<b>Figure 4.1</b> $^1\text{H}$ NMR spectrum of the suspected ZE isomer <b>ZE4.2</b> .....	46
<b>Figure 4.2 a)</b> NOESY spectrum of <b>4.2</b> (500 MHz, $\text{CDCl}_3$ , 25 °C); <b>b)</b> molecular structure; <b>c)</b> molecular view of the crystal structure of the <b>ZE4.2</b> .....	47
<b>Figure 4.3</b> E to Z isomerization promoted by TFA ( $^1\text{H}$ NMR, $\text{CDCl}_3$ , 25 °C).....	49
<b>Figure 4.4</b> Crystal structure of <b>4.4Z</b> .....	51
<b>Figure 4.5</b> Crystal structure of <b>4.5E</b> . <b>a)</b> monoclinic at room temperature <b>b)</b> non-merohedrally twinned triclinic at -93 °C. ....	52
<b>Figure 4.6 a)</b> Observed formamidoxime isomers.....	53
<b>Figure 4.7 a),b)</b> NOESY studies of isomeric mixtures of acetyl formamidoximes (500 MHz, $\text{CDCl}_3$ , 25 °C).....	54
<b>Figure 4.8</b> Molecular structure of <b>4.7E</b> .....	54
<b>Figure 4.9 a)</b> Kinetic study of the E/Z isomerization monitored by $^1\text{H}$ NMR spectroscopy (500 MHz, $\text{CDCl}_3$ , 25 °C); <b>b)</b> isomerization scheme; <b>c)</b> graphical summary and <b>d)</b> $\text{Ln}[E]$ as a function of time .....	56
<b>Figure 4.10</b> E to Z isomerization monitored by UV-vis spectroscopy in chloroform (25 °C, conc. $4 \times 10^{-5}$ M, 0.6 eq. of TFA). .....	56
<b>Figure 4.11</b> Kinetic studies monitored by $^1\text{H}$ NMR spectroscopy ( $\text{CDCl}_3$ ; 25 °C): acyl-formamidine reacted with alkoxyamine in the presence of <b>1.0 eq. of acetic acid</b> (the concentration of the reactants in <b>F4.11a</b> , <b>F4.11b</b> and <b>F4.11c</b> are 0.29 M, 0.31 M and 0.24 M respectively). SM: starting materials.....	58
<b>Figure 4.12</b> Kinetic studies monitored by $^1\text{H}$ NMR spectroscopy ( $\text{CDCl}_3$ ; 25 °C):	

acyl-formamidine reacted with alkoxyamine in the presence of <b>2.0 eq.</b> of trifluoroacetic acid (the concentration of the reactants in <b>F4.12a</b> , <b>F4.12b</b> and <b>F4.12c</b> are 0.22 M, 0.27 M and 0.24 M respectively). SM: starting materials.	59
<b>Figure 4.13</b> Kinetic studies monitored by $^1\text{H}$ NMR spectroscopy ( $\text{CDCl}_3$ ; 25 °C): alkyl-and aryl-formamidine reacted with alkoxyamine in the presence of <b>1.0 eq.</b> of acetic acid (the concentration of the reactants in <b>F4.13a</b> and <b>F4.13b</b> are 0.31 M and 0.32 M respectively). SM: starting materials.....	60
<b>Figure 4.14</b> Similar outcome observed by $^1\text{H}$ NMR spectroscopy on the condensation reaction with different alkoxyamine as nucleophile. SM: starting materials ...	61
<b>Figure 4.15</b> Reversible isomerization from Z to E ( $^1\text{H}$ NMR, $\text{DMSO-d}_6$ , 500 MHz). ....	62
<b>Figure 5.1</b> Curved Z and linear E intermediates leading to different products.. ..	75

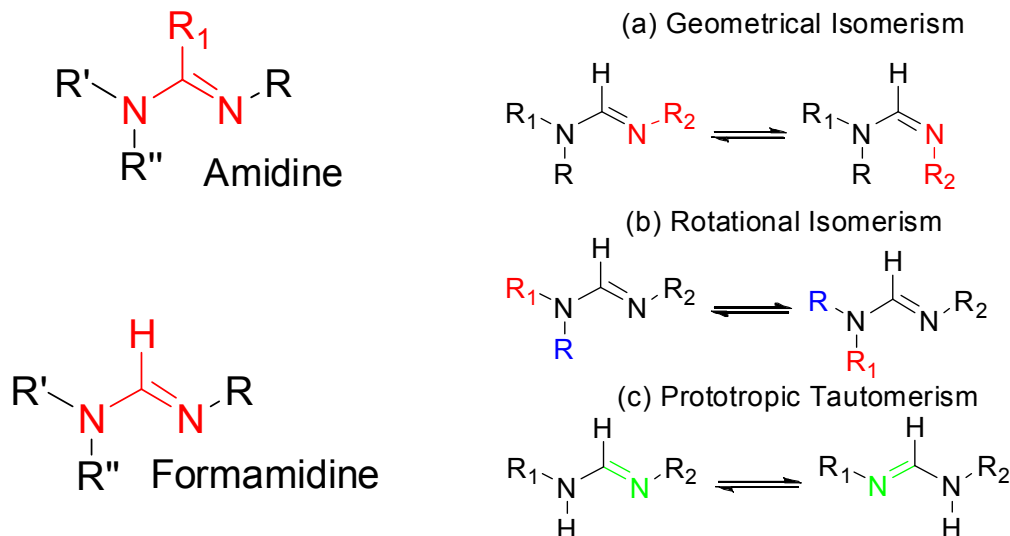
# Chapter 1

## Shape control using formamidine and pyridine-amide derivatives

### 1.1 Amidines and Formamidines

Amidines with different substitution patterns are important chemical compounds with a variety of properties. They find many applications in self-assembly,<sup>[1]</sup> coordination chemistry,<sup>[2]</sup> biological recognition<sup>[3]</sup> and as switchable solvents.<sup>[4]</sup> They have also attracted people's eyes as DNA groove binders.<sup>[5]</sup> The formamidine motif belongs to the amidine family (**Scheme 1.1**).

#### 1.1.1 Isomerisms within the formamidine unit



**Scheme 1.1:** Amidines, formamidines and different isomerisms present within formamidine unit.

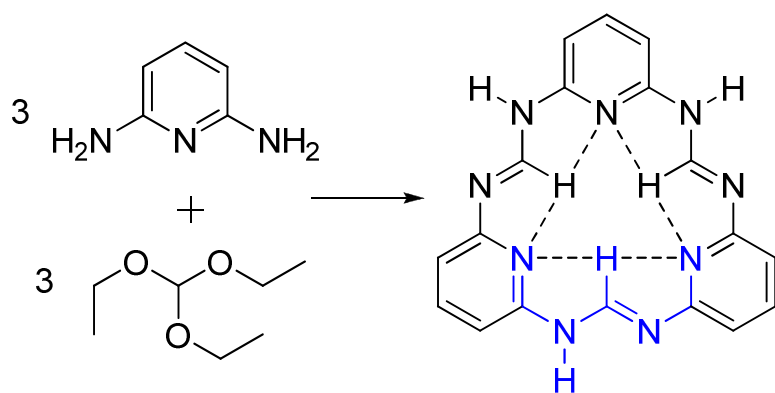
In solution, formamidines may be involved in three isomeric processes (**Scheme 1.1**):<sup>[6]</sup> (1) geometrical isomerism, giving E and Z isomers; (2) rotational isomerism, whereby the

C-N single bond can rotate to give different isomers; (3) prototropic tautomerism (for N,N'-disubstituted amidines), whereby the C=N double bond switches from one-side to the other and thus gives different tautomers.

Such complicated isomeric processes define the shape of the amidine unit, and it is interesting to be able to have **control** over the equilibria, and therefore over **the shape of the molecule**.

### 1.1.2 Shape control on formamidine unit

In an effort to prepare an amidine polymer via the reaction of 2,6-diaminopyridine and triethylorthoformate, Böhme surprisingly observed that a cyclic trimer formed rather than a polymer (**Scheme 1.2**).<sup>[6]</sup> This cyclic trimer was rationalized through the preorganization induced by weak hydrogen bonds between the basic pyridyl nitrogen and the formamidine hydrogen. The introduction of hydrogen-bonding sites within formamidine motifs indeed allows the formation of unusual folded structures.



**Scheme 1.2** Cyclic formamidine trimers observed by Böhme.<sup>[6]</sup>

Our group observed that there was an equilibrium between two isomers of di-2-pyridyl-formamidine in chloroform (**Figure 1.1**).<sup>[7]</sup> The E isomer of di-pyridyl-formamidine contains similar substructures to the cyclic formamidine trimers observed by Böhme (highlighted in blue). The uncommon Z isomer which is stabilized by intramolecular hydrogen bond between basic nitrogen and acidic NH coexists with the E

isomer in similar proportions in chloroform.

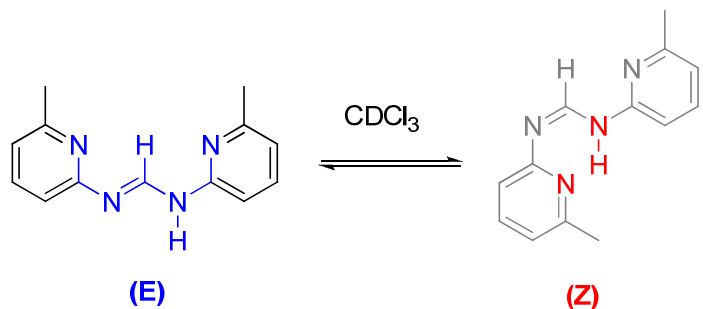


**Figure 1.1** Configurational equilibrium within the formamidine motif.<sup>[7]</sup>

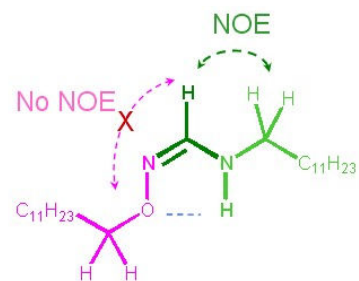


**Figure 1.2** Hydrogen bond within the alkoxyformamidine unit.

In our previous studies, we demonstrated that the introduction of one alkoxyamine substituent within the formamidine motif completely locks the structure in a Z form (**Figure 1.2**).

## 1.2 Design of folding motifs

Research on synthetic foldamers (oligomers or polymers that display well-defined structures), has been greatly emphasized over the past 20 years.<sup>[8,9]</sup> In the design of a certain class of foldamers, one may need to consider several essential factors.<sup>[9]</sup> First, the folding needs to be predictable. The prediction comes from a large amount of empirical studies of a particular type of folding structures. Second, the synthetic routes need to be feasible. For example, the synthesis of amide-functionalized folding motifs is easy and thus catches much attention.<sup>[10]</sup> Third, stability is also important. It is not possible to build a tertiary structure when using unstable secondary building blocks. Finally, the foldamer needs to be tunable, *i. e.* a wide variety of structures should be accessible under the same design principle.

### 1.2.1 Conformational control based on aryl-amide bonds

It is known that rotation around amide-aryl bonds is restricted because of the conjugation of the CONH and aryl groups. Energy minima are achieved when the aryl and amide groups are coplanar or close to coplanar in both the *syn* and *anti* conformations.<sup>[11]</sup> The *syn* and *anti* conformations could be selectively controlled by introducing specific attractive interaction or repulsive interaction between the amide and substituents on the aryl moieties.<sup>[9]</sup>

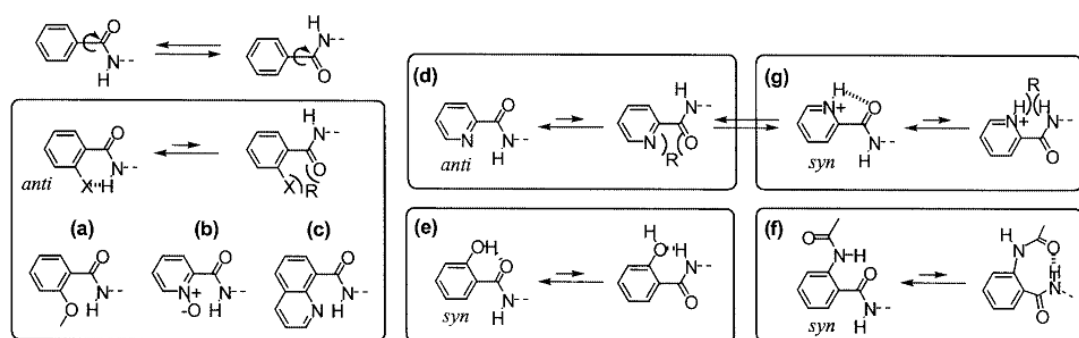


**Figure 1.3** Favorable conformations of different NHCO-aryl linkages.<sup>[9]</sup>

Conformational control of the amide-aryl bond is achieved by limitating its rotation, most often with a hydrogen-bond between the amide proton and a hydrogen-bond acceptor at the aryl group *ortho* position. The *anti* conformation is stabilized by the formation of either 5- or 6-membered hydrogen-bonded rings and disfavored by electrostatic repulsions between the carbonyl group and the *ortho* substituents on the aryl moieties (**Figure 1.3 a,b,c&d**). The strength of these hydrogen bonds is determined by the acceptor. For example, an ether oxygen is not as good an acceptor as an N-oxide group.<sup>[12]</sup> The *syn* conformation is favoured by attractive interactions between the carbonyl group and certain *ortho* substituents on the aryl moieties (**Figure 1.3 e,f&g**). The carbonyl oxygen acts as a hydrogen-bond acceptor and the phenol –OH, the protonated pyridine <sup>+</sup>NH and the amide –NH act as hydrogen-bond donors individually.

### 1.2.2 Pyridine-2,6-dicarboxamide derivatives leading to helical structures

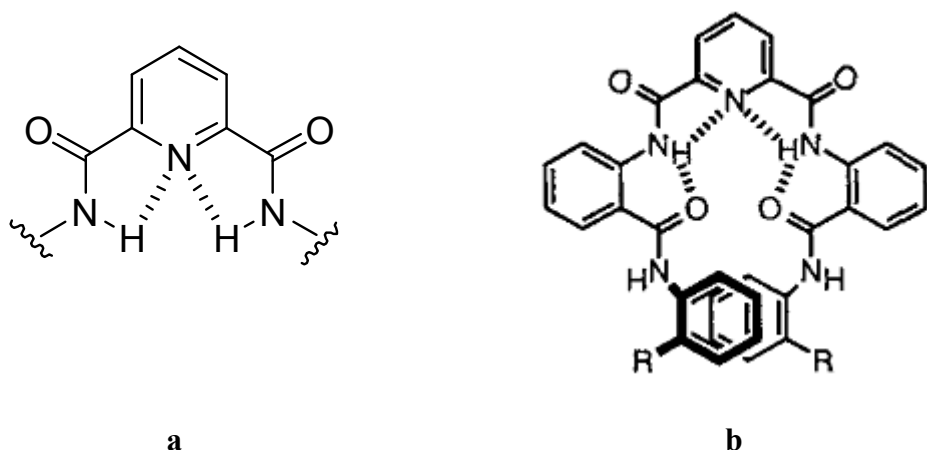


**Figure 1.4** **a)** Pyridine-2,6-dicarboxamide derivatives showing strong intramolecular H-bonds, **b)** folded helical structure observed by Hamilton.<sup>[15]</sup>

Pyridine-2,6-dicarboxamide (**Figure 1.4a**) shows a very strong hydrogen-bonding network in both condensed state and in solution.<sup>[13]</sup> In this case, one hydrogen-bond acceptor is bonded to two donor hydrogen atoms, and the hydrogen-bond will be cooperatively strengthened.<sup>[14]</sup> 2,6-Pyridylcarboxamide subunits can be used to fold many interesting structures. Hamilton demonstrated that a simple combination of pyridylcarboxamide derivatives and anthranilamide can lead to a helical structure (**Figure 1.4b**). This helical structure is stabilized by intramolecular hydrogen-bonds (amide protons with pyridine nitrogen and carbonyl oxygens) and  $\pi$ - $\pi$  interaction between two aniline groups. The amide-aryl bond takes up a *syn* conformation with only a small deviation from planarity.<sup>[15]</sup> Bearing pyridine-2,6-dicarboxamide folding motifs, a new family of oligomeric molecular strands was reported by Lehn et al. to display a bent conformation.<sup>[16, 17a]</sup> These structures were folded into single helical conformers by intramolecular hydrogen bonds and in dynamic exchange with double helices in solution.<sup>[17b]</sup> In the single helix (**Figure 1.5b**), the pyridine nitrogen atoms were bonded to neighbouring amide protons to form 4 or 5 membered hydrogen-bonded rings which direct the structure to adopt a helical shape without any template. The single helix (shown

in **Figure 1.5**) requires 4.5 pyridine-amide units per turn and leads to a one-and-a-half helical turn. The aromatic ring  $n$  overlaps with aromatic ring  $n+4$  and the distance between the terminal rings is around 3.6 Å which indicates a strong interaction between them. This may suggest that stacking provides an additional driving force for the folding of the helix.<sup>[18]</sup>

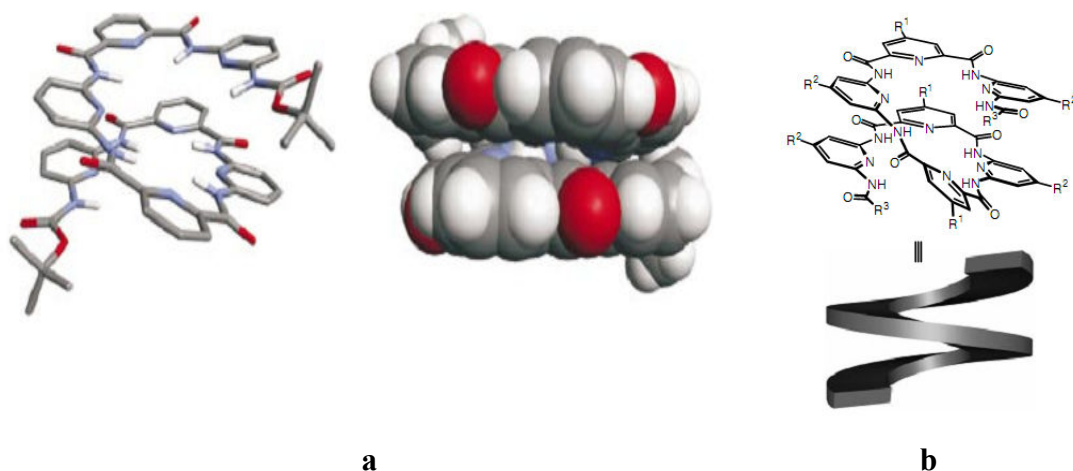


**Figure 1.5** a) Crystal structure of a single helix, grown from DMSO/CH<sub>3</sub>CN b) molecular structure of the single helix.<sup>[16]</sup>

Synthetic helical molecules are common, but double helices formed by the recognition of two strands are not very frequently observed.<sup>[19]</sup> When increasing the concentration of the single helix in CDCl<sub>3</sub>, double helices formed through dimerization with extensive intermolecular aromatic stacking.<sup>[16]</sup>

At the concentration of 0.91 mM (**Figure 1.6a**), three strongly deshielded amide protons (10.86, 10.43 and 10.27 ppm are observed indicating the formation of intramolecular hydrogen-bonds within single helix. As the concentration increases (**Figure b-d**), a second set of <sup>1</sup>H NMR signals shows up indicating the formation of double helices with a dimerization constant K<sub>d</sub><sub>im</sub> of 25–30 M<sup>-1</sup> in CDCl<sub>3</sub> at 25 °C.

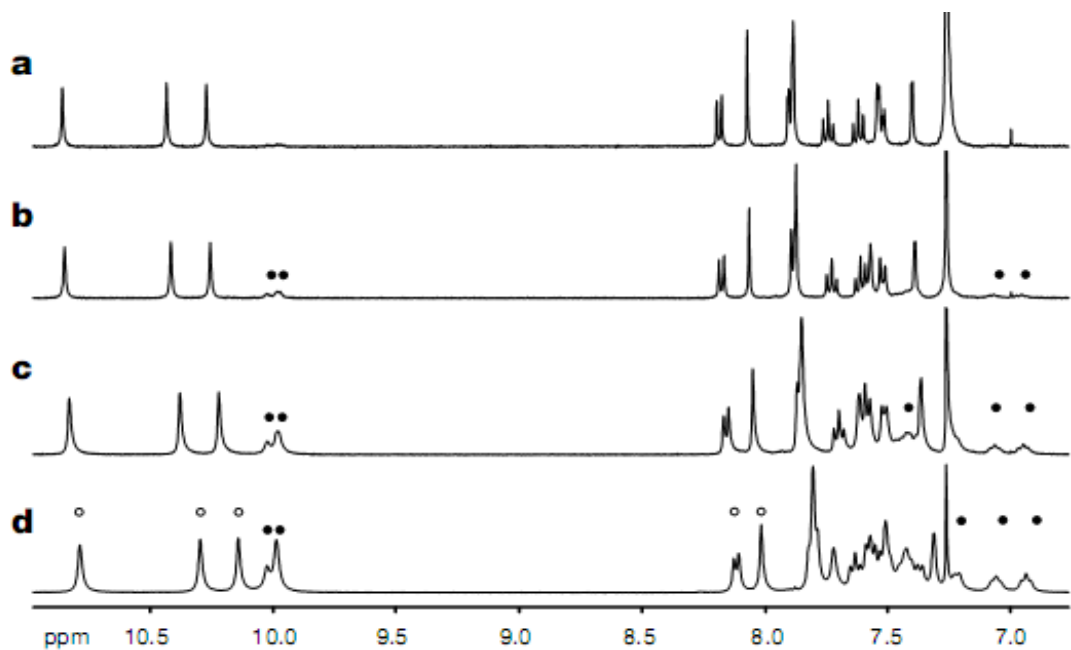


**Figure 1.6** Double helices formed in  $\text{CDCl}_3$  at various concentrations at  $25\text{ }^\circ\text{C}$ , 400 MHz  $^1\text{H}$  NMR.<sup>[16]</sup> Signals assigned to the monomer (unfilled circles), and to the dimer (filled circles) are labeled. a) 0.91 mM. b) 2.7 mM. c) 8.2 mM and d) 24.5 mM.  $K_{\text{dim}} = 25\text{--}30\text{ M}^{-1}$ .

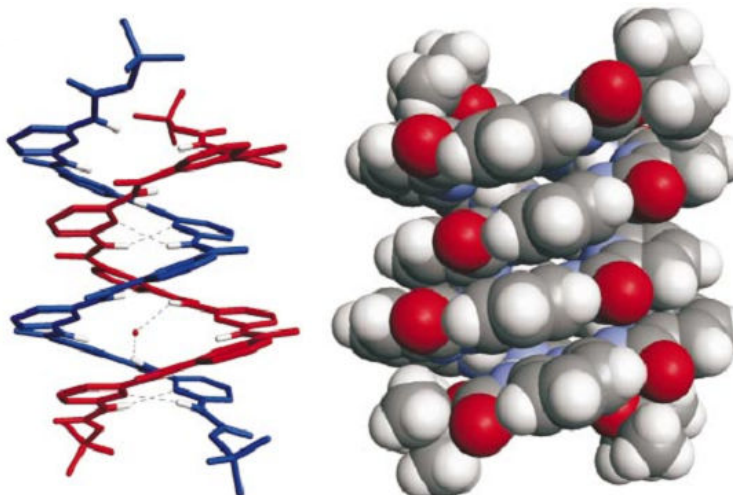


**Figure 1.7** Crystal structure of the double helical dimer, grown from nitrobenzene/heptane.<sup>[16]</sup>

The crystal of helical dimers was grown from a non-hydrogen bonding solvent mixture (nitrobenzene/heptane), compared to a hydrogen-bonding solvent (DMSO/ $\text{CH}_3\text{CN}$ )

which was used to crystallize the single helix. There are tight aromatic contacts within double helices and the average distance between contacting rings is 3.5 Å which corresponds to van der Waals contact (**Figure 1.7**). Aromatic stacking probably provides attractive interactions between two strands. Compared to the single helix, the double helices require only four pyridine-amide units per turn, although the single helix requires 4.5 pyridine-amide units per turn. This probably results from the attractive interstrand contacts which shorten the length of the helical conformer, in a similar way as a spring being compressed and extended.<sup>[17b]</sup>

### 1.2.3 Pyridine-2,6-dicarboxamide derivatives: folded to macrocycles and knot

In the course of the synthesis of the single helix reported by Lehn et al.,<sup>[17a]</sup> a tetrameric macrocycle was formed by the reaction of 2,6-diaminopyridine and 4-decyloxy-2,6-pyridine dicarbonyl chloride (**Figure 1.8**). Since it is a macrocyclization reaction, the yield (30%) is good considering the relatively concentrated conditions (3.6 mM). Besides, no other larger macrocycle was detected which indicated that the folding of this tetrameric macrocycle was pre-organized by intramolecular hydrogen-bonds between basic pyridine nitrogen atoms and slightly acidic amide protons.

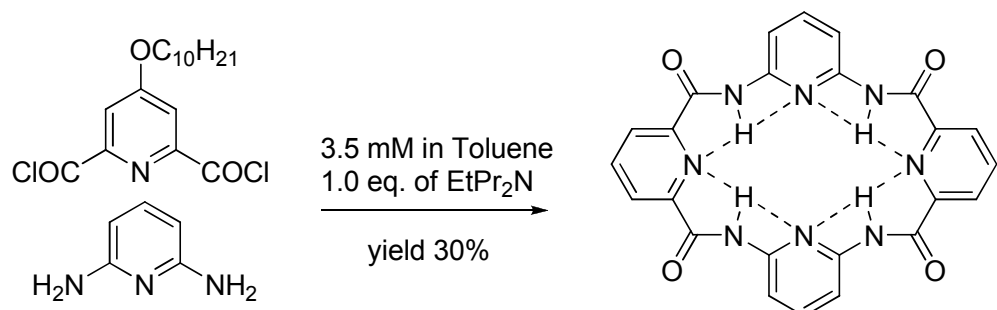


**Figure 1.8** Intramolecular hydrogen bonds lead to the folding of a tetrameric macrocycle.<sup>[17a]</sup>

Another example for using pyridine-2,6-dicarboxamide derivatives to fold a macrocycle is the quinone receptor investigated by Hunter.<sup>[14]</sup> In this case, the amide NH protons are not only hydrogen-bonded to the pyridine nitrogen to form a bis-*anti* conformation

around the amide bond, but also serve as hydrogen-bond donors to one of the quinone oxygen atoms. The association constant for quinone in  $\text{CDCl}_3$  reaches  $1800 \text{ M}^{-1}$ .<sup>[14]</sup>

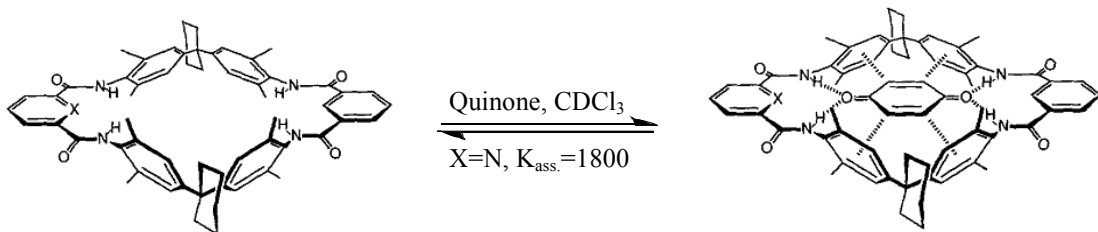


**Figure 1.9** Macrocycle bearing pyridine-2,6-dicarboxamide units as quinone receptor.<sup>[14]</sup>

In an attempt to synthesize a macrocycle used as wheels for constructing higher [n]catenane (more than 2 interlocked rings), a reaction of 2,6-pyridinedicarboxylic acid **1** and diamine **2** was carried out under dilution conditions (concentration  $10^{-3}$  mM) (**Figure 1.10a**).<sup>[20]</sup> In the reaction crude, besides a dimeric macrocycle (15%) and a tetrameric macrocycle (23%), a trefoil molecular knot (**Figure 1.10b**) was obtained by chance with a yield of 20%. It is the first example of a molecular knot synthesized without the help of transition metals. This molecular knot also contains 2,6-pyridine-dicarboxamide subunits and the formation of the knot is controlled by hydrogen-bond driven self-organization.

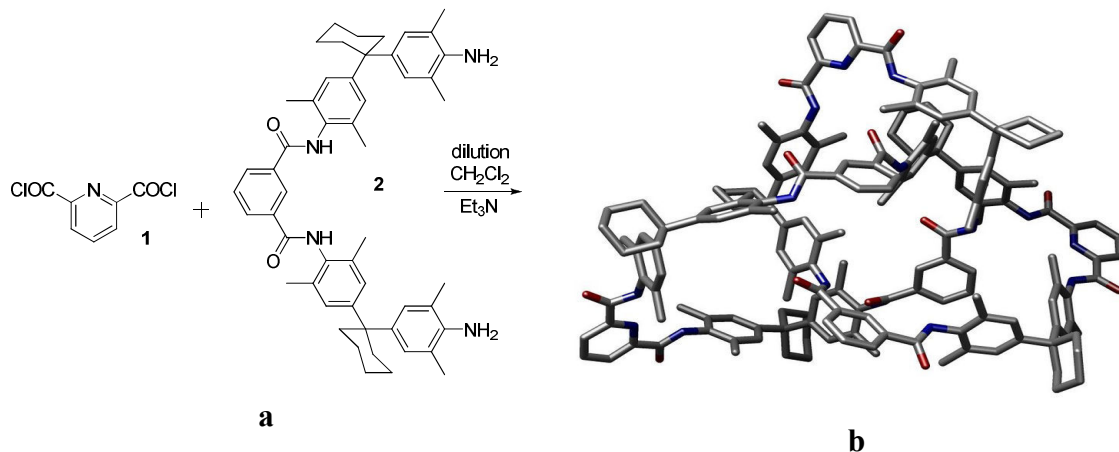


**Figure 1.10** a) Synthetic schemes targeting at macrocycles b) crystal structure of the trefoil molecule knot obtained by Vogtle.<sup>[20]</sup>

## 1.3 New formamidoxime folding motifs

### 1.3.1 Foldamers based on 2,6-pyridine-dicarboxamide and formamidoxime

Combining the 2,6-pyridine-dicarboxamide and formamidoxime (alkoxyformamidine) subunits we mentioned before, we are interested in folding more elaborate structures, such as: 1) folded open-ended structures (**Figure 1.11a**) which are very similar to the helical structure discussed by Hamilton;<sup>[15]</sup> 2) Macrocyclic **M2** (**Figure 1.11b**, the intramolecular hydrogen bonds would probably help pre-organize this macrocycle).

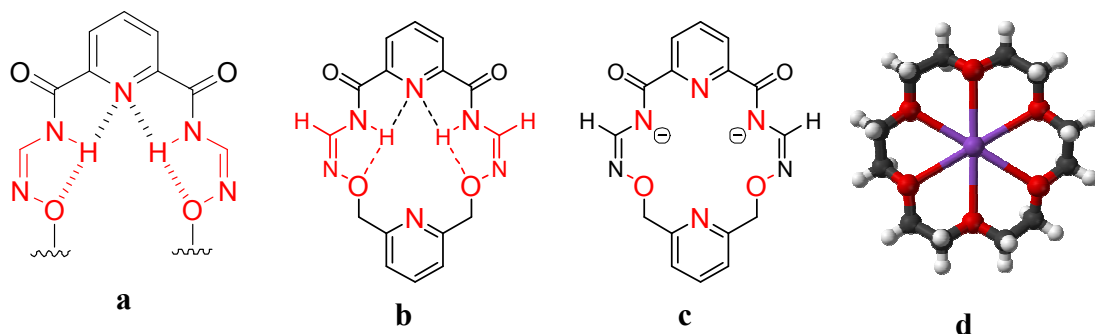


**Figure 1.11** **a)** Folded open-ended structure; **b)** macrocycle **M2**; **c)** deprotonated form of macrocycle **M2**; **d)** crystal structure of 18-C-6 crown ether coordinating to a potassium.<sup>[21]</sup>

The interest for macrocycle **M2** derives from the fact that it is structurally similar to 18-C-6 crown ether (**Figure 1.11d**) which displays pre-organized binding sites for cations. More interestingly, its acidic amide protons may be deprotonated by a base and thus induce negative charges on the amide nitrogen atoms (**Figure 1.11c**). When a crown ether binds a cation, all the binding sites are not in a plane.<sup>[22]</sup> Macrocycle **M2**, however, may become more planar because of its conjugated system. Thus, compared to crown ethers, deprotonated macrocycle **M2** is probably more selective (more rigid) for cations and may lead to higher affinities (negative charges on nitrogen atoms).

### 1.3.2 Macrocycles M1 and M3

In order to compare the shape effect, different macrocycles bearing formamidoxime units are designed. Macrocycle **M1** is much less conjugated than **M2**. Therefore it is much more flexible (two pyridine rings can flip out of the medial plane in **M1**, whereas only the methylene-pyridine can flip in **M2**, and no pyridine can flip in **M3**) and less planar. **M3** is much more rigid and planar compared to **M2**. Due to their relatively planar structures, macrocycles **M2** and **M3** may find applications in DNA quadruplex targeting.<sup>[23]</sup>

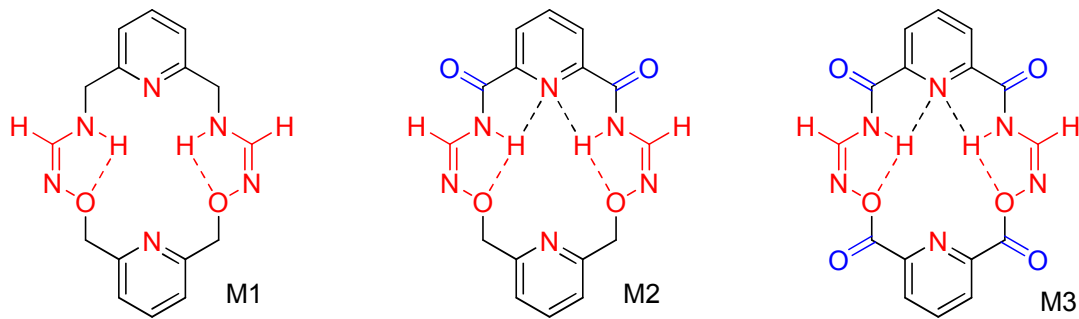


**Figure 1.12** Shapes of different macrocycles: flexible, not planar **M1**; less flexible, mostly planar **M2**; rigid, almost planar **M3**.

## References

- [1] (a) Hosseini, M. W.; Ruppert, R.; Schaeffer, P.; De Cian, A.; Kyritsakas, N. and Fischer, J. *J. Chem. Soc., Chem. Commun.* **1994**, 18, 2135-2136; (b) Auer, F.; Nelles, G. and Sellergen, B. *Chem.- Eur. J.* **2004**, 10, 3232-3240; (c) Ikeda, M.; Tanaka, T.; Hasegawa, T. and Furusho, Y.; Yashima, E. *J. Am. Chem. Soc.* **2006**, 128, 6806-6807.
- [2] (a) Barker, J. and Kilner, M. *Coord. Chem. Rev.* **1994**, 133, 219-300; (b) Cotton, F. A.; Lin, C. and Murillo, C. A. *Acc. Chem. Res.* **2001**, 34, 759-771; (c) Chisholm, M. H. and Macintosh, A. M. *Chem. Rev.* **2005**, 105, 2949-2976; (d) Coles, M. P. *Dalton Trans.* **2006**, 8, 985-1001; (e) Junk, P. C. and Cole, M. L. *Chem. Commun.* **2007**, 16, 1579-1590.
- [3] (a) Bailly, C.; Donkor, I. O.; Gentle, D.; Thornalley, M. and Waring, M. *J. Mol. Pharmacol.* **1994**, 46, 313-322; (b) Nguyen, B.; Lee, M. P. H.; Hamelberg, D.; Joubert, A.; Bailly, C.; Brun, R.; Neidle, S. and Wilson, W. D. *J. Am. Chem. Soc.* **2002**, 124, 13680-13681; (c) Mathews, T. P.; Kennedy, A. J.; Kharel, Y.; Kennedy, P. C.; Nicoara, O.; Sunkara, M.; Morris, A. J.; Wamhoff, B. R.; Lynch, K. R. and MacDonald, T. L. *J. Med. Chem.* **2010**, 53, 2766-2778.
- [4] Liu, Y.; Jessop, P. G.; Cunningham, M.; Eckert, C. A. and Liotta, C. L. *Science* **2006**, 313, 958-960.
- [5] Nguyen, B.; Lee, M. P. H.; Hamelberg, D.; Joubert, A.; Bailly, C.; Brun, R.; Neidle, S. and W. D. Wilson, *J. Am. Chem. Soc.* **2002**, 124, 13680-13681.
- [6] Komber, E.; Limbach, H.; Böhme, F. and Kunert, C.; *J. Am. Chem. Soc.* **2002**, 124, 11955-11963.
- [7] Xing, L.; Wiegert, C. and Petitjean, A.; *J. Org. Chem.* **2009**, 74, 9513-9516.
- [8] (a) Gellman, S. H.; *Acc. Chem. Res.* **1998**, 31, 173-180; (b) Hill, D. J.; Mio, M. J.; Prince, R. B.; Hughes, T. S. and Moore, J. S.; *Chem. Rev.* **2001**, 101, 3893-4011.
- [9] Huc, I.; *Eur. J. Org. Chem.* **2004**, 1, 17-29.
- [10] (a) Seebach, D. and Matthews, J. L.; *Chem. Commun.* **1997**, 2015-2022; (b) Cheng, R. P.; Gellman, S. H. and Degrado, W. F.; *Chem. Rev.* **2001**, 101, 3219-3232.
- [11] Malone, J. F.; Murray, C. M.; Dolan, G. M.; Docherty, R. and Lavery, A. J.; *Chem. Mater.* **1997**, 9, 2983-2989.
- [12] Su, C.-W. and Watson, J. W.; *J. Am. Chem. Soc.* **1974**, 76, 1854-1857.

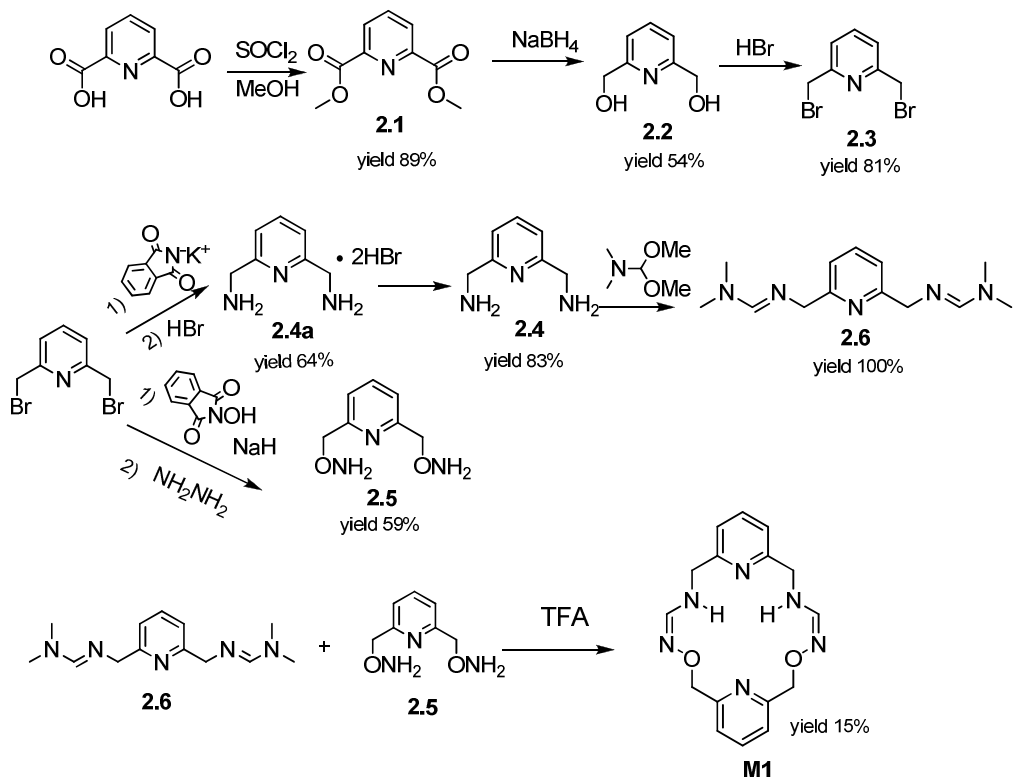
- [13] Marlin, D. S.; Olmstead, M. M. and Mascharak, P. K.; *J. Mol. Struct.*, **2000**, 554, 211-223.
- [14] Comparison of calculated lowest energies for anti/anti and anti/syn conformations of pyridine-2,6-dicarboxamide derivatives. For details, see Hunter, C. A. and Purvis, D. H.; *Angew. Chem. Int. Ed. Engl.*, **1992**, 31, 792-795.
- [15] See other examples: Garcia-Tellado, F.; Goswami, S.; Chang, S. K.; Geib, S. J. and Hamilton, A. D.; *J. Am. Chem. Soc.*, **1990**, 112, 7393-7394.
- [16] Berl, V.; Huc, I.; Khoury, R. G.; Krische, M. J. and Lehn, J.-M.; *Nature*, **2000**, 407, 720.
- [17] (a) Berl, V.; Huc, I.; Khoury, R. G.; Krische, M. J. and Lehn, J.-M.; *Chem. Eur. J.* **2001**, 7, 2798-2809 (b) Berl, V.; Huc, I.; Khoury, R. G.; Krische, M. J. and Lehn, J.-M.; *Chem. Eur. J.* **2001**, 7, 2810-2820.
- [18] (a) Zhu, J.; Parra, R. D.; Zeng, H.; Skrzypczak-Jankun, E.; Zeng, X. C. and Gong, B.; *J. Am. Chem. Soc.* **2000**, 122, 4219-4220. (b) Hamuro, Y.; Geib, J. S. and Hamilton, A. D.; *J. Am. Chem. Soc.* **1997**, 119, 10587-10593.
- [19] For a few examples: (a) Langs, D. A.; *Science* **1988**, 241, 188–191. (b) Kusanagi,H.; *Polymer J.*, **1996**, 28, 708–711. (c) Engelkamp, H.; Middelbeek, S. and Nolte, R. J. M.; *Science*, **1999**, 284, 785–788. (d) Koert, M.; Harding, M. and Lehn, J.-M; *Nature* **1990**, 346, 339–342.
- [20] Safarowsky, O.; Nieger, M.; Frohlich, R. and Vogtle, F.; *Angew. Chem. Int. Ed. Engl.*, **2000**, 39, 1616-1618.
- [21] Kotlyar, S. A.; Zubatyuk, R. I.; Shishkin, O. V.; Chuprin, G. N.; Kiriyak, A. V. and Kamalov, G. L.; *Acta Cryst.*, **2005**, E61, m293-m295.
- [22] Supramolecular Chemistry, 2nd edition; Steed, J. W. and Atwood, J. L.; **2009**, John Wiley & Sons, Ltd.
- [23] Neidle, S. and Thurston, D. E.; *Nat. Rev. Cancer*, **2005**, 5, 285-296.

## Chapter 2

### Macrocycle M1

#### 2.1 Synthetic route to macrocycle M1

The target macrocycle **M1** can be synthesized by condensation of two components: an electrophilic bis-dimethylformamidine and a nucleophilic bis-alkoxyamine (**Scheme 2.1**).



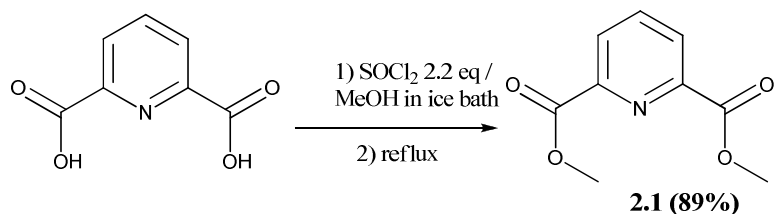
**Scheme 2.1** Synthetic route for macrocycle **M1**.

All synthetic concerns therefore focus on obtaining these two components and then condensing them into macrocycle **M1**. 2,6-Pyridinedicarboxylic acid was used as starting material, and underwent esterification to give diester **2.1**.<sup>[1]</sup> Reduction of **2.1** to dialcohol **2.2**, followed by bromination gave dibromide **2.3**<sup>[1]</sup> which is a precursor to both fragments

of the macrocycle. Compound **2.3** underwent amination and alkoxyamination separately to give compounds **2.4** and **2.5** respectively. Diamine **2.4** was transformed into formamidine **2.6**, which was then condensed with alkoxyamine **2.5** to give the target macrocycle **M1**.

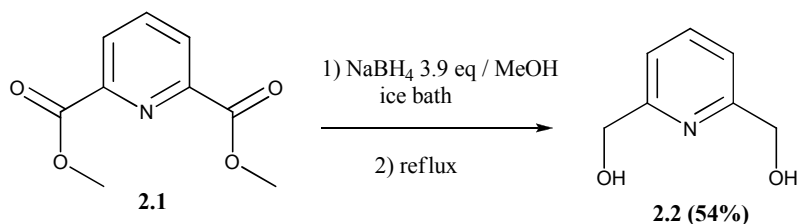
### 2.1.1 Synthesis of pyridine-2,6-dimethylalcohol (**2.2**)

In the literature protocol,<sup>[1]</sup> 1.0 equivalent of pyridine-2,6-dicarboxylic acid was added into the mixture of 2.2 equivalents of thionyl chloride and excess ethanol to give pyridine-2,6-diethylester. The diethylester was then reduced to dimethylalcohol (**2.2**) by sodium borohydride in ethanol. The method used herein was slightly different from the literature. Pyridine-2,6-dicarboxylic acid (1.0 equivalent) was also used as starting material, but added into the mixture of 2.2 equivalents of thionyl chloride and excess anhydrous methanol to give pyridine-2,6-dimethylester (**2.1**) in 89% yield.



**Scheme 2.2** Synthesis of pyridine-2,6-dimethylester (**2.1**).

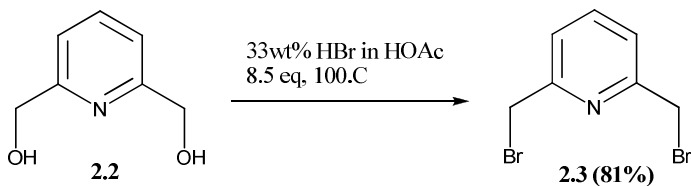
Compound (**2.1**) was then reduced by 3.9 equivalents of sodium borohydride in methanol to give dialcohol (**2.2**) in 54% yield.



**Scheme 2.3** Synthesis of dimethylalcohol (**2.2**) starting with compound **2.1**.

### 2.1.2 Synthesis of 2,6-bis(bromomethyl)pyridine (**2.3**)

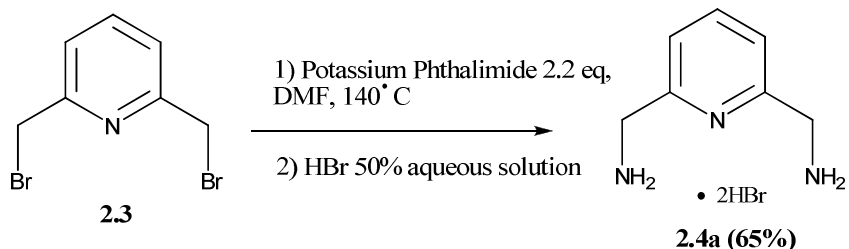
The synthesis of 2,6-bis(bromomethyl)pyridine was performed using 33 wt% hydrobromic acid in acetic acid as bromination reagent.<sup>[1]</sup>



**Scheme 2.4** Bromination of pyridine-2,6-dimethylalcohol.

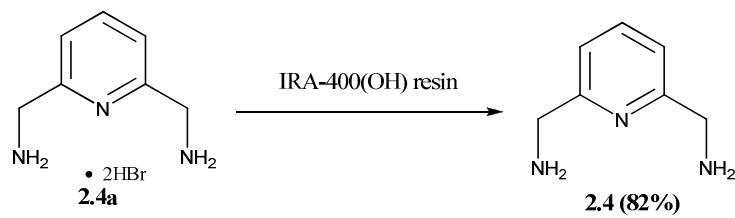
### 2.1.3 Synthesis of pyridine-2,6-diylidemethanamine (2.4)

In the literature protocol,<sup>[2]</sup> 2,6-dichloromethylpyridine was converted to the diamine via Gabriel's method ( $S_N2$  using potassium phthalimide as a nucleophile, followed by hydrolysis in aqueous hydrobromic acid) to give diaminomethylpyridine hydrobromide. In our case, 1.0 equivalent of 2,6-bis(bromomethyl)pyridine and 2.2 equivalents of potassium phthalimide were suspended in DMF and heated at 140 °C for 5 hours. After cooling to room temperature, Milli-Q water was added to induce precipitation. The precipitate was then suspended in aqueous hydrobromic acid at 120 °C for 3 hours and treated similarly to the literature work-up: neutralization with NaOH to pH 5 and inducing precipitation<sup>[2]</sup> to give the crude hydrobromide salt (**2.4a**).



**Scheme 2.5** Synthesis of hydrobromide salt by Gabriel's method.

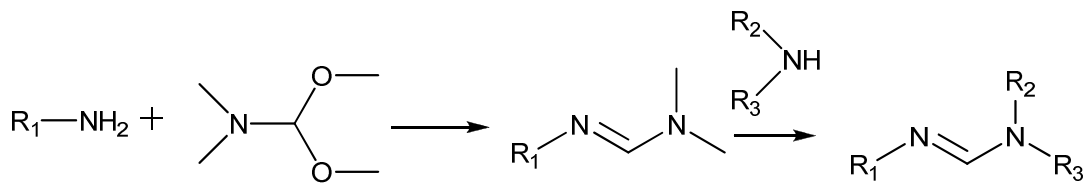
The hydrobromide salt **2.4a** was neutralized on an IRA-400(OH) resin to give the neutral diamine **2.4** in a 83% yield.



**Scheme 2.6** Neutralization of the hydrobromide salt to give pyridine-2,6-diylidemethanamine.

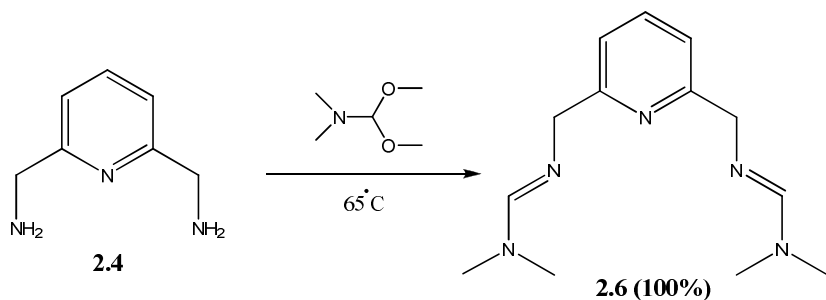
#### 2.1.4 Synthesis of pyridine-2,6-bis-(N,N-dimethylformamidine) (2.6)

The general routes for the synthesis of formamidines and related compounds involve the reaction between primary amines and N,N-dimethylformamide dimethylacetals (DMF-DMA) under neutral conditions.<sup>[3]</sup> The most common way to prepare symmetrical and unsymmetrical formamidines consists of the exchange of the electron donating dimethylamino fragment in N,N-dimethylformamidines with a variety of amines (**Scheme 2.7**).



**Scheme 2.7** General method of preparation of di-and tri-substituted formamidines.<sup>[3]</sup>

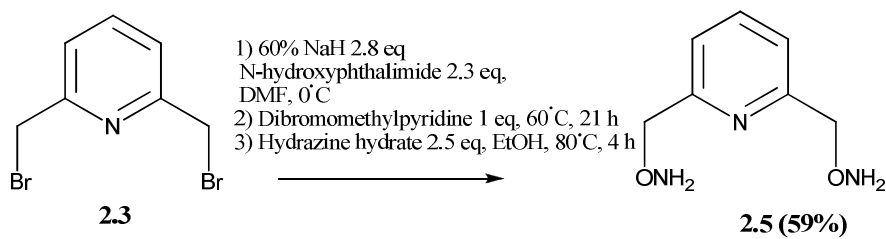
The preparation of N,N-dimethylformamidines can be conducted in different solvents or under solvent-free conditions. For the synthesis of compound **2.6**, 1.0 equivalent of pyridine-2,6-diylidemethanamine **2.4** was dissolved into 3.0 equivalents of N,N-dimethylformamide dimethylacetal (DMF-DMA) and heated at 65 °C for 2.5 h. After removal of excess amount of DMF-DMA, the desired N,N-dimethylformamidine product **2.6** was obtained in quantitative yield.



**Scheme 2.8** Synthesis of N,N-dimethylformamidine **2.6**.

### 2.1.5 Synthesis of O,O'-(pyridine-2,6-diylbis(methylene))bis(hydroxylamine) (2.5)

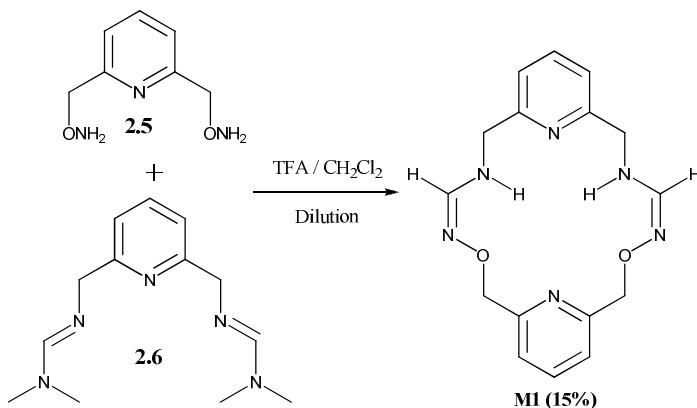
In a similar design to Gabriel synthesis, bis-alkoxyamine **2.5** was prepared in two steps: O-alkylation using an N-protected alkoxyide nucleophile, followed by deprotection of the nitrogen functionality. In the first step, 2.8 equivalents of sodium hydride (60% dispersion in mineral oil) was washed with hexane under argon and suspended in dry dimethylformamide. N-hydroxyphthalimide (2.3 equivalents) was then added portion-wise, as the mixture was stirred in an ice/water bath (exothermic reaction). 2,6-bis(bromomethyl)pyridine **2.3** (1.0 equivalent) was then added at once and the mixture was stirred at 60 °C for 21 hours to give the N-phthalimide intermediate (83%). In the second step, the N-phthalimide was deprotected using hydrazine hydrate (2.5 equivalents) in 95% ethanol at 80 °C for 4 hours. Purification by column chromatography (silica) gave the desired dialkoxyamine **2.5** in an overall 59% yield.



**Scheme 2.9** Synthesis of pyridine-2,6-bisalkoxyamine **2.5**.

### 2.1.6 Synthesis of Macrocycle M1

Under relatively dilute conditions (5 mmol/L), the cyclic products are likely to form by intramolecular reaction faster than polymers which come from intermolecular reactions.<sup>[4]</sup>



**Scheme 2.10** Cyclic condensation by bis-reactive N,N-dimethylformamidine **2.6** and alkoxyamine **2.5** under dilute conditions.

N,N-dimethylformamidine **2.6** (1.0 equivalent) and pyridine-2,6-bisalkoxyamine **2.5** (1.0 equivalent) were dissolved into anhydrous dichloromethane separately. These two solutions were combined and additional anhydrous dichloromethane was added to dilute the solution further. Then TFA (1.2 equivalent) was added and the solution refluxed for 10 days under argon. The crude was washed with aqueous NaOH solution and finally purified by column chromatography (silica) and then recrystallized from hot 95% ethanol to give the pure macrocycle **M1** (15%).

## 2.2 Results and Discussion

### 2.2.1 Characterization of macrocycle M1.

The first generation of macrocycle **M1** based on the alkoxylformamidine unit was characterized by <sup>1</sup>H NMR spectroscopy, mass spectrometry and single crystal X-ray crystallography.

### 2.2.1.1 $^1\text{H}$ NMR of macrocycle M1

From the  $^1\text{H}$  NMR spectrum of **M1** (Figure 2.1), the anticipated large  $^3\text{J}$  coupling constant for formamidine proton  $\text{H}_f$  (chemical shift at 6.70 ppm,  $^3\text{J} = 11.1$  Hz) may be seen as a sign of the formation of the alkoxyformamidine subunit (highlighted in structure). The high coupling constant reflects the facts that, in solution, the  $\text{H}_f$  and NH protons are trans to each other, and the exchange of the (possibly labile) NH proton is fairly slow. This also results in the coupling of the  $\text{CH}_2$  protons (chemical shift at 4.32 ppm) to the adjacent NH proton. The  $\text{CH}_2$  groups adjacent to oxygen have a higher chemical shift (5.08 ppm) than the ones next to the nitrogen. Since the chemical environments of the two pyridines are not the same, their respective aromatic protons show one doublet and one triplet at different chemical shifts (for the pyridine coming from the diamine, the chemical shifts of the triplet and doublet are 7.65 and 7.04 ppm respectively; for the pyridine coming from the dialkoxyamine, chemical shifts of the triplet and doublet are 7.58 and 7.26 ppm respectively). All the protons in **M1** have been assisted assigned by COSY (see appendix A) and are reported in Figure 2.1.

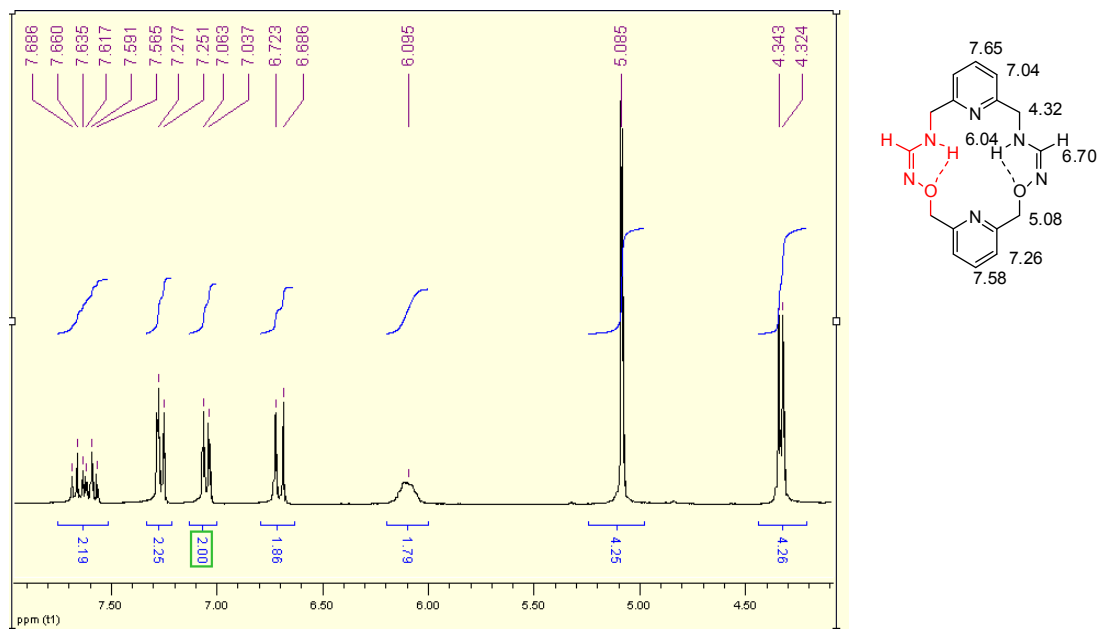


**Figure 2.1**  $^1\text{H}$  NMR spectrum of macrocycle **M1** in  $\text{CDCl}_3$  (300 MHz, 25 °C).

### 2.2.1.2 Mass spectrometry study of Macrocyclic M1

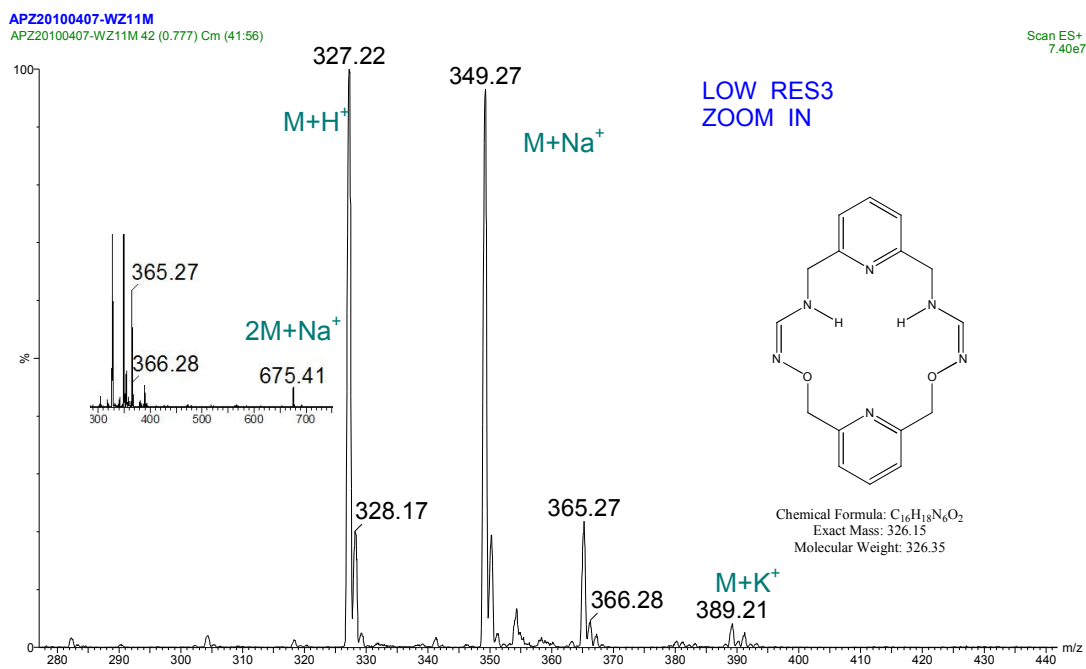


**Figure 2.2** ESI-mass spectrum of macrocycle M1 (in  $CH_2Cl_2$ ).

The electrospray ionization mass spectrum (**Figure 2.2**) clearly shows molecular peaks at 327.22 ( $M+H^+$ ), at 349.27 ( $M+Na^+$ ), and at 365.27 ( $M+K^+$ ). More importantly, the peak at 675.41, which is the mass of  $(2M+Na^+)$ , indicates that the macrocycle tends to form a dimer promoted by the binding to a sodium cation.

### 2.2.1.3 Single crystal X-ray structure of M1

According to the crystal structure presented in **Figure 2.3a**, the anticipated hydrogen-bonded pattern is clearly present within the alkoxyamine-formamidine unit. In the solid state, the macrocycles tend to form two kinds of dimers. One dimer is linked through intermolecular hydrogen bonding between the pyridine nitrogen (on the “amine” side) and the formamidine N-H (**Figure 2.3b**). Another dimer is linked by  $\pi$ - $\pi$  interactions between two pyridine rings and very weak hydrogen bonds between the pyridine nitrogen (on the “alkoxyamine side”) and the pyridine H4 hydrogen on the “amine” side (**Figure 2.3c**).

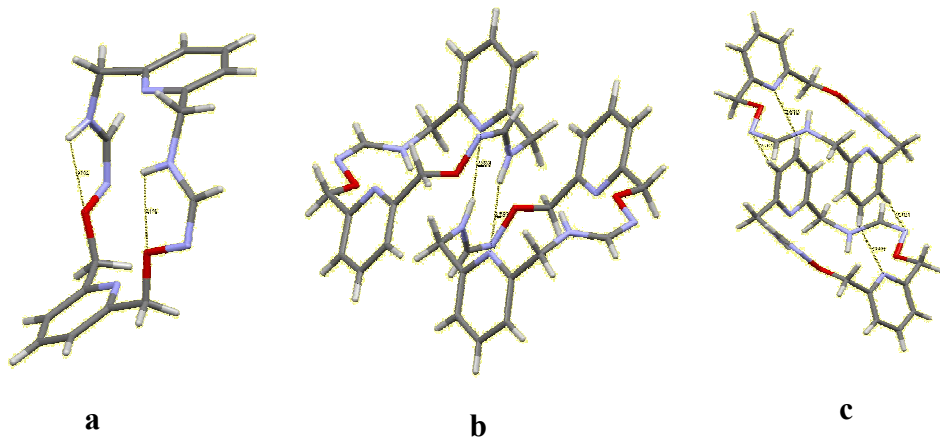


**Figure 2.3** Crystal structure of macrocycle **M1**; **a)** side view highlighting the anticipated intramolecular H-bond and the Z formamidine motif; **b)** view of the solid-state dimer maintained by intermolecular  $\text{N}_{\text{py}}\text{-NH}$  H-bonds; **c)** view of the solid-state dimer held by intermolecular  $\text{N}_{\text{py}}\text{-H}_{\text{py}}$  H-bonds. Crystallization from  $\text{Et}_2\text{O}/\text{CH}_2\text{Cl}_2$  (a), (b) and (c)).

## 2.2.2 Other isolated products

In addition to the desired macrocycle **M1**, other species were isolated in the purification process. One of them seems to be a topological molecule<sup>[5]</sup> which is described below.

### 2.2.2.1 Introduction of interlocked molecules: Catenanes

Catenanes are interlocked molecules. Different from classical molecular structures, they contain several separate components which are not connected by chemical bonds. They are true molecules but not supramolecular species since each component is intrinsically locked by each other.<sup>[5b]</sup> Catenanes are composed of two or more interlocked macrocyclic rings. For a [2]catenane shown in **Figure 2.4**, the number 2 in square brackets indicates there are two mechanically interlocked components (two rings). If both rings are identical, the molecule is a homocircuit catenane. Otherwise, it is a heterocircuit catenane when both rings are different.

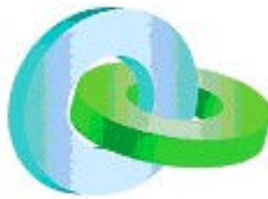


**Figure 2.4** Cartoon representation of a [2]catenane.

Up until the early 1980s, catenanes and other interlocked architectures were considered to be useless but just satisfied academic curiosities. The synthetic methods for catenane at that time were low-yielding, simply depending on the chance-induced interlocking of components during their formation. Since the first templated catenane synthesis was conducted in 1983,<sup>[6]</sup> great achievements have been made in the past two decades. With the development of supramolecular chemistry, chemists have been interested in applying their newly-discovered knowledge of non-covalent interactions to chemical synthesis. As a consequence, nowadays, a variety of templating methods (for example, transition metal templation,  $\pi$ -donor/acceptor templates, hydrogen bond templation etc)<sup>[7]</sup> are used efficiently to make catenanes and many other interesting interlocked molecules.

In today's interlocked molecules studies, chemists are paying much more attention to the interesting properties and potential applications of the molecules themselves rather than to the synthetic challenge. Compared to non-interlocked molecules, interlocked molecules usually show remarkably different properties, for example, in spectroscopic responses, chemical reactivity or mechanical properties. How to control motions of components in mechanically interlocked molecules is a big issue for the creation of novel functional molecules – molecules that are able to alter their properties in response to an external stimulus (e.g. light, electricity or a chemical reagent).<sup>[8]</sup> Such functional molecules will help produce molecular machines and molecular devices (**Figure 2.5**) which are described as “the key protagonists in the development of a “bottom-up” nanotechnology for the 21st century”.<sup>[9]</sup>

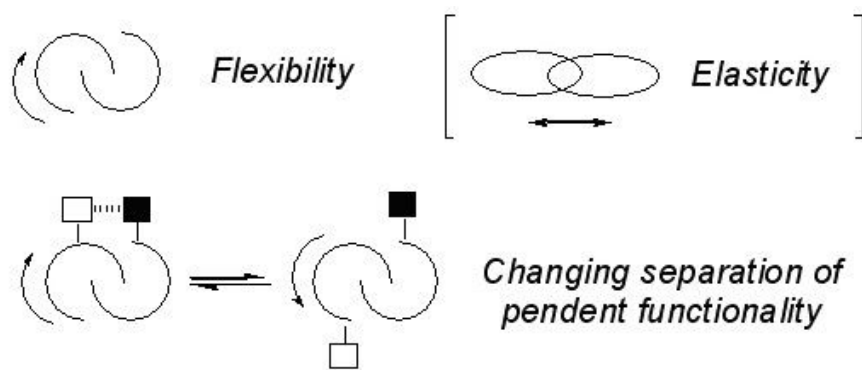


**Figure 2.5** Mechanically interlocked architectures as components for molecular machines.<sup>[9]</sup>

#### 2.2.2.2 Larger structures made of four pyridine units: large macrocycles or catenane?

In the course of the reaction, four-pyridine-unit species were also formed as by-products according to mass spectrometry analysis, and tentatively separated from the main two-unit macrocycle by column chromatography. In the ESI-MS analysis of the four-pyridine-unit system (**Figure 2.6**),  $M+H^+$  and  $M+Na^+$  peaks are clearly seen at  $m/z = 653$  and  $675$  respectively. The molecular weight of  $652$  g/mol corresponds to two possible molecules which are topological isomers. One is larger macrocycle (four pyridine units) and another is a catenane where two two-pyridine-unit macrocycles **M1** would be interlocked together mechanically. In order to know whether a catenane had formed, MS-MS experiment was used. In this experiment, collisions with gas induce the cleavage of covalent bonds. If a catenane is present, when one ring breaks, it will leave another intact ring behind and this ring should be seen in the spectrum. In the experiment, we indeed saw peaks coming from small macrocycles. This suggests that the catenane did form in this reaction. However, the catenane structure still needs to be confirmed by crystallography. Future work will focus more on the study and disclosure of the secret face of formamidine-based catenanes.

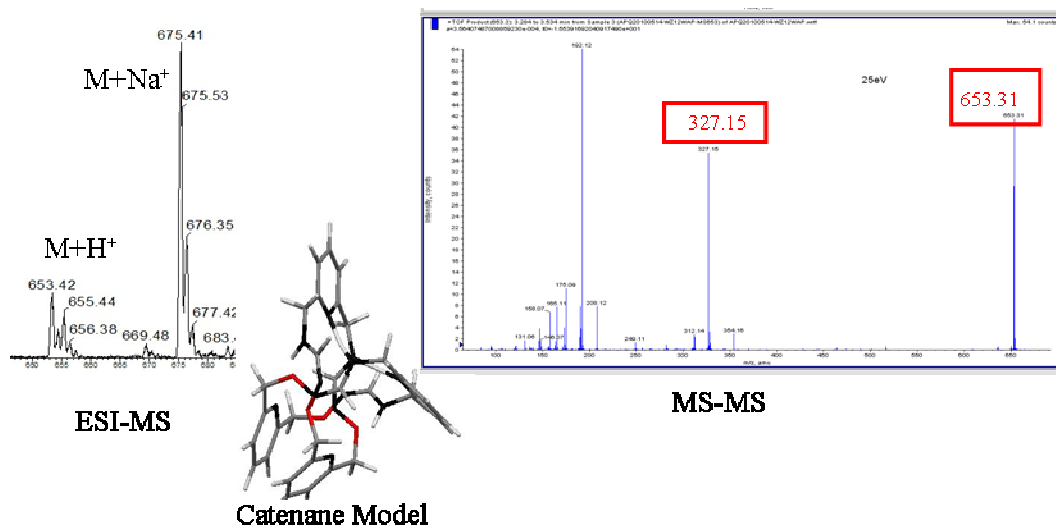


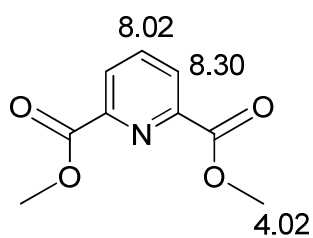
**Figure 2.6** MS evidence for existing catenane, and catenane crude model.

## 2.3 Conclusion of Chapter 2

As described in this chapter, the first generation of macrocycle **M1** with alkoxyamine-formamidine subunits has been successfully obtained and fully characterized by  $^1\text{H}$  NMR spectroscopy, mass spectrometry and single crystal X-ray diffraction. Moreover, a four-pyridine-unit interlocked molecules-catenane was discovered by accident and confirmed by mass spectrometry techniques.

## 2.4 Experimental details

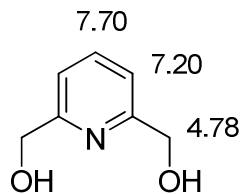
### Pyridine-2,6-dimethylester (2.1)



The synthetic method was adapted from literature protocols.<sup>[10]</sup> To ice-cold anhydrous methanol (50 mL, 1.2 mol, 40 eq) was added thionyl chloride (4.85 mL, 66.5 mmol, 2.2 eq) dropwise under argon. Pyridine-2,6-dicarboxylic acid (5.02 g, 30 mmol, 1.0 eq) was then added as a solid and the mixture was refluxed for 15 hours under argon. After cooling to room temperature, the formed shiny white precipitate was filtered, taken up in dichloromethane and saturated aqueous potassium

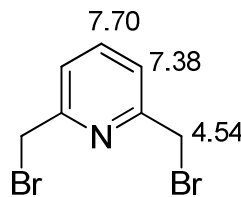
bicarbonate solution. The organic layer was isolated, dried over by sodium sulphate and evaporated in vacuo to afford the desired diester as a white powder (5.2 g, 89%).  $\delta^1\text{H}$  (300 MHz;  $\text{CDCl}_3$ ; 25 °C): 8.02 (t,  $^3J = 7.8$  Hz, 1 H), 8.30 (d,  $^3J = 7.8$  Hz, 2 H), 4.02 (s, 6 H).

### Pyridine-2,6-dimethylalcohol (2.2)



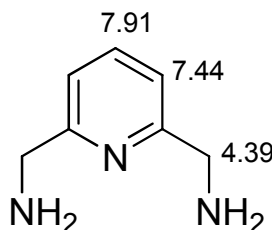
The synthetic method is slightly modified from literature protocols.<sup>[10]</sup> Dimethyl-pyridine-2,6-dicarboxylate (5.01 g, 26 mmol, 1.0 eq) was suspended in methanol (85 mL). After cooling in an ice/water bath, sodium borohydride (3.82 g, 0.1 mol, 3.9 eq) was added portion-wise as a solid. After the mixture was warmed up to room temperature, stirred for 30 minutes and then refluxed for 3 hours. The solvent was then evaporated, saturated aqueous potassium carbonate (150 mL) added and the solution heated at 60 °C for 3 hours. After cooling to room temperature, the mixture was extracted with dichloromethane (75 mL + 12×40 mL) for 13 times, the combined organic layers isolated and dried on sodium sulphate, filtered and concentrated in vacuo to give the crude diol (1.86 g, 54%) as a white solid.  $\delta^1\text{H}$  (300 MHz;  $\text{CDCl}_3$ ; 25 °C): 7.70 (t,  $^3J = 7.8$  Hz, 1 H), 7.20 (d,  $^3J = 7.8$  Hz, 2 H), 4.78 (s, 4 H).

### 2,6-Bis(bromomethyl) pyridine (2.3)



The synthetic method is slightly modified from literature protocols.<sup>[10]</sup> Pyridine-2,6-diyldimethanol (4.9 g, 35 mmol, 1.0 eq) was dissolved in a solution of hydrobromic acid in acetic acid (hydrobromic acid 33% in acetic acid, 55 mL, 0.3 mol, 8.5 eq), and heated at 100 °C for 1.5 hours. The solution was cooled down in an ice/water bath, and gently neutralized with 10 M sodium hydroxide. The formed precipitate was filtered, washed with a little amount of water, air dried overnight and in vacuum with phosphorus pentoxide for 20 minutes to give the desired dibromide as a white powder (7.56 g, 81 %).  $\delta^1\text{H}$  (300 MHz;  $\text{CDCl}_3$ ; 25 °C): 7.70 (t,  $^3J = 7.5$  Hz, 1 H), 7.38 (d,  $^3J = 7.5$  Hz, 2 H), 4.54 (s, 4 H).

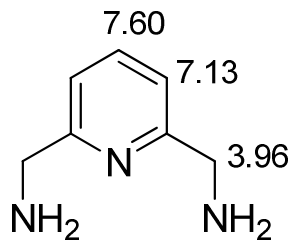
### Pyridine-2,6-diylidemethanammonium bromide (2.4a)



The synthetic method is slightly modified from literature protocols.<sup>[11]</sup> 2,6-Bis(bromomethyl) pyridine (0.9 g, 3.4 mmol, 1.0 eq) and potassium phthalimide (1.4 g, 7.5 mmol, 2.2 eq) were suspended in DMF (6 mL) and heated at 140 °C for 5 hours. After cooling to room temperature, Milli-Q water (50 mL) was added to induce precipitation. The precipitate was filtered and rinsed with water. The solid was then heated with hydrobromic acid (20 mL, 50% in water) at 120 °C for 3 hours. After cooling to room temperature, the precipitate was filtered and washed with a small amount of water. The filtrate was then concentrated to half of its volume, allowed to cool and the newly formed precipitate was collected by filtration and washed with 95% ethanol to give the crude diamine bis-hydrobromide (0.66 g, 65 %).  $\delta^1\text{H}$  (300 MHz; D<sub>2</sub>O; 25 °C): 7.91 (t, <sup>3</sup>J = 7.8 Hz, 1 H), 7.44 (d, <sup>3</sup>J = 7.8 Hz, 2 H), 4.39 (s, 4 H).

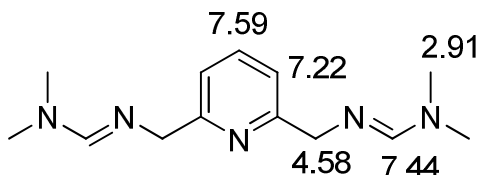
### Pyridine-2,6-diylidemethanamine (2.4)

IRA 400(OH) resin was conditioned with Milli-Q water and loaded with pyridine-2,6-diylidemethanammonium bromide (1.89 g, 6.32 mmol). The free diamine



was eluted with Milli-Q water and collected until pH was neutral. The water was evaporated (rotavap) to give the desired neutral pyridine-2,6-diylidemethanamine (0.72 g, 5.18 mmol, 82 %)  $\delta^1\text{H}$  (300 MHz; CDCl<sub>3</sub>; 25 °C): 7.60 (t, <sup>3</sup>J = 7.8 Hz, 1 H), 7.13 (d, <sup>3</sup>J = 7.8 Hz, 2 H), 3.96 (s, 4 H).

### Pyridine-2,6-diylbis(methylene)bis(N,N-dimethylformamidamide) (2.6)

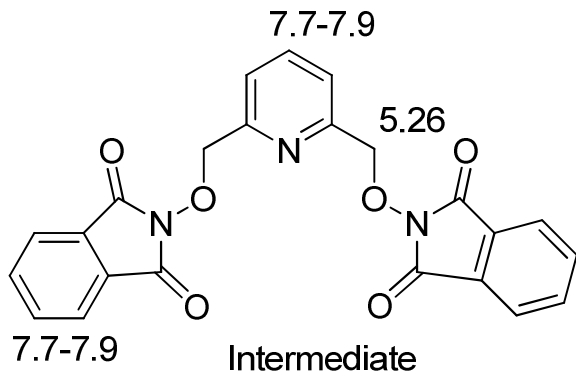


In a 10 mL RBF were solubilized 260 mg of Pyridine-2,6-diylidemethanamine (1.9 mmol, 1.0 eq) in 0.8 mL of N,N-dimethylformamide

dimethylacetal (DMF-DMA, 6 mmol, 3.2 eq). The solution was heated at 65 °C under argon for 2.5 hours. At room temperature, the solvent was co-evaporated with dichloromethane to give 0.48 g (1.9 mmol, 100 %) of the desired dimethylformamidine product as a pale yellow oil.  $\delta$   $^1\text{H}$  (300 MHz;  $\text{CDCl}_3^*$ ; 25 °C): 7.59 (t,  $^3J = 7.5$  Hz, 1 H), 7.44 (s, 2 H), 7.22 (d,  $^3J = 7.5$  Hz, 2 H), 4.58 (s, 4 H), 2.91 (s, 12 H).

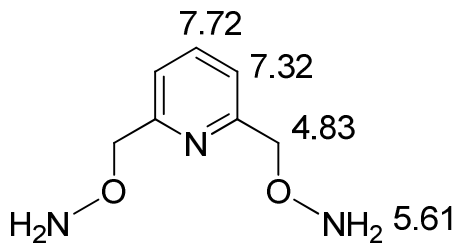
### O,O'-(pyridine-2,6-diylbis(methylene))bis(hydroxylamine) (2.5)

1<sup>st</sup> process: In hexane (5 mL) was suspended 1.24 g (31 mmol, 2.8 eq) of 60% sodium hydride (60% dispersion in mineral oil) under argon. The hexane washing was then removed, and dry DMF was added under argon. N-hydroxyphthalimide (4.24 g, 26 mmol, 2.4 eq) was then added portionwise as a solid, as the mixture was stirred in an ice/water bath (exothermic reaction). 2,6-Bis(bromomethyl) pyridine (3.0 g, 11 mmol, 1.0 eq) was then added at once and the mixture was stirred at 60 °C for 21 hours under argon. At room temperature, water was added, and the precipitate filtered and washed with copious amounts of water. The solid was then dissolved in dichloromethane and



washed with water. The organic layer was isolated, dried on sodium sulphate and concentrated in vacuo to give 3.83 g of a light yellow solid (81 %).  $\delta$   $^1\text{H}$  (300 MHz;  $\text{CDCl}_3$ ; 25 °C): 7.7-7.9 (m, 11 H), 5.26 (s, 4H).

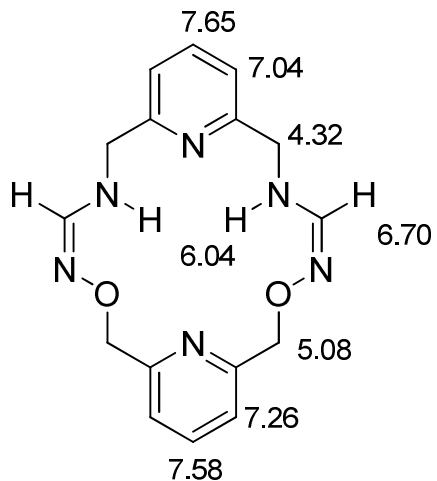
2<sup>nd</sup> process: in 95% ethanol (150 mL) was suspended 3.83 g of the previous intermediate (8.9 mmol, 1.0 eq). Most of the reagent was dissolved by heating gently, and hydrazine hydrate (1.1 mL, 22 mmol, 2.5 eq) was added. The mixture was then heated at 80 °C for 4 hours. Back to room temperature, the suspension was concentrated in vacuo to give a white solid which was taken up in diethyl ether (80 mL). The precipitate was filtered and washed with more diethyl ether (6×50 mL). The combined filtrates were concentrated in vacuo to give 1.53 g of a crude oil which was purified by column chromatography (silica gel, 100:1:5 diethyl ether, triethylamine and methanol as the eluent) to give 1.12 g (6.63 mmol,



73 %) of a colourless oil which solidified into a white solid in the freezer.  $\delta$  <sup>1</sup>H (300 MHz; CDCl<sub>3</sub>\*; 25 °C): 7.72 (t,  $^3J = 7.8$  Hz, 1 H), 7.32 (d,  $^3J = 7.8$  Hz, 2 H), 5.61 (s, 4 H), 4.83 (s, 4 H).  $\delta$  <sup>13</sup>C NMR (CDCl<sub>3</sub>\*, 125 MHz, 25°C) 157.6, 137.2, 120.7,

78.4. R<sub>f</sub> (SiO<sub>2</sub>, 100:1:15 Et<sub>2</sub>O/Et<sub>3</sub>N/CH<sub>3</sub>OH) = 0.25.

## Macrocycle M1



Bis-reactive dimethylformamidine **2.6** (110 mg, 0.445 mmol, 1.0 eq) was dissolved in 5 mL of dry dichloromethane, as 75 mg of compound **2.5** (0.45 mmol, 1.0 eq) was dissolved in 5 mL of dry dichloromethane. These two solutions were combined into the RBF and another 80 mL of dry dichloromethane were added. Then 42  $\mu$ L (0.53 mmol, 1.2 eq) of trifluoroacetic acid were added and the solution refluxed for 5 days under argon (some white solid came out during the reaction). At room

temperature, the suspension was successively washed with Milli-Q water and 0.1 M sodium hydroxide. The organic layer was concentrated and then the residue was loaded onto a silica gel column. The desired product was eluted with a 100:5 dichloromethane/methanol as mixture, and then recrystallized from hot ethanol to give the

pure macrocycle **M1** (21 mg, 0.064 mmol, 15%).  $\delta$   $^1\text{H}$  (300 MHz;  $\text{CDCl}_3^*$ ; 25 °C): 7.65 (t,  $^3J = 7.8$  Hz, 1 H), 7.58 (t,  $^3J = 7.8$  Hz, 1 H), 7.26 (d,  $^3J = 7.8$  Hz, 2 H), 7.04 (d,  $^3J = 7.8$  Hz, 2 H), 6.70 (d,  $^3J = 11$  Hz, 2 H), 6.04 (br s, 2 H), 5.08 (s, 4 H), 4.32 (d,  $^3J = 5.7$  Hz, 4 H). TLC :  $R_f$  ( $\text{SiO}_2$ , 100:5  $\text{CH}_2\text{Cl}_2/\text{CH}_3\text{OH}$ ) = 0.17. Mp decomposed around 200 °C. Details of the crystal structure are given in the appendix.

## References

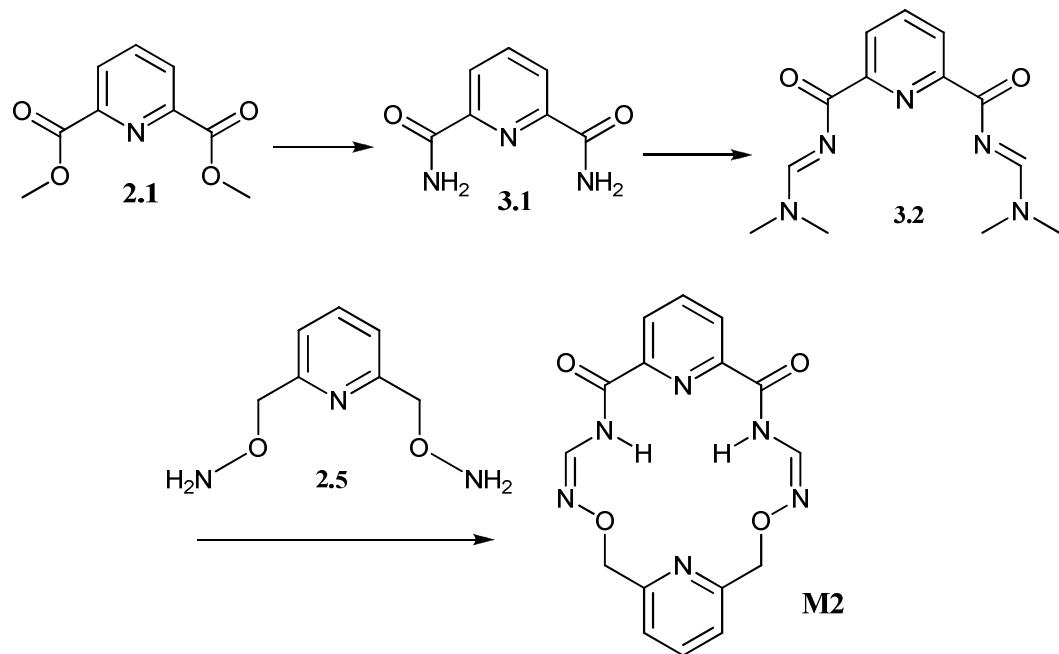
- [1] Chifuku, K.; Sawada, T.; Kuwahara, Y. and Shosenji, H.; *Mol. Cryst. Liq. Cryst.*, **2007**, 470, 369-381.
- [2] Zepik, H. and Benner, S., A.; *J. Org. Chem.* **1999**, 64, 8080-8083.
- [3] Porcheddu, A.; Giacomelli and G.; Piredda, I.; *J. Comb. Chem.* **2009**, 11, 126-130.
- [4] Supramolecular Chemistry, 2nd edition; Steed, J. W. and Atwood, J. L.; **2009**, John Wiley & Sons, Ltd.
- [5] (a) Dietrich-Buchecker, C. D. and Sauvage, J. P.; *Chem. Rev.* **1987**, 87, 795-810. (b) Molecular Catenanes, Rotaxanes and Knots: A Journey Through the World of Molecular Topology; Sauvage, J. -P. and Dietrich-Buchecker, C. D.; **1999**, Wiley-VCH.
- [6] Dietrich-Buchecker, C. D. and Sauvage, J. P.; *Tetrahedron Lett.* **1983**, 24, 5095-5098.
- [7] Arico, F.; Badjic, J. D.; Cantrill, S. J.; Flood, A. H.; Leung, K. C. -F.; Liu, Y. and Stoddart, J. F.; *Top Curr. Chem.* **2005**, 249, 203-259.
- [8] Leigh, D. A.; Wong, J. K. Y.; Dehez, F. and Zerbetto, F.; *Nature* **2003**, 424, 174-179.
- [9] Leigh's research homepage, [www.catenane.net](http://www.catenane.net) (5<sup>th</sup>, July, 2011).
- [10] Chifuku, K.; Sawada, T.; Kuwahara, Y. and Shosenji, H.; *Mol. Cryst. Liq. Cryst.*, **2007**, 470, 369-381.
- [11] Zepik, H. and Benner, S., A.; *J. Org. Chem.* **1999**, 64, 8080-8083.

## Chapter 3

### Macrocyclic M2

#### 3.1 Synthesis of macrocycle M2

Similar to **M1**, target macrocycle **M2** can also be obtained by the condensation of two similar components, namely a formamidine and the alkoxyamine described in chapter 2. The difference resides in the use of pyridine-2,6-diamide **3.1** which can either be purchased or synthesized from diester **2.1**. Diamide **3.1** was then transformed to N,N-dimethylformamidine **3.2** as a precursor to the macrocycle. Compound **3.2** was finally condensed with bis-alkoxyamine **2.5** to give the second generation macrocycle (**M2**).

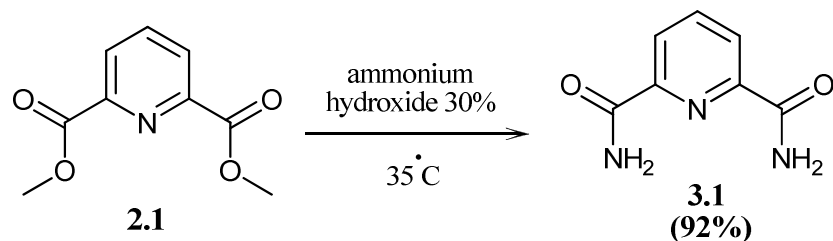


**Scheme 3.1** Synthetic route for macrocycle **M2**.

#### 3.1.1 Synthesis of pyridine-2,6-dicarboxamide (3.1)

The preparation of pyridine-2,6-dicarboxamide followed literature methods.<sup>[1]</sup> The diester

was used as starting material to give the pure diamide in 92% yield.

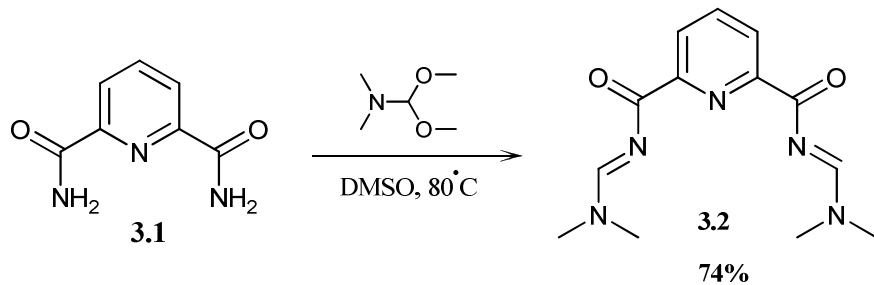


**Scheme 3.2** Synthesis of pyridine-2,6-dicarboxamide.

### 3.1.2 Synthesis of (N<sub>2</sub>E,N<sub>6</sub>E)-N<sub>2</sub>,N<sub>6</sub>-bis((dimethylamino)methylene)-pyridine-2,6-dicarboxamide (**3.2**)

Diamide **3.1** shows a very strong hydrogen-bond network both in the condensed state and in solution.<sup>[2]</sup> This special property limits its solubility in many solvents like chloroform and methanol. The best solvent to dissolve this diamide is DMSO (dimethylsulfoxide). But as DMSO is a solvent that has a very high boiling point and is difficult to remove, the synthesis of N,N-dimethylformamidine **3.2** was first carried out in non-solvent conditions. Diamide **3.1** (1.0 equivalent) was mixed with 3.2 equivalents of N,N-dimethylformamide dimethylacetal (DMF-DMA) and heated at 70 °C for 5 hours. During the reaction, the colour of the solution turned into a deeper and deeper red. At the end, a dark-red oil-like mixture was obtained and was difficult to analyze by <sup>1</sup>H NMR.

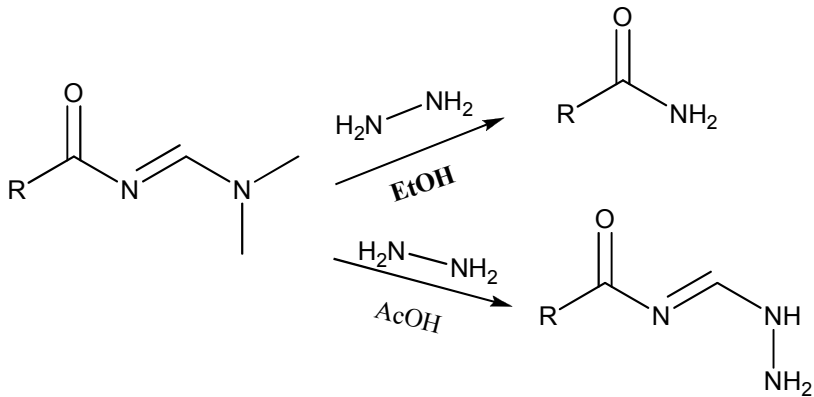
In order to understand what was happening, an NMR scale reaction study was conducted in DMSO-d<sub>6</sub>, and monitored by <sup>1</sup>H NMR spectroscopy. Diamide **3.1** (1.0 equivalent) was mixed with 4.0 equivalents of DMF-DMA in DMSO-d<sub>6</sub> at 80°C (**Scheme 3.3**).



**Scheme 3.3** Synthesis of pyridine-dicarbonylformamidine **3.2**.

<sup>1</sup>H NMR spectroscopy showed that the major product was N,N-dimethylformamidine **3.2**,

mixed with some impurity. Lin et al.<sup>[3]</sup> observed that acylformamides decomposed by reaction with hydrazine in the presence of ethanol (**Scheme 3.4**), but that by switching the solvent from ethanol to acetic acid, formamidinyl exchange occurred and no decomposition was observed. The presence of alcohol will probably accelerate the decomposition of N,N-dimethylformamidine.

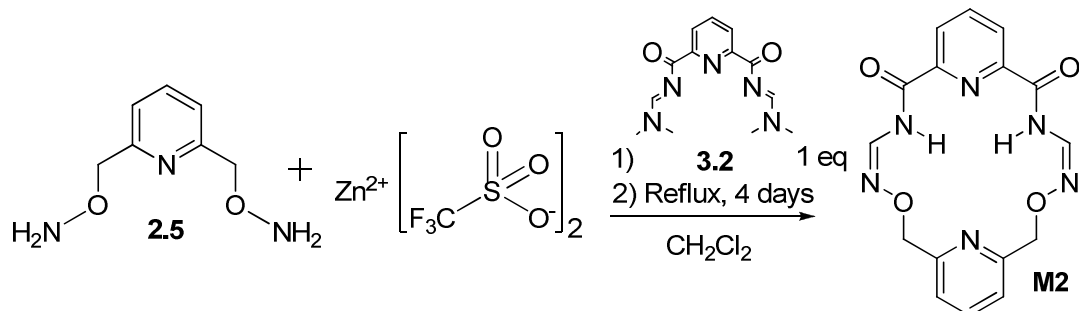


**Scheme 3.4** Acylformamides were decomposed by hydrazine in the presence of ethanol.<sup>[3]</sup>

Therefore, an improved method was introduced to maximize the formation of N,N-dimethylformamidine **3.2**: during the reaction, the formed methanol was distilled out and collected. In these experimental conditions, only a trace amount of impurity was observed in the crude by <sup>1</sup>H NMR spectroscopy. Interestingly, the precursor diamide **3.1** was only soluble in dimethyl sulfoxide. However the formed N,N-dimethyl-formamidine **3.2** product was not soluble in DMSO at room temperature. As a consequence, compound **3.2** precipitated out from the solution when the reaction was cooled down, facilitating its isolation. N,N-dimethylformamidine **3.2** is very reactive and will decompose when exposed to methanol and water. However, it is stable in chloroform, tetrahydrofuran and acetonitrile.

### 3.1.3 Synthesis of Macrocycle M2

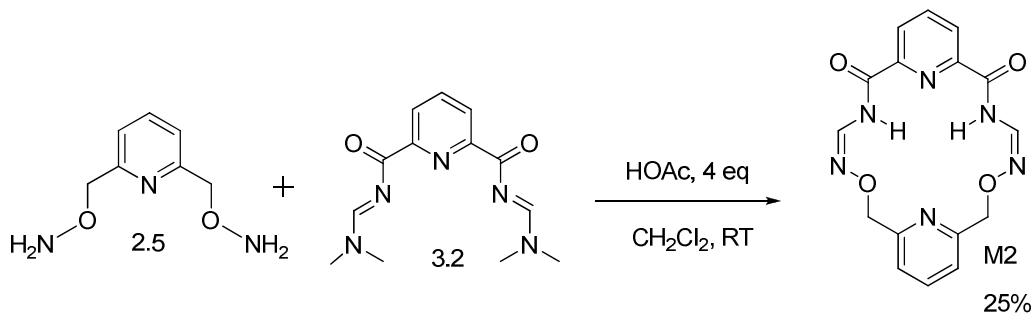
#### Method A: in the presence of a Lewis Acid catalyst



**Scheme 3.5** Macrocyclization to form **M2** in the presence of a Lewis Acid catalyst.

Alkoxyamine **2.5** (1.0 equivalent) was mixed with 1.1 equivalent of  $Zn(OTf)_2$  (zinc triflate) in acetonitrile/dichloromethane. Then 1.0 equivalent of **N,N**-dimethylformamidine **3.2** was added and the reaction was refluxed at 60 °C for 4 days. The crude was finally purified by preparative TLC to give pure macrocycle **M2**. Zinc triflate plays two roles here: first, as a Lewis Acid to promote formamidinyl exchange reactions; second, the  $Zn^{2+}$  cation would hopefully serve as a template for the macrocyclization. In the work-up, an unknown white pasty compound suspended in mixed acetonitrile/dichloromethane tended to form a yellow-coloured gel after evaporating all the solvent.

#### Method B: in the presence of Brønsted acids as catalysts



**Scheme 3.6** Macrocyclization to form **M2** in the presence of a Brønsted acid.

Alkoxyamine **2.5** (1.0 equivalent) and 1.0 equivalent of N,N-dimethylformamidine **3.2** were mixed in anhydrous dichloromethane in the presence of 4.0 equivalents of acetic acid. The reaction was carried out at room temperature for 3 days and the crude was finally purified by preparative TLC to give pure **M2** (26%). In method B, temperature was considered to affect the yield of macrocyclization. At the reflux temperature of dichloromethane (55 °C), a white precipitate came out from the solution after 10 minutes. When the reaction was finished, a white emulsion formed which made purification complicated. However, when the reaction was carried out at room temperature, neither precipitate nor emulsion formed.

## 3.2 Results and Discussion

### 3.2.1 Characterization of macrocycle **M2**

The second generation of macrocycle **M2** based on the alkoxyformamidine unit has been characterized by  $^1\text{H}$  NMR spectroscopy, mass spectrometry and single crystal X-ray diffraction.

#### 3.2.1.1 $^1\text{H}$ NMR of macrocycle **M2**

From the  $^1\text{H}$  NMR spectrum of **M2**, the anticipated high  $^3\text{J}$  coupling constant for the formamidine H<sub>F</sub> proton (chemical shift at 7.86 ppm,  $^3\text{J} = 10.0$  Hz) was seen as a sign of the formation of alkoxyamine-formamidine subunit (highlighted structure in **Figure 3.1**). The high coupling constant provides structural information: in solution, the formamidine proton points in opposite direction compared to the NH proton. In this typical alkoxyamine-formamidine subunit, the NH proton is not only locked by the oxygen but also by the pyridine nitrogen through hydrogen-bonding. Moreover, it is an amide type of NH, so the high chemical shift was rationalized to match this slightly acidic proton. The aliphatic CH<sub>2</sub> groups adjacent to the oxygen have a higher chemical shift around 5.08 ppm. Since the chemical environments of the two pyridines are not the same, their aromatic protons show two sets of doublet and triplet at different chemical shifts (for the pyridine coming from the amide, the chemical shifts of triplet and doublet are 8.11 and

8.48 ppm respectively; for the pyridine coming from the alkoxyamine, the chemical shifts of the triplet and doublet 7.75 and 7.31 ppm respectively. All the protons are assisted assigned by HMBC, see appendix A).

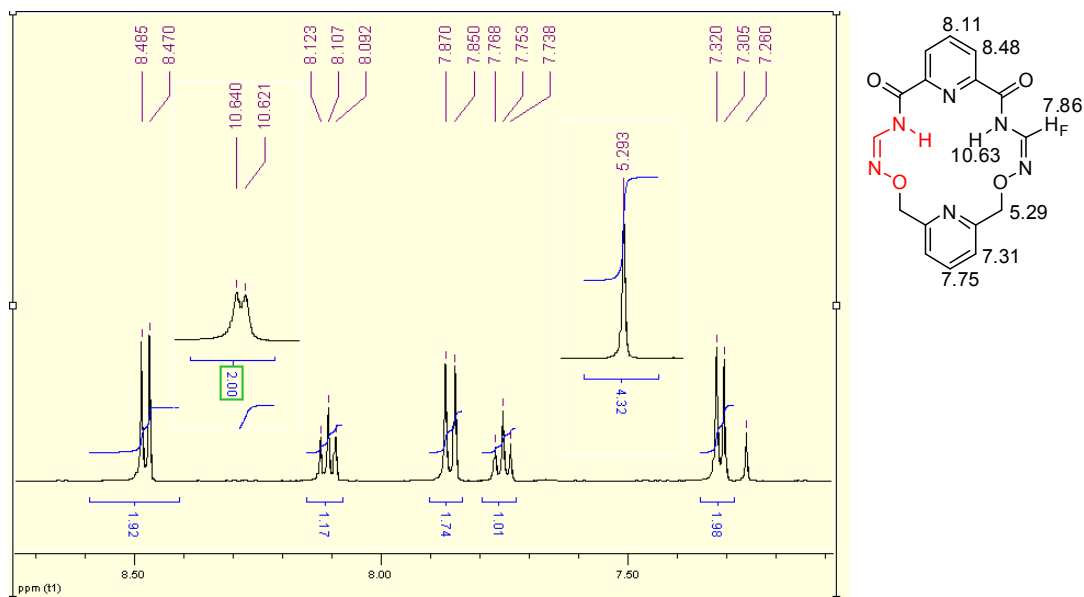
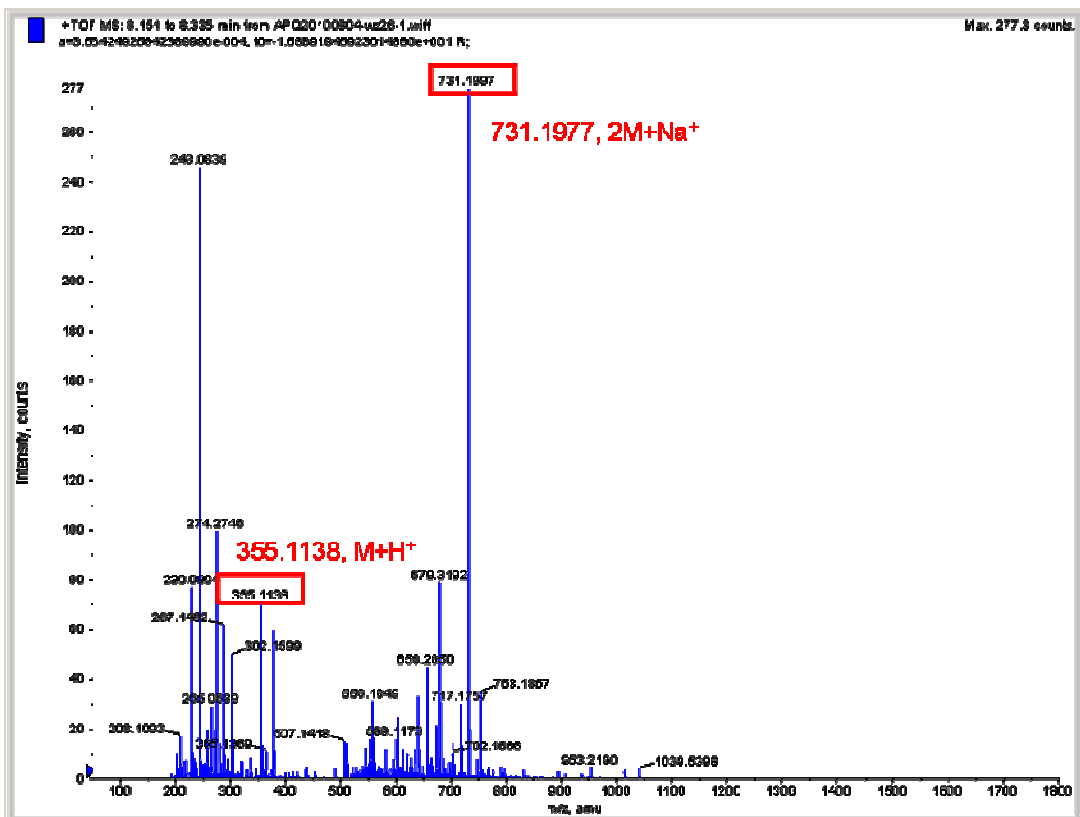
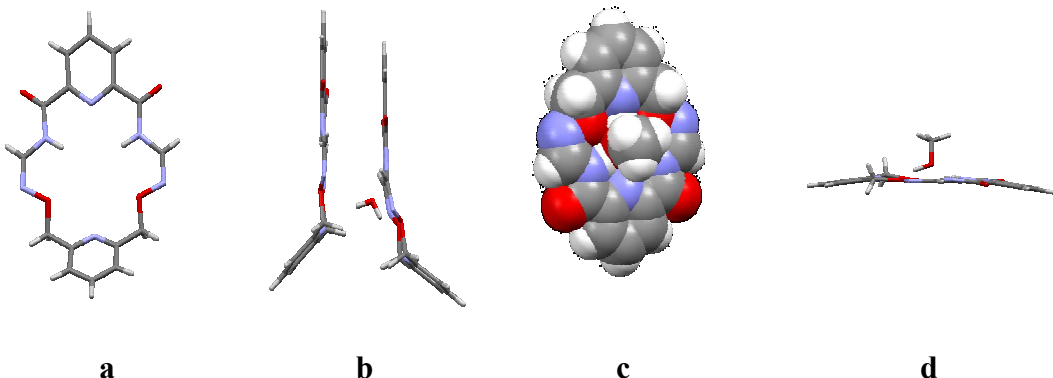


Figure 3.1  $^1\text{H}$  NMR spectrum of macrocycle M2 in  $\text{CDCl}_3$  (500 MHz, 25 °C).

### 3.2.1.2 Mass spectrometry study of macrocycle M2

The mass spectrum of macrocycle **M2** (**Figure 3.2**) clearly shows the  $M+H^+$  peak at m/z 355.1138. More interestingly, the intense peak at 731.1997 gives a hint that in the presence of sodium cations, macrocycle **M2** is prone to form dimers. Possibly, the stability of dimers for **M2** is higher than that for **M1** (in the case of **M1**, the  $2M+Na^+$  peak is much less intense than  $M+H^+$  peak, for details, see **2.2.1.2**).





**Figure 3.3** Crystal structure of macrocycle **M2** for two different crystals; **a-b**: crystal grown by slow diffusion of Et<sub>2</sub>O to a solution of CH<sub>2</sub>Cl<sub>2</sub>, CH<sub>3</sub>CN and dimethylammonium triflate ; **c-d**: crystal grown from NaOH /MeOH. **a)** side view highlighting the anticipated intramolecular H-bond and the Z formamide motif; **b)** view of the solid-state dimer maintained by intermolecular N<sub>py</sub>-H<sub>H2O</sub> H-bonds; **c)** CPK view of the **M2**-MeOH adduct; **d)** side view of the **M2**-MeOH adduct.

A crystal of **M2** was also grown by slow evaporation of a solution in methanol in the presence of sodium hydroxide. The crystal structure shows that a methanol molecule is bound inside the cavity of **M2** (CPK view and crystal structure in **Figure 3.3c,d**) and is held by three interaction points: the OH hydrogen is hydrogen-bonded to the basic pyridine nitrogen, while the methanol oxygen is involved in two hydrogen bonds with the formamide NH groups, probably through the involvement of both its lone pairs. The size of the methanol OH group perfectly matches the cavity of **M2**, just as a key to a lock. It is also worth noticing that, compared to the crystal structure grown in the absence of methanol (see above), the methanol adduct is much more planar (the binding of methanol aligns the flexible pyridine fragment in the plane with the conjugated fragment constituting the rest of the molecule). This crystal structure gives a hint that the binding of methanol in solution could enable macrocycle **M2** to become more planar and moreover, lead to molecular recognition of alcohol molecules.

### 3.2.2 Incredibly large macrocycle: “Maxi-M2”

In the reaction leading to macrocycle M2, one interesting compound was isolated by preparative TLC (~8% yield) and showed very similar  $^1\text{H}$  NMR signals to M2 (all the NH, HF, pyridine protons and CH<sub>2</sub> are shown in **Figure 3.4**). This suggests a molecule bearing exactly the same subunits and symmetry as M2. However, mass spectrometry indicates (Electrospray Ionization, see appendix A) a peak at m/z 1063 suggesting that a molecule three times as large as M2 had been generated (“trimer” of M2).

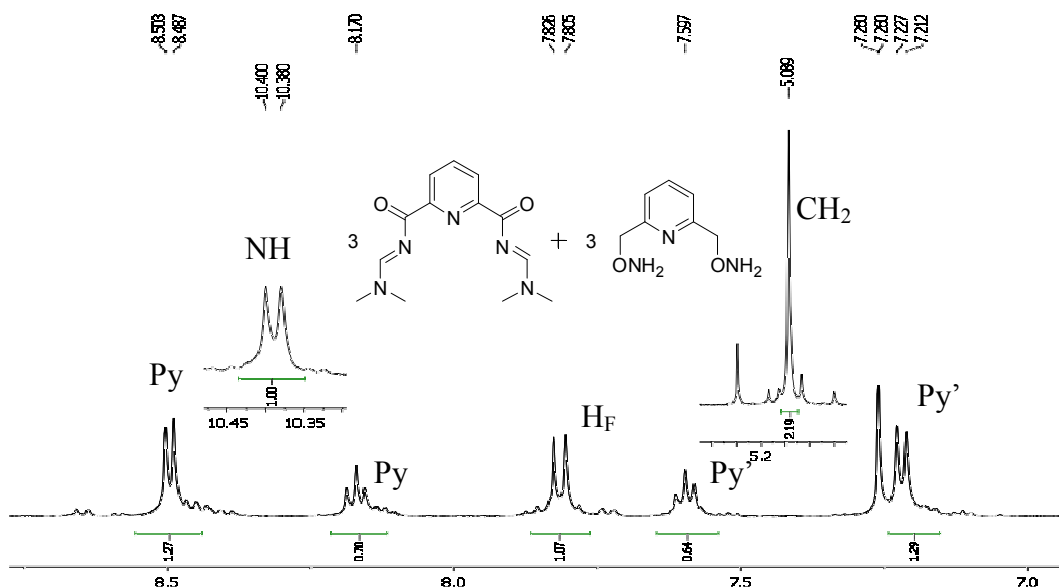


**Figure 3.4**  $^1\text{H}$  NMR spectrum of “Maxi-M2” in  $\text{CDCl}_3$  (500 MHz, 25 °C).

As seen in chapter 2, dimers or trimers may correspond to two different topological isomers individually: macrocycle or catanane, and macrocycle or molecule knot. Catenanes and knots are both interlocked molecules and the properties of catenanes have been briefly discussed in chapter 2. Molecular knots are less well-known compounds and only a few types of knots have been synthesized, based on phenanthrolines by Dietrich-Buchecker and Sauvage,<sup>[4]</sup> on nucleic-acid type by Seeman,<sup>[5]</sup> crown/quat (a complex formed by an  $\pi$ -electron rich 1,5-di-oxyphenanthroline-based polyether and an acyclic  $\pi$ -electron deficient bipyridinium-based tetracation) type by Stoddart<sup>[6]</sup> and 2,6-pyridinedicarboxamide type by Vogtle.<sup>[7]</sup> Vogtle’s trefoil molecular knot (**Figure 3.5a**) is probably the most intriguing one since it was the first example of a molecular knot

synthesized without the help of transition metals. Moreover, this molecular knot was obtained in a one-step synthesis to give a reasonable yield (20%) and the formation of the knot was controlled by hydrogen-bond driven self-organization. The molecular knots in a trefoil configuration are chiral and exist as different enantiomers (**Figure 3.5b**).

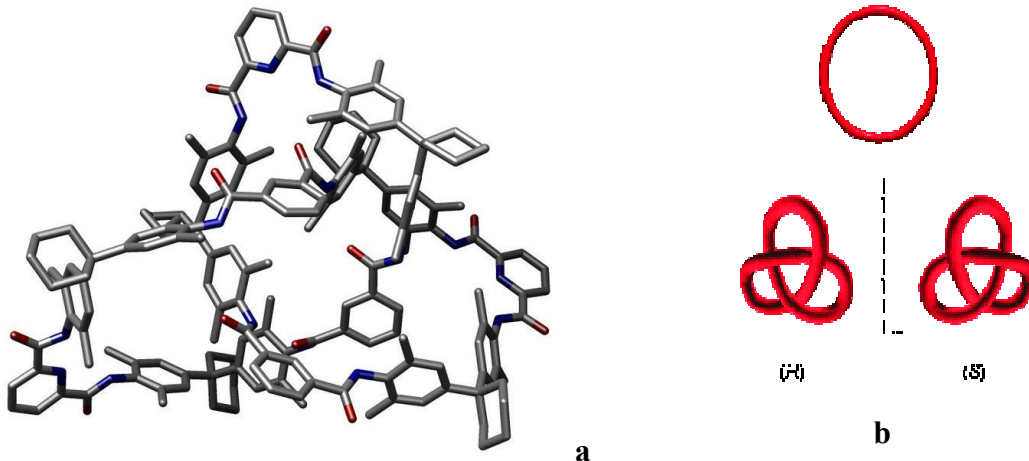


**Figure 3.5** **a)** Trefoil molecular knot obtained by Vogtle<sup>[7]</sup>; **b)** knot enantiomers.

X-ray crystallography is the best way to distinguish topological isomers and, fortunately, this large “trimer of **M2**” crystallized by slow evaporation from a dichloromethane solution.

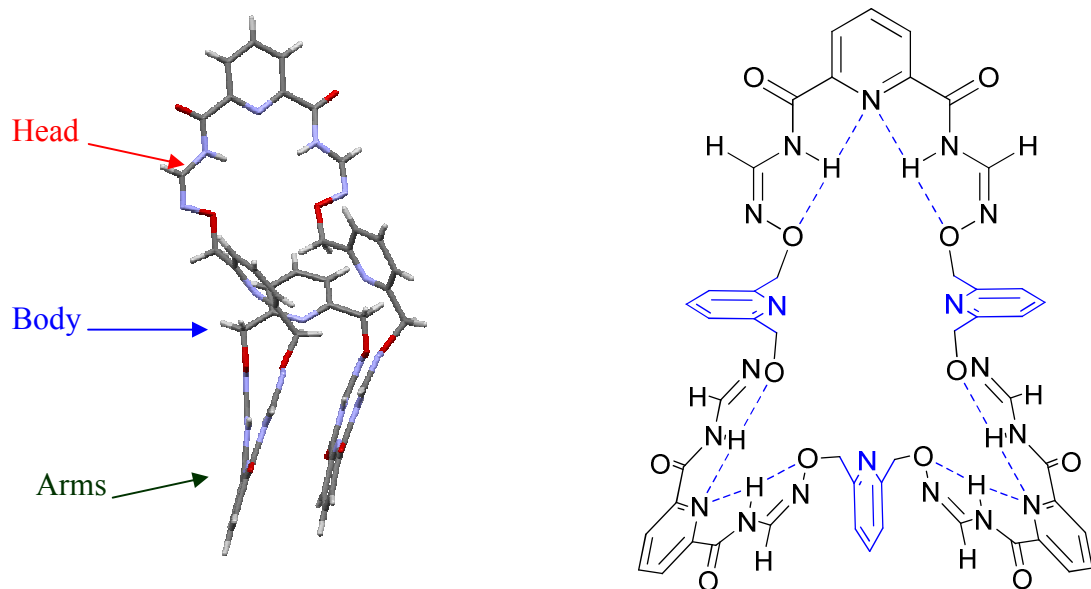


**Figure 3.6** Crystal structure of “Maxi-M2” and molecule structure.

It turned out to be a surprisingly large macrocycle rather than a mechanical knot, hence the name “**Maxi-M2**” (**Figure 3.6**). As anticipated from the mass spectrometry results, **Maxi-M2** is three times as large as **M2** and has the same repeating units (Py-Acyl-Formamidoxime-Methylene-Py). It consists of three curved segments, two of them being stacked together (coined “arms” in the section below), and the third one, named “head” below, pointing in a nearly perpendicular direction. Three flexible methylene pyridines can be seen as a body to bridge the head and arms.

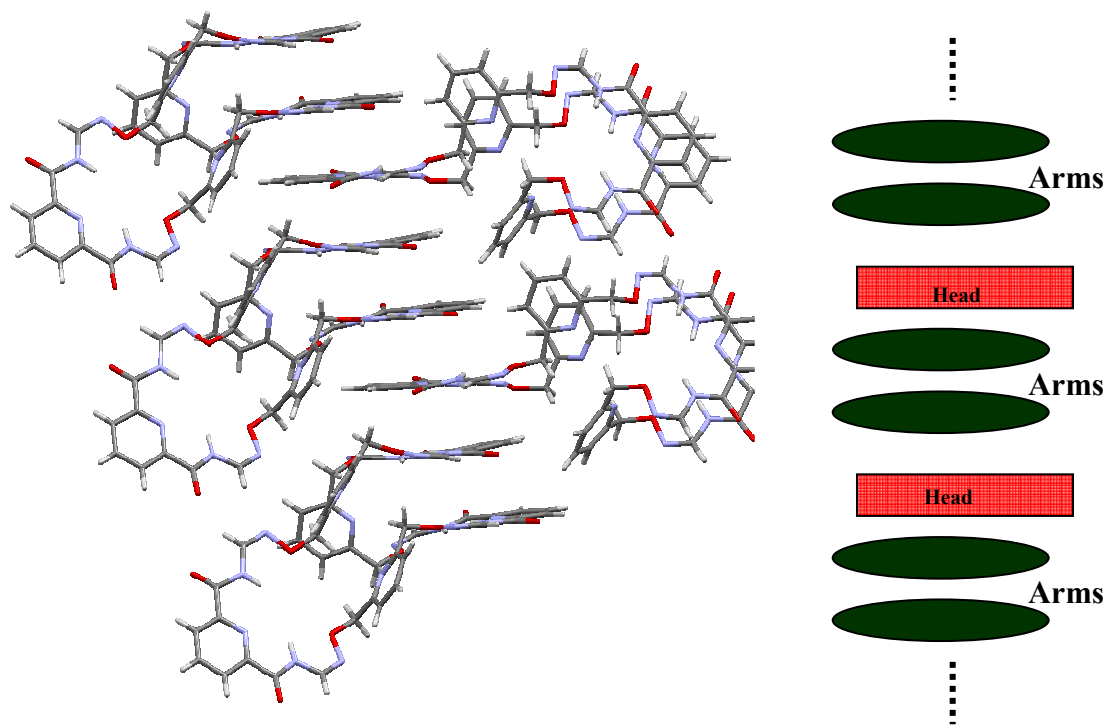


**Figure 3.7** Stacking of “**Maxi-M2**”- The arms stack against the head alternatively.

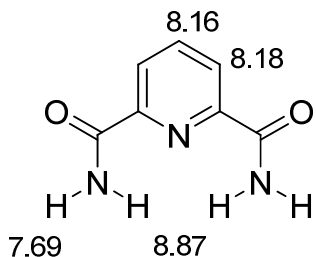
The packing results in the arms being stacked against the heads alternatively, creating a tubular assembly in one direction (**Figure 3.7 right**). Interestingly, the arms attached to the head within a 1 D tubule (*e. g.* in the plane of the page, **Figure 3.7 left**) also self-assemble in a perpendicular direction (*e. g.* through the page, **Figure 3.7 left**), leading to a cross-linked network of tubular assemblies.

### 3.3 Conclusion of Chapter 3

As described in this chapter, the second generation of macrocycle **M2** with alkoxyamine-formamidine subunit has been successfully synthesized and fully characterized by  $^1\text{H}$  NMR spectroscopy, mass spectrometry and Single crystal X-ray crystallography. The crystal structure of the **M2**-MeOH adduct indicates that molecular recognition may be achieved by such receptor. In addition, the unexpected formation of “Maxi-**M2**” and its solid-state self-assembly gave interesting structural information.

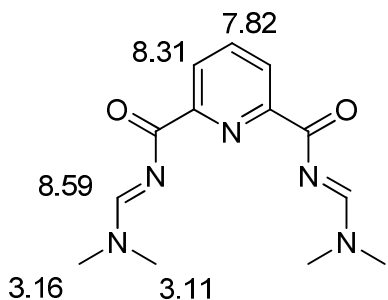
### 3.4 Experiment details

#### 2,6-Pyridine dicarboxamide (3.1)



The synthetic method is slightly modified from literature protocols.<sup>[8]</sup> Pyridine-2,6-dimethylester (4.98 g, 25.5 mmol) was suspended in 20 mL of ammonium hydroxide (28%-30% aqueous solution). The reaction was warmed up to 35 °C and stirred rigorously for 4 hours. After cooling in an ice-water bath, the suspension was filtered and the precipitate washed with water, dried in air overnight and under vacuum ( $\text{P}_2\text{O}_5$ ) to give the crude 2,6-pyridinedicarboxamide (4.2 g, 92 %) as a white solid. The crude is soluble in DMSO but neither in chloroform nor methanol.  $\delta$   $^1\text{H}$  (300 MHz;  $\text{DMSO-d}_6$ ; 25 °C): 8.87 (br s, 2 H), 8.18 (d,  $^3J$  = 5.4 Hz, 2 H), 8.16 (t,  $^3J$  = 5.4 Hz, 1 H), 7.69 (br s, 2 H).

#### (N2E,N6E)-N2,N6-bis((dimethylamino)methylene)pyridine-2,6-dicarboxamide (3.2)



Pyridine-2,6-dicarboxamide (11 mmol, 1.0 eq) was mixed with N,N-dimethylformamide dimethylacetal (DMF-DMA, 35 mmol, 3.2 eq) in dimethyl sulfoxide (20 mL). The reaction was heated at 85°C for 3.5 hours while the methanol by-product was distilled off. After

cooling to room temperature, the formed white solid precipitate was filtered and washed with diethyl ether to remove residual dimethyl sulfoxide. The resulting N,N-dimethylformamidine product (74 %) was then used without further purification.  $\delta$   $^1\text{H}$  NMR ( $\text{CDCl}_3^*$ , 500 MHz, 25°C) 8.59 (s, 2 H), 8.31 (d,  $^3J = 7.5$  Hz, 2 H), 7.82 (t,  $^3J = 7.5$  Hz, 1 H), 3.16 (br s, 6 H), 3.11 (br s, 6 H).  $\delta$   $^{13}\text{C}$  NMR ( $\text{CDCl}_3^*$ , 125 MHz, 25 °C) 176.0, 161.3, 153.5, 137.0, 126.5, 41.3, 35.4. EI $^+$ -HRMS: calc. for  $\text{C}_{13}\text{H}_{17}\text{N}_5\text{O}_2$ : 275.1382; found: 275.1382 [M] $^+$ , 232.0981 [M-Me<sub>2</sub>N-H] $^+$ , 220.0929 [M-Me<sub>2</sub>N-H-C] $^+$ , 205.0839 [M-Me<sub>2</sub>N-H-C-NH] $^+$ . EA calc. for  $\text{C}_{13}\text{H}_{17}\text{N}_5\text{O}_2$ : %C 56.71, %H 6.22, %N 25.44; found %C 56.38, %H 6.20, %N 25.22. Mp decomposed around 204 °C.

## Macrocycle M2 and Maxi-M2

### Method A, in the presence of Lewis Acid as catalyst:

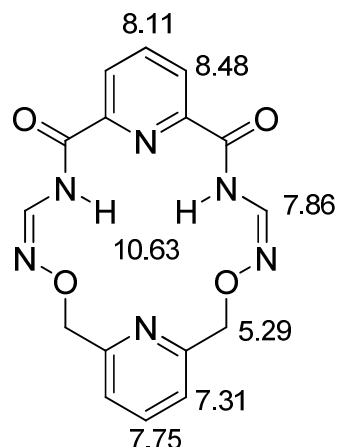
Bis-reactive Alkoxyamine **2.5** (154 mg, 0.91 mmol, 1.0 eq) and zinc(II) triflate (364 mg, 1.0 mmol, 1.1 eq) was dissolved in a mixture of anhydrous acetonitrile (7 mL) and anhydrous dichloromethane (5 mL). Compound **3.2** (250 mg, 0.91 mmol, 1.0 eq) was then added and the reaction mixture was refluxed (60°C) for 4 days (some solid formed after 2 days). The suspension was washed with 10 mL of water (pH 5), and the aqueous layer extracted with dichloromethane 7 times. Attempts to purify the crude by column chromatography (silica gel) with 5:100 methanol/dichloromethane as an eluent failed

(giving mixed fractions).

The mixture was purified by preparative TLC with 5:100 MeOH/CH<sub>2</sub>Cl<sub>2</sub> as an eluent to give 11 mg of pure **M2**.  $\delta$   $^1\text{H}$  NMR ( $\text{CDCl}_3^*$ , 500 MHz, 25°C) 10.63 (d,  $^3J = 10$  Hz, 2 H), 8.48 (d,  $^3J = 7.5$  Hz, 2 H), 8.11 (t,  $^3J = 7.5$  Hz, 1 H), 7.86 (d,  $^3J = 10$  Hz, 2 H), 7.75 (t,  $^3J = 7.5$  Hz, 1 H), 7.31 (d,  $^3J = 7.5$  Hz, 2 H), 5.29 (s, 4 H). Details of crystal structures are given in appendix. Mp decomposed around 200 °C.

### Method B, in the presence of Brønsted acids as catalysts:

Bis-reactive Alkoxyamine **2.5** (18.4 mg, 0.108 mmol, 1.0 eq) and Compound **3.2** (29.9 mg, 0.108 mmol, 1.0 eq) were mixed in 2 mL of anhydrous dichloromethane in the



presence of acetic acid ( $24.7 \mu \text{L}$ ,  $0.43 \text{ mmol}$ ,  $4.0 \text{ eq}$ ). The reaction was carried out at room temperature for 3 days and then the crude solution was washed with  $2 \text{ mL}$  of saturated aqueous potassium bicarbonate. The aqueous layer was extracted with dichloromethane and the combined organic layers were dried over sodium sulphate, concentrated in vacuo and purified by preparative TLC with  $2:100$  methanol/ dichloromethane as an eluent to give  $10 \text{ mg}$  of pure **M2** ( $26\%$ ) and  $3 \text{ mg}$  of **Maxi-M2** as a more polar fraction (mixed with minor impurities,  $8\%$  yield).

## References

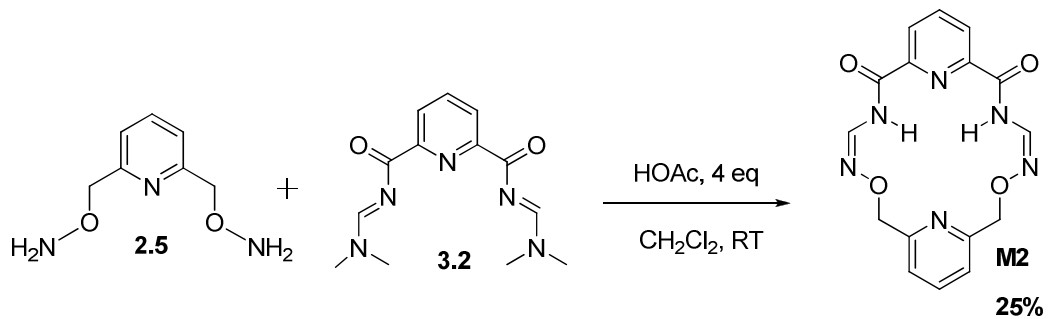
- [1] Tondreau, A. M.; Darmon, J. M.; Wile, B. M.; Floyd, S., K.; Lobkovsky, E. and Chirik, P. J.; *Organometallics* **2009**, *28*, 3928-3940.
- [2] Marlin, D. S.; Olmstead, M. M and Mascharak, P. K; *J. Mol. Struc.* **2000**, *554*, 211-223.
- [3] Lin, Y.; Lang, S. A.; Jr. Lovell, M. F. and Perkinson, N. A.; *J. Org. Chem.* **1979**, *44*, 4160-4164.
- [4] Dietrich-Buchecker, C. D. and Sauvage, J.-P; *Angew. Chem, Int. Ed. Engl.* **1989**, *28*, 189-201.
- [5] Seeman, N. C.; *Acc. Chem. Res.*, **1997**, *30*, 357-363.
- [6] Ashton, P. R.; Matthews, O. A.; Menzer, S.; Raymo, F. M.; Spencer, N. and Stoddart F. M.; *Liebigs Ann.* **1997**, 2485-2494.
- [7] Safarowsky, O.; Nieger, M.; Frohlich, R. and Vogtle, F.; *Angew. Chem, Int. Ed. Engl.* **2000**, *39*, 1616-1618.
- [8] Tondreau, A. M.; Darmon, J. M.; Wile, B. M.; Floyd, S., K.; Lobkovsky, E. and Chirik, P. J.; *Organometallics*, **2009**, *28*, 3928-3940.

## Chapter 4

### Configurational control in alkoxyamine-derived formamidines

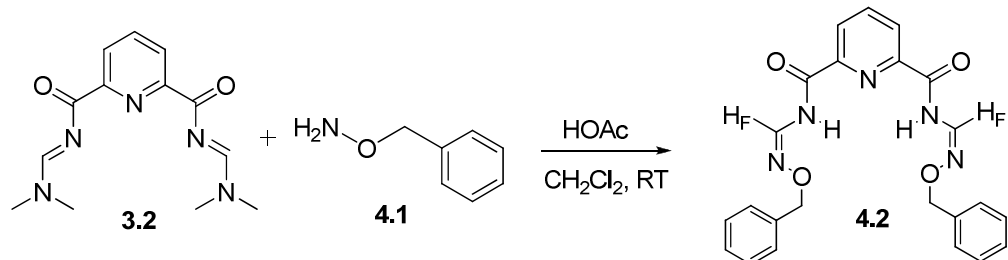
#### 4.1 Reflections on the macrocyclization to M2

As seen in chapter 3, the reaction to give macrocycle **M2** (**Scheme 4.1**) did not result in a very high yield (25%). At the same time, in the course of reaction, many by-products formed as observed by both  $^1\text{H}$  NMR spectroscopy and TLC. In an attempt to improve the yield of macrocyclization, a systematic study of the condensation reaction (alkoxyamines reacting with acyl-dimethylformamidine) was carried out and is described in this chapter.



**Scheme 4.1** Macrocyclization to form **M2** in the presence of acetic acid.

For the reaction shown in **Scheme 4.1**, the bis-reactive alkoxyamine was condensed with the bis-reactive acyl-dimethylformamidine. Since each reactant has two reactive sides, polymerization competes with macrocyclization. In the course of the reaction, polymer-like by-products formed and precipitated out from the dichloromethane solution.



**Scheme 4.2** Simplified reaction used to optimize reaction conditions.

In order to identify and fully understand the formation of by-products, a simplified condensation reaction was studied, so that optimized condensation conditions may be found to avoid polymerization (**Scheme 4.2**).

## 4.2 First evidence of the existence of the E isomer

### 4.2.1 ZE isomer

Based on previous study in our group and on crystal structures from the Cambridge Crystallographic Database, compound **4.2** with two Z (cis) C=N double bonds was anticipated to form in the condensation reaction. It is a symmetrical molecule and, therefore, its  $^1\text{H}$  NMR spectrum should display only one set of NH, H<sub>F</sub> and CH<sub>2</sub> protons. However, in one of the products isolated from the reaction crude by column (silica) chromatography, two sets of NH, H<sub>F</sub> and CH<sub>2</sub>  $^1\text{H}$  NMR signals were observed within the same molecule, with a 1 to 1 ratio (**Figure 4.1**).

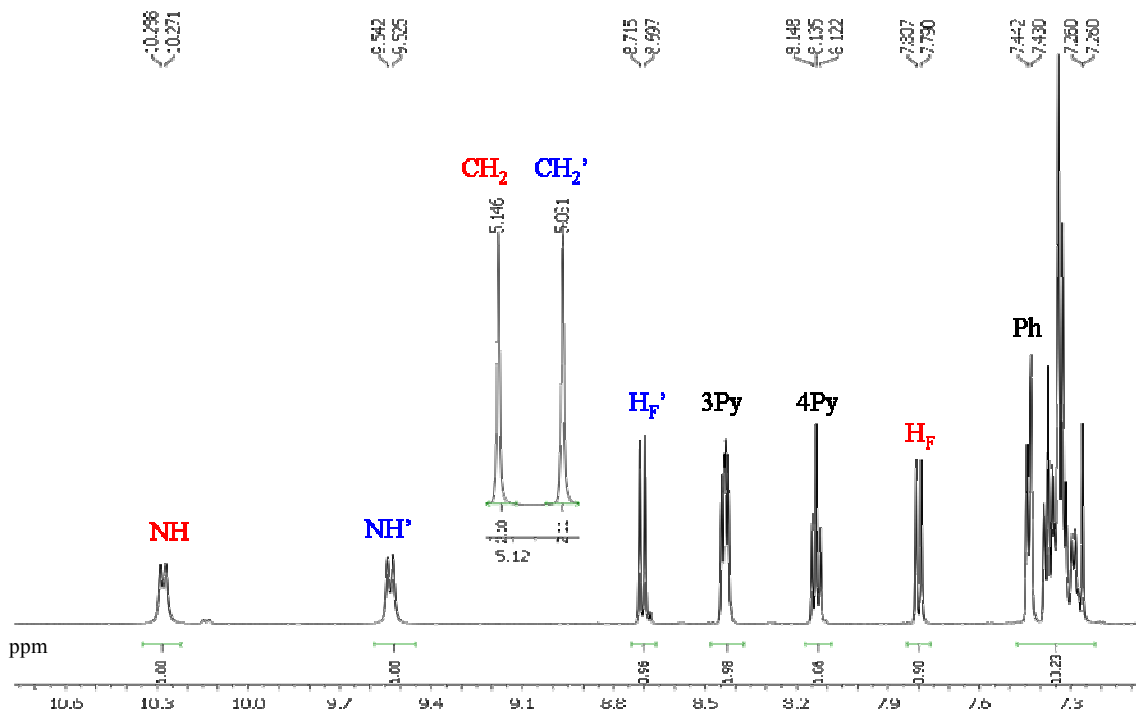


**Figure 4.1**  $^1\text{H}$  NMR spectrum of the suspected ZE isomer **ZE4.2**  
(500 MHz,  $\text{CDCl}_3$ , 25 °C)

This observation suggested that two types of alkoxy-formamidine subunits coexisted within the same molecule. As seen in chapter 1, different kinds of formamidine isomers may exist. We suspected that the ZE configurational isomer formed. In order to test our hypothesis, a 2D NOESY experiment was conducted. As shown in **Figure 4.2a,b**, the suspected  $\text{CH}_{2\text{Z}}$  has a weak correlation with both  $\text{NH}_\text{Z}$  and  $\text{H}_{\text{FZ}}$  which suggested both  $\text{NH}_\text{Z}$  and  $\text{H}_{\text{FZ}}$  are fairly distant from  $\text{CH}_{2\text{Z}}$ . However, the suspected  $\text{CH}_{2\text{E}}$  has a relatively strong correlation with  $\text{H}_{\text{FE}}$  but not with  $\text{NH}_\text{E}$  which gives a hint that the  $\text{CH}_{2\text{E}}$  stays much closer to  $\text{H}_{\text{FE}}$  than to  $\text{NH}_\text{E}$ . In addition to the 2D data, the 1D  $^1\text{H}$  NMR spectrum is also consistent with a ZE isomer. Indeed, in the Z form of the formamidoxime subunit, the NH proton is deshielded ( $\sim 10.3$  ppm) due to the formation of a 5-membered hydrogen-bonded ring (**Figure 4.2b**).

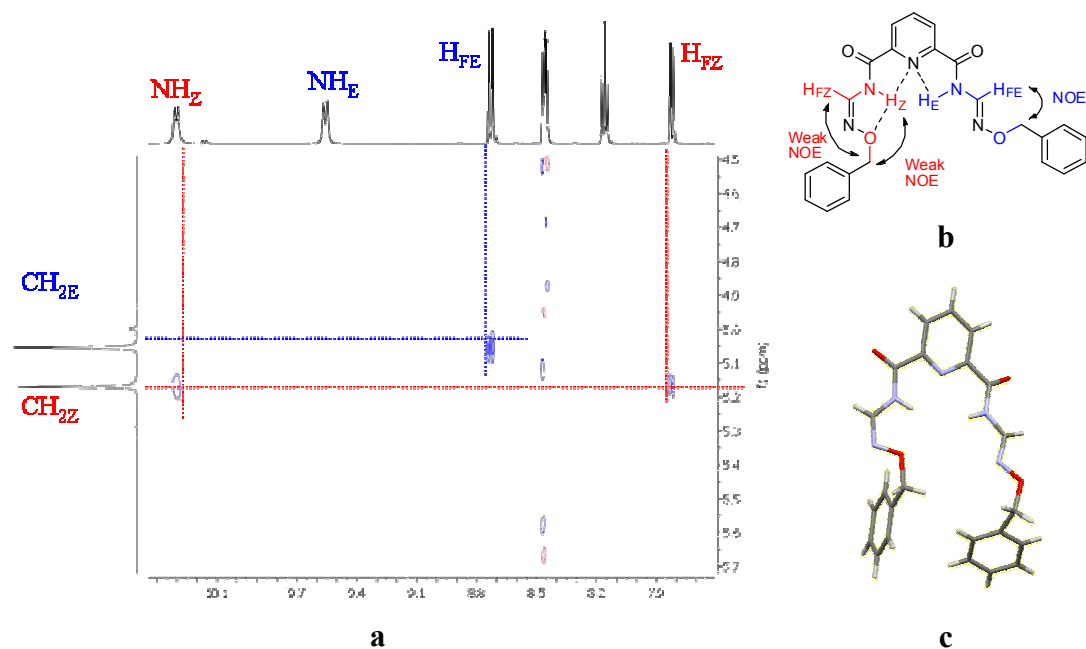


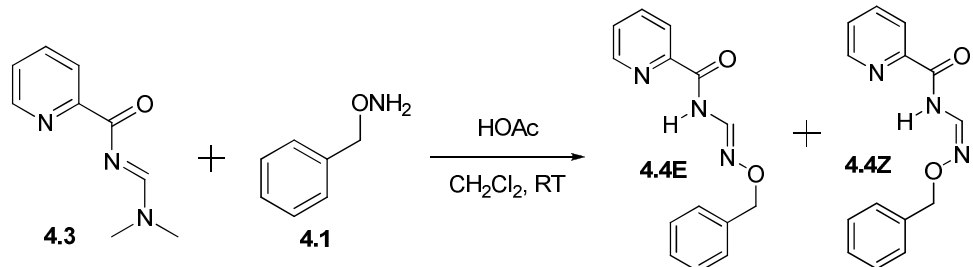
**Figure 4.2** a) NOESY spectrum of **4.2** (500 MHz,  $\text{CDCl}_3$ , 25 °C); b) molecular structure; c) molecular view of the crystal structure of the **ZE4.2**

This pattern is also observed in what is suspected to be the Z portion of 4.2. However, a distinctly different pattern is displayed by what is suspected to be an E formamidine unit: the NH proton (blue NH' around 9.5 ppm in Figure 4.1) is not involved in an intramolecular H-bond anymore and appears at lower chemical shifts, while HFE (blue

HF' around 8.7 ppm in Figure 4.1) is in a more electron-rich environment than HFZ (red HF around 7.7 ppm), and therefore appears at lower field. In consequence, based on 1D and 2D  $^1\text{H}$  NMR experiments, the existence of ZE isomer in solution was confirmed. Moreover, product 4.2 was crystallized and the ZE isomeric pattern was also clearly shown in the solid state structure (Figure 4.2c).

#### 4.2.2 E/Z isomeric mixtures and isomerization

It is important to note that the E isomer of formamidoxime has never been reported before. Since the E form of the formamidoxime subunit was observed within the ZE isomer of compound 4.2, we thought it was important to understand the conditions for the formation of such an unusual and stable E isomer. As a result, an even simplified system was studied, with only one reactive formamidine unit. As shown in **Scheme 4.3**, mono-reactive pyridine-acyl-formamidine 4.3 was reacted with mono-reactive O-benzylhydroxylamine 4.1 in the presence of acetic acid to give E and Z isomeric mixtures (4.4E and 4.4Z).



**Scheme 4.3** Mono-reactive formamidine and alkoxyamine condensed to give E and Z isomeric mixtures.

To this mixture was then added TFA and, surprisingly, the E isomer disappeared. As shown in **Figure 4.3**, both the  $^1\text{H}$  NMR signals of E and Z isomers were observed in the first (bottom) spectrum, before TFA addition. After addition of TFA, the signals of the E isomer disappeared and the Z isomer remained while no new peak formed. This indicates that protons facilitate the isomerization of the E to Z isomers.

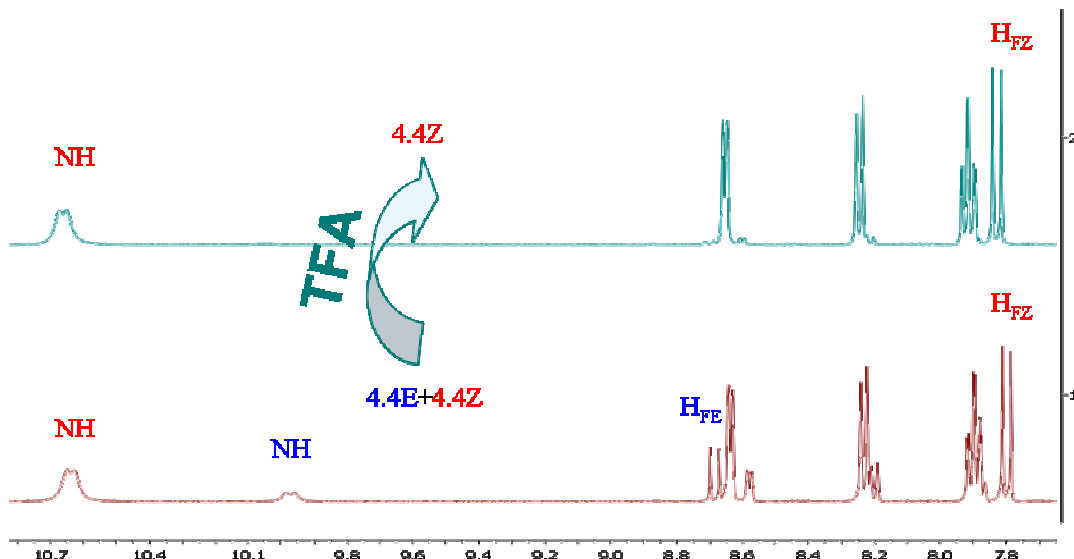
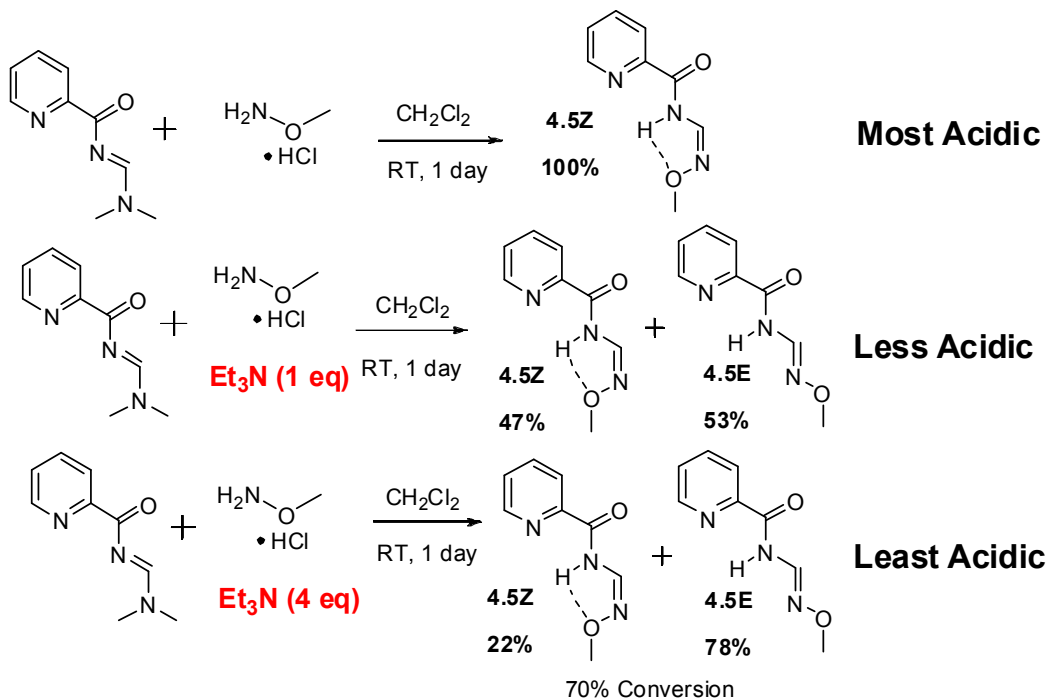


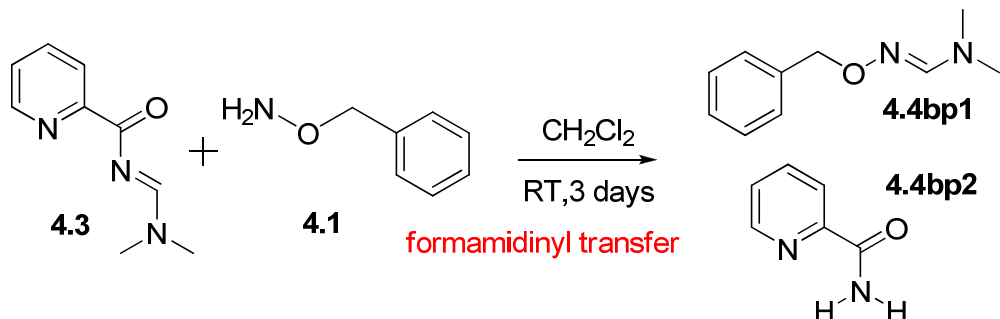
**Figure 4.3** E to Z isomerization promoted by TFA ( $^1\text{H}$  NMR,  $\text{CDCl}_3$ , 25 °C).

#### 4.2.3 Relationship between yield of E/Z isomers and acidity of reaction mixture

Since the isomerization is promoted by protons, a series of reactions were conducted under different acidic conditions (**Scheme 4.4**). In the most acidic conditions, the pyridine-acyl-formamidine was reacted with methoxylamine in the presence of 1.0 equivalent of HCl to give the exclusive Z isomer product. In less acidic case, the same reactants except that 1.0 equivalent of HCl was neutralized by 1.0 equivalent of  $\text{Et}_3\text{N}$  gave 47% of the Z isomer and 53% of the E isomer. In the least acidic condition, 1.0 equivalent of HCl was mixed with 4.0 equivalents of  $\text{Et}_3\text{N}$  to give 22% of the Z isomer and 78% of the E isomer, with 70% conversion. These observations suggested that the more available protons in the reaction, the more Z isomer could be generated. However, when there is no proton added to the condensation reaction, formamidinyl transfer took place to predominantly give by-products **4.4bp1**, **4.4bp2**, and trace amounts of the E and Z formamidoxime isomers (**Scheme 4.5**).



**Scheme 4.4** condensation reaction carried out under various acidic conditions.



**Scheme 4.5** Condensation reaction carried out in the absence of protons.

#### 4.2.4 Isolation condition for E mono-pyridyl-acyl-formamidoximes

The condensation reactions (alkoxyamines reacting with pyridyl-acyl-dimethyl-formamidines) always lead to E/Z isomeric mixtures. Therefore, it is important to find conditions to isolate these two configurational isomers. The E and Z isomers show different  $R_f$  value on silica-coated TLC (see details in Chapter 5) but have no resolution on alumina-coated TLC. Unfortunately, the silica surface is acidic and promotes the E/Z

isomerization, thus consumes the E isomer. Therefore, preparative HPLC was used and successfully allowed to separate the two isomers. E/Z isomeric mixtures of N-((methoxyimino)methyl)-picolinamide (**4.5Z** and **4.5E**) were separated by CHIRALPAK IC HPLC column (5 cm ID × 50 cmL, 20  $\mu$ ) with 15:100 ethyl acetate/dichloromethane as the eluent.

#### 4.2.5 X-ray crystallographic analysis of Z and E mono-pyridyl-acyl-formamidoximes

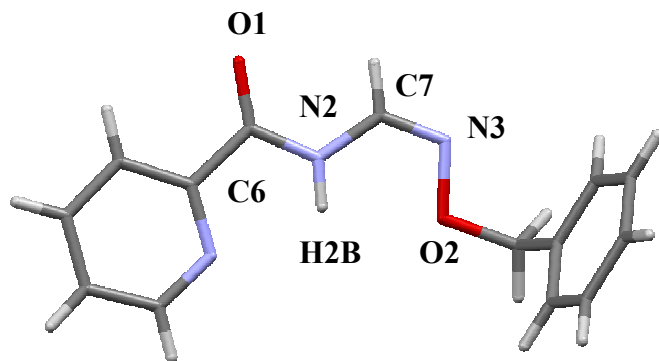


**Figure 4.4** Crystal structure of **4.4Z**. Selected bond distances ( $\text{\AA}$ ): C6-O1: 1.220, C6-N2: 1.364, N2-C7: 1.374, C7-N3: 1.275. H2B-O2: 2.243.

The anticipated intra-molecular hydrogen bond within the formamidoxime unit is clearly observed in compound **4.4Z** (**Figure 4.4**). The distance between the formamidine NH (H2B) and the ether oxygen (O2) is 2.243  $\text{\AA}$ . The C7-N3 bond distance is 1.275  $\text{\AA}$ , meaning that the C=N double bond localizes between the formamidine carbon and nitrogen in the alkoxyamine part. The C7-N2 bond length of 1.364  $\text{\AA}$  also gives a hint that it is neither a traditional C-N single bond (1.469  $\text{\AA}$  for neutral amine) nor a C=N double bond (1.279  $\text{\AA}$  for imine),<sup>[1]</sup> but a partial double bond. The lone pair electrons in the nitrogen atoms N2 delocalize throughout the conjugated acyl-formamidine system.

In the crystal structure of **4.5E**, a linear structure is observed. The bond length of N3-C7

is 1.255 Å and that of C7-N2 is 1.375 Å (**Figure 4.5a**) indicating C=N still localizes on the alkoxyamine side even in the absence of the intra-molecular hydrogen bond present in the Z form. The crystal structure confirms that the configurational E isomer forms rather than its tautomer (discussed in chapter 1). Worth mentioning here is the fact that the crystal is monoclinic at room temperature (**Figure 4.5a**), but undergoes a phase transformation when cooled to 180K (-93 °C) to a non-merohedrally twinned triclinic (**Figure 4.5b**) with a 180° rotation about the reciprocal axis (0,0,1).

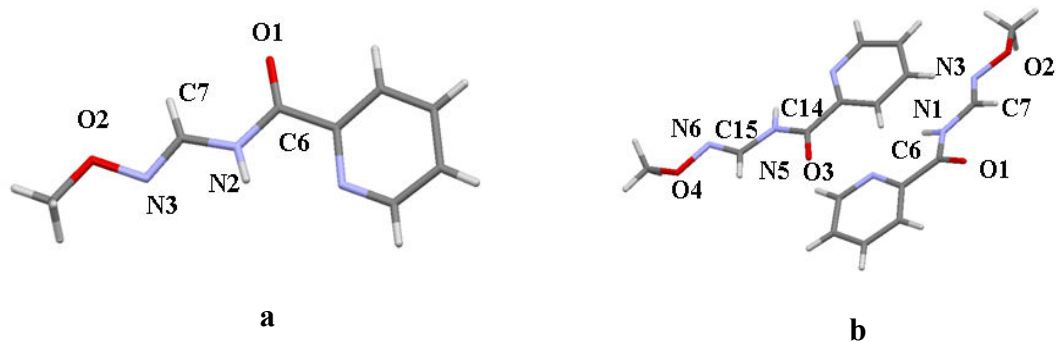


**Figure 4.5** Crystal structure of **4.5E**. **a)** monoclinic at room temperature **b)** non-merohedrally twinned triclinic at -93 °C. Selected bond distances (Å): for a: N3-C7: 1.255, C7-N2: 1.375; for b: N6-C15: 1.265, C15-N5: 1.374, N3-C7: 1.271, C7-N1: 1.376.

#### 4.2.6 Short Summary

In a short summary, the E and Z isomers of pyridinyl-acyl formamidine were fully characterized and studied.<sup>[2]</sup> It is the first time that such E isomer is observed and isolated (**Figure 4.6a**). Indeed, in alkyl and aryl-substituted formamidines, only Z isomers have been reported. The compounds shown in **Figure 4.6a** all show intramolecular hydrogen-bonds. Maybe the formation of the uncommon E isomer is related to the presence of a hydrogen-bond between the basic pyridine nitrogen and the acidic amide NH. One may therefore wonder whether or not the E isomer can still be identified and isolated when the pyridine group is absent.

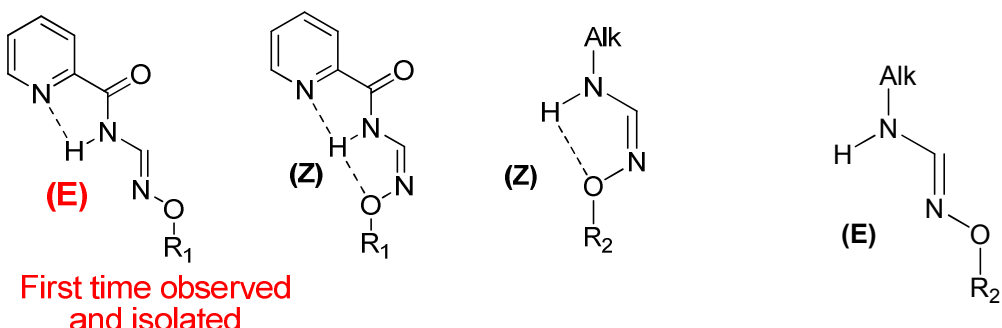
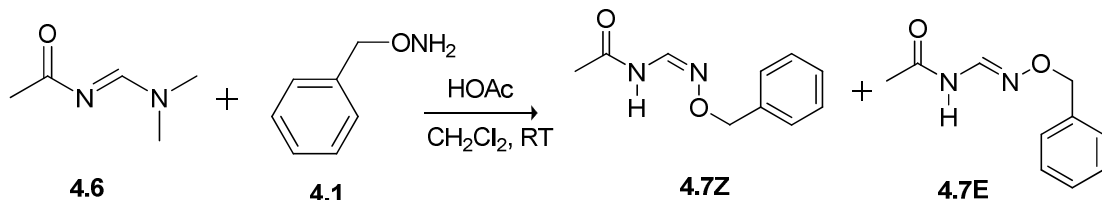


**Figure 4.6** a) Observed formamidoxime isomers. b) never observed.

#### 4.2.7 E isomers of acetyl formamidoxime

In order to assess the effect of the pyridyl group, it was replaced by an acetyl functionality. In a modified reaction, N-acetyl,N'-dimethylformamidine was reacted with alkoxyamine **4.1** in the presence of acetic acid (**Scheme 4.6**).



**Scheme 4.6** Acetyl-formamidine condensed with O-benzylhydroxyamine to give both E and Z isomers.

In the reaction crude, two types of NH and HF hydrogens were observed by  $^1\text{H}$  NMR spectroscopy<sup>[3]</sup> which indicated that the E isomer was probably generated. A NOESY experiment on isomeric mixtures of **4.7Z** and **4.7E** was performed to confirm the formation of the E isomer. As shown in **Figure 4.7a**, the  $\text{CH}_{2Z}$  has weak correlations with both  $\text{NH}_Z$  and  $\text{HF}_Z$ . On the other hand, the  $\text{CH}_{2E}$  only has a relatively strong correlation with  $\text{H}_{FE}$  (the  $\text{CH}_2\text{-O}$  bond can rotate in solution which is different from the crystal structure shown in solid state) but not with  $\text{NH}_E$ . The NOESY results on isomeric mixtures of acetyl-based formamidoxime (**Figure 4.5b**) is therefore consistent with the NOESY experiment of Z/E **4.2** isomer (**Figure 4.2b**), thus confirming the formation of E

isomer in solution. As a result, the acyl group also allows generating the E isomer.

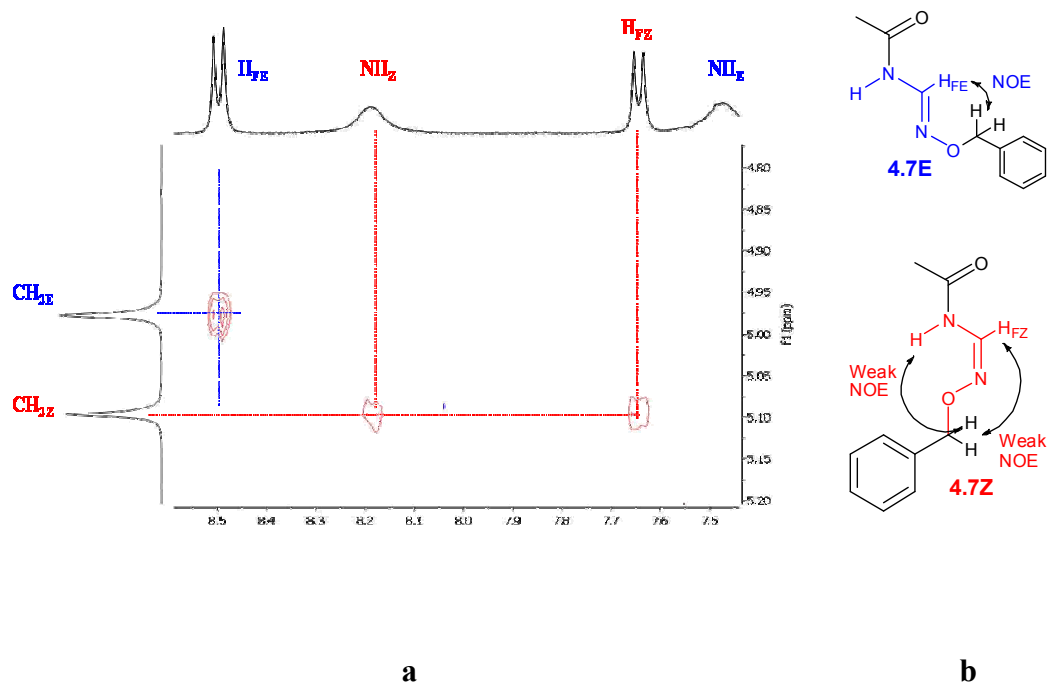


**Figure 4.7 a),b)** NOESY studies of isomeric mixtures of acetyl formamidoximes (500 MHz,  $\text{CDCl}_3$ , 25 °C).

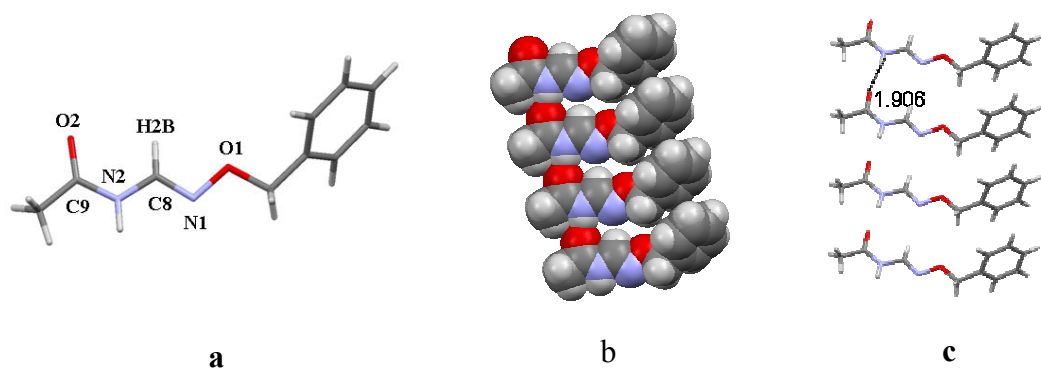


**Figure 4.8** Molecular structure of **4.7E** (a), and self-assembly in the solid state (b&c)  
Selected bond distances (Å): C9-N2: 1.358, N2-C8: 1.380, C8-N1: 1.282

Despite the absence of stabilization through the five-membered intramolecular hydrogen-bonded ring involving the pyridine, the E isomer (**4.7E**) could still be generated and isolated. Moreover, crystallization of **4.7E** was achieved and X-ray crystallographic analysis also confirmed its stereochemical identity (E), as highlighted below (**Figure 4.8**).

The bond length of C8-N1 is 1.282 Å, indicating that the C=N double-bond still localizes between the formamidine carbon atom (C8) and the nitrogen in alkoxyamine part (N1). Surprisingly, the solid-state self-assemby of **4.7E** (**Figure 4.8b**) is very different from most N,N'-disubstituted formamidines which tend to self-assemble into dimers.<sup>[4]</sup> However, in the present case, the E isomer tends to self-assemble in a structure similar to N,N-disubstituted ureas.<sup>[5]</sup> N,N-Disubstituted ureas can act as both hydrogen-bond donors through two NH protons, and acceptors through the lone pairs of the carbonyl group. These hydrogen-bonded self-associations result into one-dimensional hydrogen-bonded chains.

### 4.3 Conditions for isolation of the E isomer

It turns out that the amount of the acid added to condensation reaction (reactive N,N-dimethyl-formamidine as electrophile attacked by alkoxyamine as nucleophile) is critical to the stereochemical outcome (proportion of E and Z isomers, see **Scheme 4.4**). Therefore, the reaction conditions were systematically studied in order to determine conditions for the exclusive formation of the uncommon E isomer.

#### 4.3.1 Kinetic study of E/Z isomerization promoted by acid

The kinetics of E/Z isomerization was studied by  $^1\text{H}$  NMR (**Figure 4.9**) and UV-vis spectroscopies (**Figure 4.10**). The sample was a mixture of E and Z isomers of toluene-derived acyl-formamidoxime (**4.8E&4.8Z**). In the first (bottom) spectrum shown on **Figure 4.9a**, the signals from both E and Z isomers are clearly observed ( $\text{NH}_Z$ ,  $\text{H}_{FZ}$ ,  $\text{NH}_E$ ,  $\text{H}_{FE}$ ). TFA was then added, both  $\text{NH}_E$  and  $\text{H}_{FE}$  showed downfield shifts which indicated that the E isomer of the toluene-derived acyl-formamidoxime (**4.8E**) was bound to TFA and being activated towards isomerization. The E isomer was then rapidly converted to the Z isomer and only trace amount of E isomer remained after 45 minutes (**Figure 4.9c**). When we plot  $\ln[\text{E}]$  as a function of time, a line could be obtained and the slope (-k) is -0.0501. Therefore the rate constant k is 0.0501 and half life of the isomerization reaction  $t_{1/2}$  could be calculated as  $t_{1/2}= \ln 2/k = 13.8$  mins.

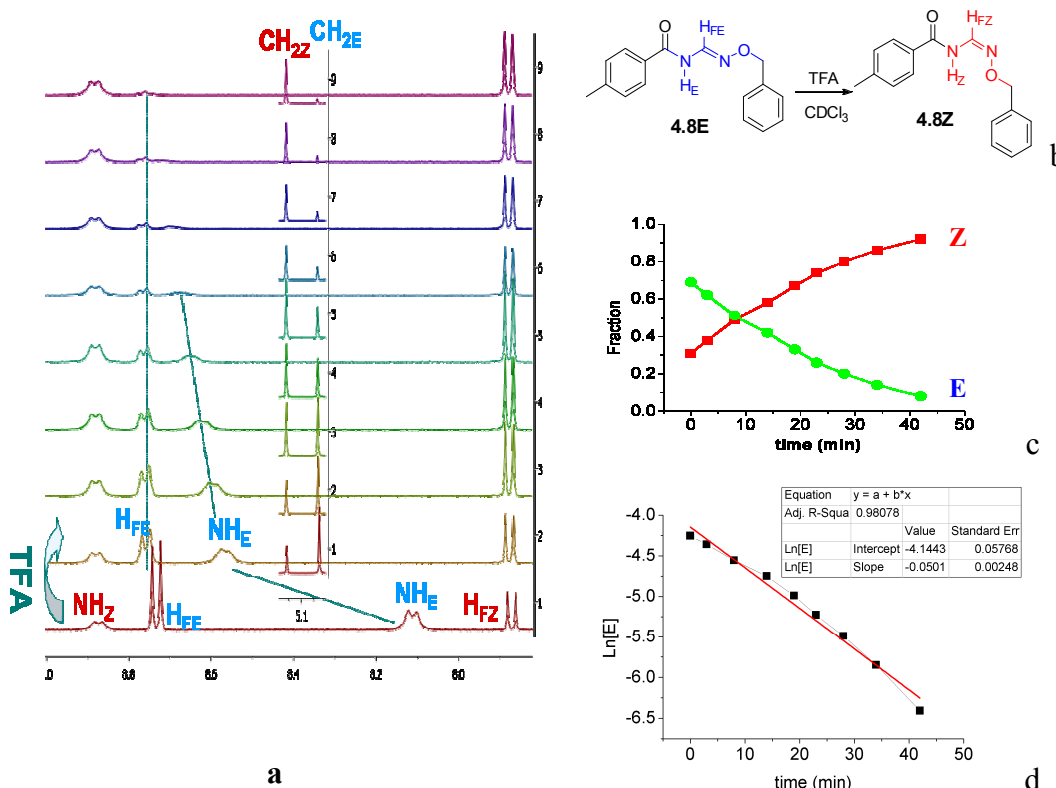


**Figure 4.9** a) Kinetic study of the E/Z isomerization monitored by  $^1\text{H}$  NMR spectroscopy (500 MHz,  $\text{CDCl}_3$ , 25 °C); b) isomerization scheme; c) graphical summary and d)  $\ln[\text{E}]$  as a function of time

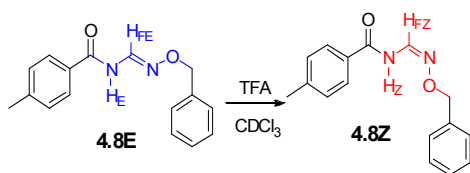
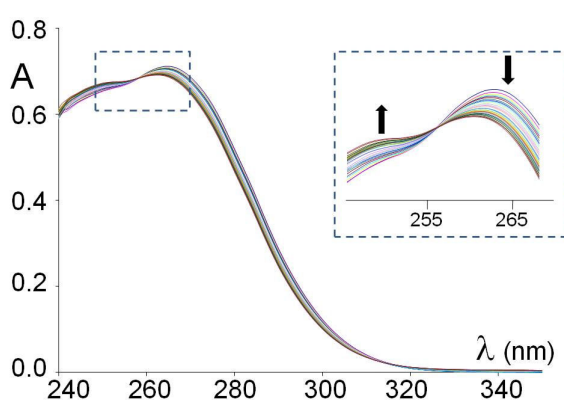
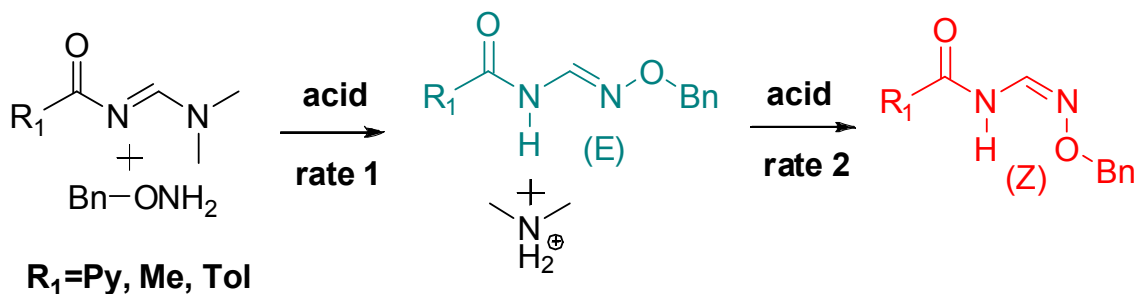


**Figure 4.10** E to Z isomerization monitored by UV-vis spectroscopy in chloroform (25 °C, conc.  $4 \times 10^{-5}$  M, 0.6 eq. of TFA).

The UV-vis experiment (**Figure 4.10**) also showed similar results, with an isobestic point indicating a clean E to Z transformation.

#### 4.3.2 Kinetic study of the condensation and isomerization reactions



**Scheme 4.7** Cascade processes giving E and Z isomers.

A mechanism was proposed and studied based on two facts: (i) both E and Z isomers could be generated in the reaction promoted by acid, and (ii) the E isomer could be isomerized to Z form by additions of protons (**Scheme 4.7**). In the first stage, the condensation of N,N-dimethylformamidine with alkoxyamine promoted by acid would generate the E isomer and dimethylamine as a basic by-product which could easily bind protons. The condensation reaction rate is **rate 1**. In a second stage, the formed E isomer would isomerize to the Z form in the presence of acid, with an isomerization rate **rate 2**. In order to find the best conditions for the isolation of the E isomer, kinetic studies on both condensation and isomerization processes were carried out and monitored by <sup>1</sup>H NMR.

As shown in **Figure 4.11**, pyridine-derived (**F4.11a**), acetyl-derived (**F4.11b**) and toluene-derived (**F4.11c**) acyl-formamidines were reacted with benzylhydroxyamine individually in the presence of 1.0 equivalent of acetic acid. In the pyridine-derived case (**F4.11a**), both condensation and isomerization happened at the early stage of the reaction to give both E and Z isomers. The formed dimethylamine would consume protons and thus reduce not only the condensation **rate 1** but also the isomerization **rate 2**. In both acetyl-(**F4.11b**) and toluene- (**F4.11c**) derived cases, only the condensation process happened at the early stage to give exclusive the E isomer. The isomerization then took place to generate the Z isomers gradually. Comparing **F4.11b** with **F4.11c**, it turned out that the condensation **rate 1** in the acetyl case was faster than in the toluene case. This is probably due to a more electron-rich (lower reactivity) N,N-dimethylformamidine

induced by the toluyl group.

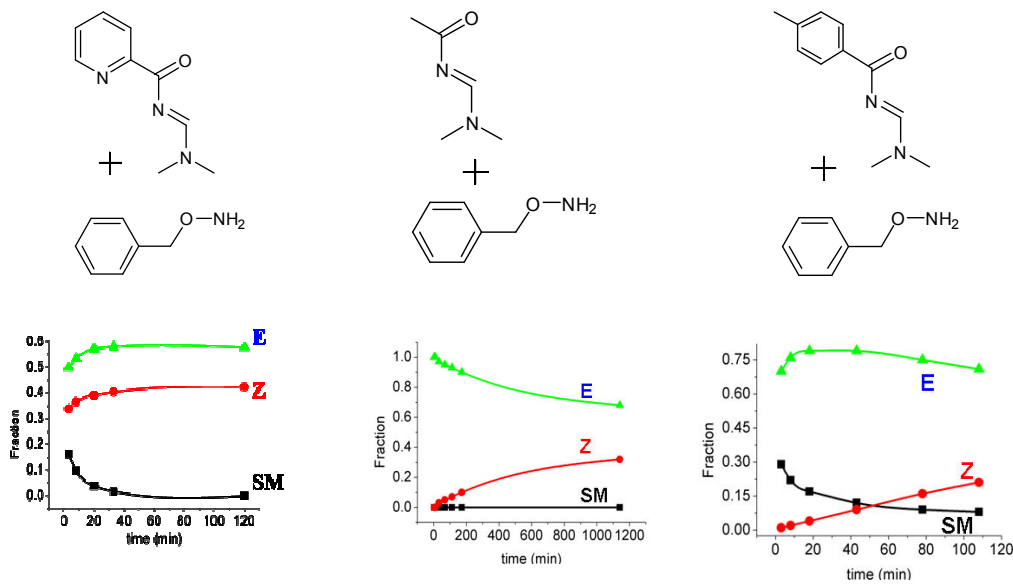
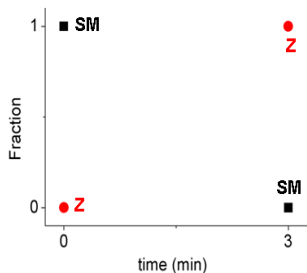
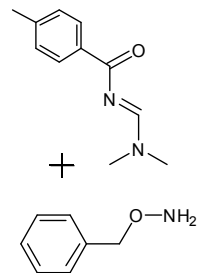
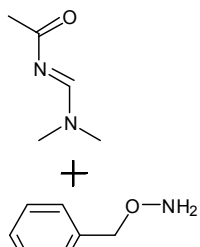
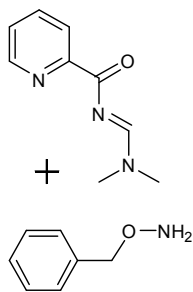
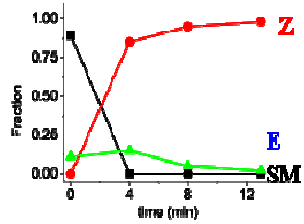


**Figure 4.11** Kinetic studies monitored by  $^1\text{H}$  NMR spectroscopy ( $\text{CDCl}_3$ ; 25 °C): acyl-formamidine reacted with alkoxyamine in the presence of **1.0 eq. of acetic acid** (the concentration of the reactants in **F4.11a**, **F4.11b** and **F4.11c** are 0.29 M, 0.31 M and 0.24 M respectively). SM: starting material.

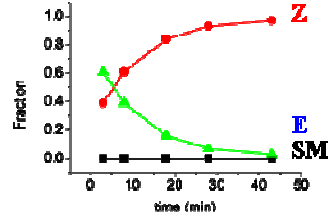
When the reaction was promoted by 2.0 equivalents of trifluoroacetic acid (**Table 4.2**), the provided extra protons greatly accelerated not only the condensation process, but also the isomerization step. After 45 minutes, in all three cases (**F4.12a**, **F4.12b&F4.12c**), all the starting materials was converted to the E isomers and rapidly isomerized to the Z form (in **F4.12a**, the isomerization was too fast to be recorded by  $^1\text{H}$  NMR spectroscopy, but when the reaction was slowed down (1 eq. of TFA added) the E isomer was observed by  $^1\text{H}$  NMR spectroscopy). The comparison of **F4.12a**, **F4.12b** and **F4.12c** suggests that the more electron-rich the formamidine center of E isomer is, the slower of the isomerization would take place.



F4.12a



F4.12b

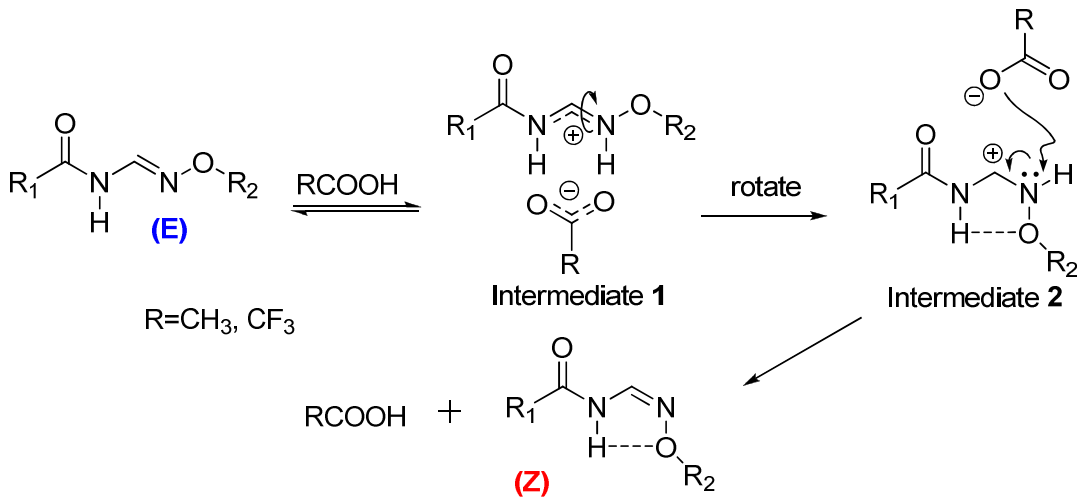


F4.12c

**Figure 4.12** Kinetic studies monitored by  $^1\text{H}$  NMR spectroscopy ( $\text{CDCl}_3$ ; 25 °C):

acyl-formamidine reacted with alkoxyamine in the presence of **2.0 eq.** of **trifluoroacetic acid** (the concentration of the reactants in **F4.12a**, **F4.12b** and **F4.12c** are 0.22 M, 0.27 M and 0.24 M respectively). SM: starting material.

Based on the isomerization kinetic studies, a mechanism may be proposed (**Scheme 4.8**). When the E isomer is exposed to acidic conditions, it would bind to the carboxylic acid and form **intermediate 1** (evidence shown on **Figure 4.9a**) and lead to a C=N double bond cleavage. Then the N-O single bond could rotate to give **intermediate 2** which finally would lose a proton to generate the Z isomer. The formation of the formamidine-carboxylic adduct (**intermediate 1**) is a key step in the whole isomerization process.<sup>[6]</sup> When the formamidine is in a very electron rich environment (toluene derived E isomer **F4.12c**), it would tend to form a more stable adduct with carboxylic acids. This would make the rotation of the N-O single bond more difficult and thus slow down the whole isomerization process.



**Scheme 4.8** Proposed mechanism for E/Z isomerization promoted by acid

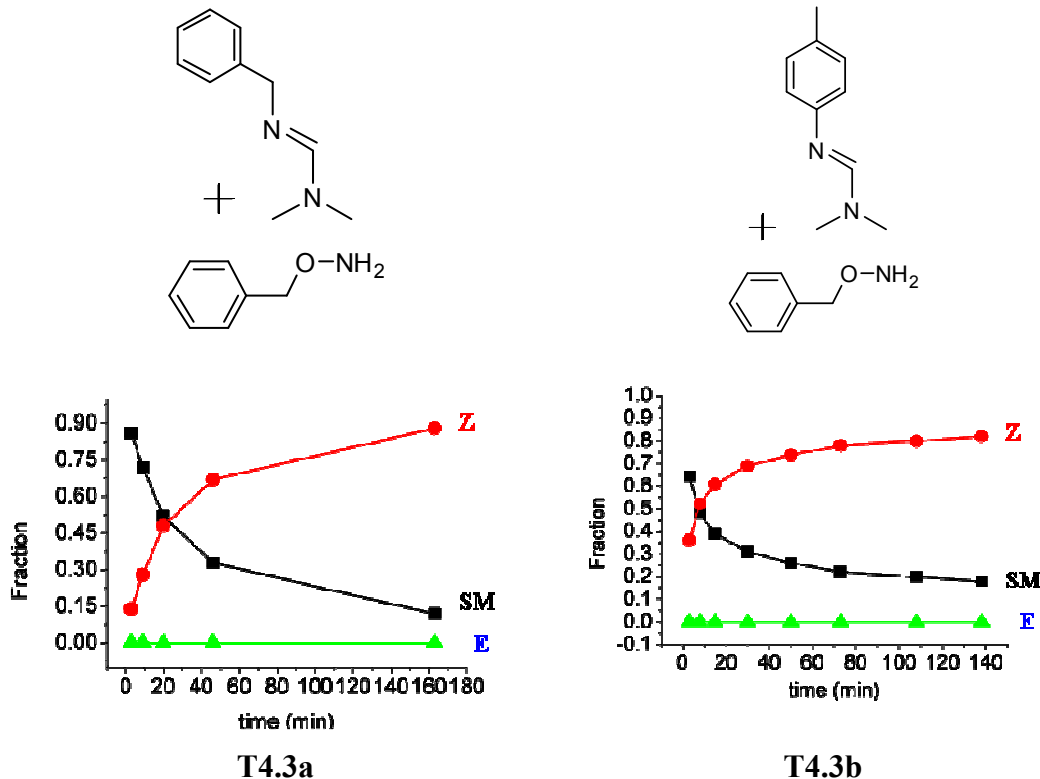


**Figure 4.13** Kinetic studies monitored by <sup>1</sup>H NMR spectroscopy (CDCl<sub>3</sub>; 25 °C): alkyl-and aryl-formamidine reacted with alkoxyamine in the presence of 1.0 eq. of acetic acid (the concentration of the reactants in **F4.13a** and **F4.13b** are 0.31 M and 0.32 M respectively). SM: starting material.

In an effort to understand the role of the acyl group on the relative kinetics of the condensation and isomerizations processes, alkyl- and aryl-substituted formamidines were also studied and compared with the acyl substituted formamidines (**Figure 4.13**). However, in the whole reaction process, no E isomer was observed. This probably meant that the isomerization rate 2 was much faster than the condensation rate 1 (**Scheme 4.7**). Once the starting material alkyl substituted N,N-dimethylformamidines converted to the E product, it probably instantly isomerize to the Z form.

Since different types of N,N-dimethylformamidines were studied and compared in the kinetic experiments, it is also interesting to investigate whether different alkoxyamines would have any effect on the kinetics and outcome of the reaction. When changing the alkoxyamine alkyl group, a control experiment was performed ( $\text{Ph}-\text{CH}_2-\text{ONH}_2$  vs  $\text{C}_{12}\text{H}_{25}-\text{O}-\text{NH}_2$ ). The kinetic data showed very similar results for both cases (**Figure 4.14**) and suggested that changing the alkyl group of the alkoxyamine had no effect on the outcome.

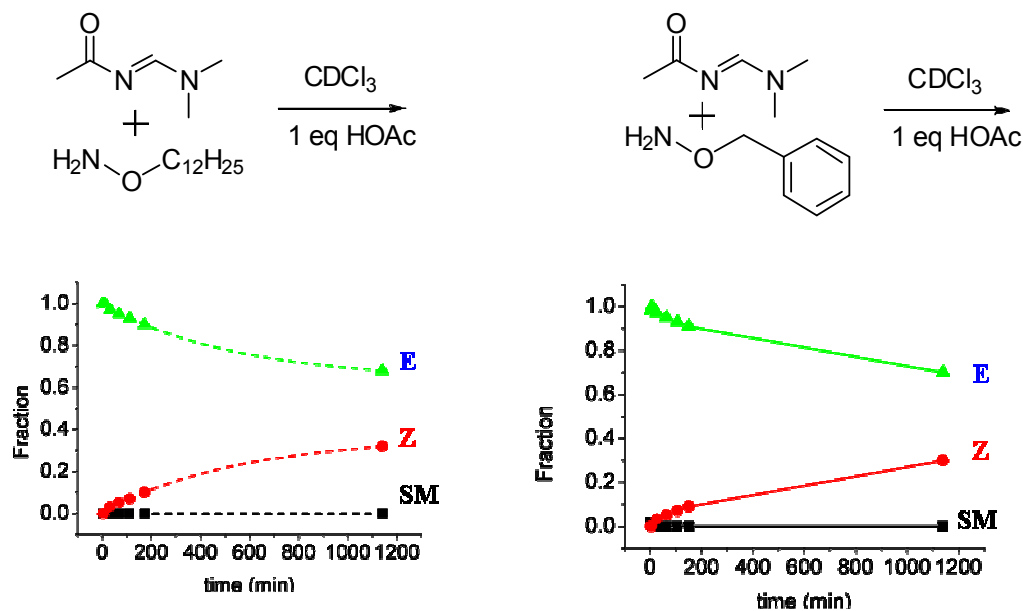


**Figure 4.14** Similar outcome observed by <sup>1</sup>H NMR spectroscopy on the condensation reaction with different alkoxyamine as nucleophile. SM: starting materials. (concentration of reactants: 0.31 M;  $\text{CDCl}_3$ ; 25 °C).

### 4.3.3 Reversible Z to E isomerization

As indicated above, the E isomers can be isomerized to the Z form. What about the reverse process? One report<sup>[7]</sup> suggested that the minute amount of E isomer of N-aryl-N'-formamidoxime may be generated while the corresponding Z isomer was heated in DMSO-d<sub>6</sub>. In order to test this hypothesis, a pure Z-acetyl derived formamidine was heated in DMSO-d<sub>6</sub> at various temperatures. New sets of NH and H<sub>F</sub> gradually grew when the temperature increased (Figure 4.15). Based on the higher chemical shift of the new formed H<sub>F</sub>, the E isomer was probably generated (no NOESY experiment was performed in DMSO at high temperature to confirm this interpretation, but these results are consistent with the analysis in CDCl<sub>3</sub> presented above).

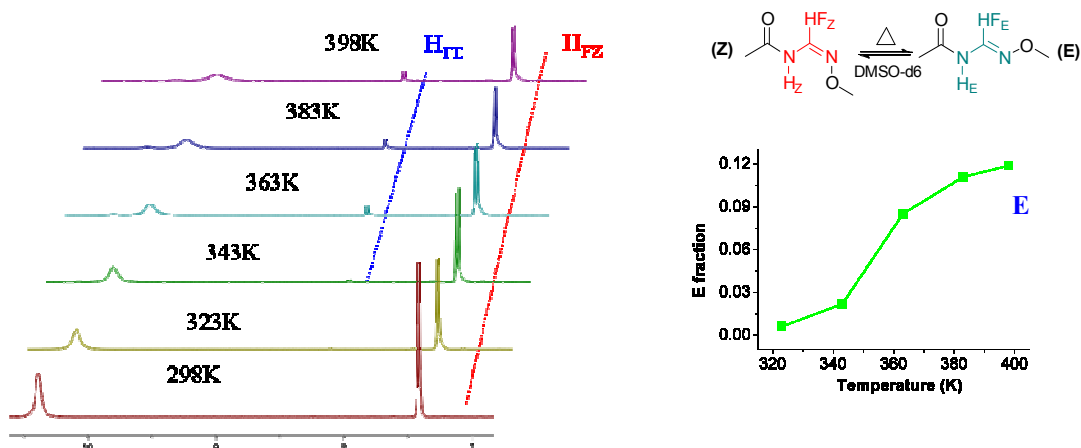


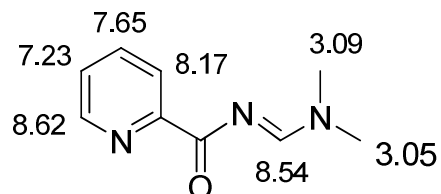
Figure 4.11 Reversible isomerization from Z to E (<sup>1</sup>H NMR, DMSO-d<sub>6</sub>, 500 MHz).

## 4.4 Conclusion

In conclusion, for the first time, the E isomer derived from N-acyl-N'-substituted formamidoxime were isolated and fully studied. The acyl group plays a key role in generating the E isomer in the condensation step. Tuning the acidity in the reaction allows to give either E isomers as major products (just enough protons to promote the condensation but prevent isomerization from being too fast) or exclusive Z isomers (excess amount of protons facilitating the isomerization). The E/Z isomerization is reversible and may find applications in biomimetic chemistry,<sup>[8]</sup> chemically/thermally controlled configurational rotary switches<sup>[9]</sup> and pH-induced drug release.<sup>[10]</sup>

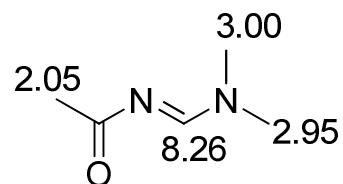
## 4.5 Experimental details

### (E)-N-((Dimethylamino)methylene)picolinamide (4.3)



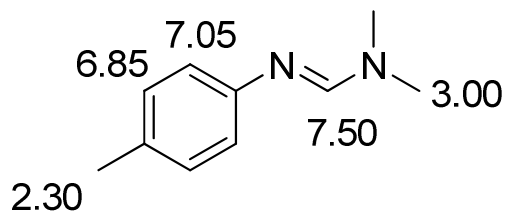
Picolinamide (2.44 g, 20 mmol, 1.0 eq) was mixed with N,N-dimethylformamide dimethylacetal (DMF-DMA, 30 mmol, 1.5 eq) in anhydrous toluene (30 mL). The reaction mixture was heated at 90°C for 3.5 hours while methanol distilled off. After cooling to room temperature, the solvent was evaporated to give the desired N,N-dimethylformamidine product as a white solid (85 %) which was used without further purification.  $\delta$   $^1\text{H}$  NMR ( $\text{CDCl}_3^*$ , 500 MHz, 25°C) 8.62 (d,  $^3J = 4.5$  Hz, 1 H), 8.54 (s, 1 H), 8.17 (d,  $^3J = 8.0$  Hz, 1 H), 7.65 (t,  $^3J = 7.5$  Hz, 1 H), 7.23 (dd,  $^3J = 8.0$  Hz, 5.5 Hz, 1 H), 3.09 (s, 3 H), 3.05 (s, 3 H).  $\delta$   $^{13}\text{C}$  NMR ( $\text{CDCl}_3^*$ , 125 MHz, 25 °C) 176.2, 161.2, 153.6, 149.2, 136.2, 125.3, 124.6, 41.2, 35.3. EI $^+$ -HRMS: calc. for  $\text{C}_9\text{H}_{11}\text{N}_3\text{O}$ : 177.0902; found: 177.0908  $[\text{M}]^+$ , 122.0454  $[\text{M}-(\text{CH}_3)_2\text{NCH}+2\text{H}]^+$ , 85.9483  $[\text{M-Py-CH}_3+\text{H}]^+$ , 73.0527  $[\text{M-PyCO+2H}]^+$ . Mp 58-61 °C.

### (E)-N-((Dimethylamino)methylene)acetamide (4.6)



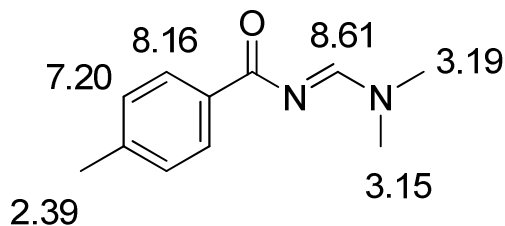
Acetyl amide (3.65, 32 mmol, 1 eq) was mixed with N,N-dimethylformamide dimethylacetal (DMF-DMA, 48 mmol, 1.5 eq) in 30 mL of anhydrous toluene. The reaction was heated at 90°C for 4 hours while the methanol by-product was distilled out. At room temperature, the solvent was evaporated to give the desired N,N-dimethylformamidine product as light yellow oil in quantitative yield. It was used without further purification in the following step.  $\delta$   $^1\text{H}$  NMR ( $\text{CDCl}_3^*$ , 500 MHz, 25°C) 8.26 (s, 1 H), 3.00 (s, 3 H), 2.95 (s, 3 H), 2.05 (s, 3 H).  $\delta$   $^{13}\text{C}$  NMR ( $\text{CDCl}_3^*$ , 125 MHz, 25°C) 184.4, 159.7, 41.0, 34.9, 26.7. EI $^+$ -HRMS: calc. for  $\text{C}_5\text{H}_{10}\text{N}_2\text{O}$ : 114.0793; found: 114.0797  $[\text{M}]^+$ , 99.0557  $[\text{M-NH}]^+$ , 85.9492  $[\text{M-CH}_3*2]^+$ , 83.9511  $[\text{M-CH}_3*2-2]^+$ , 73.0542  $[\text{M-CH}_3\text{CO+2H}]^+$ , 59.0376  $[\text{M-}(\text{CH}_3)_2\text{N-CH}+2\text{H}]^+$ .

### (E)-N,N-Dimethyl-N'-p-tolylformamidamide (4.9)



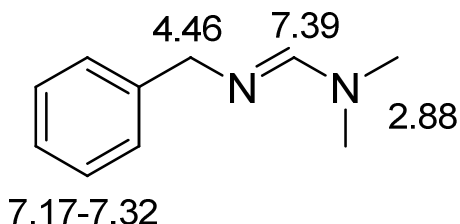
The synthetic method is different from the literature<sup>[11]</sup>. *p*-Toluidine (2.0 g, 18.7 mmol, 1.0 eq) was dissolved in N,N-dimethylformamide dimethylacetal (DMF-DMA, 7.44 mL, 56 mmol, 3.0 eq). The solution was heated at 85°C for 3 hours while the methanol by-product distilled off. After cooling to room temperature, the solvent was evaporated to give the desired N,N-dimethylformamidine product as a colourless liquid in quantitative yield. It was used without further purification in the following step.  $\delta$   $^1\text{H}$  NMR ( $\text{CDCl}_3^*$ , 500 MHz, 25°C) 7.50 (s, 1 H), 7.05 ( $d$ ,  $^3J = 8.0$  Hz, 2 H), 6.85 ( $d$ ,  $^3J = 8.0$  Hz, 2 H), 3.00 (s, 6 H), 2.30 (s, 3 H).

### (E)-N-((Dimethylamino)methylene)-4-methylbenzamide (4.13)



The synthetic method was slightly different from the literature.<sup>[12]</sup> 4-Methylbenzamide (2.41 g, 17.8 mmol, 1.0 eq) was mixed with N,N-dimethylformamide dimethylacetal (DMF-DMA, 26.7 mmol, 1.5 eq) in 30 mL anhydrous toluene. The reaction was heated at 90°C for 4 hours while the methanol by-product distilled off. After cooling to room temperature, the solvent was evaporated to give the desired N,N-dimethylformamidine product as a white solid in quantitative yield. It was used without further purification in the following step.  $\delta$   $^1\text{H}$  NMR ( $\text{CDCl}_3^*$ , 500 MHz, 25 °C) 8.61 (s, 1 H), 8.16 ( $d$ ,  $^3J = 8.0$  Hz, 2 H), 7.20 ( $d$ ,  $^3J = 8.0$  Hz, 2 H), 3.19 (s, 3 H), 3.15 (s, 3 H), 2.39 (s, 3 H). Mp 88-90 °C (lit. 89-90 °C).<sup>[12]</sup>

### (E)-N'-Benzyl-N,N-dimethylformimidamide (4.10)

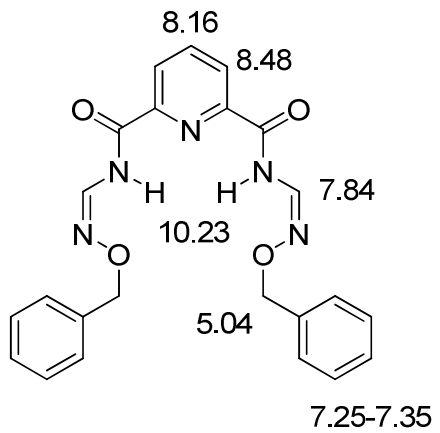


The synthetic method was adapted from literature protocols.<sup>[13]</sup> Benzylamine (1.0 mL, 9.16 mmol, 1.0 eq) was mixed with DMF-DMA (3.65 mL, 27.5 mmol, 3.0 eq) in 30 mL of anhydrous methanol and heated at 65°C for 3 hours. After

cooling to room temperature, the solution was concentrated to give the desired N,N-dimethylformamidine product as a colourless liquid in quantitative yield.  $\delta$  <sup>1</sup>H NMR (CDCl<sub>3</sub>\* , 500 MHz, 25°C) 7.39 (s, 1H), 7.17-7.32 (m, 4H), 4.46 (s, 2H), 2.88 (s, 6H).

### N2,N6-Bis((Z)-(benzyloxyimino)methyl)pyridine-2,6-dicarboxamide (4.2ZZ)

Compound 3.2 (131 mg, 0.48 mmol, 1.0 eq) was mixed with 117 mg of O-benzylhydroxylamine (0.95 mmol, 2.0 eq) in anhydrous dichloromethane (2 mL), followed by 147  $\mu$ L of trifluoroacetic acid (1.90 mmol, 4.0 eq). The reaction solution was stirred overnight at room temperature. The crude solution was washed with saturated aqueous potassium carbonate (2 mL) and the aqueous layer was extracted with dichloromethane. The

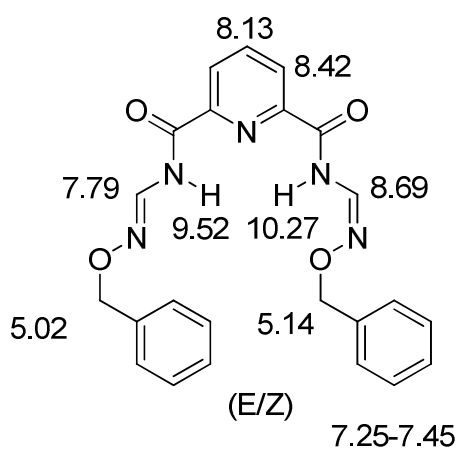


combined organic layers were dried over sodium sulphate and concentrated in vacuo. Recrystallization of the crude from hot 95% ethanol gave 150 mg of pure product as a white solid (72 %).  $\delta$  <sup>1</sup>H NMR (CDCl<sub>3</sub>\* , 500 MHz, 25°C) 10.23 (d, <sup>3</sup>J = 10 Hz, 2H), 8.48 (d, <sup>3</sup>J = 8.0 Hz, 2H), 8.16 (t, <sup>3</sup>J = 8.0 Hz, 1H), 7.84 (d, <sup>3</sup>J = 10 Hz, 2H), 7.25-7.35 (m, 10 H), 5.04 (s, 4 H).  $\delta$  <sup>13</sup>C NMR (CDCl<sub>3</sub>\* , 125 MHz, 25 °C) 160.4, 147.8, 139.7, 137.5, 133.8,

128.5, 128.0, 127.5, 127.2, 76.1. EI<sup>+</sup>-HRMS: calc. for C<sub>23</sub>H<sub>21</sub>N<sub>5</sub>O<sub>4</sub>: 431.1594; found: 431.1603 [M]<sup>+</sup>, 324.1182 [M-BnO]<sup>+</sup>, 218.0715 [M-2\*BnO+H]<sup>+</sup>, 148.0552 [M-2\*BnO-CONHCHN]<sup>+</sup>. Mp 162-163 °C. EA: C<sub>23</sub>H<sub>21</sub>N<sub>5</sub>O<sub>4</sub>, calculated: %C 64.03, %H

4.91, %N 16.23; found: %C 64.16, %H 4.88, %N 16.25.

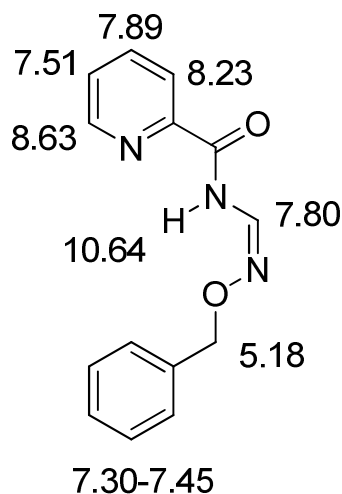
**N2-((E)-(Benzylxyimino)methyl)-N6-((Z)-(benzylxyimino)methyl)pyridine-2,6-dicarboxamide (4.2ZE)**



Compound **3.2** (207 mg, 0.75 mmol, 1.0 eq) was mixed with 185 mg of O-benzylhydroxylamine (1.50 mmol, 2 eq) in 4 mL of anhydrous dichloromethane, followed by addition of 172  $\mu$ L of acetic acid (3 mmol, 4.0 eq). The reaction was stirred overnight at room temperature. The crude solution was washed with 3 mL of saturated potassium carbonate aqueous solution and the aqueous layer was extracted with

dichloromethane. The combined organic layers were dried over sodium sulphate and concentrated in vacuo to give the crude isomeric mixture (EE, EZ, ZZ). Then 39 mg of the crude mixture was purified by Preparative TLC to give 12 mg pure E/Z isomer and 14 mg EE, ZZ isomeric mixture. EZ isomer:  $\delta$  <sup>1</sup>H NMR ( $\text{CDCl}_3^*$ , 600 MHz, 25°C) 10.27 (d,  $^3J$ = 10 Hz, 1 H), 9.52 (d,  $^3J$ = 11 Hz, 1 H), 8.69 (d,  $^3J$ = 11 Hz, 1 H), 8.42 (m, 2 H), 8.13 (t,  $^3J$ = 7.8 Hz, 1 H), 7.79 (d,  $^3J$ = 10 Hz, 1 H), 7.25-7.45 (m, 10 H), 5.14 (s, 2 H), 5.02 (s, 2 H). Due to the small amount of product, <sup>13</sup>C NMR was not recorded. Details of the crystal structure of the EZ isomer are given in appendix.

**(Z)-N-((Benzyl oxyimino)methyl)picolinamide (4.4Z)**



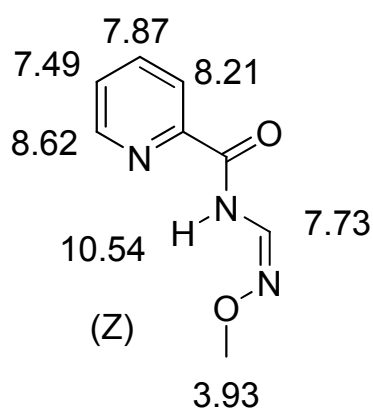
(E)-N-((Dimethylamino)methylene)picolinamide (302 mg, 1.70 mmol, 1.0 eq) was mixed with 199 mg of O-benzylhydroxylamine (1.62 mmol, 0.95 eq) in anhydrous dichloromethane (3 mL), followed by addition of trifluoroacetic acid (262 µL, 3.40 mmol, 2.0 eq). The reaction was stirred overnight at room temperature. The crude solution was washed with saturated aqueous potassium carbonate (3 mL) and the aqueous layer was extracted with CH<sub>2</sub>Cl<sub>2</sub>. The combined organic layers were dried over sodium sulphate and concentrated in vacuo.

Recrystallization from hot 95% ethanol gave the pure product as a white solid (217 mg, 85%).  $\delta$  <sup>1</sup>H NMR (CDCl<sub>3</sub>\* , 500 MHz, 25 °C) 10.64 (br s, 1 H), 8.63 (d, <sup>3</sup>J = 4.5 Hz, 1 H), 8.23 (d, <sup>3</sup>J = 8.0 Hz, 1 H), 7.89 (t, <sup>3</sup>J = 8.0 Hz, 1 H), 7.80 (d, <sup>3</sup>J = 10 Hz, 1 H), 7.50-7.52 (m, 1 H), 7.30-7.45 (m, 5 H), 5.18 (s, 2 H).  $\delta$  <sup>13</sup>C NMR (CDCl<sub>3</sub>\* , 125 MHz, 25°C) 161.7, 148.6, 148.2, 137.6, 137.5, 134.1, 128.4, 128.1, 128.0, 127.3, 123.2, 76.2. EI<sup>+</sup> HRMS: calc. for C<sub>14</sub>H<sub>13</sub>N<sub>3</sub>O<sub>2</sub>: 255.1008; found: 255.1016 [M]<sup>+</sup>, 134.0491 [M-PyCONH-H]<sup>+</sup>, 91.0556 [M-PyCONHCHNO-H]<sup>+</sup>. Mp 79-80 °C. Details of the crystal structure are given in the appendix.

**(Z)-N-((Methoxyimino)methyl)picolinamide (4.5Z)**  
**and (E)-N-((methoxyimino)methyl)picolinamide (4.5E)**

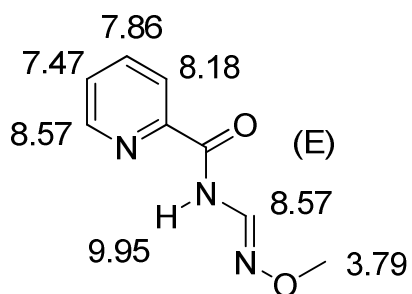
Methoxylamine hydrochloride (181 mg, 2.17 mmol, 1.0 eq) was suspended in anhydrous dichloromethane (3 mL), and 301 µL of triethylamine (2.17 mmol, 1.0 eq) were added. After 5 minutes, 384 mg of (E)-N-((dimethylamino)methylene)picolinamide (2.17 mmol, 1.0 eq) were added and the solution was left to stir at room temperature overnight. The crude solution was washed with 1 N aqueous sodium hydroxide (3 mL) and the aqueous layer was extracted with dichloromethane. The combined organic layers were dried over sodium sulphate and concentrated in vacuo. The crude was purified by column

chromatography with 2.5:100 ethyl acetate/dichloromethane as the eluent to give 267 mg of E/Z isomeric mixture (69 %). The isomeric mixtures were further separated by CHIRALPAK IC HPLC column (5 cm ID × 50 cmL, 20  $\mu$ ) with 15:100 ethyl acetate/dichloromethane as eluent to give pure E isomer and Z isomer.



Z isomer:  $^1\text{H}$  NMR ( $\text{CDCl}_3^*$ , 500 MHz, 25°C) 10.54 (br s, 1 H), 8.62 (d,  $^3J = 4.5$  Hz, 1 H), 8.21 (d,  $^3J = 8.0$  Hz, 1 H), 7.87 (t,  $^3J = 8.0$  Hz, 1 H), 7.73 (d,  $^3J = 11$  Hz, 1 H), 7.49 (m, 1 H), 3.93 (s, 3H).  $^{13}\text{C}$  NMR ( $\text{CDCl}_3^*$ , 125 MHz, 25 °C) 161.6, 148.5, 148.1, 137.5, 133.6, 127.3, 123.1, 62.1.  $R_f$  ( $\text{SiO}_2$ , 2.5:100 EtOAc/CH<sub>2</sub>Cl<sub>2</sub>) = 0.20. EI<sup>+</sup>-HRMS: calc. for C<sub>8</sub>H<sub>9</sub>N<sub>3</sub>O<sub>2</sub>: 179.0695; found: 179.0703 [M]<sup>+</sup>, 148.0538 [M-OCH<sub>3</sub>]<sup>+</sup>, 106.0334 [M-OCH<sub>3</sub>-N=CH-NH]<sup>+</sup>.

Mp 78-80 °C. EA: C<sub>8</sub>H<sub>9</sub>N<sub>3</sub>O<sub>2</sub>, calculated: %C 53.63, %H 5.06, %N 23.45; found: %C 53.96, %H 5.03, %N 23.22.

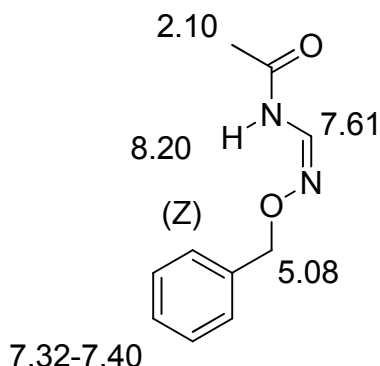


E isomer:  $\delta$   $^1\text{H}$  NMR ( $\text{CDCl}_3^*$ , 300 MHz, 25 °C) 9.95 (br s, 1 H), 8.57 (d,  $^3J = 11$  Hz, 1 H), 8.57 (d,  $^3J = 4.8$  Hz, 1 H), 8.18 (d,  $^3J = 7.8$  Hz, 1 H), 7.86 (t,  $^3J = 7.8$  Hz, 1 H), 7.48 (m, 1 H), 3.79 (s, 3H).  $R_f$  ( $\text{SiO}_2$ , 2.5:100 EtOAc/CH<sub>2</sub>Cl<sub>2</sub>) = 0.28. Mp 85-86 °C. Details of the crystal structure are given in appendix.

**(Z)-N-((Benzylxyimino)methyl)acetamide (4.7Z)**

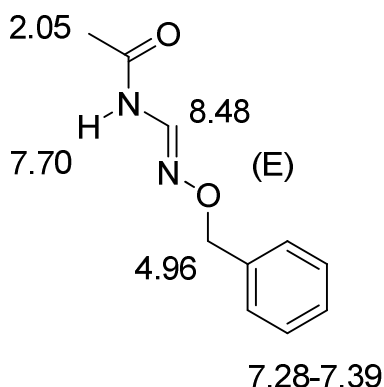
and

**(E)-N-((benzyloxyimino)methyl)acetamide (4.7E)**



(E)-N-((Dimethylamino)methylene)acetamide (111 mg, 0.97 mmol, 1.0 eq) was mixed with 119 mg of O-benzylhydroxylamine (0.97 mmol, 1.0 eq) in anhydrous dichloromethane (2 mL), followed by addition of triethylamine (270  $\mu$ L, 1.94 mmol, 2.0 eq). The solution was stirred overnight at room temperature, concentrated and uploaded onto a silica column which was then eluted with 10:100:1 ethyl acetate/dichloromethane/triethylamine to give 18.5 mg of Z isomer (10 %) and 131 mg of E isomer (70 %). EA:  $C_{10}H_{12}N_2O_2$ , calculated: %C 62.49, %H 6.29, %N 14.57; found: %C 62.54, %H 6.33, %N 14.29.

Z isomer:  $\delta^{1}\text{H}$  NMR ( $\text{CDCl}_3^*$ , 500 MHz, 25°C) 8.20 (br s, 1 H), 7.61 (d,  ${}^3J = 9.5$  Hz, 1 H), 7.32-7.40 (m, 5 H), 5.08 (s, 2 H), 2.10 (s, 3 H).  $\delta^{13}\text{C}$  NMR ( $\text{CDCl}_3^*$ , 125 MHz, 25 °C) 167.3, 136.9, 134.2, 128.5, 128.4, 128.3, 76.4, 23.3.  $R_f$  ( $\text{SiO}_2$ , 10:100:1 EtOAc/ $\text{CH}_2\text{Cl}_2/\text{Et}_3\text{N}$ ) = 0.42. EI $^+$ -HRMS: calc. for 192.0899; found 192.0907 [M] $^+$ , 150.0830 [M- $\text{CH}_3\text{CO-H}$ ] $^+$ , 91.0551 [M- $\text{CH}_3\text{CO-NHCHNO}$ ] $^+$ , 85.9518 [M- $\text{BnO+H}$ ] $^+$ . 83.9533 [M-BnO-H] $^+$ . Mp 94-95 °C.



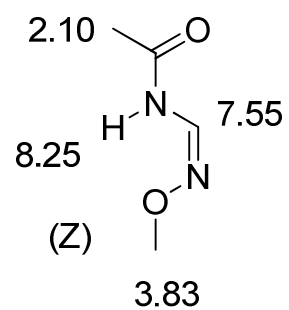
E isomer:  $\delta^{1}\text{H}$  NMR ( $\text{CDCl}_3^*$ , 500 MHz, 25°C) 8.48 (d,  ${}^3J = 10$  Hz, 1 H), 7.70 (br s, 1 H), 7.28-7.39 (m, 5 H), 4.96 (s, 2 H), 2.05 (s, 3 H).  $\delta^{13}\text{C}$  NMR ( $\text{CDCl}_3$ , 125 MHz, 25°C) 168.0, 141.6, 137.5, 128.4, 128.1, 127.9, 75.9, 23.3.  $R_f$  ( $\text{SiO}_2$ , 10:100:1 EtOAc/ $\text{CH}_2\text{Cl}_2/\text{Et}_3\text{N}$ ) = 0.27. Mp 105-107 °C. Details of crystal structures are given in the appendix.

**(Z)-N-((Methoxyimino)methyl)acetamide(4.11Z)**

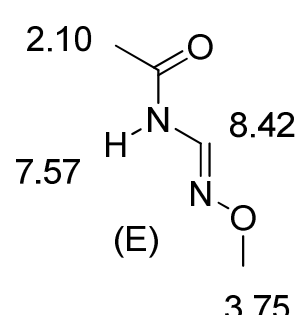
and

**(E)-N-((methoxyimino)methyl)acetamide(4.11E)**

(E)-N-((Dimethylamino)methylene)acetamide (256 mg, 2.24 mmol, 1.0 eq) was mixed with 187 mg of methoxylamine hydrochloride (2.24 mmol, 1.0 eq) in anhydrous dichloromethane (3 mL), followed by triethylamine (312  $\mu$ L, 2.24 mmol, 1.0 eq). The solution was stirred overnight at room temperature and concentrated, uploaded on silica column, eluted with 15:100 ethyl acetate/dichloromethane to give 158 mg of Z isomer (61 %) and 36 mg of E isomer (14 %).

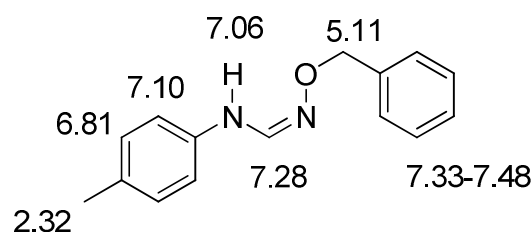


Z isomer:  $\delta^1\text{H}$  NMR ( $\text{CDCl}_3^*$ , 500 MHz, 25 °C) 8.25 (br s, 1 H), 7.55 (d,  $^3J = 10.0$  Hz, 1 H), 3.83 (s, 3 H), 2.10 (s, 3 H).  $\delta^{13}\text{C}$  NMR ( $\text{CDCl}_3^*$ , 125 MHz, 25°C) 167.4, 133.9, 61.8, 23.2.  $R_f$  ( $\text{SiO}_2$ , 15:100 EtOAc/CH<sub>2</sub>Cl<sub>2</sub>) = 0.28. EI<sup>+</sup>-HRMS : calc. for C<sub>4</sub>H<sub>8</sub>N<sub>2</sub>O<sub>2</sub>: 116.0586; found 116.0591 [M]<sup>+</sup>, 74.0475 [M-CH<sub>3</sub>CO+H]<sup>+</sup>. Mp 120-121 °C. EA: C<sub>4</sub>H<sub>8</sub>N<sub>2</sub>O<sub>2</sub>, calculated: %C 41.37, %H 6.94, %N 24.12; found: %C 41.48, %H 6.81, %N 23.92.



E isomer :  $\delta^1\text{H}$  NMR ( $\text{CDCl}_3^*$ , 300 MHz, 25°C) 8.42 (d,  $^3J = 10.2$  Hz, 1 H), 7.57 (br s, 1 H), 3.75 (s, 3 H), 2.10 (s, 3 H).  $R_f$  ( $\text{SiO}_2$ , 15:100 EtOAc/CH<sub>2</sub>Cl<sub>2</sub>) = 0.17.

**(Z)-N'-(Benzylxy)-N-p-tolylformimidamide (4.12)**



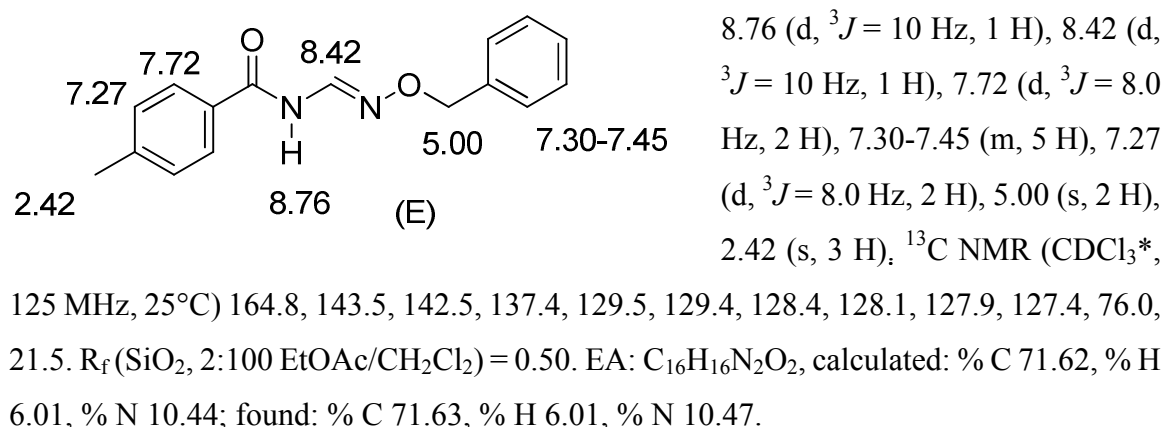
5.80 mmol, 2.5 eq). The solution was stirred for 1.5 hours at room temperature and washed

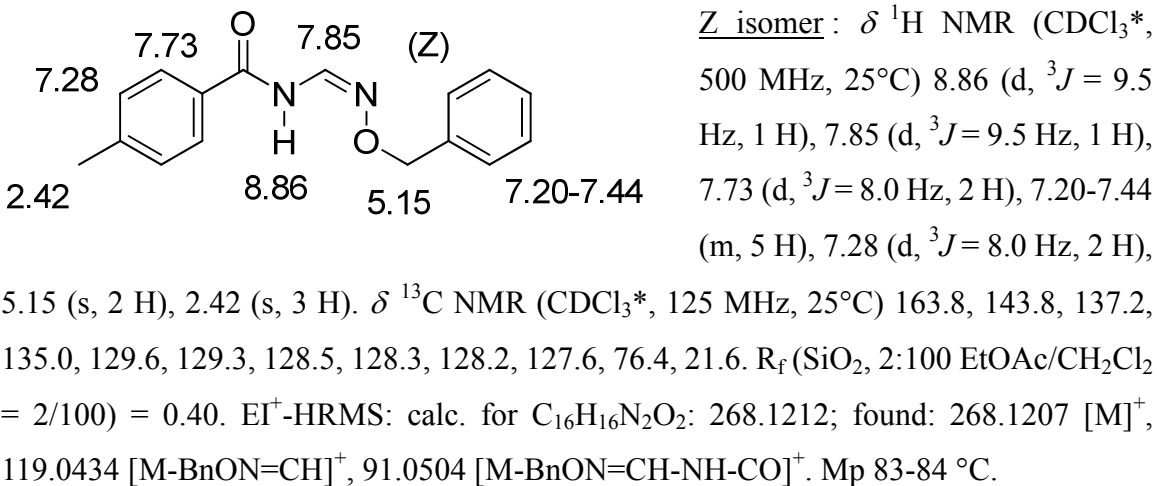
(E)-N,N-Dimethyl-N'-p-tolylformimidamide (376 mg, 2.32 mmol, 1.0 eq) was mixed with 285 mg of O-benzylhydroxylamine (2.32 mmol, 1.0 eq) in anhydrous CH<sub>2</sub>Cl<sub>2</sub> (3 mL), followed by addition of acetic acid (331  $\mu$ L,

with 3 N sodium hydroxide (3 mL). The aqueous layer was extracted with dichloromethane. The combined organic layers were dried over sodium sulphate and concentrated in vacuo. The crude was purified by column chromatography with 5:100 ethyl acetate/dichloromethane as the eluent to give 510 mg of the desired product (92 %).  $\delta$ <sup>1</sup>H NMR (CDCl<sub>3</sub>\* , 500 MHz, 25°C) 7.33-7.48 (m, 5 H), 7.28 (d, <sup>3</sup>J = 11 Hz, 1 H), 7.10 (d, <sup>3</sup>J = 8.0 Hz, 2 H), 7.06 (br d, <sup>3</sup>J = 11 Hz, 1H), 6.81 (d, <sup>3</sup>J = 8.0 Hz, 2 H), 5.11 (s, 2 H), 2.32 (s, 3 H).  $\delta$ <sup>13</sup>C NMR (CDCl<sub>3</sub>\* , 125 MHz, 25°C) 139.1, 137.8, 137.0, 131.7, 130.1, 128.4, 128.2, 127.9, 115.4, 75.8, 20.5. R<sub>f</sub> (SiO<sub>2</sub>, 5:100 EtOAc/CH<sub>2</sub>Cl<sub>2</sub>) = 0.57. EI<sup>+</sup>-HRMS: calc. for C<sub>15</sub>H<sub>16</sub>N<sub>2</sub>O :240.1263; found: 240.1257 [M]<sup>+</sup>, 223.1281 [M-CH<sub>3</sub>-2H]<sup>+</sup>, 118.0652 [M-BnO-N=CH-H]<sup>+</sup>, 91.0529 [M- M-BnO-N=CH-NH]<sup>+</sup>. Mp 58-60 °C. EA: C<sub>15</sub>H<sub>16</sub>N<sub>2</sub>O, calculated: %C 74.97, %H 6.71, %N 11.66; found: %C 74.87, %H 6.72, %N 11.69.

**(E)-N-((Benzylxyimino)methyl)-4-methylbenzamide (4.8E)** and **(Z)-N-((benzyloxyimino)methyl)-4-methylbenzamide (4.8Z)**

(E)-N-((Dimethylamino)methylene)-4-methylbenzamide **4.13** (271 mg, 1.43 mmol, 1.0 eq) was mixed with 175 mg of O-benzylhydroxylamine (1.43 mmol, 1.0 eq) in anhydrous dichloromethane (3mL), followed by addition of acetic acid (90  $\mu$ L, 1.57 mmol, 1.1 eq). The solution was stirred for 3 hours at room temperature and washed with 2 N sodium hydroxide (3 mL) .The aqueous layer was extracted with dichloromethane. The combined organic layers were dried over sodium sulphate, concentrated in vacuo and purified by column chromatography with 2:100 ethyl acetate/dichloromethane as the eluent to give 295 mg of E/Z isomeric mixture (77 %). E isomer:  $\delta$ <sup>1</sup>H NMR (CDCl<sub>3</sub>\* , 500 MHz, 25°C)





## References

- [1] Allen, F. H.; Kennard, O. and Watson, D. G.; *J. Chem. Soc. Perkin Trans. 2*, **1987**, S1-S19.
- [2] Zhao, W.; Wang, R. and Petitjean, A.; manuscript submitted in July **2011**
- [3] See Appendix A.
- [4] Petitjean, A.; Xing, L. and Wang, R. *CrystEngComm.* **2010**, 12, 1397-1401.
- [5] Dannecker,W.; Kopf, J. and Rust, H.; *Cryst. Struct. Commun.* **1979**, 8, 429-432.
- [6] Xing, L.; Wiegert, C. and Petitjean, A.; *J. Org. Chem.* **2009**, 74, 9513-9516.
- [7] Hayakawa, K.; Eguchi, Y.; and Nakayama, A. *J. Pesticide Sci.* **1993**, 18, 191-196.
- [8] Tew, G. N.; Scott, R. W.; Klein, M. L. and De Grado, W. F. *Acc. Chem. Res.* **2010**, 43, 30-39.
- [9] (a) Feringa, B. L; *J. Org. Chem.* **2007**, 72, 6635-6652; (b) Landge, S. M. and Aprahamian, I.; *J. Am. Chem. Soc.* **2009**, 131, 18269–18271.
- [10] Leblond, J.; Gao, H.; Petitjean, A. and Leroux, J.-C.; *J. Am. Chem. Soc.* **2010**, 132, 8544-8545.
- [11] Enthalter, S.; Schroder, K.; Inoue, S.; Eckhardt, B.; Junge, K.; Beller, M. and Drieb, M.; *Eur. J. Org. Chem.* **2010**, 25, 4893-4901.
- [12] Blake A.J.; McNab, H. and Murray, E-A.; *J. Chem. Soc. Perkin Trans. I*, **1989**, 589-595.

[13] Porcheddu, A.; Giacomelli, G. and Piredda, I.; *J. Comb. Chem.*, **2009**, 11, 126-130.

# Chapter 5

## Conclusion and perspectives

### 5.1 Summary and conclusion

Two years ago, my MSc research started with the synthesis of macrocycle **M1**, as a potential anionic analog of 18-crown-6. The first generation of macrocycle **M1** with alkoxyamine-formamidine subunits was successfully obtained by cyclic condensation of a bis-alkoxyamine and a bis-formamidine, and fully characterized, as described in chapter 2. More interesting is the existence of a four-pyridine-unit interlocked catenane as confirmed by MS-MS.

As it was anticipated that **M1** would be difficult to deprotonate, the second generation macrocycle **M2** was introduced which involved more acidic amide NH protons. Moreover, the highly conjugated system in **M2** would favor a more planar conformation and may promote a high cation affinity. **M2** was successfully synthesized and fully characterized, as reported in chapter 3. A crystal of an **M2-MeOH** adduct indicated molecular recognition may happen in solution. The unexpected formation and isolation of “**Maxi-M2**” gave interesting structural information about the assembly of bis-formamidoxime type compounds.

Driven by the desire to understand how these by-products (catenane, large macrocycle) formed, we performed a systematic study of such condensation. In chapter 4, we report, for the first time, a full study of the E isomers derived from N-acyl-N'-substituted formamidoximes. The acyl group plays a key role in generating the E isomer in the condensation step. Either Z or E isomers derived from N-acetyl-N'-substituted formamidoxime could be selectively formed and isolated by tuning the acidic conditions in the reaction. The E/Z configurational switch is reversible and it may find potential applications in chemically/thermally controlled rotary switches and pH-induced drug release.

## 5.2 Future directions

As mentioned in chapter 4, the formation of the uncommon E isomer was probably the main reason that diminished the yield of macrocycle **M2**. We have demonstrated that the E isomers of acyl-formamidoxime were favorable kinetic products. Therefore in the final condensation step to give **M2**, two mono-condensed intermediates may form (**Figure 5.1**). The curved (Z) intermediate would probably cyclize to generate **M2**, but the linear (E) intermediate may lead to polymerization or oligomerization. This may explain the formation of **Maxi-M2** and several highly polar by-products observed by TLC.

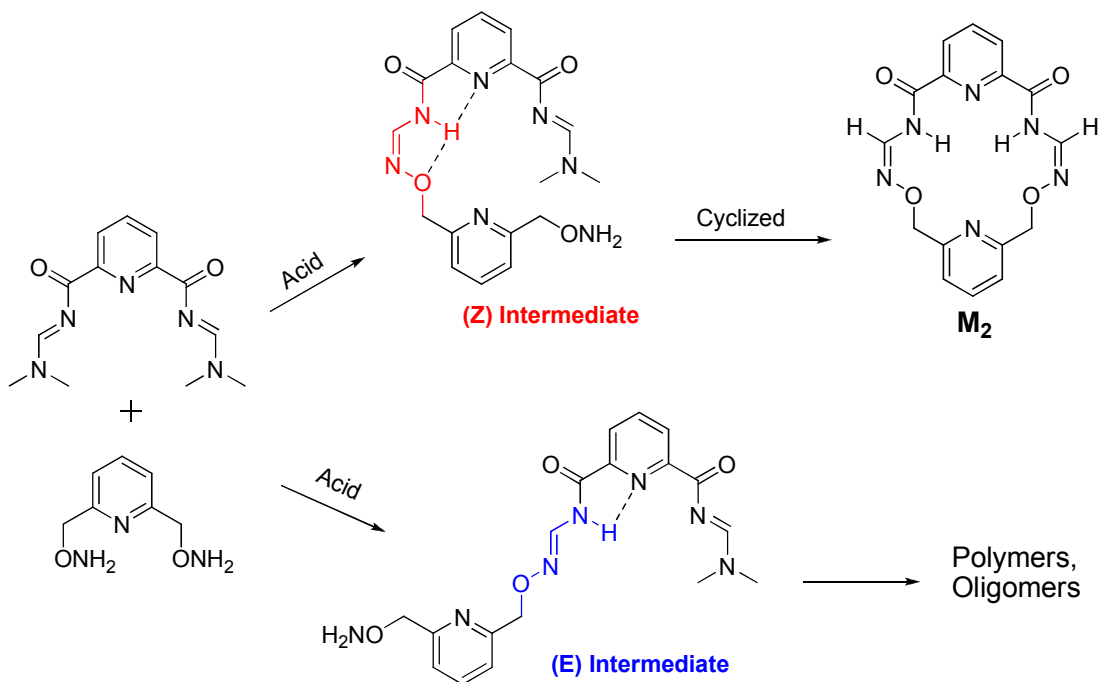
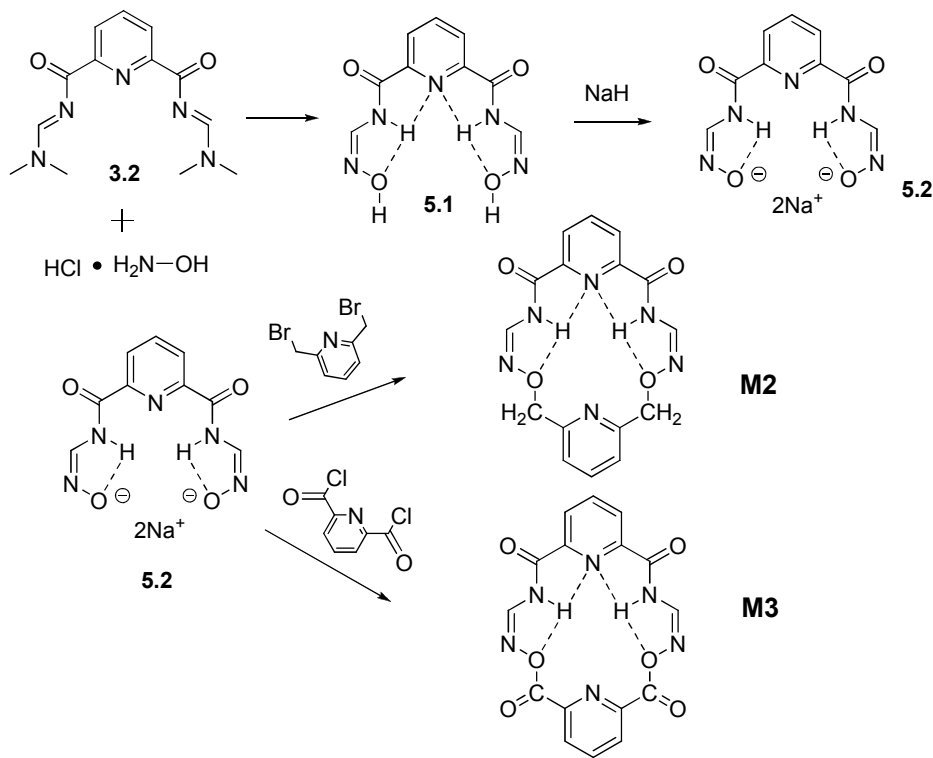


**Figure 5.1** Curved Z and linear E intermediates leading to different products.

In the future, an improved synthetic method for the target macrocycles is considered as shown in **Scheme 5.1** and is being explored by Alexandre Faurie, a summer student (May-August 2011). We already know that bis-acyl-formamidine **3.2** reacts with hydroxylamine hydrochloride in the presence of acetic acid (4.0 equivalents) to give the Z/Z isomer of compound **5.1** as the major product.



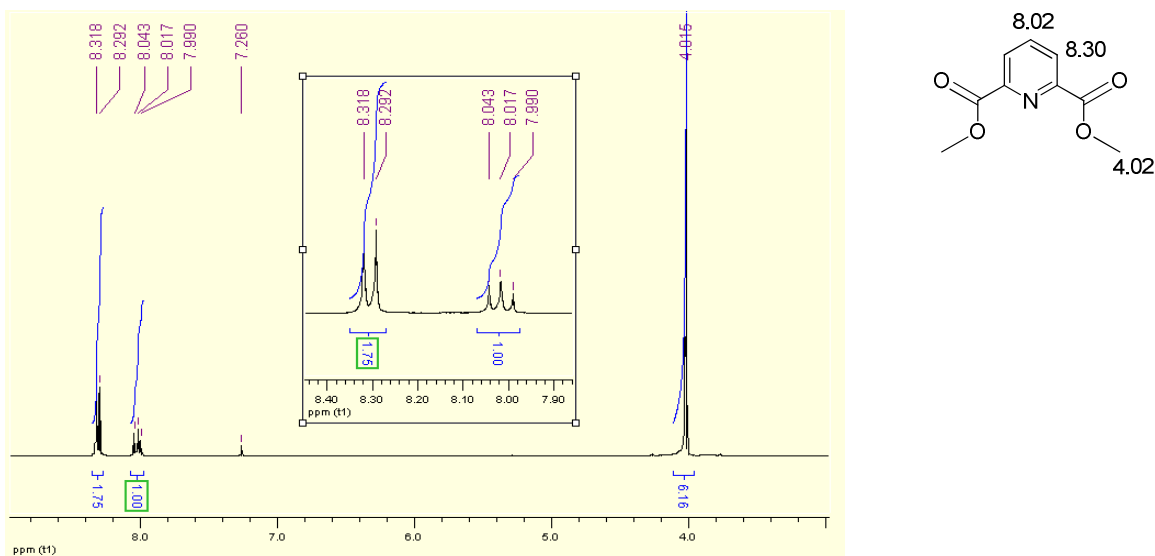
**Scheme 5.1** Improved synthetic method for **M2** and **M3**.

The next step to be explored is its deprotonation by sodium hydride (for instance) to form the **5.2** bis-anion, hopefully in a pre-organized, curved (*Z* form), and as a good nucleophile (equivalent of an alkoxide). Electrophiles such as dibromomethylpyridine and pyridine-dicarbonyl dichloride may then be able to condense with **5.2** to generate **M2** and the even more planar **M3** macrocycle, respectively.

## Appendix A: NMR and MS spectra

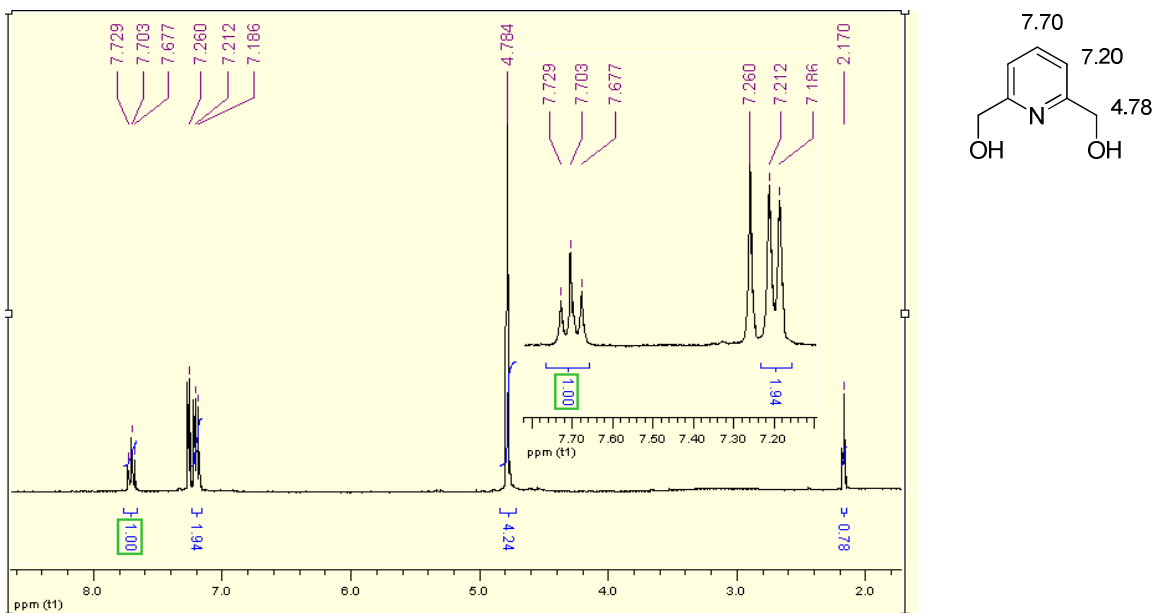
### **Pyridine-2,6-dimethylester (2.1)**

<sup>1</sup>H NMR (300 MHz; CDCl<sub>3</sub>; 25 °C)



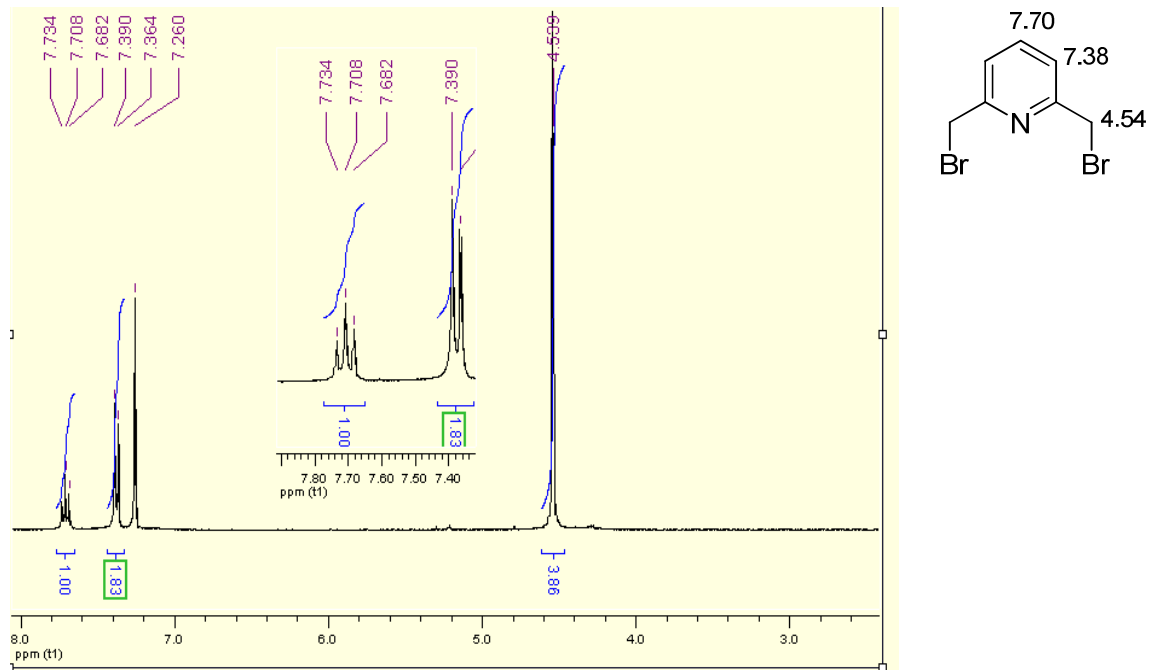
### **Pyridine-2,6-dimethylalcohol (2.2)**

<sup>1</sup>H NMR (300 MHz; CDCl<sub>3</sub>; 25 °C)



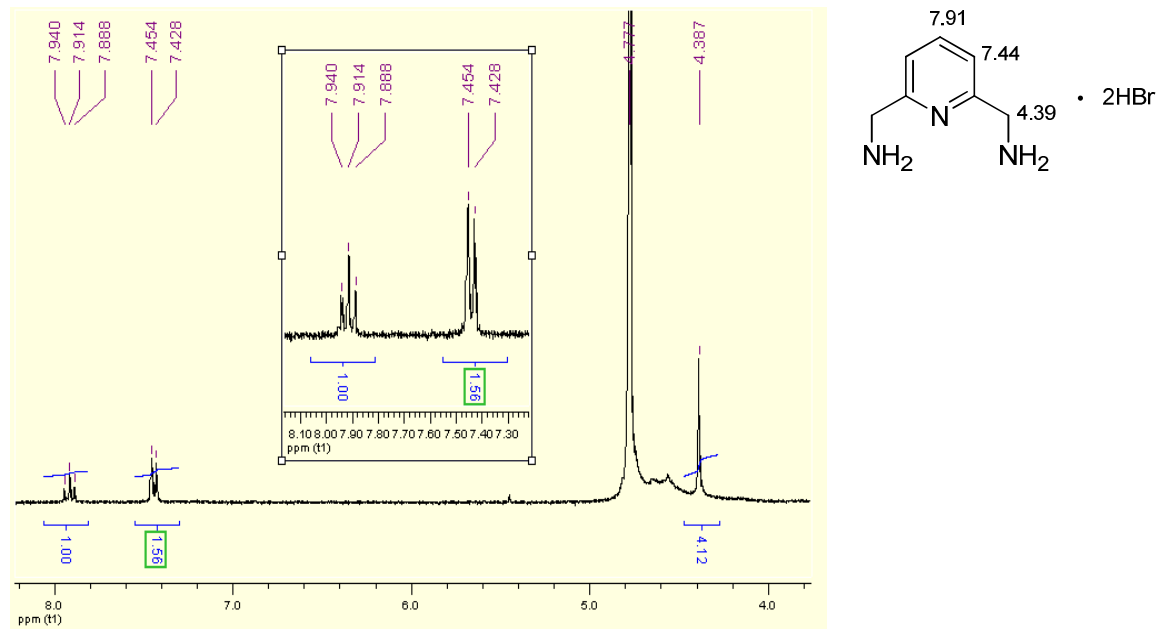
### 2,6-Bis(bromomethyl)-pyridine (2.3)

<sup>1</sup>H NMR (300 MHz; CDCl<sub>3</sub>; 25 °C)



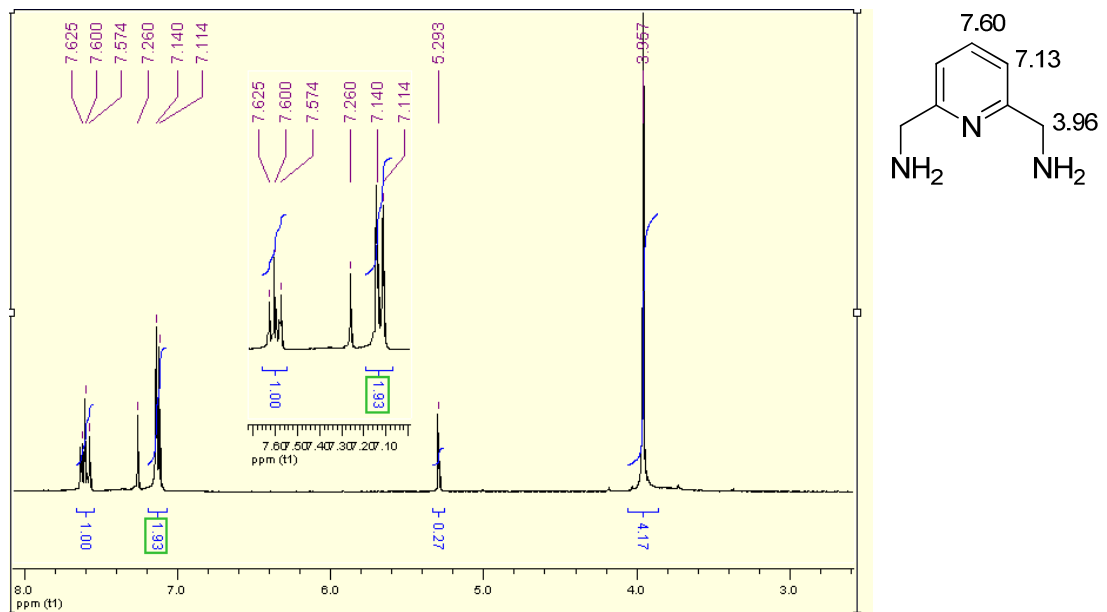
### Pyridine-2,6-diylidemethanammonium bromide (2.4a)

<sup>1</sup>H NMR (300 MHz; D<sub>2</sub>O; 25 °C)



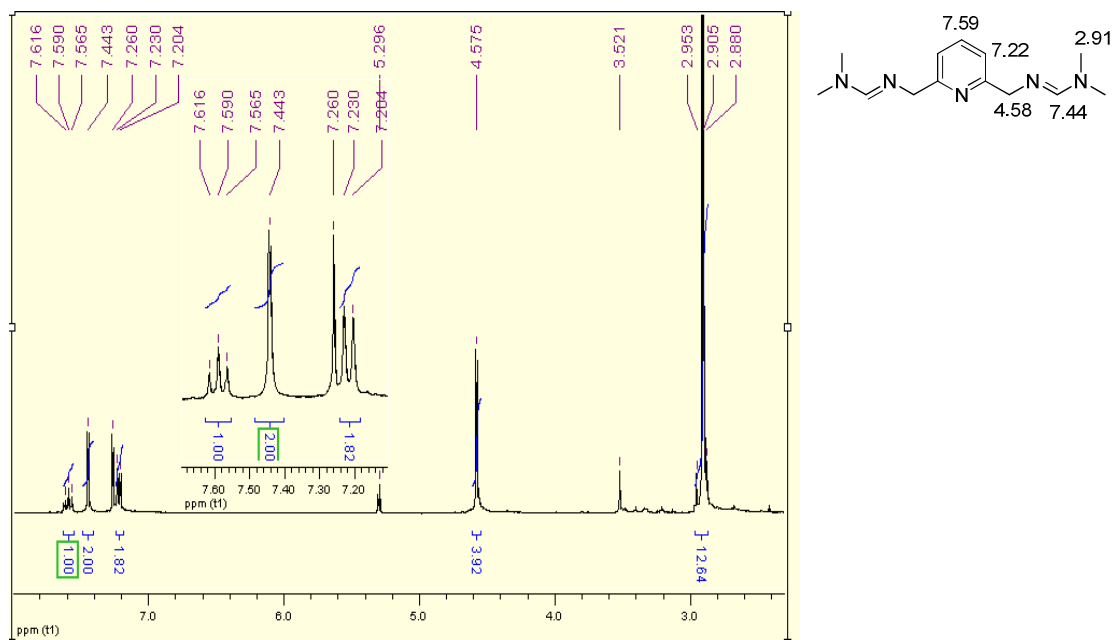
## **Pyridine-2,6-diylidemethanamine (2.4)**

<sup>1</sup>H NMR (300 MHz; CDCl<sub>3</sub>; 25 °C)



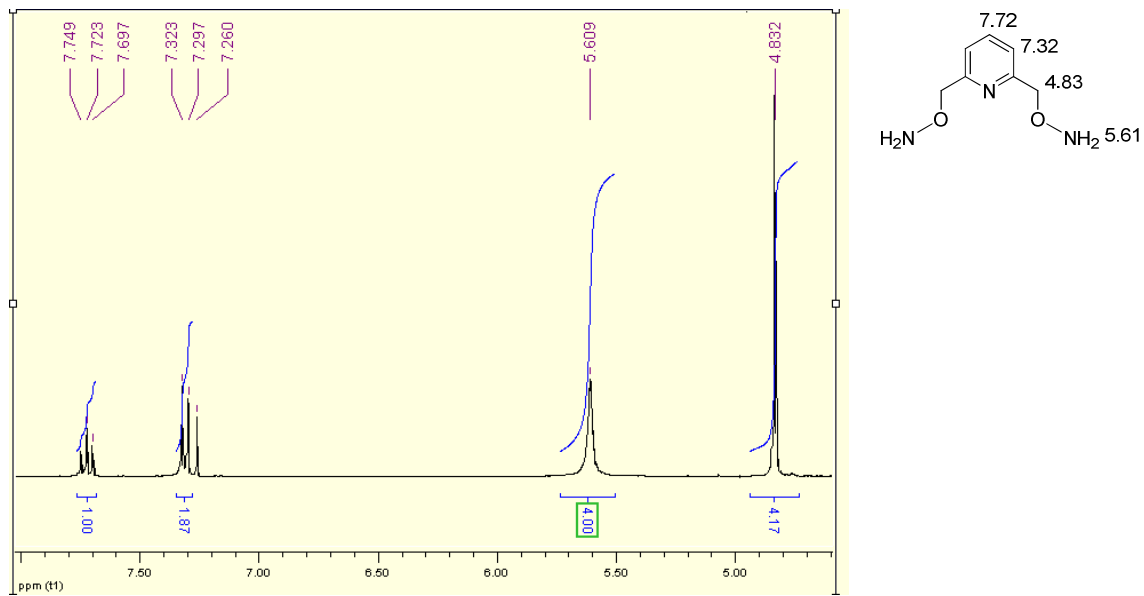
### **Pyridine-2,6-diylbis(methylene)bis(N,N-dimethylformamidamide) (2.6)**

<sup>1</sup>H NMR (300 MHz; CDCl<sub>3</sub>; 25 °C)



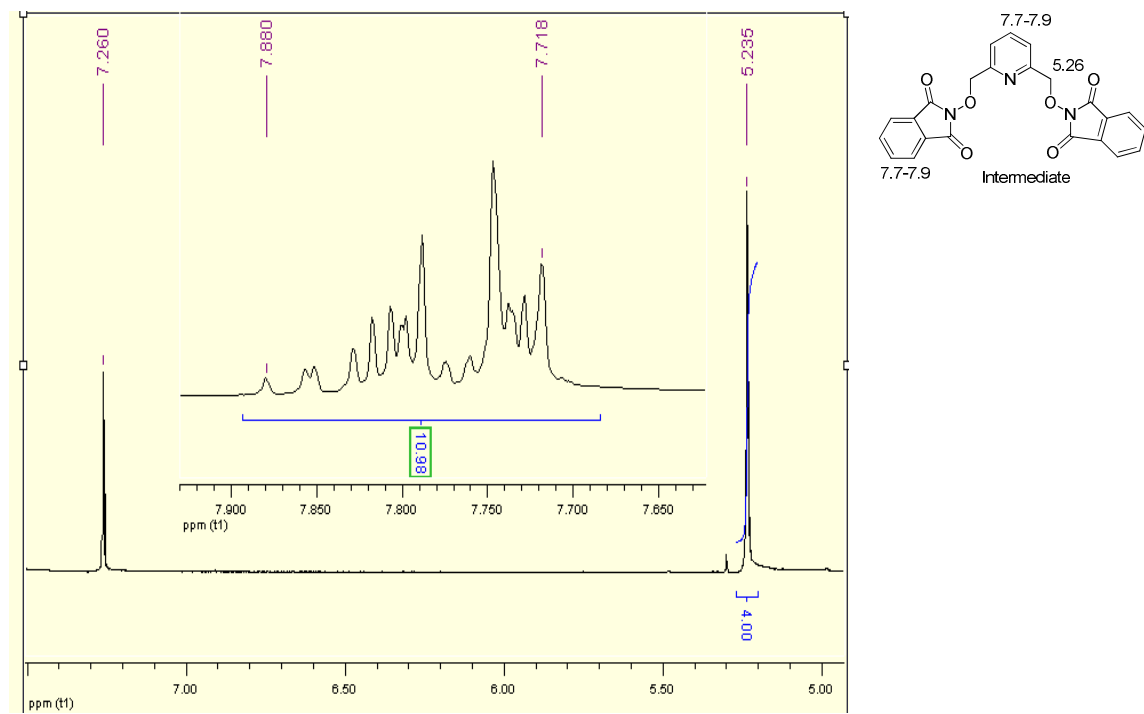
**O,O'-(pyridine-2,6-diylbis(methylene))bis(hydroxylamine) (2.5)**

<sup>1</sup>H NMR (300 MHz; CDCl<sub>3</sub>; 25 °C)

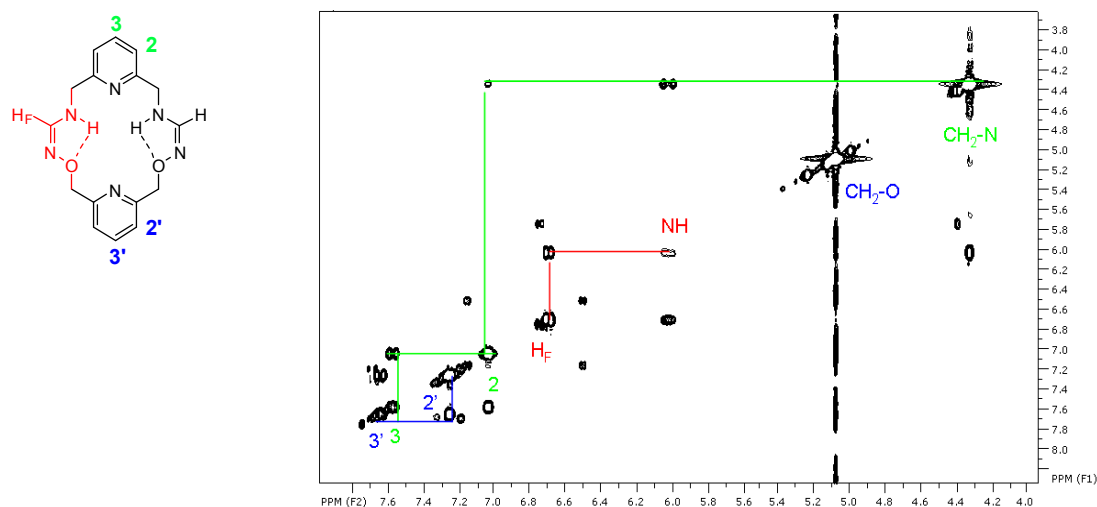


**Intermediate (precursor for compound 2.5)**

<sup>1</sup>H NMR (300 MHz; CDCl<sub>3</sub>; 25 °C)



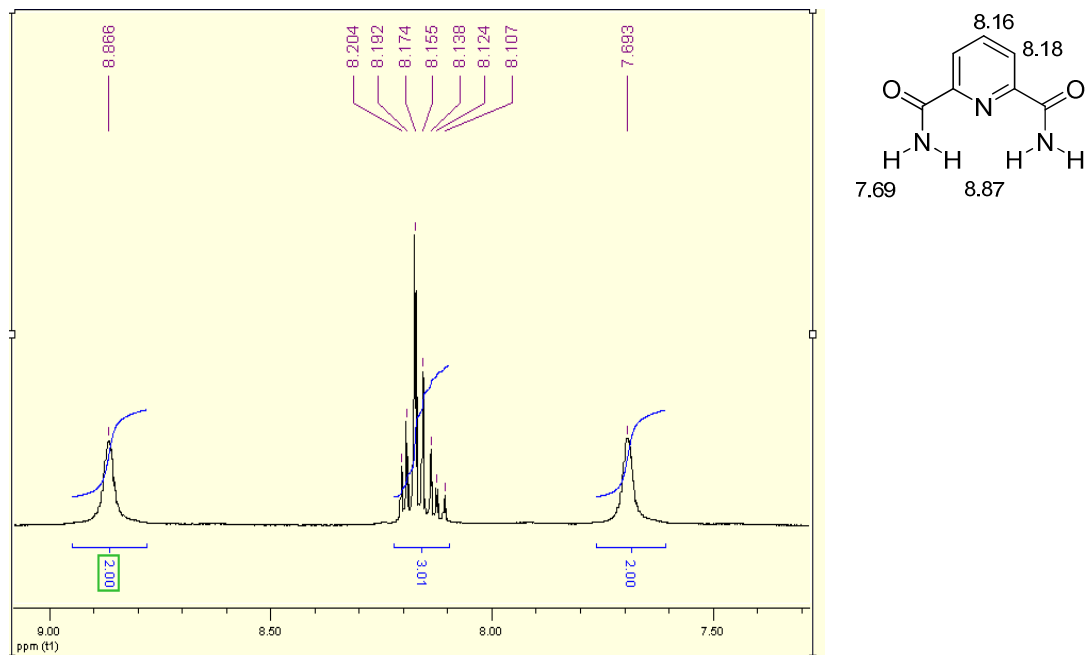
### Macrocyclic M1- COSY (400 MHz; CDCl<sub>3</sub>; 25 °C)



The COSY spectrum was assigned by the lines and labels shown above. The CH<sub>2</sub> (4.32 ppm) adjacent to nitrogen has correlation with the pyridine protons at 7.04 ppm which correlates with the neighbouring pyridine proton at 7.65 ppm. The pyridine protons at 7.26 ppm correlate with the neighbouring pyridine proton at 7.58 ppm. The NH at 6.04 ppm correlates with the H<sub>F</sub> at 6.70 ppm.

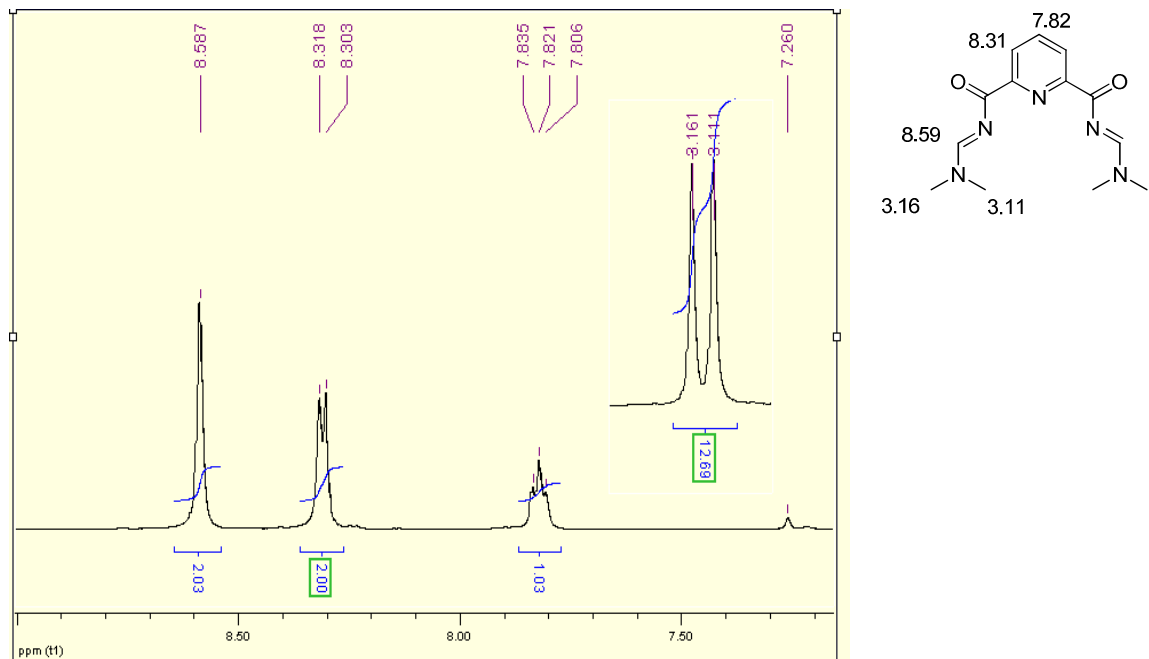
### 2,6-Pyridine dicarboxamide (3.1)

#### <sup>1</sup>H NMR (300 MHz; DMSO-d6; 25 °C)

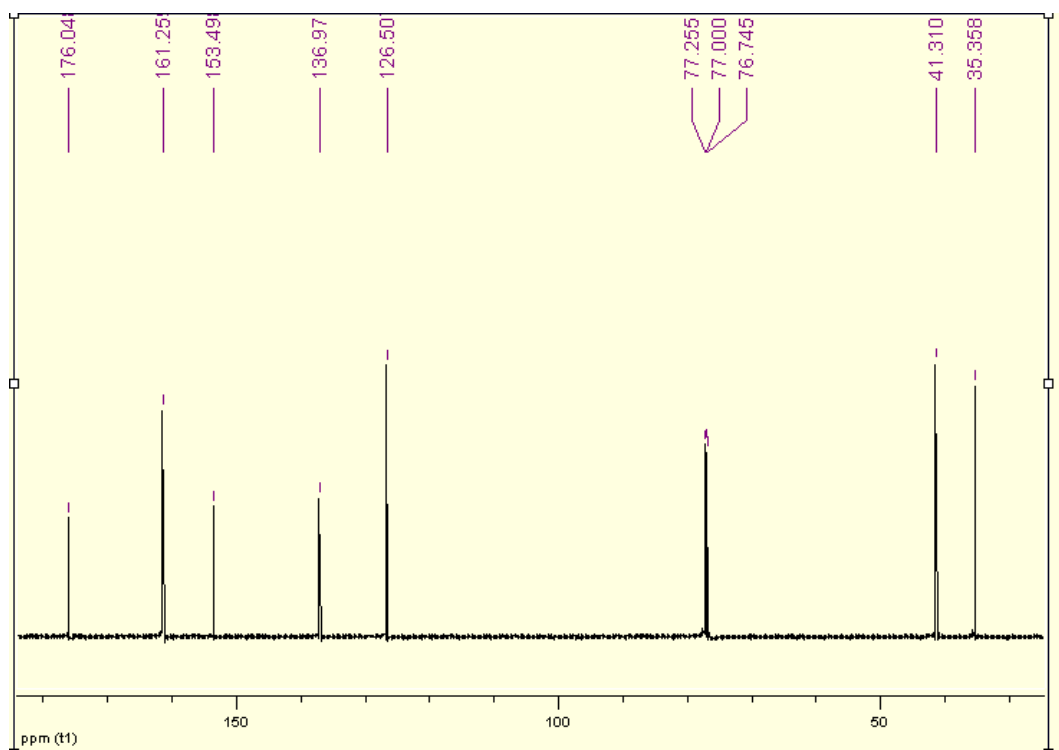


(N<sub>2</sub>E,N<sub>6</sub>E)-N<sub>2</sub>,N<sub>6</sub>-bis((dimethylamino)methylene)pyridine-2,6-dicarboxamide (3.2)

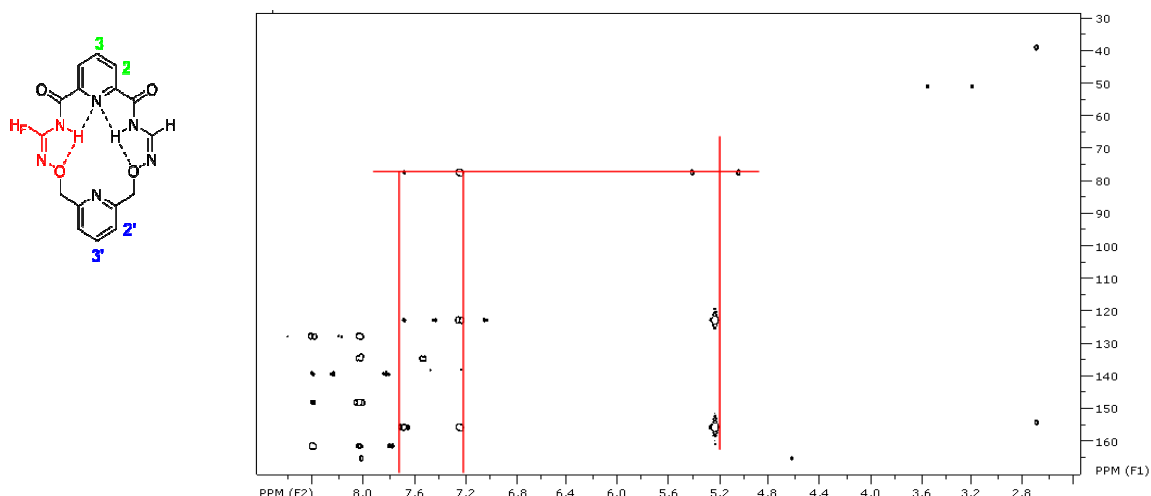
<sup>1</sup>H NMR (500 MHz; CDCl<sub>3</sub>; 25 °C)



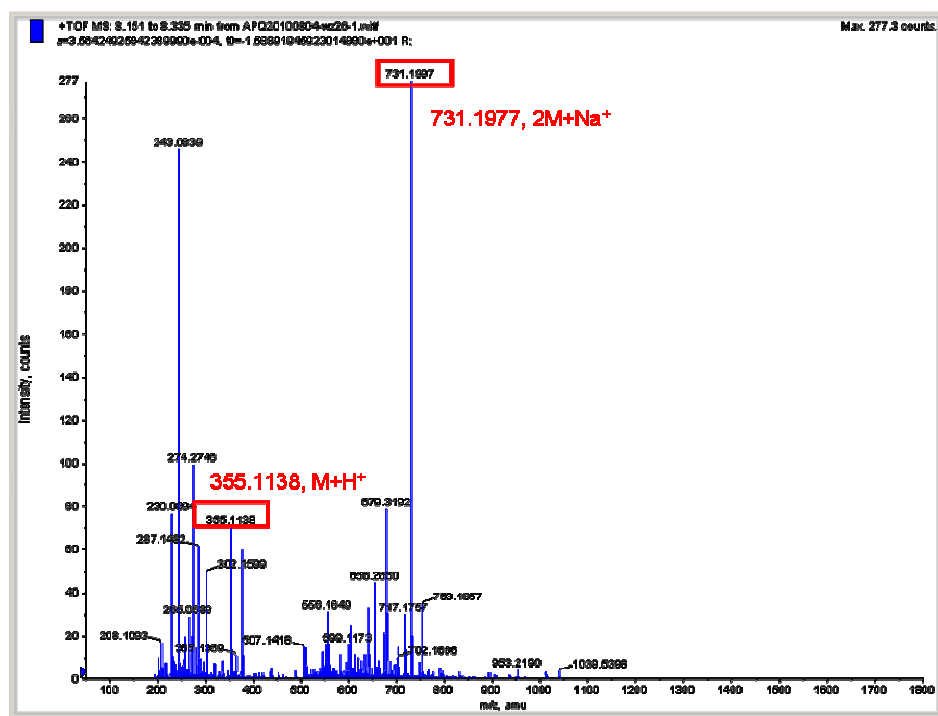
<sup>13</sup>C NMR (125 MHz; CDCl<sub>3</sub>; 25 °C)



### Macrocyclic M2-HMBC (500 MHz; CDCl<sub>3</sub>; 25 °C)

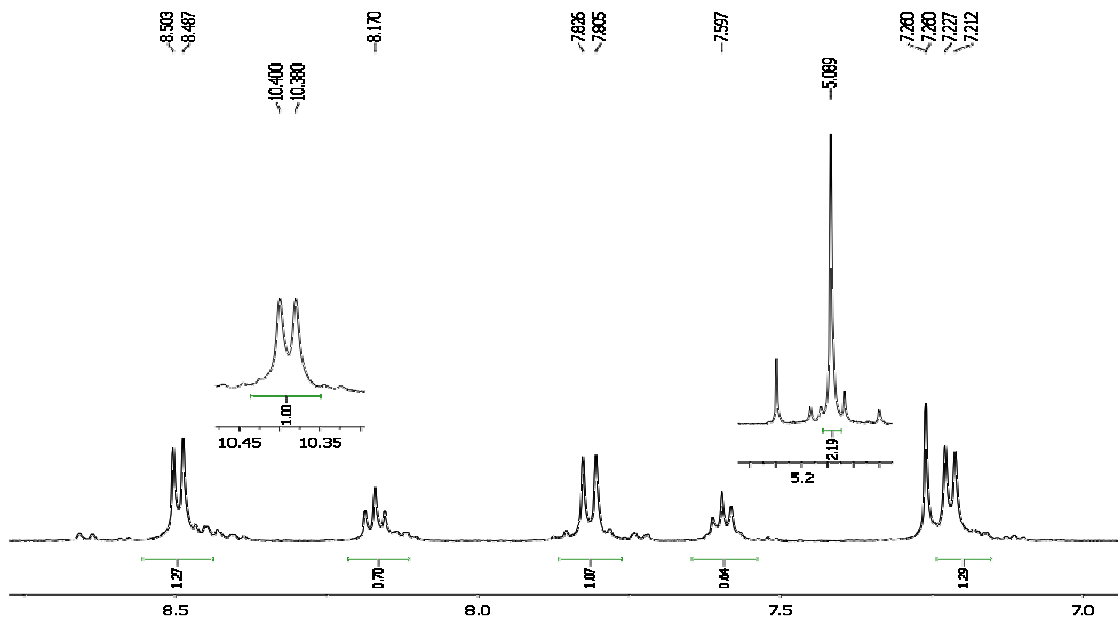


### ESI<sup>+</sup>-MS



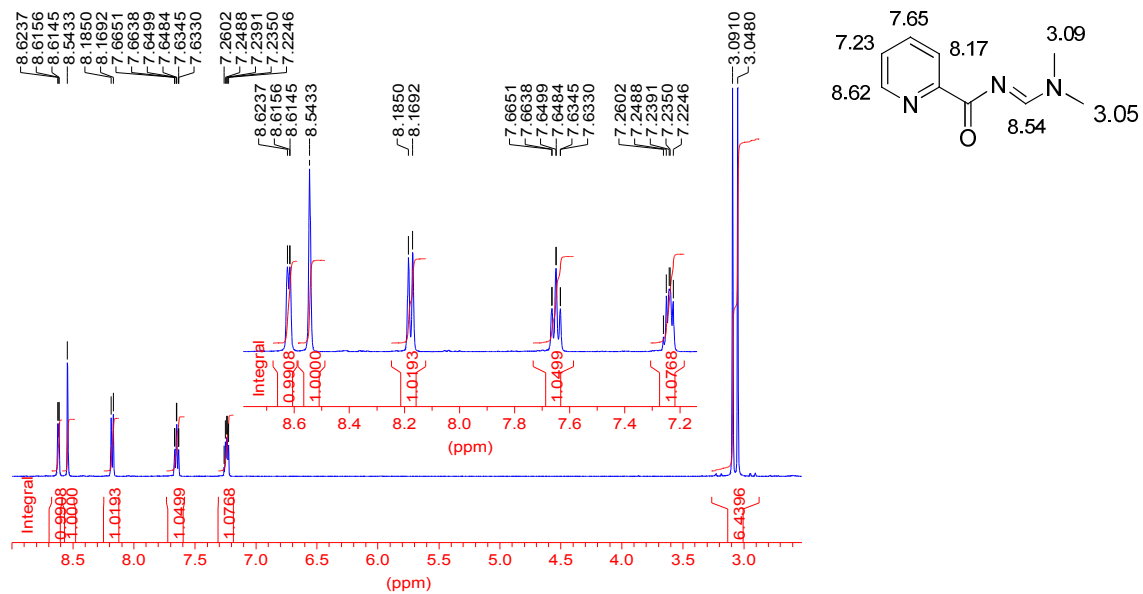
## Maxi-M2

<sup>1</sup>H NMR (500 MHz; CDCl<sub>3</sub>; 25 °C)

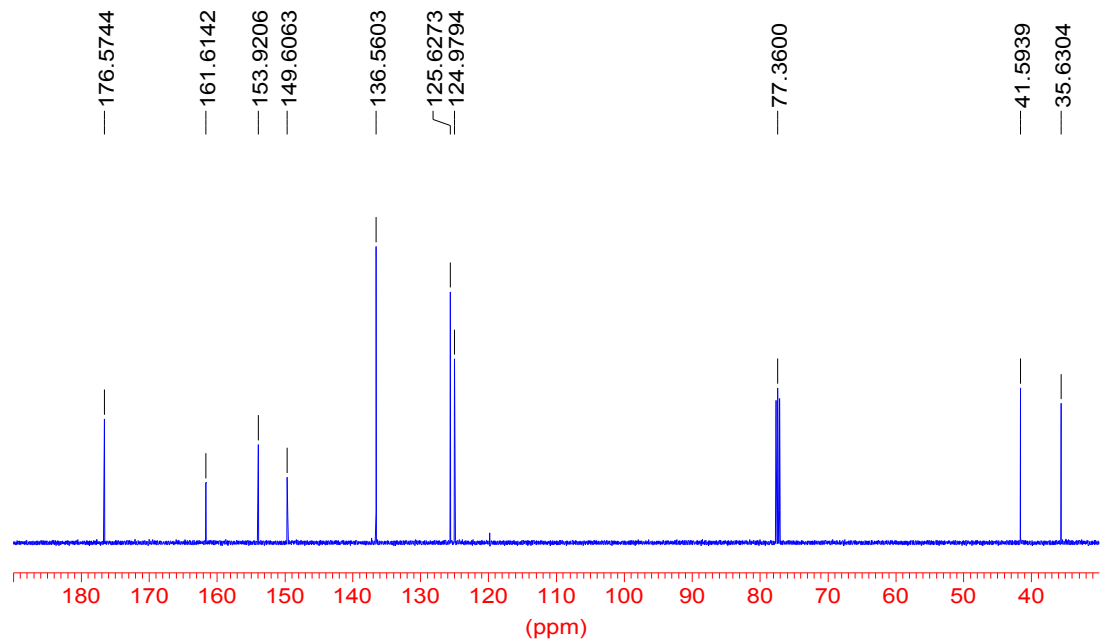


### (E)-N-((dimethylamino)methylene)picolinamide (4.3)

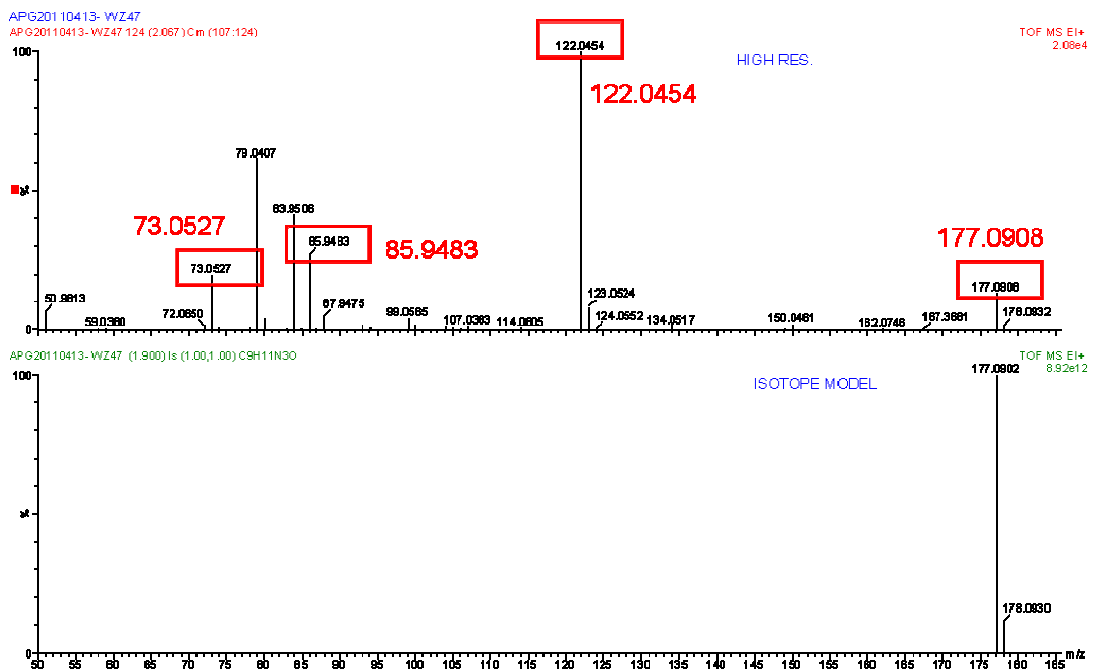
<sup>1</sup>H NMR (500 MHz; CDCl<sub>3</sub>; 25 °C)



$^{13}\text{C}$  NMR (125 MHz;  $\text{CDCl}_3$ ; 25 °C)

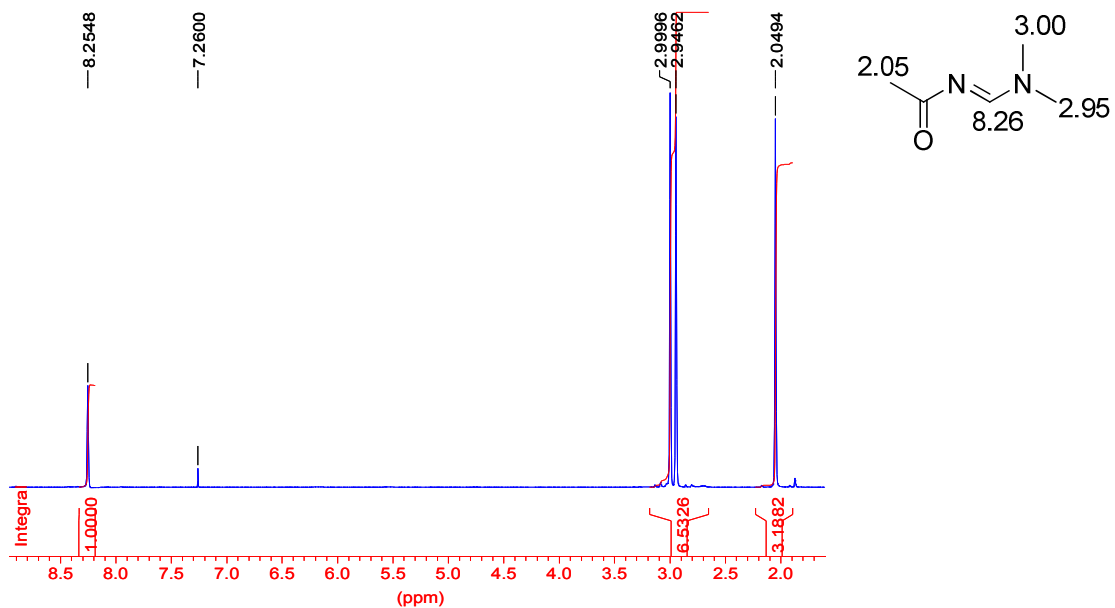


$\text{EI}^+$ -HRMS

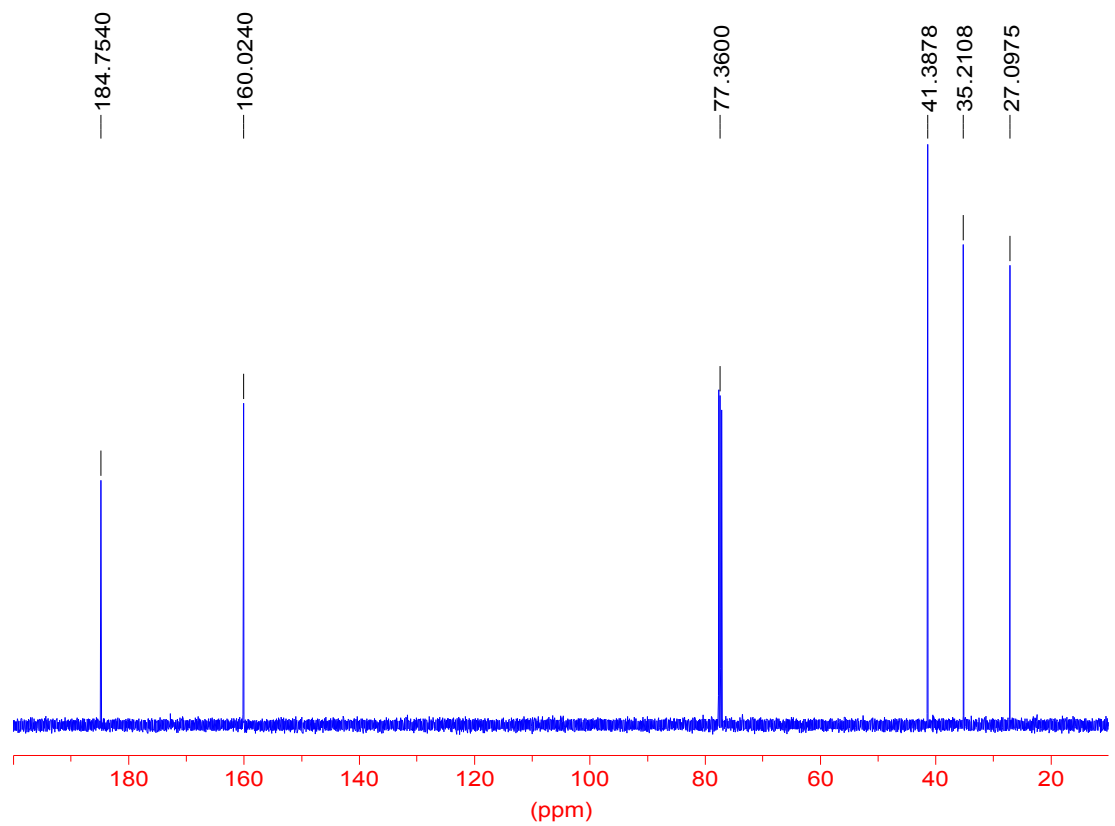


**(E)-N-((dimethylamino)methylene)acetamide (4.6)**

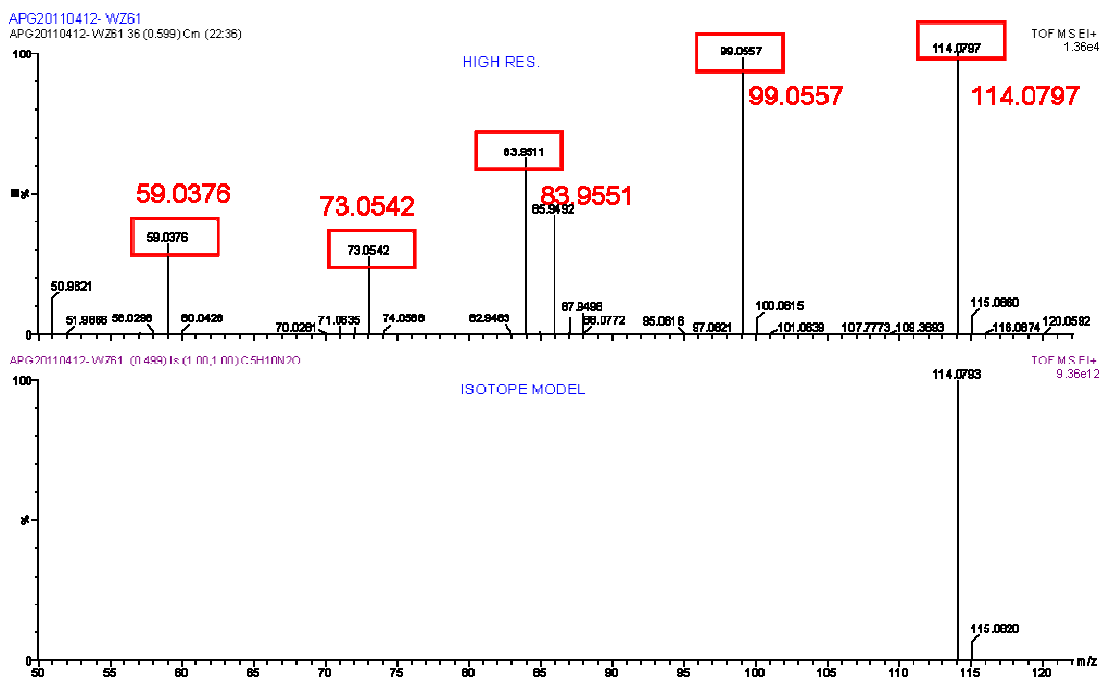
<sup>1</sup>H NMR (500 MHz; CDCl<sub>3</sub>; 25 °C)



<sup>13</sup>C NMR (125 MHz; CDCl<sub>3</sub>; 25 °C)

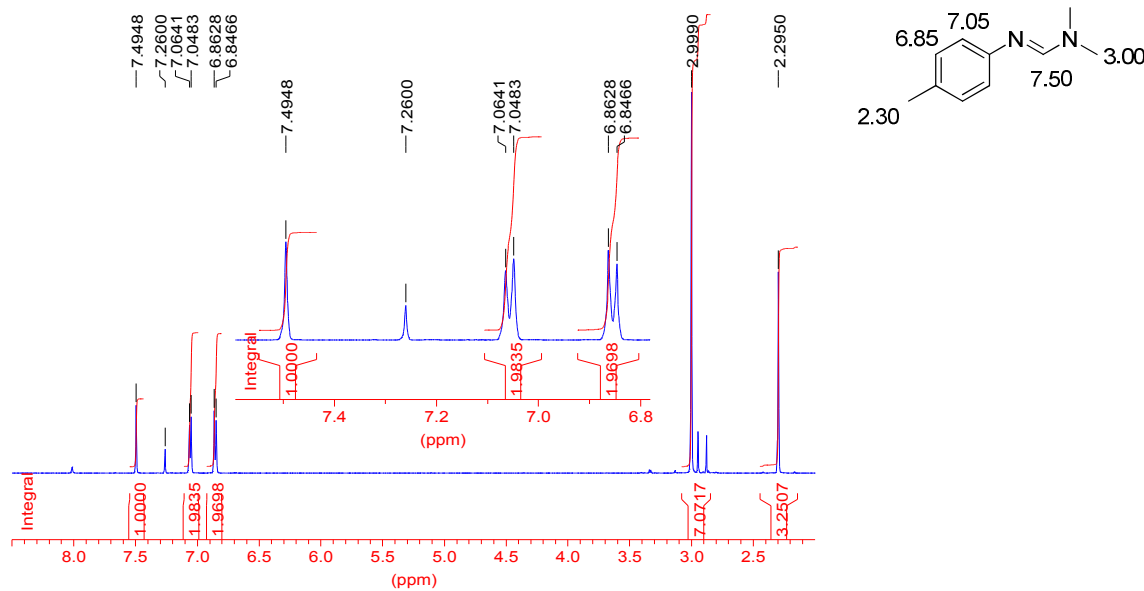


EI<sup>+</sup>-HRMS



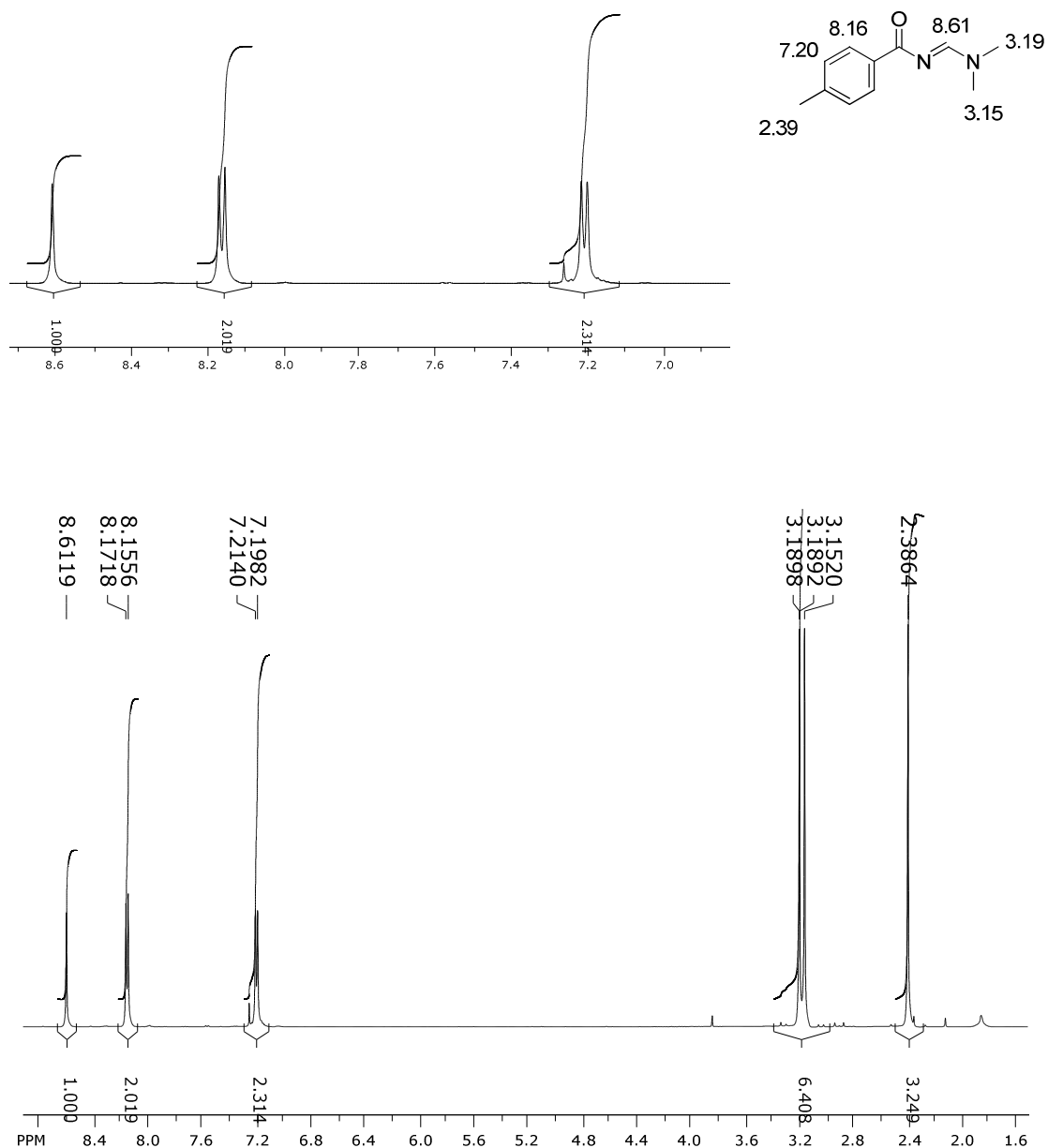
### (E)-N,N-dimethyl-N'-p-tolylformamidamide (4.9)

<sup>1</sup>H NMR (500 MHz; CDCl<sub>3</sub>; 25 °C)



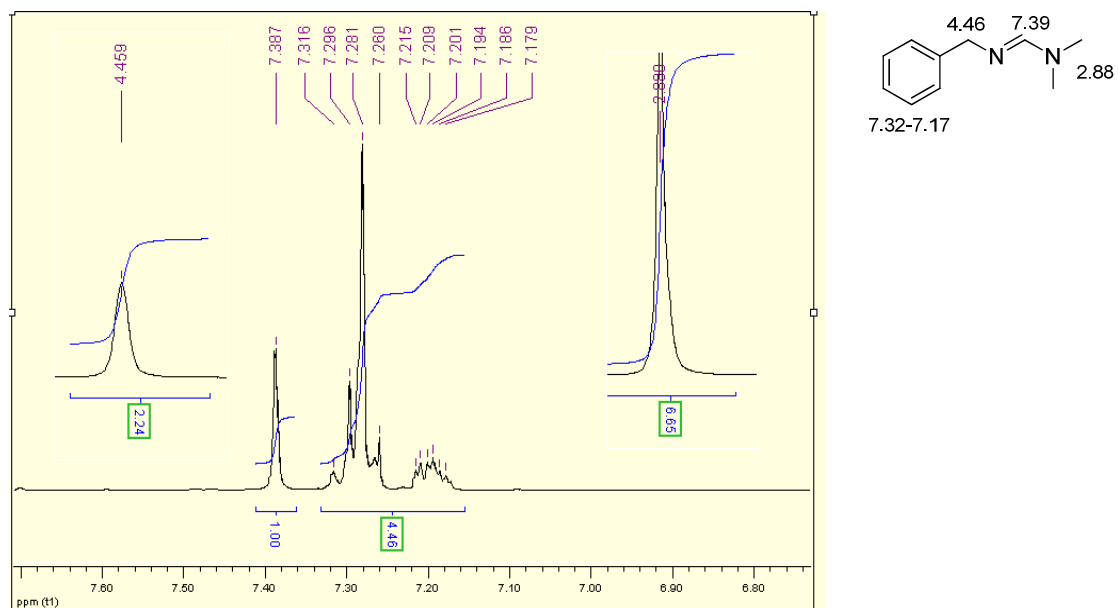
**(E)-N-((dimethylamino)methylene)-4-methylbenzamide (4.13)**

$^1\text{H}$  NMR (500 MHz;  $\text{CDCl}_3$ ; 25 °C)



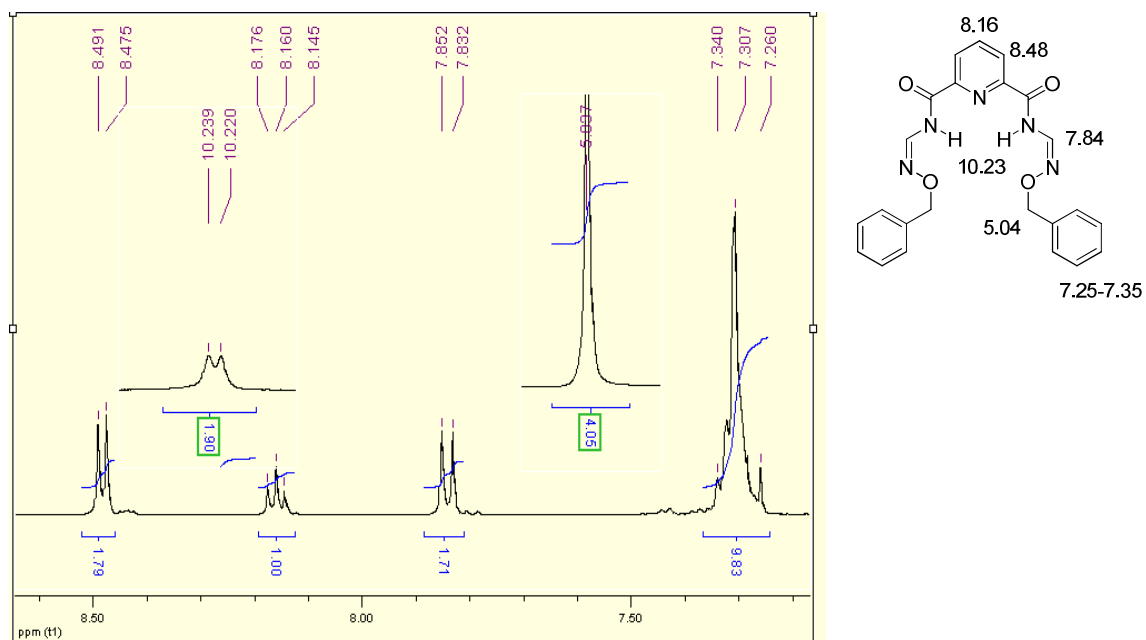
**(E)-N'-benzyl-N,N-dimethylformimidamide (4.10)**

<sup>1</sup>H NMR (500 MHz; CDCl<sub>3</sub>; 25 °C)

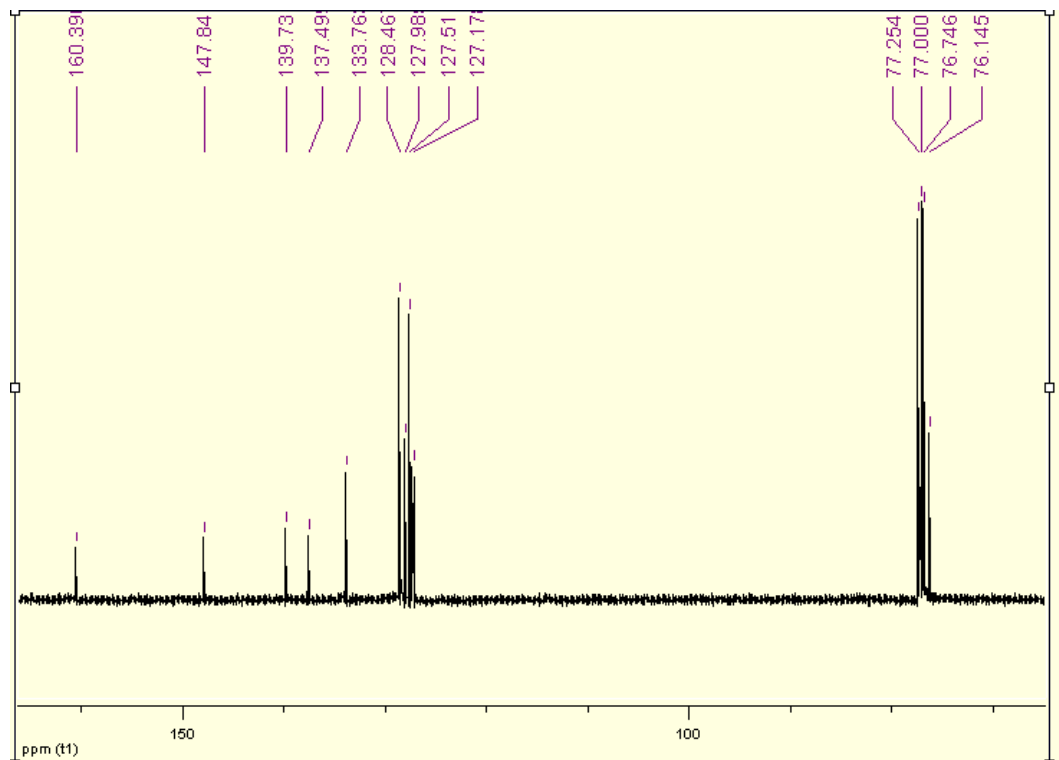


**N2,N6-bis((Z)-(benzyloxyimino)methyl)pyridine-2,6-dicarboxamide (4.2ZZ)**

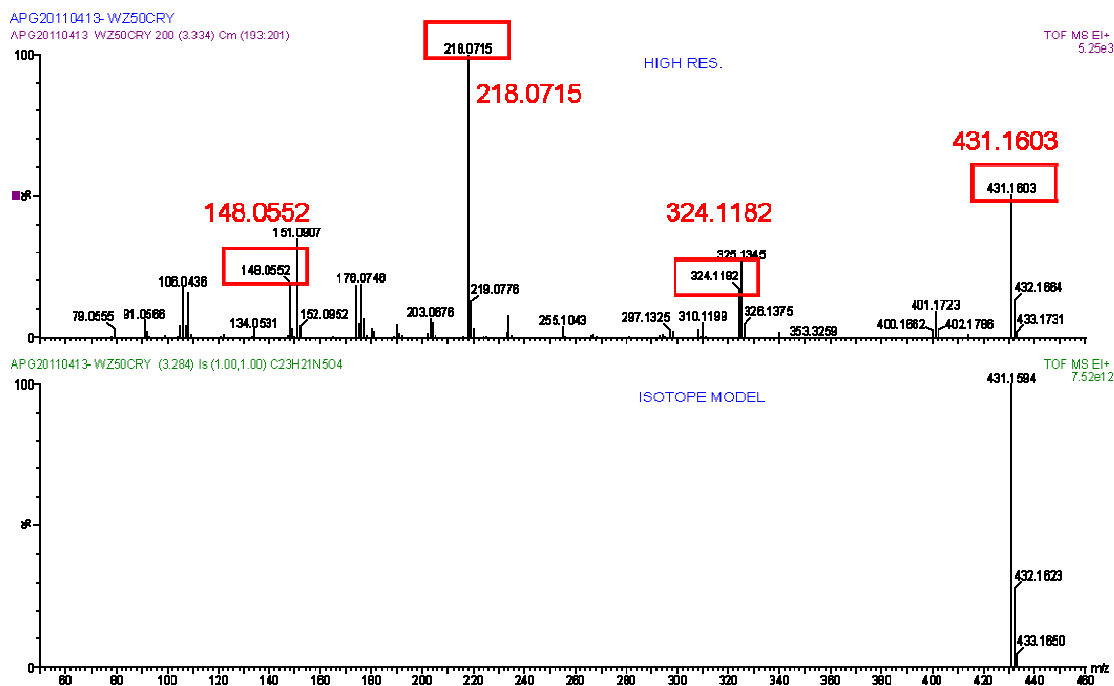
<sup>1</sup>H NMR (500 MHz; CDCl<sub>3</sub>; 25 °C)



<sup>13</sup>C NMR (125 MHz; CDCl<sub>3</sub>; 25 °C)

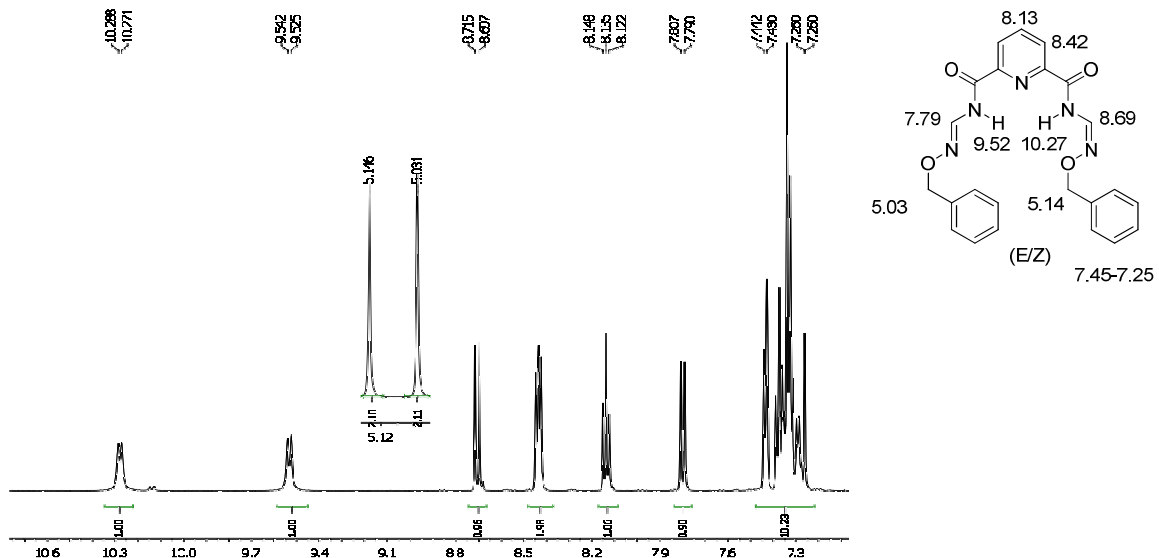


EI<sup>+</sup>-HRMS



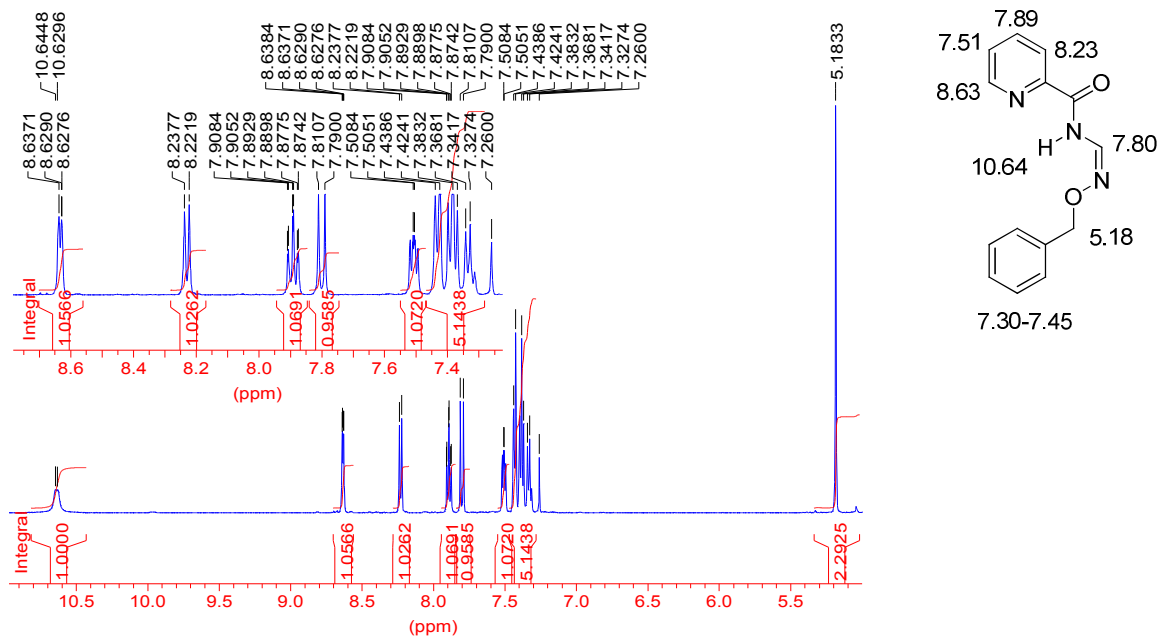
## N2-((E)-(benzyloxyimino)methyl)-N6-((Z)-(benzyloxyimino)methyl)pyridine-2,6-dicarboxamide (4.2ZE)

<sup>1</sup>H NMR (500 MHz; CDCl<sub>3</sub>; 25 °C)

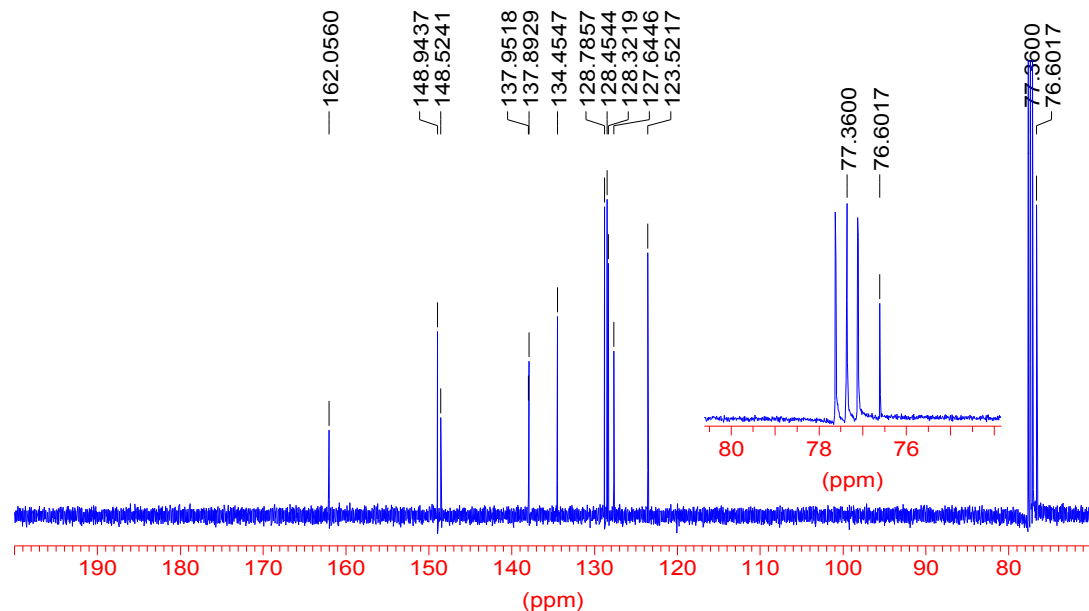


#### **Z)-N-((benzyloxyimino)methyl)picolinamide (4.4Z)**

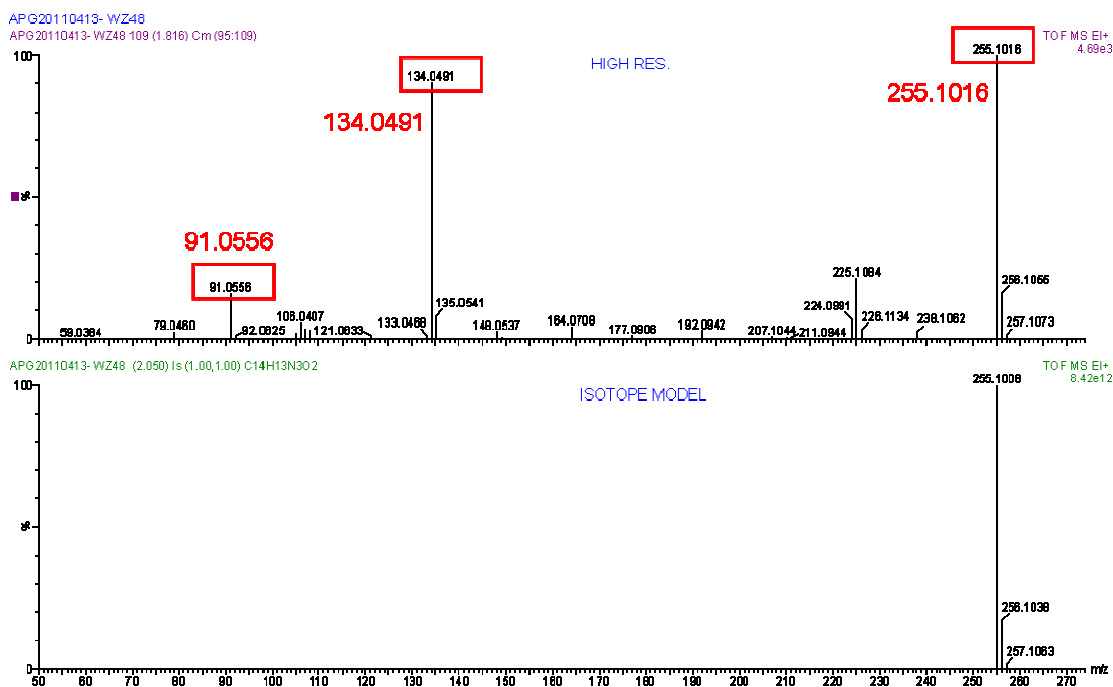
<sup>1</sup>H NMR (500 MHz; CDCl<sub>3</sub>; 25 °C)



<sup>13</sup>C NMR (125 MHz; CDCl<sub>3</sub>; 25 °C)

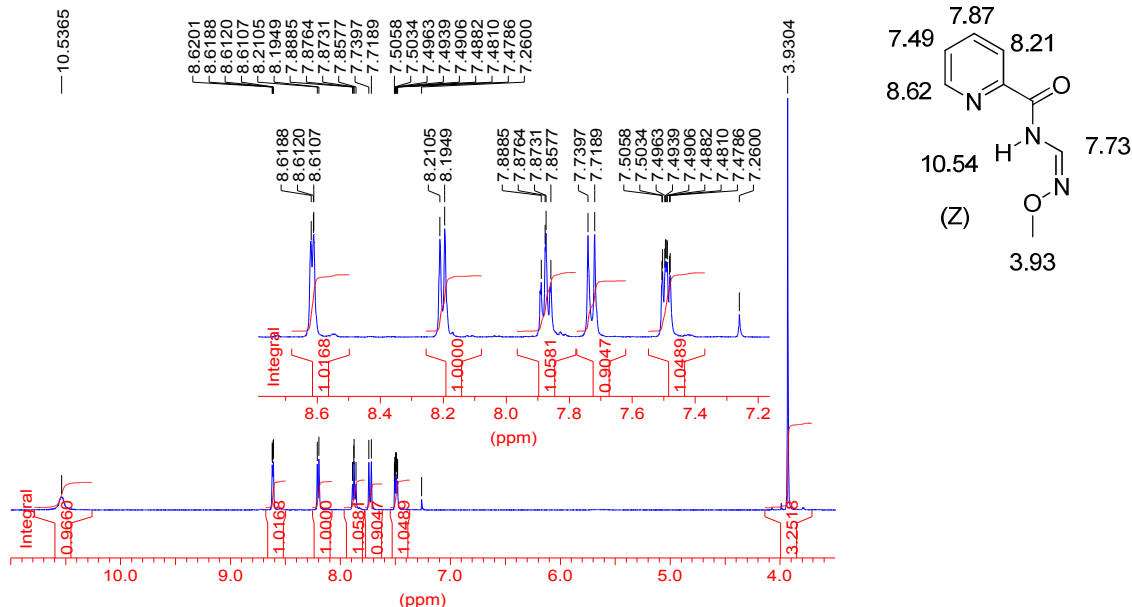


EI<sup>+</sup>-HRMS

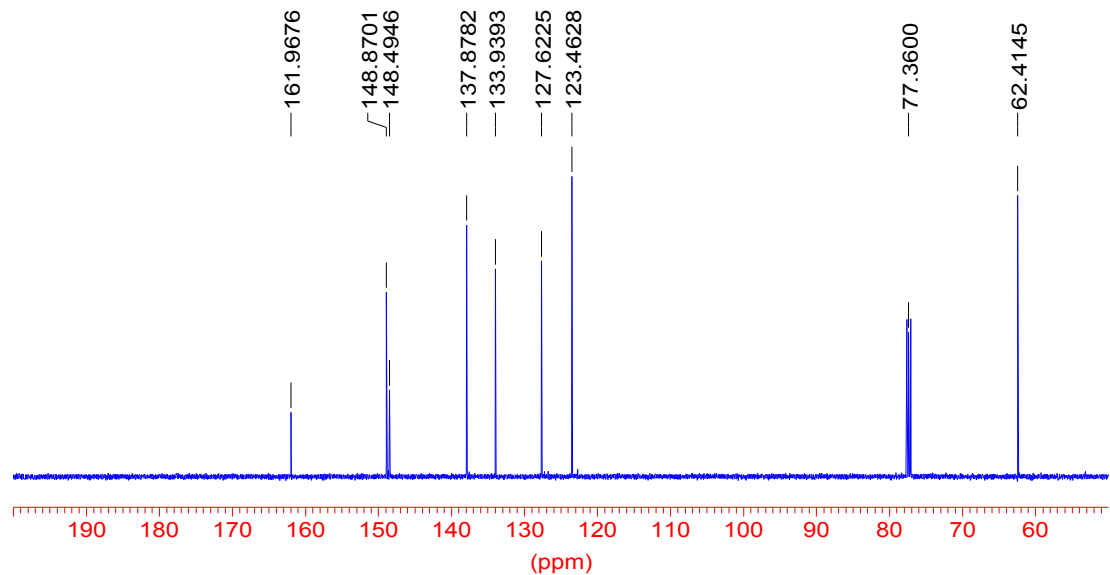


**(Z)-N-((methoxyimino)methyl)picolinamide (4.5Z)**

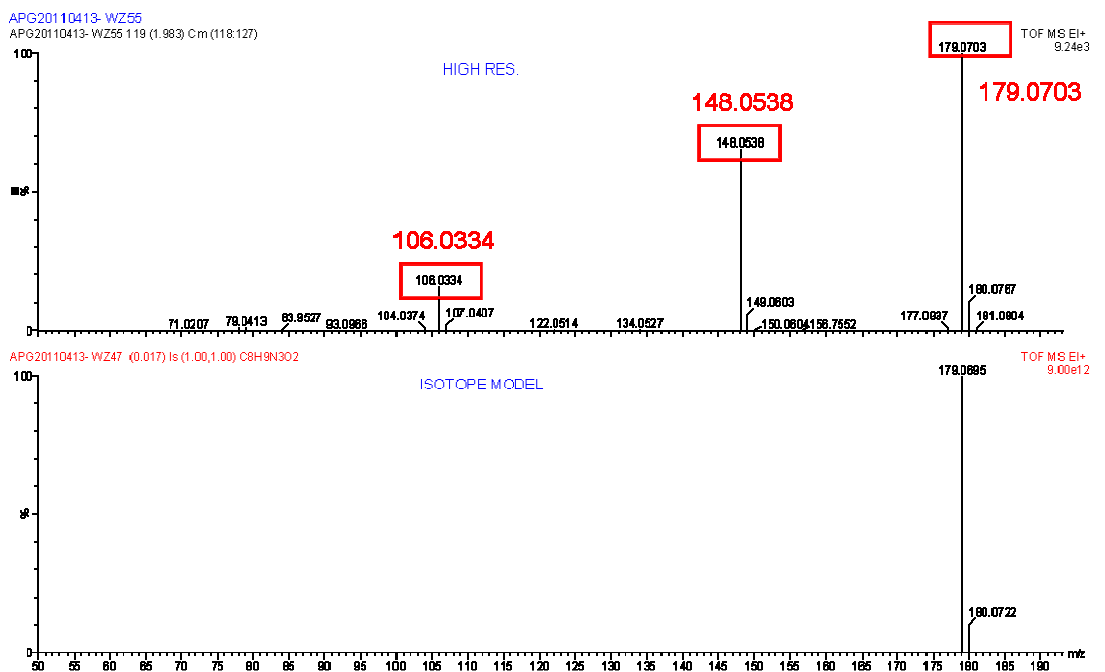
<sup>1</sup>H NMR (500 MHz; CDCl<sub>3</sub>; 25 °C)



<sup>13</sup>C NMR (125 MHz; CDCl<sub>3</sub>; 25 °C)

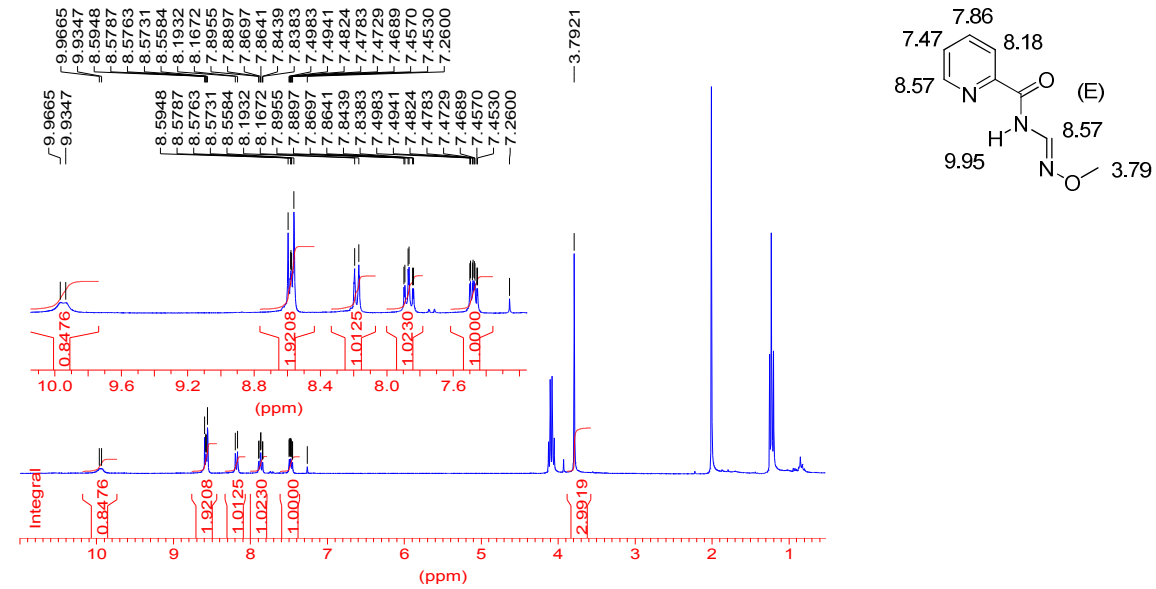


EI<sup>+</sup>-HRMS

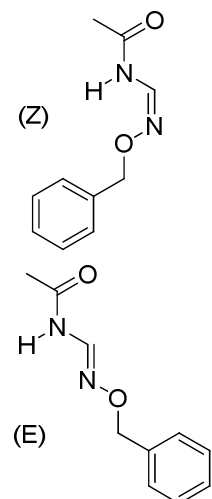
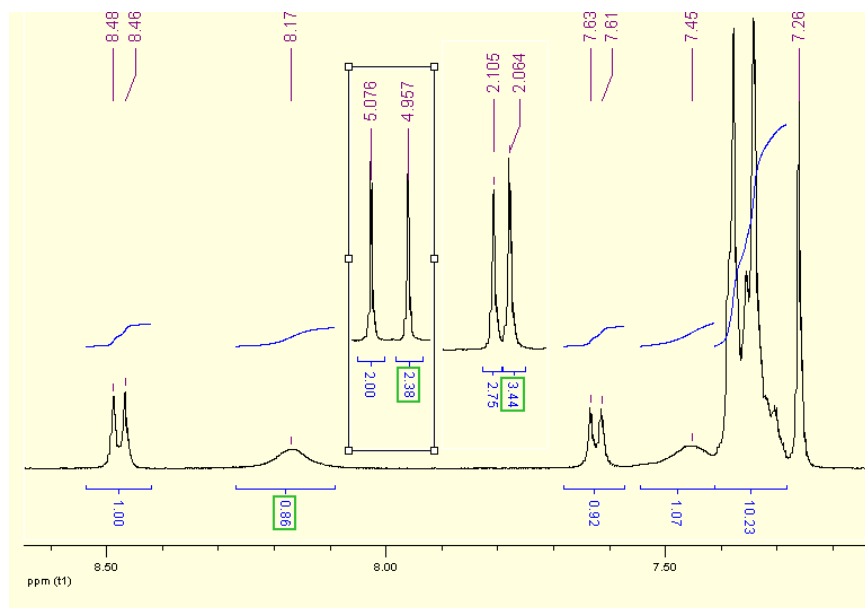


### (E)-N-((methoxyimino)methyl)picolinamide (4.5E)

<sup>1</sup>H NMR (500 MHz; CDCl<sub>3</sub>; 25 °C)

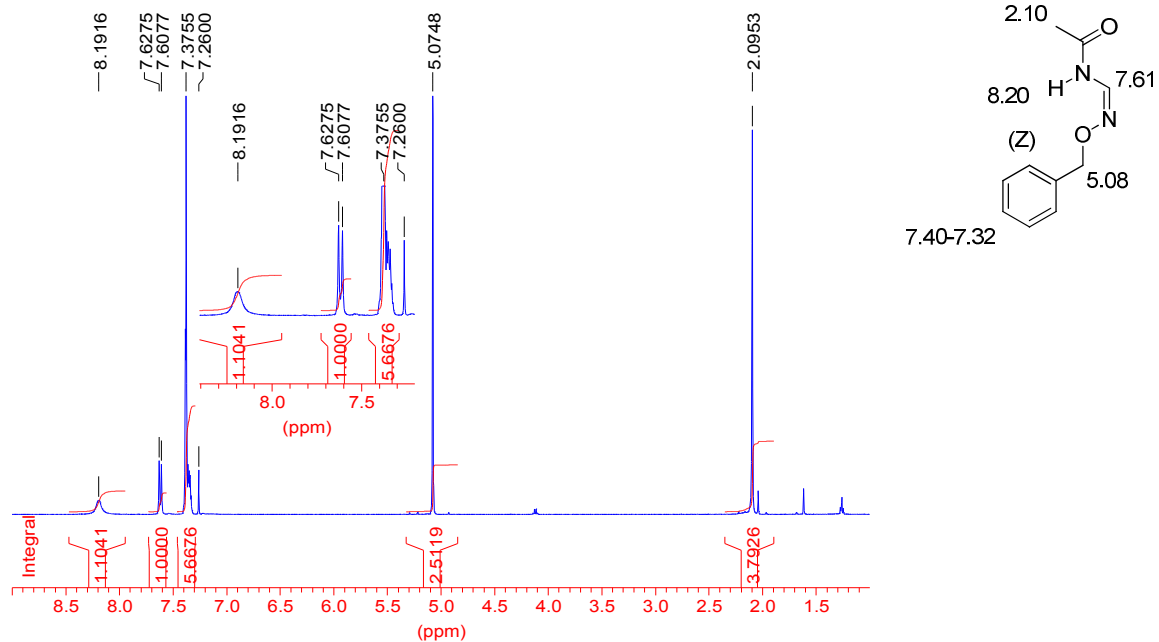


**E and Z isomeric mixtures of acetyl-formamidoxime (4.7E+4.7Z)**

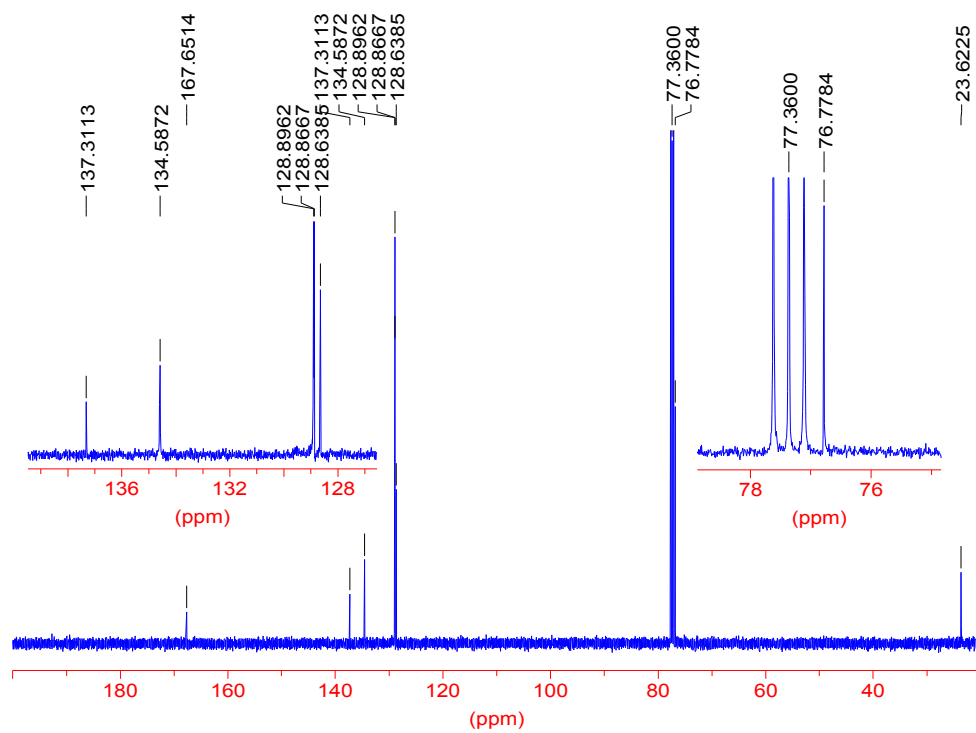


**(Z)-N-((benzyloxyimino)methyl)acetamide (4.7Z)**

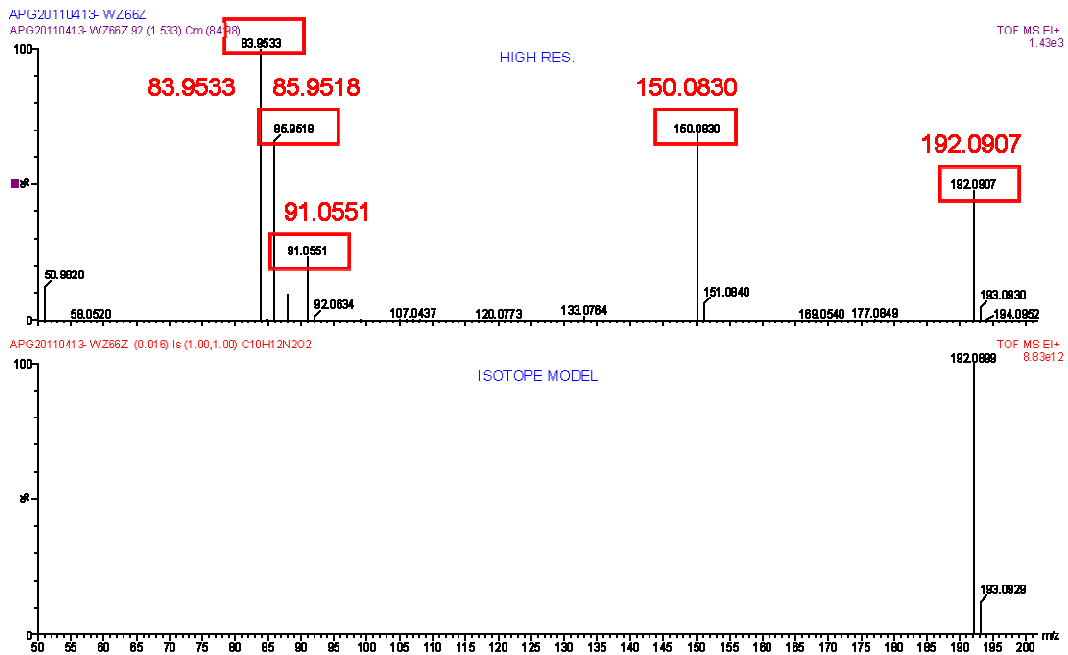
$^1\text{H}$  NMR (500 MHz;  $\text{CDCl}_3$ ; 25 °C)



<sup>13</sup>C NMR (125 MHz; CDCl<sub>3</sub>; 25 °C)

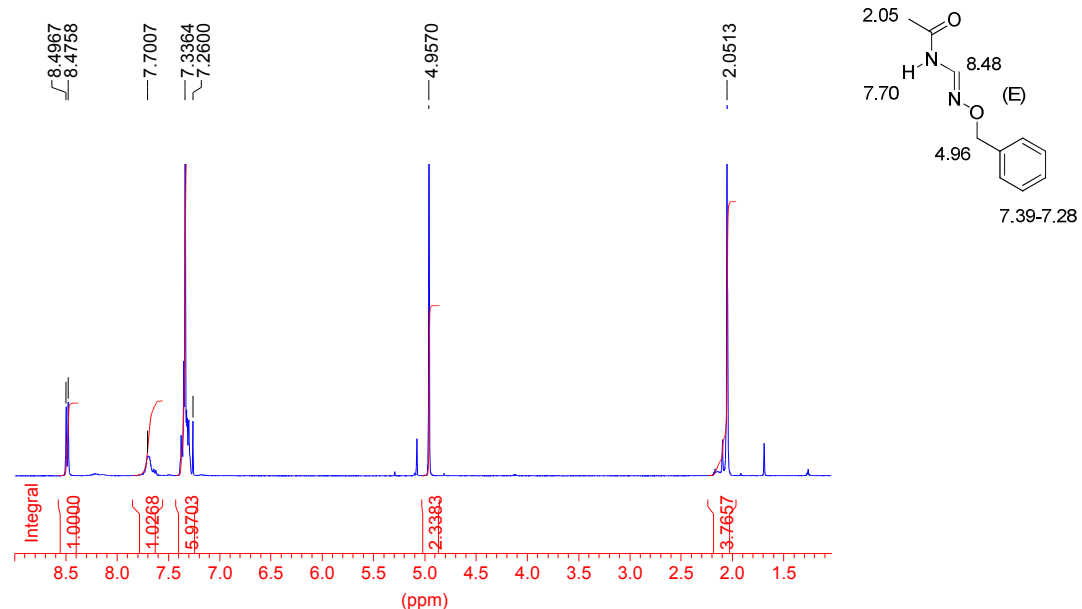


EI<sup>+</sup>-HRMS

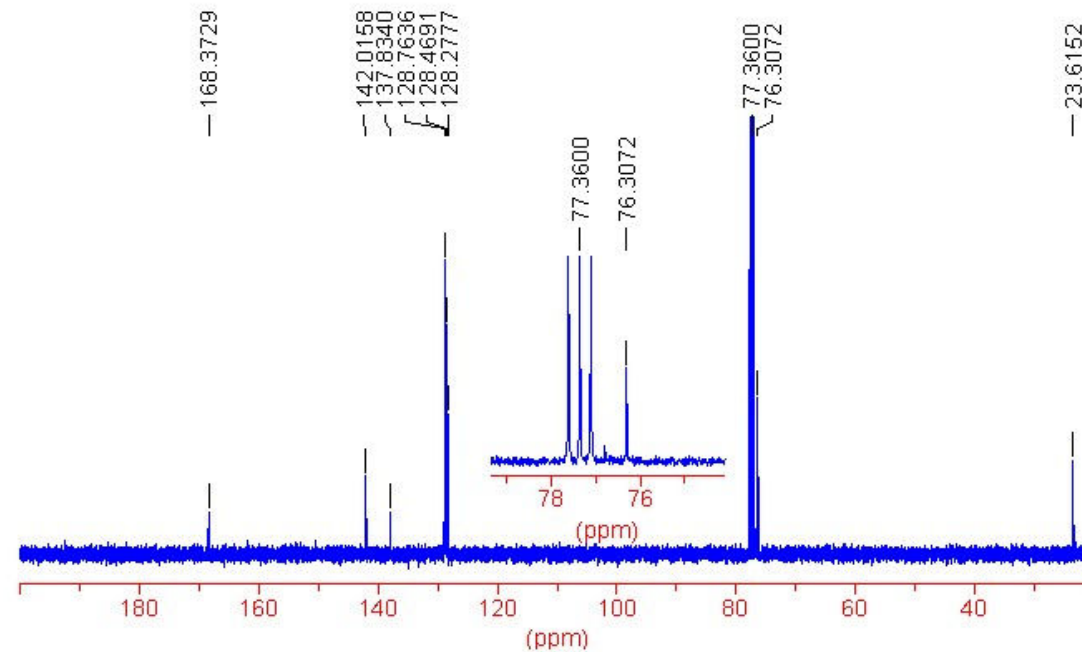


### (E)-N-((benzyloxyimino)methyl)acetamide (4.7E)

<sup>1</sup>H NMR (500 MHz; CDCl<sub>3</sub>; 25 °C)

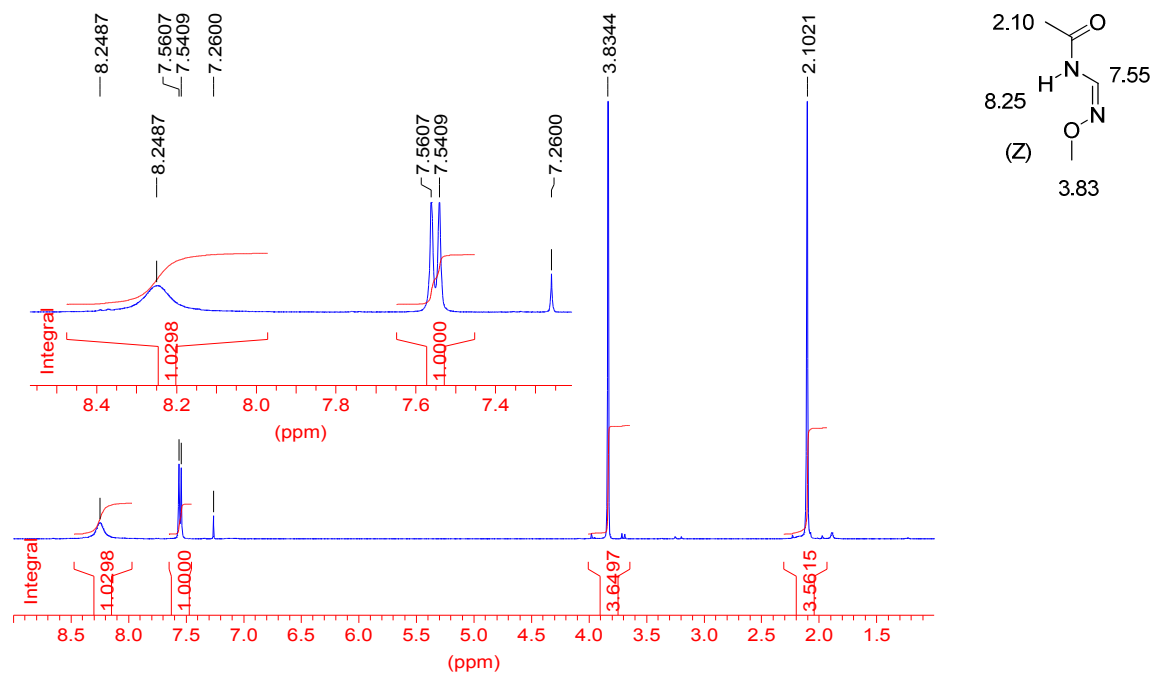


<sup>13</sup>C NMR (125 MHz; CDCl<sub>3</sub>; 25 °C)

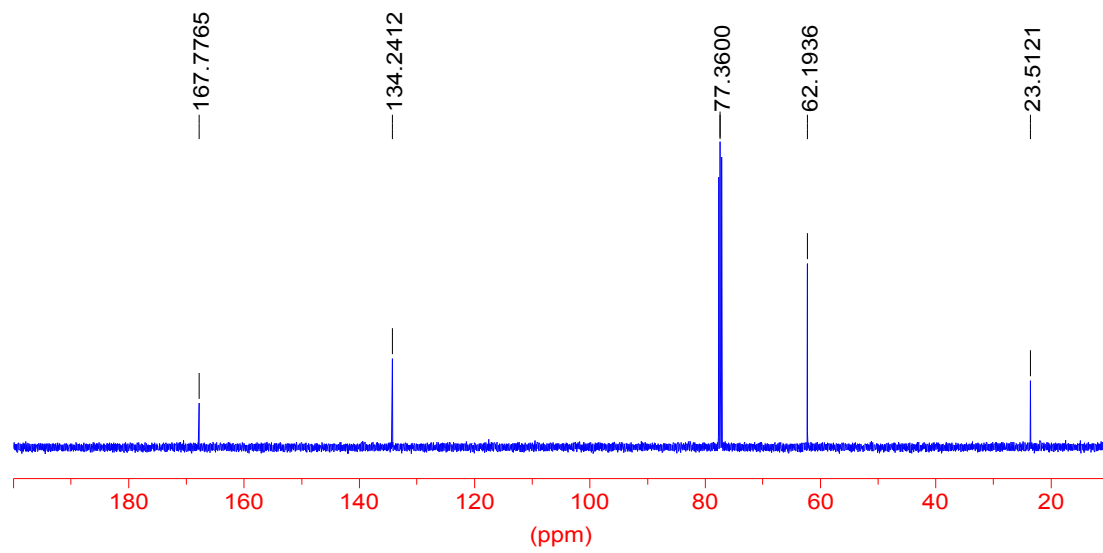


**(Z)-N-((methoxyimino)methyl)acetamide (4.11Z)**

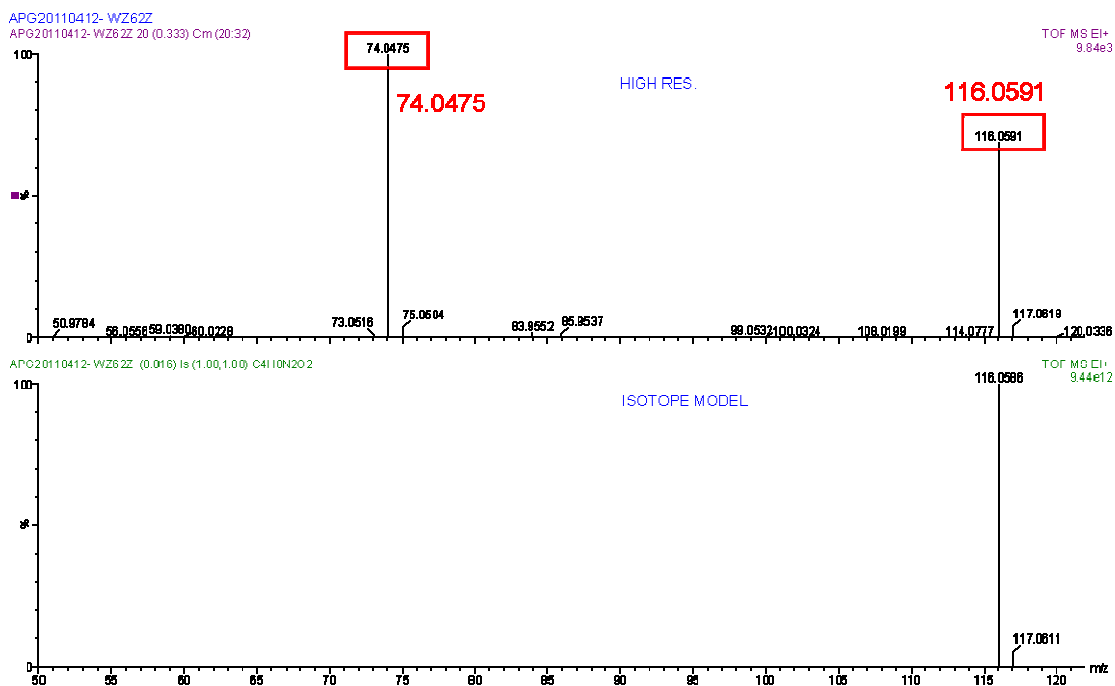
<sup>1</sup>H NMR (500 MHz; CDCl<sub>3</sub>; 25 °C)



<sup>13</sup>C NMR (125 MHz; CDCl<sub>3</sub>; 25 °C)

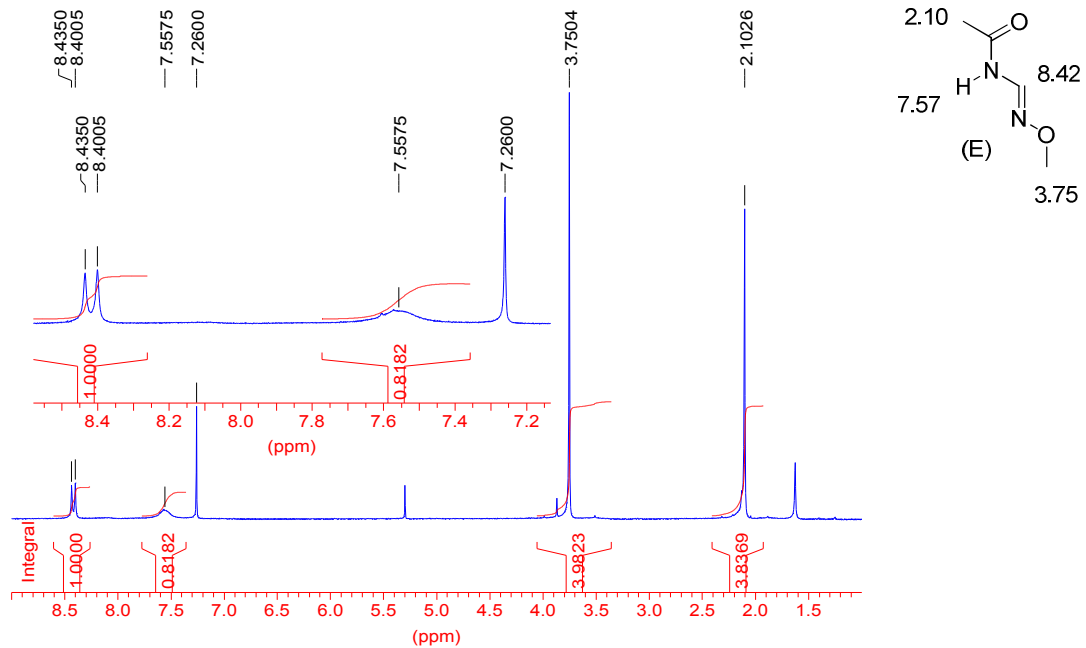


### EI<sup>+</sup>-HRMS



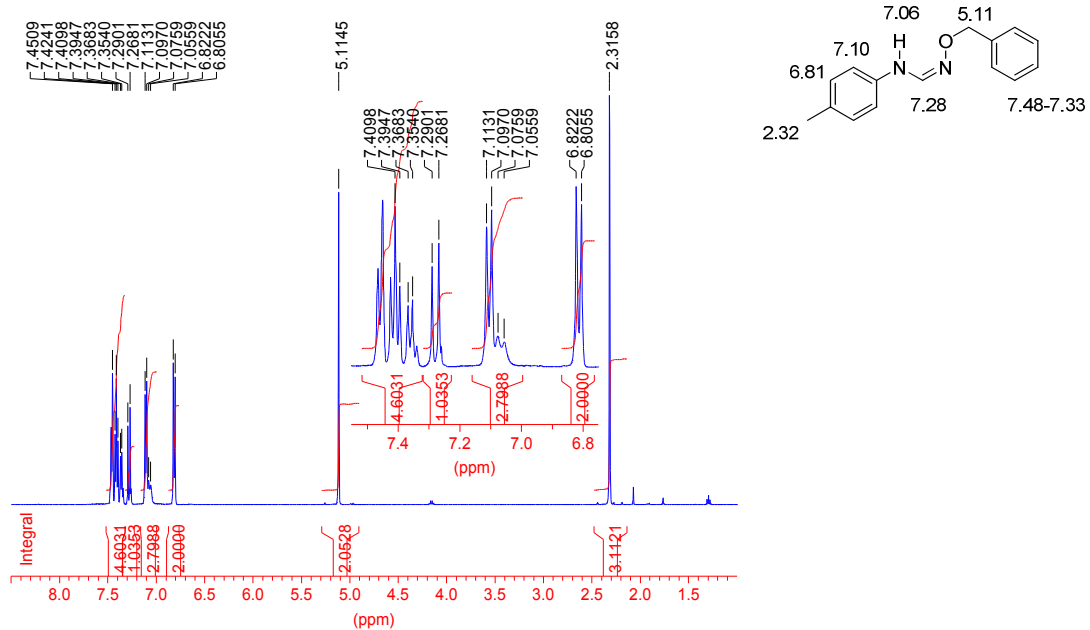
### (E)-N-((methoxyimino)methyl)acetamide (4.11E)

<sup>1</sup>H NMR (500 MHz; CDCl<sub>3</sub>; 25 °C)

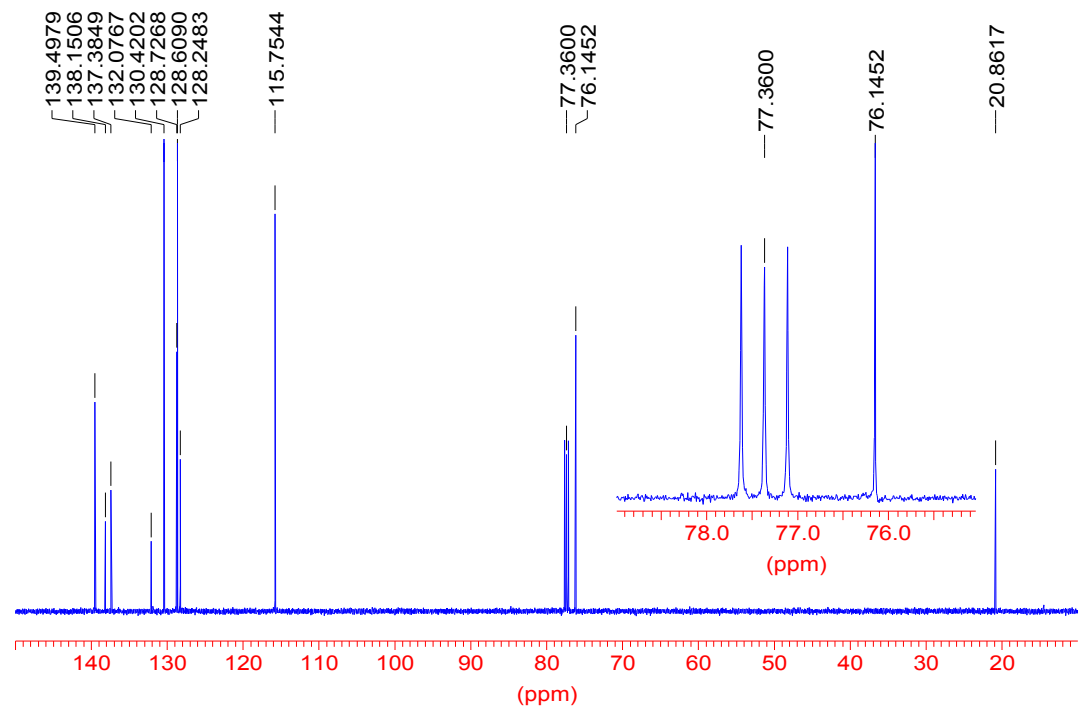


#### (Z)-N'-(benzyloxy)-N-p-tolylformimidamide (4.12)

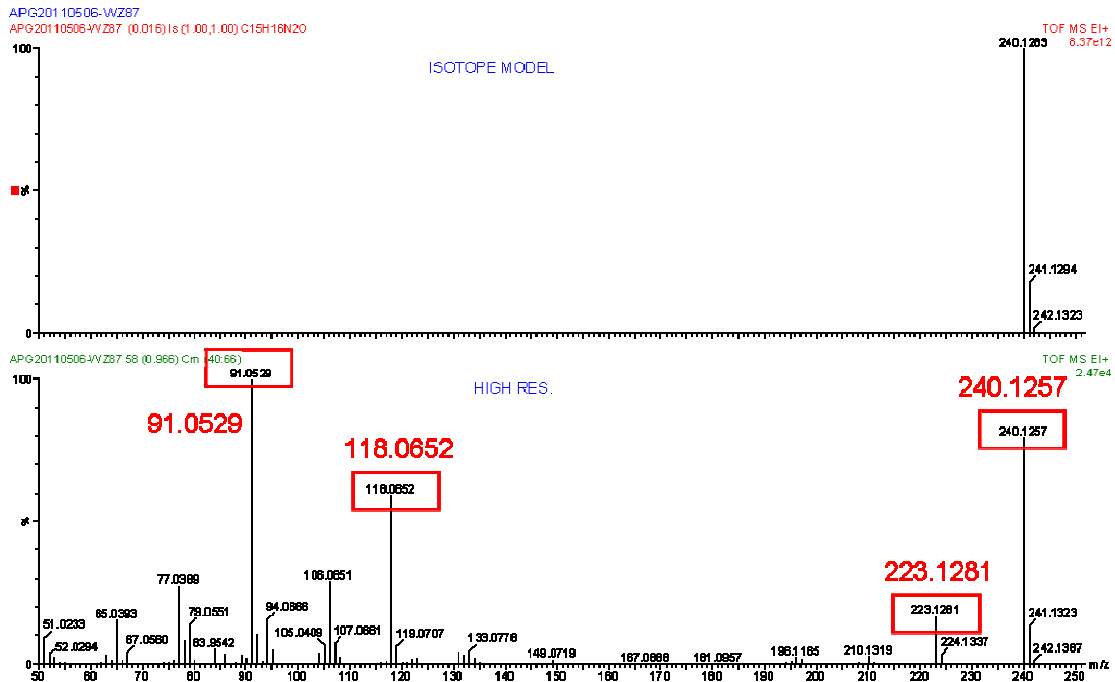
<sup>1</sup>H NMR (500 MHz; CDCl<sub>3</sub>; 25 °C)



<sup>13</sup>C NMR (125 MHz; CDCl<sub>3</sub>; 25 °C)

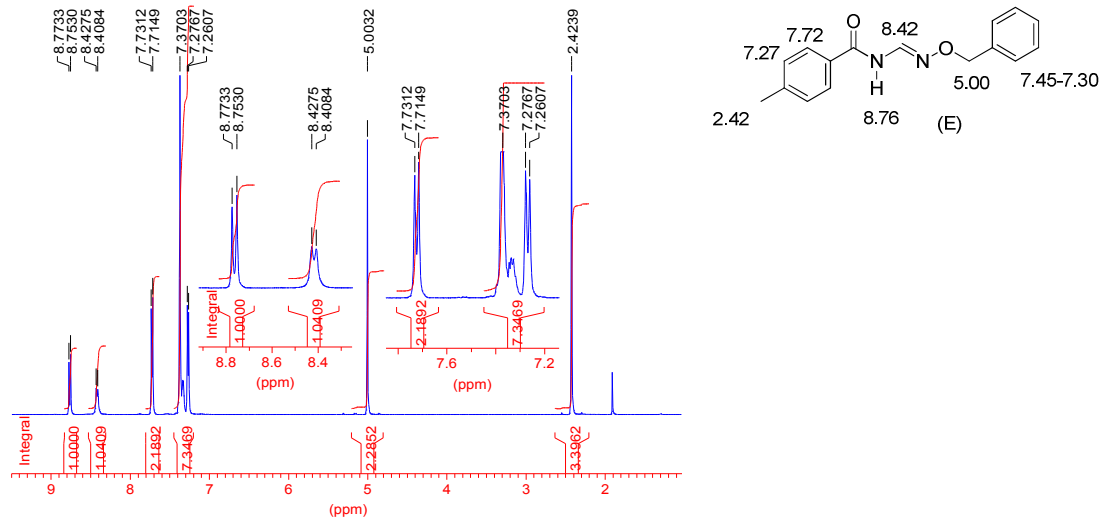


EI<sup>+</sup>-HRMS

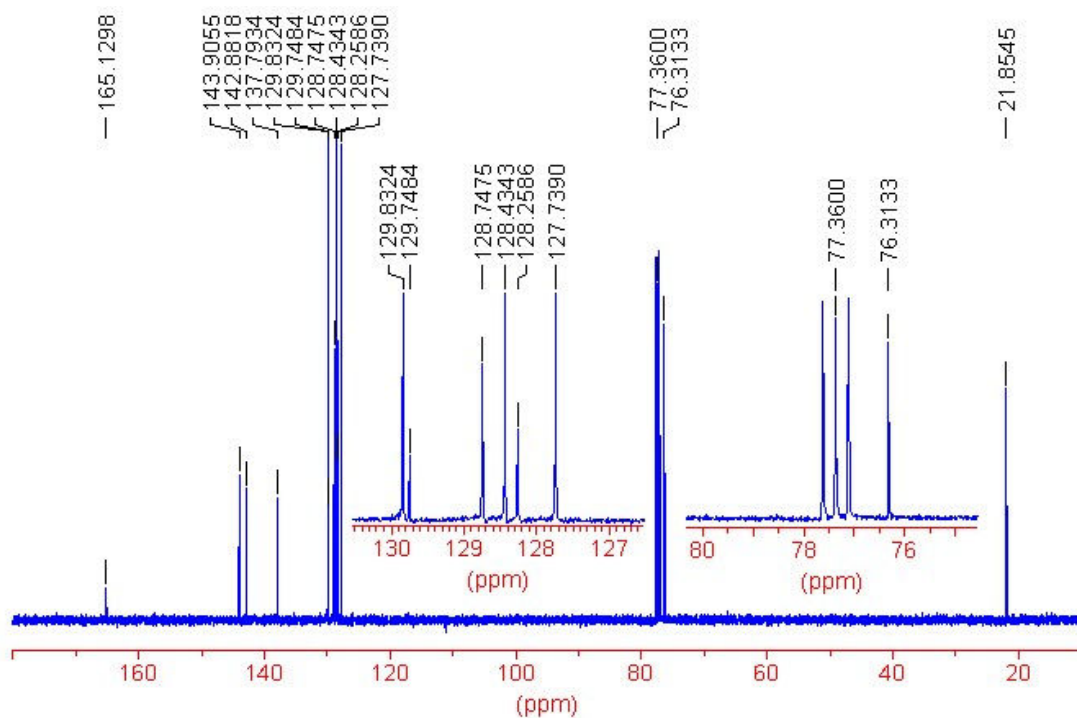


**(E)-N-((benzyloxyimino)methyl)-4-methylbenzamide (4.8E)**

<sup>1</sup>H NMR (500 MHz; CDCl<sub>3</sub>; 25 °C)

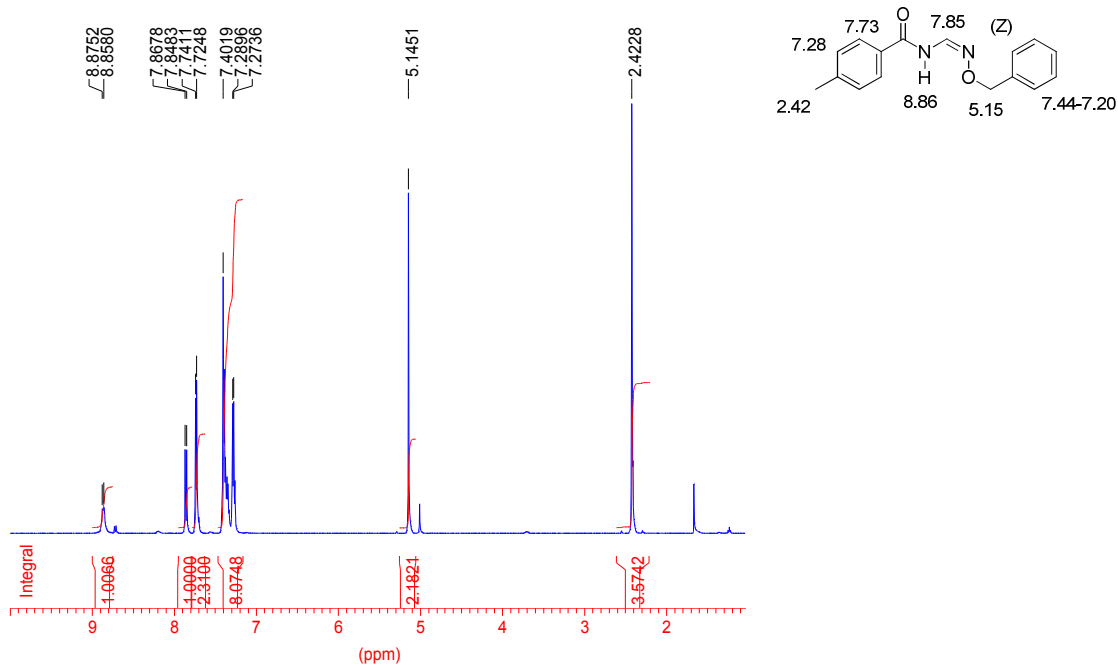


<sup>13</sup>C NMR (125 MHz; CDCl<sub>3</sub>; 25 °C)

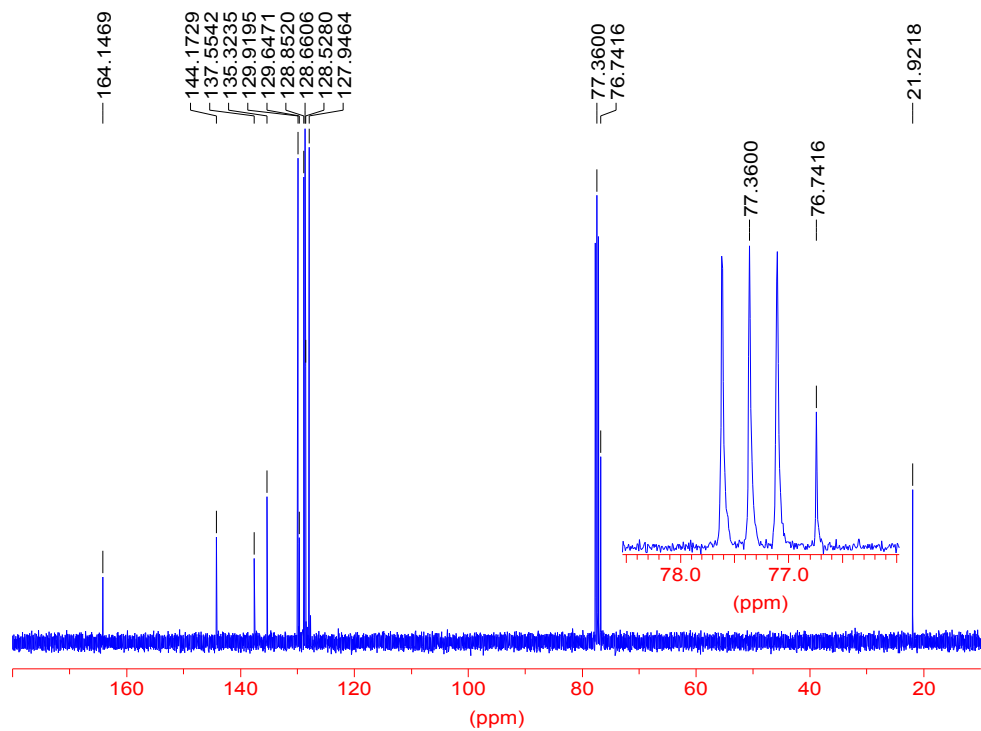


**(Z)-N-((benzyloxyimino)methyl)-4-methylbenzamide (4.8Z)**

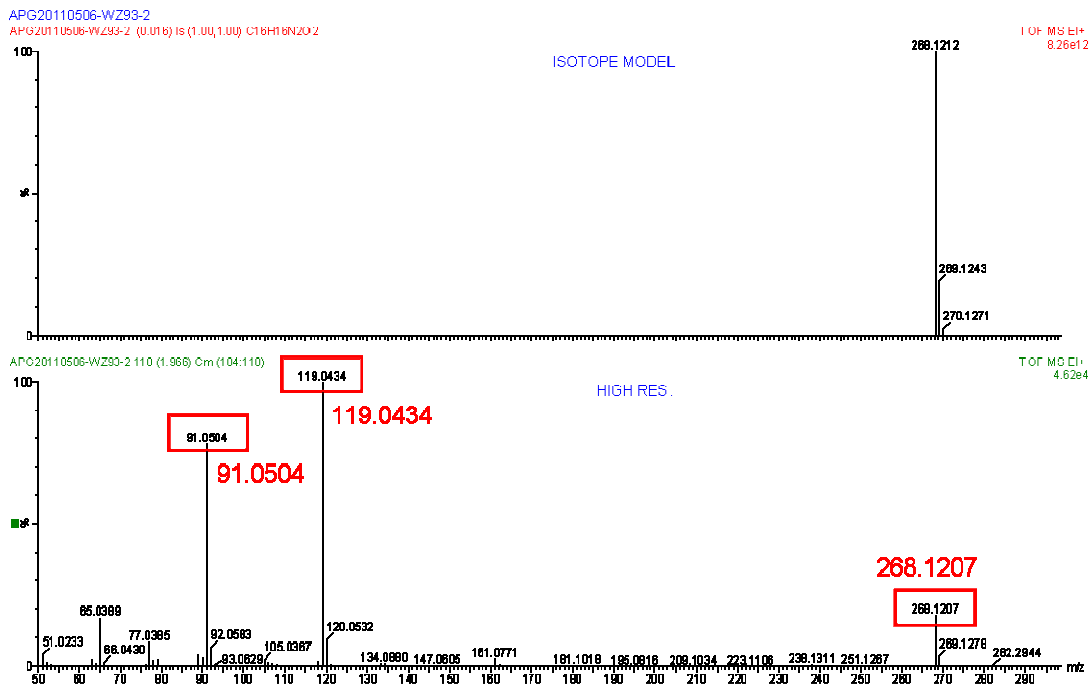
<sup>1</sup>H NMR (500 MHz; CDCl<sub>3</sub>; 25 °C)



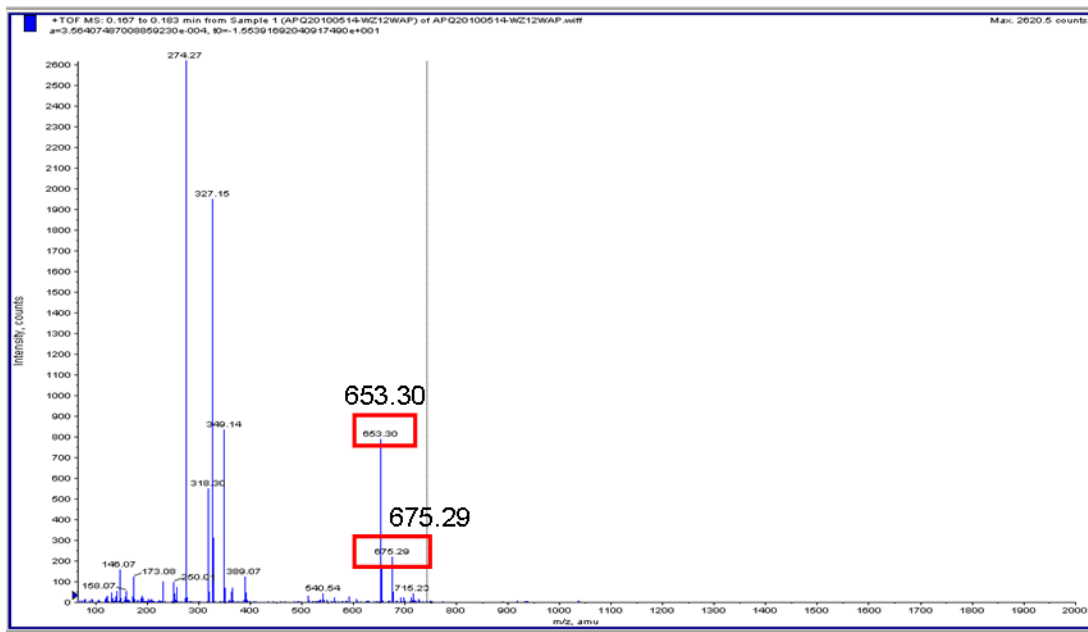
$^{13}\text{C}$  NMR (125 MHz;  $\text{CDCl}_3$ ; 25 °C)



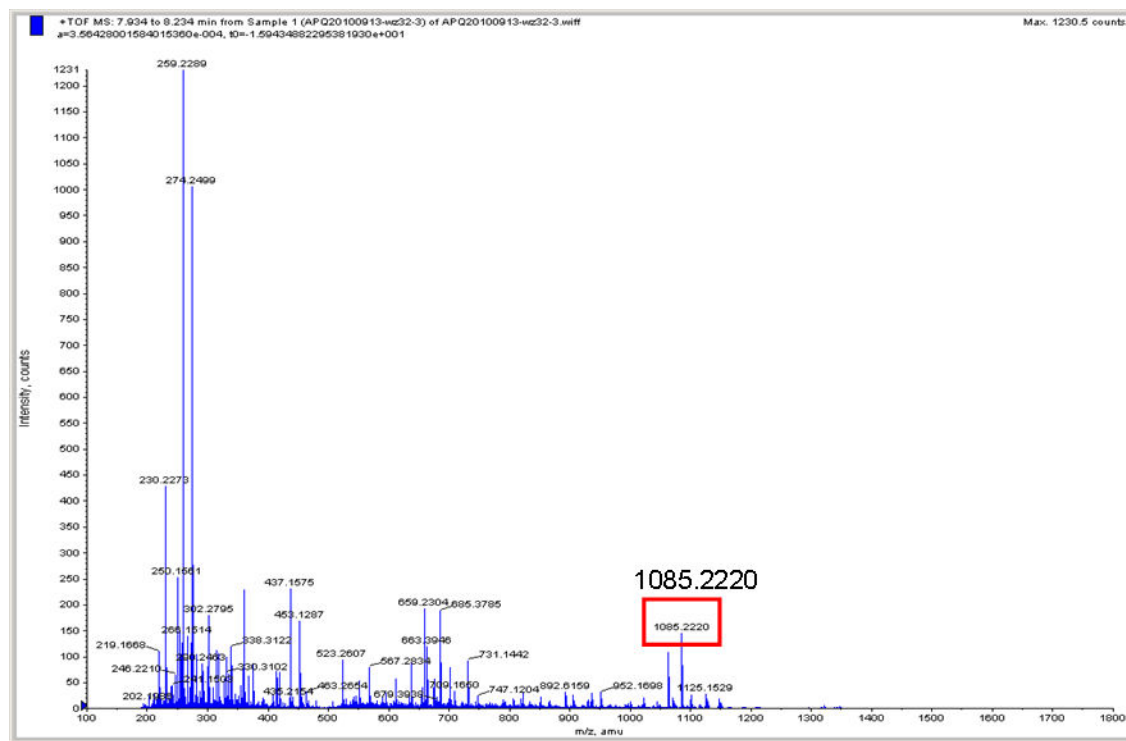
$\text{EI}^+$ -HRMS



## ESI-MS of Catenane (in CH<sub>2</sub>Cl<sub>2</sub>)



## ESI-MS of Maxi-M2 (in CH<sub>2</sub>Cl<sub>2</sub>)



## Appendix B: Crystallography Data

### 1) Macrocycle M2 dimer ((M2)<sub>2</sub>.H<sub>2</sub>O.(CH<sub>3</sub>)<sub>2</sub>NH<sub>2</sub><sup>+</sup>.OTf))

A crystal of the compound (colorless, block-shaped, size  $0.32 \times 0.28 \times 0.25$  mm) was mounted on a glass fiber with grease and cooled to -93 °C in a stream of nitrogen gas controlled with Cryostream Controller 700. Data collection was performed on a Bruker SMART APEX II X-ray diffractometer with graphite-monochromated Mo K $\alpha$  radiation ( $\lambda = 0.71073$  Å), operating at 50 kV and 30 mA over 2 $\theta$  ranges of  $3.02 \sim 52.00^\circ$ . No significant decay was observed during the data collection. Data were processed on a PC using the Bruker AXS Crystal Structure Analysis Package:<sup>[1]</sup> Data collection: APEX2 (Bruker, 2006); cell refinement: SAINT (Bruker, 2005); data reduction: SAINT (Bruker, 2005); structure solution: XPREP (Bruker, 2005) and SHELXTL (Bruker, 2000); structure refinement: SHELXTL; molecular graphics: SHELXTL; publication materials: SHELXTL. Neutral atom scattering factors were taken from Cromer and Waber.<sup>[2]</sup> The crystal is triclinic space group *P*-1, based on the systematic absences, *E* statistics and successful refinement of the structure. The structure was solved by direct methods. Full-matrix least-square refinements minimizing the function  $\sum w(F_o^2 - F_c^2)^2$  were applied to the compound. All non-hydrogen atoms were refined anisotropically. The H atoms of water were located from difference Fourier maps. All of the other H atoms were placed in geometrically calculated positions, with C-H = 0.95 (aromatic), 0.99(CH<sub>2</sub>), and 0.88(N-H) Å, and refined as riding atoms, with Uiso(H) = 1.2 Ueq(C or N). The two triflates are disordered. SHELX command, EADP, was used to resolve the disorder. Convergence to final  $R_1 = 0.0569$  and  $wR_2 = 0.1408$  for 8004 ( $I > 2\sigma(I)$ ) independent reflections, and  $R_1 = 0.0663$  and  $wR_2 = 0.1494$  for all 9507 ( $R(\text{int}) = 0.0185$ ) independent reflections, with 703 parameters and 0 restraints, were achieved.<sup>[3]</sup> The largest residual peak and hole to be 0.692 and -0.706 e/Å<sup>3</sup>, respectively. Crystallographic data, atomic coordinates and equivalent isotropic displacement parameters, bond lengths and angles, anisotropic displacement parameters, hydrogen coordinates and isotropic displacement parameters, torsion angles and H-bonding information are given in Tables B1.1 to B1.7. The molecular structure and

the cell packing are shown in Figure B1.1 and B1.2.

[1] Bruker AXS Crystal Structure Analysis Package: Bruker (2000). SHELXTL. Version 6.14. Bruker AXS Inc., Madison, Wisconsin, USA; Bruker (2005). XPREP. Version 2005/2. Bruker AXS Inc., Madison, Wisconsin, USA; Bruker (2005). SAINT. Version 7.23A. Bruker AXS Inc., Madison, Wisconsin, USA; Bruker (2006). APEX2. Version 2.0-2. Bruker AXS Inc., Madison, Wisconsin, USA.

[2] Cromer, D. T.; Waber, J. T. *International Tables for X-ray Crystallography*; Kynoch Press: Birmingham, UK, 1974; Vol. 4, Table 2.2 A.

$$[3] R_1 = \sum | |F_O| - |F_C| | / \sum |F_O|$$

$$wR_2 = \{ \sum [w(F_O^2 - F_C^2)^2] / \sum [w(F_O^2)^2] \}^{1/2}$$

$$(w = 1 / [\sigma^2(F_O^2) + (0.0625P)^2 + 3.25P], \text{ where } P = [\text{Max}(F_O^2, 0) + 2F_C^2] / 3)$$

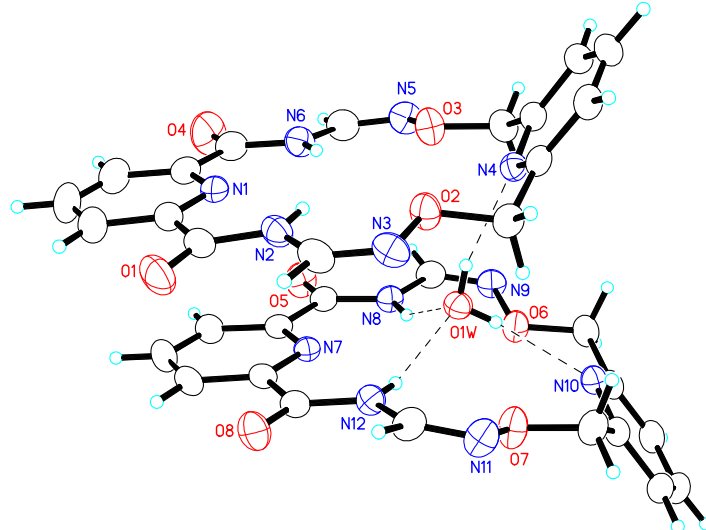


**Figure B1.1** Molecular Structure (displacement ellipsoids for non-H atoms are shown at the 50% probability level and H atoms are represented by circles of arbitrary size. The solvent molecules and the anions are omitted for clarity)

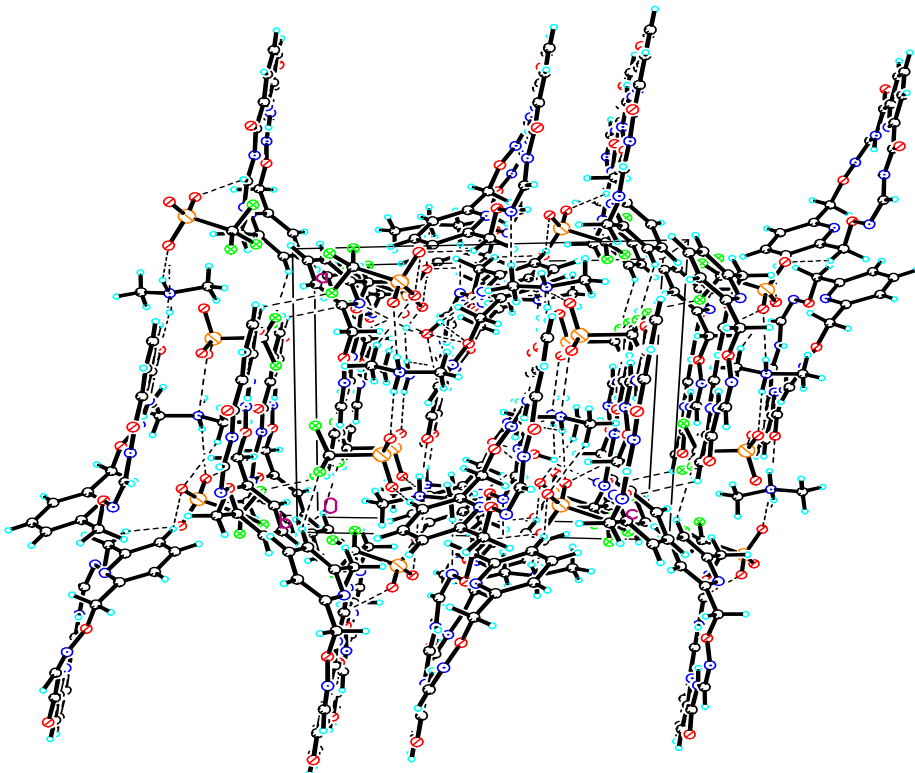


**Figure B1.2** Unit cell packing

**Table B1.1.** Crystal data and structure refinement for ap16

Identification code	ap16		
Empirical formula	C <sub>19</sub> H <sub>23</sub> F <sub>3</sub> N <sub>7</sub> O <sub>7.50</sub> S		
Formula weight	558.50		
Temperature	180(2) K		
Wavelength	0.71073 Å		
Crystal system	Triclinic		
Space group	P-1		
Unit cell dimensions	a = 14.4432(8) Å	α= 64.0350(10)°.	
	b = 14.6020(8) Å	β= 76.9770(10)°.	
	c = 14.6895(8) Å	γ = 61.12°.	
Volume	2438.6(2) Å <sup>3</sup>		
Z	4		
Density (calculated)	1.521 Mg/m <sup>3</sup>		
Absorption coefficient	0.213 mm <sup>-1</sup>		
F(000)	1156		
Crystal size	0.32 x 0.28 x 0.25 mm <sup>3</sup>		

Theta range for data collection	1.54 to 26.00°
Index ranges	-17<=h<=17, -18<=k<=18, -18<=l<=18
Reflections collected	24537
Independent reflections	9507 [R(int) = 0.0185]
Completeness to theta = 26.00°	99.4 %
Absorption correction	Multi-scan
Max. and min. transmission	0.9486 and 0.9349
Refinement method	Full-matrix least-squares on F <sup>2</sup>
Data / restraints / parameters	9507 / 0 / 703
Goodness-of-fit on F <sup>2</sup>	1.033
Final R indices [I>2sigma(I)]	R1 = 0.0569, wR2 = 0.1408
R indices (all data)	R1 = 0.0663, wR2 = 0.1494
Largest diff. peak and hole	0.692 and -0.706 e.Å <sup>-3</sup>

**Table B1.2.** Atomic coordinates ( $\times 10^4$ ) and equivalent isotropic displacement parameters

(Å<sup>2</sup> × 10<sup>3</sup>) for ap16. U(eq) is defined as one third of the trace of the orthogonalized U<sup>ij</sup> tensor.

	x	y	z	U(eq)
N(1)	5464(2)	3398(2)	8915(2)	33(1)
N(2)	3585(2)	5323(2)	8679(2)	32(1)
N(3)	1725(2)	6347(2)	8429(2)	35(1)
N(4)	1720(2)	3509(2)	8383(2)	27(1)
N(5)	4579(2)	615(2)	8675(2)	38(1)
N(6)	5472(2)	1518(2)	8875(2)	36(1)
N(7)	4895(2)	4470(2)	6277(1)	26(1)
N(8)	4806(2)	2684(2)	6175(2)	28(1)
N(9)	3938(2)	1873(2)	5785(2)	33(1)
N(10)	1308(2)	4980(2)	5027(2)	28(1)
N(11)	1224(2)	7545(2)	5661(2)	36(1)
N(12)	3046(2)	6394(2)	6059(2)	29(1)
O(1)	4485(2)	6243(2)	8670(2)	47(1)
O(2)	1836(1)	5287(1)	8542(1)	36(1)
O(3)	3681(1)	1597(2)	8728(2)	38(1)
O(4)	7246(2)	601(2)	9075(2)	64(1)
O(5)	6572(1)	1658(2)	6434(2)	44(1)

O(6)	3190(1)	3016(1)	5370(1)	34(1)
O(7)	1405(1)	6717(2)	5303(2)	38(1)
O(8)	3932(2)	7211(2)	6274(2)	40(1)
O(1W)	2799(1)	4361(2)	6532(2)	30(1)
C(1)	6390(2)	2469(2)	9038(2)	38(1)
C(2)	7346(2)	2418(3)	9160(2)	51(1)
C(3)	7354(3)	3364(3)	9144(2)	56(1)
C(4)	6419(2)	4331(3)	9002(2)	48(1)
C(5)	5495(2)	4309(2)	8899(2)	36(1)
C(6)	4487(2)	5377(2)	8741(2)	35(1)
C(7)	2618(2)	6273(2)	8521(2)	35(1)
C(8)	882(2)	5452(2)	8215(2)	33(1)
C(9)	895(2)	4304(2)	8664(2)	27(1)
C(10)	127(2)	4074(2)	9349(2)	32(1)
C(11)	220(2)	2981(2)	9771(2)	34(1)
C(12)	1087(2)	2149(2)	9510(2)	32(1)
C(13)	1816(2)	2448(2)	8810(2)	28(1)
C(14)	2774(2)	1589(2)	8496(2)	35(1)
C(15)	5415(2)	648(2)	8771(2)	39(1)
C(16)	6414(2)	1442(2)	9007(2)	42(1)
C(17)	4948(2)	5340(2)	6318(2)	28(1)
C(18)	5884(2)	5315(2)	6454(2)	34(1)
C(19)	6807(2)	4336(3)	6561(2)	40(1)
C(20)	6772(2)	3426(2)	6523(2)	36(1)
C(21)	5801(2)	3529(2)	6382(2)	28(1)
C(22)	5763(2)	2538(2)	6340(2)	30(1)
C(23)	4711(2)	1799(2)	6140(2)	32(1)
C(24)	2295(2)	3065(2)	5063(2)	35(1)
C(25)	1567(2)	4300(2)	4531(2)	28(1)
C(26)	1195(2)	4695(2)	3576(2)	33(1)
C(27)	524(2)	5828(2)	3119(2)	34(1)
C(28)	258(2)	6542(2)	3613(2)	31(1)
C(29)	668(2)	6085(2)	4565(2)	27(1)
C(30)	417(2)	6831(2)	5127(2)	33(1)
C(31)	2079(2)	7324(2)	5994(2)	33(1)

C(32)	3934(2)	6398(2)	6220(2)	29(1)
S(1)	1173(1)	2(1)	7167(1)	47(1)
C(33)	643(3)	34(3)	8398(3)	56(1)
O(11A)	174(3)	483(3)	6681(3)	52(1)
O(12A)	1894(4)	-1068(3)	7301(3)	52(1)
O(13A)	1588(5)	859(5)	6796(4)	52(1)
F(11A)	-38(3)	1046(3)	8428(3)	66(1)
F(12A)	223(4)	-645(4)	8973(3)	66(1)
F(13A)	1509(3)	-263(4)	8947(3)	66(1)
O(11B)	508(5)	-182(7)	6703(5)	52(1)
O(12B)	2150(5)	-1247(6)	7640(6)	52(1)
O(13B)	1493(8)	799(9)	6637(8)	52(1)
F(11B)	-390(6)	946(6)	8087(6)	74(2)
F(12B)	514(7)	-954(7)	8902(7)	74(2)
F(13B)	1084(7)	213(7)	8856(6)	74(2)
S(2)	2951(1)	2313(1)	2449(1)	35(1)
C(34)	2924(2)	2942(3)	1081(2)	51(1)
O(21)	1846(2)	2725(2)	2728(2)	51(1)
O(22)	3514(2)	2771(2)	2682(2)	51(1)
O(23)	3496(2)	1123(2)	2681(2)	56(1)
F(21A)	3941(5)	2440(7)	690(5)	55(1)
F(22A)	2217(7)	2889(8)	708(4)	55(1)
F(23A)	2397(5)	4173(6)	894(6)	55(1)
F(21B)	3835(5)	2827(7)	648(4)	62(1)
F(22B)	2527(7)	2458(8)	739(4)	62(1)
F(23B)	2534(5)	3983(6)	632(5)	62(1)
N(13A)	1418(3)	85(3)	3413(3)	60(1)
C(35A)	1352(3)	346(3)	4251(3)	62(1)
C(36A)	1160(20)	960(20)	2430(20)	101(3)
N(13B)	980(7)	1091(9)	3234(9)	60(1)
C(35B)	1352(3)	346(3)	4251(3)	62(1)
C(36B)	1300(60)	850(60)	2440(60)	101(3)
N(14)	4233(2)	8503(2)	7115(2)	38(1)
C(37)	4234(3)	9305(3)	6067(2)	54(1)
C(38)	3996(2)	9000(3)	7874(3)	50(1)

**Table B1.3.** Bond lengths [ $\text{\AA}$ ] and angles [ $^\circ$ ] for ap16.

N(1)-C(5)	1.341(3)	C(4)-H(4A)	0.9500	S(1)-O(13A)	1.484(5)
N(1)-C(1)	1.343(3)	C(5)-C(6)	1.499(4)	S(1)-O(12B)	1.627(7)
N(2)-C(6)	1.368(3)	C(7)-H(7A)	0.9500	S(1)-C(33)	1.810(4)
N(2)-C(7)	1.386(3)	C(8)-C(9)	1.501(3)	C(33)-F(13B)	1.199(9)
N(2)-H(2B)	0.8800	C(8)-H(8A)	0.9900	C(33)-F(12A)	1.296(6)
N(3)-C(7)	1.274(3)	C(8)-H(8B)	0.9900	C(33)-F(11A)	1.337(5)
N(3)-O(2)	1.413(3)	C(9)-C(10)	1.385(3)	C(33)-F(12B)	1.386(9)
N(4)-C(13)	1.338(3)	C(10)-C(11)	1.384(4)	C(33)-F(13A)	1.424(6)
N(4)-C(9)	1.342(3)	C(10)-H(10A)	0.9500	C(33)-F(11B)	1.436(9)
N(5)-C(15)	1.272(4)	C(11)-C(12)	1.383(4)	S(2)-O(23)	1.427(2)
N(5)-O(3)	1.414(3)	C(11)-H(11A)	0.9500	S(2)-O(21)	1.439(2)
N(6)-C(16)	1.363(4)	C(12)-C(13)	1.386(3)	S(2)-O(22)	1.442(2)
N(6)-C(15)	1.385(4)	C(12)-H(12A)	0.9500	S(2)-C(34)	1.808(3)
N(6)-H(6A)	0.8800	C(13)-C(14)	1.499(3)	C(34)-F(23B)	1.235(7)
N(7)-C(17)	1.337(3)	C(14)-H(14A)	0.9900	C(34)-F(21B)	1.291(7)
N(7)-C(21)	1.339(3)	C(14)-H(14B)	0.9900	C(34)-F(22A)	1.309(7)
N(8)-C(22)	1.356(3)	C(15)-H(15A)	0.9500	C(34)-F(22B)	1.383(7)
N(8)-C(23)	1.388(3)	C(17)-C(18)	1.393(3)	C(34)-F(21A)	1.405(8)
N(8)-H(8C)	0.8800	C(17)-C(32)	1.506(3)	C(34)-F(23A)	1.491(8)
N(9)-C(23)	1.274(3)	C(18)-C(19)	1.379(4)	N(13A)-C(35A)	1.410(5)
N(9)-O(6)	1.411(3)	C(18)-H(18A)	0.9500	N(13A)-C(36A)	1.43(3)
N(10)-C(29)	1.342(3)	C(19)-C(20)	1.380(4)	N(13A)-H(13A)	0.9200
N(10)-C(25)	1.346(3)	C(19)-H(19A)	0.9500	N(13A)-H(13B)	0.9200
N(11)-C(31)	1.272(3)	C(20)-C(21)	1.390(3)	C(35A)-H(35A)	0.9800
N(11)-O(7)	1.413(2)	C(20)-H(20A)	0.9500	C(35A)-H(35B)	0.9800
N(12)-C(32)	1.359(3)	C(21)-C(22)	1.502(3)	C(35A)-H(35C)	0.9800
N(12)-C(31)	1.385(3)	C(23)-H(23A)	0.9500	C(36A)-H(36A)	0.9800
N(12)-H(12B)	0.8800	C(24)-C(25)	1.507(3)	C(36A)-H(36B)	0.9800
O(1)-C(6)	1.221(3)	C(24)-H(24A)	0.9900	C(36A)-H(36C)	0.9800
O(2)-C(8)	1.436(3)	C(24)-H(24B)	0.9900	N(13B)-C(36B)	1.29(8)
O(3)-C(14)	1.434(3)	C(25)-C(26)	1.386(4)	N(13B)-H(13C)	0.9200
O(4)-C(16)	1.217(3)	C(26)-C(27)	1.378(4)	N(13B)-H(13D)	0.9200

O(5)-C(22)	1.226(3)	C(26)-H(26A)	0.9500	C(36B)-H(36D)	0.9800
O(6)-C(24)	1.422(3)	C(27)-C(28)	1.383(4)	C(36B)-H(36E)	0.9800
O(7)-C(30)	1.424(3)	C(27)-H(27A)	0.9500	C(36B)-H(36F)	0.9800
O(8)-C(32)	1.223(3)	C(28)-C(29)	1.387(3)	N(14)-C(37)	1.471(4)
O(1W)-H(1WB)	0.80(4)	C(28)-H(28A)	0.9500	N(14)-C(38)	1.476(3)
O(1W)-H(1WA)	0.79(4)	C(29)-C(30)	1.509(3)	N(14)-H(14C)	0.9200
C(1)-C(2)	1.394(4)	C(30)-H(30A)	0.9900	N(14)-H(14D)	0.9200
C(1)-C(16)	1.504(4)	C(30)-H(30B)	0.9900	C(37)-H(37A)	0.9800
C(2)-C(3)	1.377(5)	C(31)-H(31A)	0.9500	C(37)-H(37B)	0.9800
C(2)-H(2A)	0.9500	S(1)-O(13B)	1.318(11)	C(37)-H(37C)	0.9800
C(3)-C(4)	1.375(5)	S(1)-O(12A)	1.347(4)	C(38)-H(38A)	0.9800
C(3)-H(3A)	0.9500	S(1)-O(11A)	1.459(4)	C(38)-H(38B)	0.9800
C(4)-C(5)	1.394(4)	S(1)-O(11B)	1.470(7)	C(38)-H(38C)	0.9800

C(5)-N(1)-C(1)	116.6(2)	C(29)-C(30)-H(30A)	110.5
C(6)-N(2)-C(7)	120.5(2)	O(7)-C(30)-H(30B)	110.5
C(6)-N(2)-H(2B)	119.8	C(29)-C(30)-H(30B)	110.5
C(7)-N(2)-H(2B)	119.8	H(30A)-C(30)-H(30B)	108.7
C(7)-N(3)-O(2)	110.2(2)	N(11)-C(31)-N(12)	126.9(2)
C(13)-N(4)-C(9)	118.3(2)	N(11)-C(31)-H(31A)	116.6
C(15)-N(5)-O(3)	109.8(2)	N(12)-C(31)-H(31A)	116.6
C(16)-N(6)-C(15)	121.3(2)	O(8)-C(32)-N(12)	123.0(2)
C(16)-N(6)-H(6A)	119.3	O(8)-C(32)-C(17)	120.6(2)
C(15)-N(6)-H(6A)	119.3	N(12)-C(32)-C(17)	116.4(2)
C(17)-N(7)-C(21)	117.0(2)	O(13B)-S(1)-O(12A)	116.1(5)
C(22)-N(8)-C(23)	119.7(2)	O(13B)-S(1)-O(11A)	101.1(4)
C(22)-N(8)-H(8C)	120.1	O(12A)-S(1)-O(11A)	119.9(2)
C(23)-N(8)-H(8C)	120.1	O(13B)-S(1)-O(11B)	120.5(5)
C(23)-N(9)-O(6)	110.17(19)	O(12A)-S(1)-O(11B)	86.7(3)
C(29)-N(10)-C(25)	117.9(2)	O(11A)-S(1)-O(11B)	33.3(3)
C(31)-N(11)-O(7)	109.8(2)	O(13B)-S(1)-O(13A)	12.8(5)
C(32)-N(12)-C(31)	119.6(2)	O(12A)-S(1)-O(13A)	116.2(3)
C(32)-N(12)-H(12B)	120.2	O(11A)-S(1)-O(13A)	110.0(3)
C(31)-N(12)-H(12B)	120.2	O(11B)-S(1)-O(13A)	132.7(3)
N(3)-O(2)-C(8)	108.65(18)	O(13B)-S(1)-O(12B)	112.6(5)

N(5)-O(3)-C(14)	107.75(18)	O(12A)-S(1)-O(12B)	19.5(3)
N(9)-O(6)-C(24)	108.94(17)	O(11A)-S(1)-O(12B)	136.9(3)
N(11)-O(7)-C(30)	109.32(17)	O(11B)-S(1)-O(12B)	104.1(4)
H(1WB)-O(1W)-H(1WA)	105(3)	O(13A)-S(1)-O(12B)	108.2(4)
N(1)-C(1)-C(2)	123.2(3)	O(13B)-S(1)-C(33)	112.1(5)
N(1)-C(1)-C(16)	119.0(2)	O(12A)-S(1)-C(33)	108.1(2)
C(2)-C(1)-C(16)	117.8(3)	O(11A)-S(1)-C(33)	98.0(2)
C(3)-C(2)-C(1)	119.1(3)	O(11B)-S(1)-C(33)	110.5(3)
C(3)-C(2)-H(2A)	120.5	O(13A)-S(1)-C(33)	101.1(3)
C(1)-C(2)-H(2A)	120.5	O(12B)-S(1)-C(33)	93.4(3)
C(4)-C(3)-C(2)	118.8(3)	F(13B)-C(33)-F(12A)	113.8(5)
C(4)-C(3)-H(3A)	120.6	F(13B)-C(33)-F(11A)	74.8(4)
C(2)-C(3)-H(3A)	120.6	F(12A)-C(33)-F(11A)	105.4(3)
C(3)-C(4)-C(5)	118.6(3)	F(13B)-C(33)-F(12B)	115.9(6)
C(3)-C(4)-H(4A)	120.7	F(12A)-C(33)-F(12B)	20.2(3)
C(5)-C(4)-H(4A)	120.7	F(11A)-C(33)-F(12B)	125.6(4)
N(1)-C(5)-C(4)	123.8(3)	F(13B)-C(33)-F(13A)	26.9(4)
N(1)-C(5)-C(6)	118.7(2)	F(12A)-C(33)-F(13A)	105.8(4)
C(4)-C(5)-C(6)	117.5(3)	F(11A)-C(33)-F(13A)	101.7(4)
O(1)-C(6)-N(2)	122.5(3)	F(12B)-C(33)-F(13A)	99.3(5)
O(1)-C(6)-C(5)	121.0(2)	F(13B)-C(33)-F(11B)	111.8(5)
N(2)-C(6)-C(5)	116.4(2)	F(12A)-C(33)-F(11B)	90.3(4)
N(3)-C(7)-N(2)	127.0(2)	F(11A)-C(33)-F(11B)	37.0(3)
N(3)-C(7)-H(7A)	116.5	F(12B)-C(33)-F(11B)	106.7(5)
N(2)-C(7)-H(7A)	116.5	F(13A)-C(33)-F(11B)	138.7(4)
O(2)-C(8)-C(9)	105.78(19)	F(13B)-C(33)-S(1)	118.1(4)
O(2)-C(8)-H(8A)	110.6	F(12A)-C(33)-S(1)	119.0(3)
C(9)-C(8)-H(8A)	110.6	F(11A)-C(33)-S(1)	116.9(3)
O(2)-C(8)-H(8B)	110.6	F(12B)-C(33)-S(1)	104.1(4)
C(9)-C(8)-H(8B)	110.6	F(13A)-C(33)-S(1)	106.1(3)
H(8A)-C(8)-H(8B)	108.7	F(11B)-C(33)-S(1)	98.1(4)
N(4)-C(9)-C(10)	122.4(2)	O(23)-S(2)-O(21)	115.00(14)
N(4)-C(9)-C(8)	115.5(2)	O(23)-S(2)-O(22)	115.03(14)
C(10)-C(9)-C(8)	122.1(2)	O(21)-S(2)-O(22)	114.85(12)
C(11)-C(10)-C(9)	118.9(2)	O(23)-S(2)-C(34)	104.01(16)

C(11)-C(10)-H(10A)	120.5	O(21)-S(2)-C(34)	102.72(15)
C(9)-C(10)-H(10A)	120.5	O(22)-S(2)-C(34)	102.81(14)
C(12)-C(11)-C(10)	118.9(2)	F(23B)-C(34)-F(21B)	92.0(6)
C(12)-C(11)-H(11A)	120.5	F(23B)-C(34)-F(22A)	91.1(4)
C(10)-C(11)-H(11A)	120.5	F(21B)-C(34)-F(22A)	122.3(5)
C(11)-C(12)-C(13)	118.8(2)	F(23B)-C(34)-F(22B)	111.7(4)
C(11)-C(12)-H(12A)	120.6	F(21B)-C(34)-F(22B)	108.0(4)
C(13)-C(12)-H(12A)	120.6	F(22A)-C(34)-F(22B)	23.7(3)
N(4)-C(13)-C(12)	122.6(2)	F(23B)-C(34)-F(21A)	110.3(6)
N(4)-C(13)-C(14)	115.9(2)	F(21B)-C(34)-F(21A)	20.2(3)
C(12)-C(13)-C(14)	121.5(2)	F(22A)-C(34)-F(21A)	111.5(4)
O(3)-C(14)-C(13)	107.15(19)	F(22B)-C(34)-F(21A)	92.5(4)
O(3)-C(14)-H(14A)	110.3	F(23B)-C(34)-F(23A)	19.2(3)
C(13)-C(14)-H(14A)	110.3	F(21B)-C(34)-F(23A)	101.3(6)
O(3)-C(14)-H(14B)	110.3	F(22A)-C(34)-F(23A)	99.8(5)
C(13)-C(14)-H(14B)	110.3	F(22B)-C(34)-F(23A)	123.0(4)
H(14A)-C(14)-H(14B)	108.5	F(21A)-C(34)-F(23A)	121.3(6)
N(5)-C(15)-N(6)	126.6(2)	F(23B)-C(34)-S(2)	120.2(5)
N(5)-C(15)-H(15A)	116.7	F(21B)-C(34)-S(2)	114.3(3)
N(6)-C(15)-H(15A)	116.7	F(22A)-C(34)-S(2)	113.2(3)
O(4)-C(16)-N(6)	122.6(3)	F(22B)-C(34)-S(2)	109.2(3)
O(4)-C(16)-C(1)	120.7(3)	F(21A)-C(34)-S(2)	109.4(3)
N(6)-C(16)-C(1)	116.7(2)	F(23A)-C(34)-S(2)	101.1(4)
N(7)-C(17)-C(18)	123.6(2)	C(35A)-N(13A)-C(36A)	120.2(12)
N(7)-C(17)-C(32)	117.8(2)	C(35A)-N(13A)-H(13A)	107.3
C(18)-C(17)-C(32)	118.6(2)	C(36A)-N(13A)-H(13A)	107.3
C(19)-C(18)-C(17)	118.3(2)	C(35A)-N(13A)-H(13B)	107.3
C(19)-C(18)-H(18A)	120.9	C(36A)-N(13A)-H(13B)	107.3
C(17)-C(18)-H(18A)	120.9	H(13A)-N(13A)-H(13B)	106.9
C(18)-C(19)-C(20)	119.2(2)	N(13A)-C(35A)-H(35A)	109.5
C(18)-C(19)-H(19A)	120.4	N(13A)-C(35A)-H(35B)	109.5
C(20)-C(19)-H(19A)	120.4	H(35A)-C(35A)-H(35B)	109.5
C(19)-C(20)-C(21)	118.6(2)	N(13A)-C(35A)-H(35C)	109.5
C(19)-C(20)-H(20A)	120.7	H(35A)-C(35A)-H(35C)	109.5
C(21)-C(20)-H(20A)	120.7	H(35B)-C(35A)-H(35C)	109.5

N(7)-C(21)-C(20)	123.4(2)	N(13A)-C(36A)-H(36A)	109.5
N(7)-C(21)-C(22)	118.1(2)	N(13A)-C(36A)-H(36B)	109.5
C(20)-C(21)-C(22)	118.5(2)	H(36A)-C(36A)-H(36B)	109.5
O(5)-C(22)-N(8)	122.8(2)	N(13A)-C(36A)-H(36C)	109.5
O(5)-C(22)-C(21)	120.5(2)	H(36A)-C(36A)-H(36C)	109.5
N(8)-C(22)-C(21)	116.6(2)	H(36B)-C(36A)-H(36C)	109.5
N(9)-C(23)-N(8)	126.5(2)	C(36B)-N(13B)-H(13C)	105.7
N(9)-C(23)-H(23A)	116.8	C(36B)-N(13B)-H(13D)	105.7
N(8)-C(23)-H(23A)	116.8	H(13C)-N(13B)-H(13D)	106.2
O(6)-C(24)-C(25)	107.18(19)	N(13B)-C(36B)-H(36D)	109.5
O(6)-C(24)-H(24A)	110.3	N(13B)-C(36B)-H(36E)	109.5
C(25)-C(24)-H(24A)	110.3	H(36D)-C(36B)-H(36E)	109.5
O(6)-C(24)-H(24B)	110.3	N(13B)-C(36B)-H(36F)	109.5
C(25)-C(24)-H(24B)	110.3	H(36D)-C(36B)-H(36F)	109.5
H(24A)-C(24)-H(24B)	108.5	H(36E)-C(36B)-H(36F)	109.5
N(10)-C(25)-C(26)	122.6(2)	C(37)-N(14)-C(38)	113.3(2)
N(10)-C(25)-C(24)	116.8(2)	C(37)-N(14)-H(14C)	108.9
C(26)-C(25)-C(24)	120.6(2)	C(38)-N(14)-H(14C)	108.9
C(27)-C(26)-C(25)	118.9(2)	C(37)-N(14)-H(14D)	108.9
C(27)-C(26)-H(26A)	120.6	C(38)-N(14)-H(14D)	108.9
C(25)-C(26)-H(26A)	120.6	H(14C)-N(14)-H(14D)	107.7
C(26)-C(27)-C(28)	119.3(2)	N(14)-C(37)-H(37A)	109.5
C(26)-C(27)-H(27A)	120.4	N(14)-C(37)-H(37B)	109.5
C(28)-C(27)-H(27A)	120.4	H(37A)-C(37)-H(37B)	109.5
C(27)-C(28)-C(29)	118.5(2)	N(14)-C(37)-H(37C)	109.5
C(27)-C(28)-H(28A)	120.7	H(37A)-C(37)-H(37C)	109.5
C(29)-C(28)-H(28A)	120.7	H(37B)-C(37)-H(37C)	109.5
N(10)-C(29)-C(28)	122.9(2)	N(14)-C(38)-H(38A)	109.5
N(10)-C(29)-C(30)	116.6(2)	N(14)-C(38)-H(38B)	109.5
C(28)-C(29)-C(30)	120.6(2)	H(38A)-C(38)-H(38B)	109.5
O(7)-C(30)-C(29)	106.28(19)	N(14)-C(38)-H(38C)	109.5
O(7)-C(30)-H(30A)	110.5	H(38A)-C(38)-H(38C)	109.5
		H(38B)-C(38)-H(38C)	109.5

**Table B1.4.** Anisotropic displacement parameters ( $\text{\AA}^2 \times 10^3$ ) for ap16. The anisotropic

displacement factor exponent takes the form:  $-2\pi^2 [ h^2 a^{*2} U^{11} + \dots + 2 h k a^* b^* U^{12} ]$

	$U^{11}$	$U^{22}$	$U^{33}$	$U^{23}$	$U^{13}$	$U^{12}$
N(1)	32(1)	42(1)	24(1)	-8(1)	0(1)	-21(1)
N(2)	38(1)	32(1)	34(1)	-13(1)	2(1)	-21(1)
N(3)	42(1)	27(1)	39(1)	-16(1)	4(1)	-17(1)
N(4)	27(1)	30(1)	27(1)	-12(1)	0(1)	-13(1)
N(5)	33(1)	29(1)	46(1)	-18(1)	4(1)	-6(1)
N(6)	26(1)	33(1)	39(1)	-12(1)	1(1)	-9(1)
N(7)	28(1)	29(1)	22(1)	-9(1)	1(1)	-14(1)
N(8)	26(1)	21(1)	33(1)	-11(1)	-2(1)	-6(1)
N(9)	34(1)	20(1)	41(1)	-12(1)	-4(1)	-8(1)
N(10)	26(1)	28(1)	32(1)	-13(1)	0(1)	-13(1)
N(11)	40(1)	25(1)	46(1)	-20(1)	-9(1)	-7(1)
N(12)	34(1)	24(1)	32(1)	-13(1)	-3(1)	-13(1)
O(1)	59(1)	53(1)	51(1)	-24(1)	7(1)	-40(1)
O(2)	34(1)	26(1)	49(1)	-14(1)	-6(1)	-13(1)
O(3)	28(1)	32(1)	56(1)	-26(1)	3(1)	-9(1)
O(4)	32(1)	46(1)	92(2)	-18(1)	-14(1)	-4(1)
O(5)	28(1)	32(1)	62(1)	-20(1)	-4(1)	-4(1)
O(6)	31(1)	21(1)	51(1)	-13(1)	-10(1)	-8(1)
O(7)	31(1)	33(1)	58(1)	-29(1)	-8(1)	-7(1)
O(8)	48(1)	37(1)	51(1)	-24(1)	0(1)	-24(1)
O(1W)	31(1)	31(1)	28(1)	-12(1)	2(1)	-15(1)
C(1)	31(1)	47(2)	29(1)	-6(1)	-3(1)	-17(1)
C(2)	32(2)	66(2)	47(2)	-14(2)	-7(1)	-20(1)
C(3)	41(2)	89(3)	51(2)	-26(2)	-3(1)	-38(2)
C(4)	49(2)	73(2)	38(2)	-22(2)	3(1)	-40(2)
C(5)	38(1)	52(2)	24(1)	-12(1)	3(1)	-28(1)
C(6)	45(2)	47(2)	25(1)	-14(1)	6(1)	-31(1)
C(7)	43(2)	32(1)	37(1)	-17(1)	7(1)	-21(1)
C(8)	30(1)	30(1)	37(1)	-12(1)	-4(1)	-11(1)
C(9)	25(1)	29(1)	29(1)	-12(1)	-5(1)	-10(1)
C(10)	25(1)	37(1)	36(1)	-20(1)	0(1)	-10(1)
C(11)	30(1)	46(2)	33(1)	-18(1)	6(1)	-22(1)

C(12)	34(1)	32(1)	34(1)	-12(1)	-1(1)	-18(1)
C(13)	29(1)	30(1)	29(1)	-14(1)	-2(1)	-14(1)
C(14)	34(1)	35(1)	42(1)	-20(1)	3(1)	-17(1)
C(15)	31(1)	30(1)	44(2)	-14(1)	1(1)	-6(1)
C(16)	30(1)	39(2)	39(2)	-5(1)	-5(1)	-10(1)
C(17)	34(1)	31(1)	21(1)	-9(1)	3(1)	-18(1)
C(18)	40(1)	42(1)	31(1)	-15(1)	7(1)	-28(1)
C(19)	31(1)	56(2)	40(2)	-18(1)	6(1)	-28(1)
C(20)	26(1)	43(2)	35(1)	-14(1)	4(1)	-16(1)
C(21)	29(1)	31(1)	22(1)	-8(1)	2(1)	-14(1)
C(22)	27(1)	28(1)	27(1)	-9(1)	0(1)	-10(1)
C(23)	33(1)	22(1)	36(1)	-12(1)	-2(1)	-7(1)
C(24)	34(1)	28(1)	49(2)	-16(1)	-4(1)	-15(1)
C(25)	24(1)	29(1)	37(1)	-15(1)	2(1)	-14(1)
C(26)	31(1)	39(1)	40(1)	-23(1)	1(1)	-18(1)
C(27)	33(1)	41(1)	33(1)	-15(1)	-5(1)	-17(1)
C(28)	27(1)	30(1)	35(1)	-11(1)	-4(1)	-11(1)
C(29)	22(1)	28(1)	32(1)	-13(1)	0(1)	-11(1)
C(30)	29(1)	31(1)	39(1)	-18(1)	-5(1)	-8(1)
C(31)	41(1)	23(1)	37(1)	-14(1)	-8(1)	-10(1)
C(32)	38(1)	31(1)	24(1)	-11(1)	1(1)	-19(1)
S(1)	45(1)	56(1)	44(1)	-14(1)	-3(1)	-28(1)
C(33)	63(2)	48(2)	57(2)	-14(2)	8(2)	-33(2)
O(11A)	63(2)	33(1)	55(1)	-5(1)	-13(1)	-22(1)
O(12A)	63(2)	33(1)	55(1)	-5(1)	-13(1)	-22(1)
O(13A)	63(2)	33(1)	55(1)	-5(1)	-13(1)	-22(1)
F(11A)	74(2)	68(2)	56(1)	-27(1)	10(1)	-34(1)
F(12A)	74(2)	68(2)	56(1)	-27(1)	10(1)	-34(1)
F(13A)	74(2)	68(2)	56(1)	-27(1)	10(1)	-34(1)
O(11B)	28(2)	52(3)	67(3)	-21(2)	1(2)	-14(2)
O(12B)	28(2)	52(3)	67(3)	-21(2)	1(2)	-14(2)
O(13B)	28(2)	52(3)	67(3)	-21(2)	1(2)	-14(2)
F(11B)	84(3)	79(3)	91(3)	-57(3)	38(2)	-54(3)
F(12B)	84(3)	79(3)	91(3)	-57(3)	38(2)	-54(3)
F(13B)	84(3)	79(3)	91(3)	-57(3)	38(2)	-54(3)

S(2)	33(1)	35(1)	40(1)	-20(1)	3(1)	-14(1)
C(34)	44(2)	62(2)	45(2)	-10(2)	-6(1)	-29(2)
O(21)	38(1)	58(1)	74(2)	-44(1)	16(1)	-25(1)
O(22)	43(1)	65(1)	63(1)	-37(1)	1(1)	-26(1)
O(23)	58(1)	34(1)	63(1)	-17(1)	1(1)	-13(1)
F(21A)	55(2)	57(2)	52(2)	-22(2)	-5(1)	-22(2)
F(22A)	55(2)	57(2)	52(2)	-22(2)	-5(1)	-22(2)
F(23A)	55(2)	57(2)	52(2)	-22(2)	-5(1)	-22(2)
F(21B)	68(2)	63(3)	47(2)	-19(2)	2(1)	-26(2)
F(22B)	68(2)	63(3)	47(2)	-19(2)	2(1)	-26(2)
F(23B)	68(2)	63(3)	47(2)	-19(2)	2(1)	-26(2)
N(13A)	33(2)	51(2)	90(3)	-41(2)	-10(2)	1(2)
C(35A)	61(2)	59(2)	53(2)	-19(2)	3(2)	-20(2)
C(36A)	167(9)	143(8)	57(3)	-20(5)	-3(5)	-131(7)
N(13B)	33(2)	51(2)	90(3)	-41(2)	-10(2)	1(2)
C(35B)	61(2)	59(2)	53(2)	-19(2)	3(2)	-20(2)
C(36B)	167(9)	143(8)	57(3)	-20(5)	-3(5)	-131(7)
N(14)	42(1)	33(1)	48(1)	-21(1)	2(1)	-19(1)
C(37)	75(2)	42(2)	51(2)	-17(1)	6(2)	-34(2)
C(38)	40(2)	60(2)	63(2)	-42(2)	0(1)	-15(1)

**Table B1.5.** Hydrogen coordinates ( $\times 10^4$ ) and isotropic displacement parameters ( $\text{\AA}^2 \times 10^2$ ) for ap16.

	x	y	z	U(eq)
H(2B)	3618	4681	8741	39
H(6A)	4887	2131	8856	43
H(8C)	4247	3337	6091	34
H(12B)	3084	5804	5996	34
H(1WB)	2590(30)	4100(30)	7090(30)	46(9)
H(1WA)	2390(30)	4490(30)	6170(30)	48(10)
H(2A)	7982	1740	9254	61
H(3A)	7995	3348	9229	67
H(4A)	6403	5001	8974	57
H(7A)	2621	6941	8476	42

H(8A)	867	5757	7467	40
H(8B)	254	5989	8460	40
H(10A)	-455	4657	9526	38
H(11A)	-303	2804	10234	41
H(12A)	1180	1388	9805	39
H(14A)	2794	827	8868	42
H(14B)	2760	1786	7761	42
H(15A)	6066	12	8772	47
H(18A)	5887	5956	6474	41
H(19A)	7459	4289	6660	48
H(20A)	7398	2744	6592	43
H(23A)	5278	1065	6406	39
H(24A)	1931	2703	5660	42
H(24B)	2517	2663	4600	42
H(26A)	1398	4194	3243	39
H(27A)	246	6115	2471	41
H(28A)	-194	7328	3307	37
H(30A)	-41	7630	4718	39
H(30B)	48	6586	5778	39
H(31A)	2052	7854	6222	40
H(13A)	987	-264	3555	72
H(13B)	2100	-444	3378	72
H(35A)	1520	-343	4869	93
H(35B)	633	911	4310	93
H(35C)	1856	651	4155	93
H(36A)	1240	637	1938	152
H(36B)	1634	1324	2232	152
H(36C)	426	1529	2429	152
H(13C)	260	1329	3272	72
H(13D)	1078	1720	3086	72
H(35D)	1084	784	4680	93
H(35E)	2127	-15	4244	93
H(35F)	1098	-239	4519	93
H(36D)	975	1528	1838	152
H(36E)	1104	266	2504	152

H(36F)	2073	557	2374	152
H(14C)	4884	7885	7246	46
H(14D)	3738	8251	7181	46
H(37A)	4394	8928	5601	81
H(37B)	4772	9562	5986	81
H(37C)	3537	9958	5915	81
H(38A)	4015	8425	8554	75
H(38B)	3291	9642	7755	75
H(38C)	4524	9262	7815	75

**Table B1.6.** Torsion angles [°] for ap16.

C(7)-N(3)-O(2)-C(8)	-167.3(2)	C(25)-C(26)-C(27)-C(28)	1.3(4)
C(15)-N(5)-O(3)-C(14)	173.2(2)	C(26)-C(27)-C(28)-C(29)	-1.0(4)
C(23)-N(9)-O(6)-C(24)	-174.8(2)	C(25)-N(10)-C(29)-C(28)	0.8(3)
C(31)-N(11)-O(7)-C(30)	168.2(2)	C(25)-N(10)-C(29)-C(30)	-178.3(2)
C(5)-N(1)-C(1)-C(2)	1.0(4)	C(27)-C(28)-C(29)-N(10)	-0.1(4)
C(5)-N(1)-C(1)-C(16)	-176.8(2)	C(27)-C(28)-C(29)-C(30)	179.0(2)
N(1)-C(1)-C(2)-C(3)	-0.9(4)	N(11)-O(7)-C(30)-C(29)	169.4(2)
C(16)-C(1)-C(2)-C(3)	177.0(3)	N(10)-C(29)-C(30)-O(7)	58.5(3)
C(1)-C(2)-C(3)-C(4)	-0.3(5)	C(28)-C(29)-C(30)-O(7)	-120.6(2)
C(2)-C(3)-C(4)-C(5)	1.2(4)	O(7)-N(11)-C(31)-N(12)	-3.2(4)
C(1)-N(1)-C(5)-C(4)	-0.1(4)	C(32)-N(12)-C(31)-N(11)	165.6(3)
C(1)-N(1)-C(5)-C(6)	178.6(2)	C(31)-N(12)-C(32)-O(8)	-2.9(4)
C(3)-C(4)-C(5)-N(1)	-1.0(4)	C(31)-N(12)-C(32)-C(17)	177.9(2)
C(3)-C(4)-C(5)-C(6)	-179.8(3)	N(7)-C(17)-C(32)-O(8)	178.4(2)
C(7)-N(2)-C(6)-O(1)	0.6(4)	C(18)-C(17)-C(32)-O(8)	-1.0(3)
C(7)-N(2)-C(6)-C(5)	-179.2(2)	N(7)-C(17)-C(32)-N(12)	-2.4(3)
N(1)-C(5)-C(6)-O(1)	-176.3(2)	C(18)-C(17)-C(32)-N(12)	178.2(2)
C(4)-C(5)-C(6)-O(1)	2.5(4)	O(13B)-S(1)-C(33)-F(13B)	-40.3(7)
N(1)-C(5)-C(6)-N(2)	3.5(3)	O(12A)-S(1)-C(33)-F(13B)	89.0(6)
C(4)-C(5)-C(6)-N(2)	-177.7(2)	O(11A)-S(1)-C(33)-F(13B)	-145.8(5)
O(2)-N(3)-C(7)-N(2)	1.7(4)	O(11B)-S(1)-C(33)-F(13B)	-177.7(6)
C(6)-N(2)-C(7)-N(3)	178.5(2)	O(13A)-S(1)-C(33)-F(13B)	-33.4(6)
N(3)-O(2)-C(8)-C(9)	-161.58(19)	O(12B)-S(1)-C(33)-F(13B)	75.8(6)

C(13)-N(4)-C(9)-C(10)	-2.4(3)	O(13B)-S(1)-C(33)-F(12A)	174.8(5)
C(13)-N(4)-C(9)-C(8)	175.5(2)	O(12A)-S(1)-C(33)-F(12A)	-56.0(4)
O(2)-C(8)-C(9)-N(4)	-60.0(3)	O(11A)-S(1)-C(33)-F(12A)	69.2(4)
O(2)-C(8)-C(9)-C(10)	117.8(2)	O(11B)-S(1)-C(33)-F(12A)	37.3(5)
N(4)-C(9)-C(10)-C(11)	1.0(4)	O(13A)-S(1)-C(33)-F(12A)	-178.4(4)
C(8)-C(9)-C(10)-C(11)	-176.7(2)	O(12B)-S(1)-C(33)-F(12A)	-69.1(4)
C(9)-C(10)-C(11)-C(12)	1.2(4)	O(13B)-S(1)-C(33)-F(11A)	46.2(6)
C(10)-C(11)-C(12)-C(13)	-1.9(4)	O(12A)-S(1)-C(33)-F(11A)	175.5(3)
C(9)-N(4)-C(13)-C(12)	1.6(3)	O(11A)-S(1)-C(33)-F(11A)	-59.3(4)
C(9)-N(4)-C(13)-C(14)	-177.7(2)	O(11B)-S(1)-C(33)-F(11A)	-91.2(4)
C(11)-C(12)-C(13)-N(4)	0.6(4)	O(13A)-S(1)-C(33)-F(11A)	53.1(4)
C(11)-C(12)-C(13)-C(14)	179.8(2)	O(12B)-S(1)-C(33)-F(11A)	162.3(4)
N(5)-O(3)-C(14)-C(13)	165.7(2)	O(13B)-S(1)-C(33)-F(12B)	-170.5(7)
N(4)-C(13)-C(14)-O(3)	57.7(3)	O(12A)-S(1)-C(33)-F(12B)	-41.2(5)
C(12)-C(13)-C(14)-O(3)	-121.6(2)	O(11A)-S(1)-C(33)-F(12B)	84.0(5)
O(3)-N(5)-C(15)-N(6)	-2.3(4)	O(11B)-S(1)-C(33)-F(12B)	52.1(6)
C(16)-N(6)-C(15)-N(5)	177.8(3)	O(13A)-S(1)-C(33)-F(12B)	-163.7(5)
C(15)-N(6)-C(16)-O(4)	-2.6(4)	O(12B)-S(1)-C(33)-F(12B)	-54.4(6)
C(15)-N(6)-C(16)-C(1)	175.8(2)	O(13B)-S(1)-C(33)-F(13A)	-66.3(5)
N(1)-C(1)-C(16)-O(4)	177.1(3)	O(12A)-S(1)-C(33)-F(13A)	63.0(3)
C(2)-C(1)-C(16)-O(4)	-0.9(4)	O(11A)-S(1)-C(33)-F(13A)	-171.8(3)
N(1)-C(1)-C(16)-N(6)	-1.3(4)	O(11B)-S(1)-C(33)-F(13A)	156.2(4)
C(2)-C(1)-C(16)-N(6)	-179.3(3)	O(13A)-S(1)-C(33)-F(13A)	-59.5(4)
C(21)-N(7)-C(17)-C(18)	0.5(3)	O(12B)-S(1)-C(33)-F(13A)	49.8(4)
C(21)-N(7)-C(17)-C(32)	-178.94(19)	O(13B)-S(1)-C(33)-F(11B)	79.9(6)
N(7)-C(17)-C(18)-C(19)	-0.5(4)	O(12A)-S(1)-C(33)-F(11B)	-150.8(3)
C(32)-C(17)-C(18)-C(19)	178.9(2)	O(11A)-S(1)-C(33)-F(11B)	-25.6(3)
C(17)-C(18)-C(19)-C(20)	0.4(4)	O(11B)-S(1)-C(33)-F(11B)	-57.5(4)
C(18)-C(19)-C(20)-C(21)	-0.3(4)	O(13A)-S(1)-C(33)-F(11B)	86.7(4)
C(17)-N(7)-C(21)-C(20)	-0.3(3)	O(12B)-S(1)-C(33)-F(11B)	-164.0(4)
C(17)-N(7)-C(21)-C(22)	179.9(2)	O(23)-S(2)-C(34)-F(23B)	-177.2(4)
C(19)-C(20)-C(21)-N(7)	0.2(4)	O(21)-S(2)-C(34)-F(23B)	62.6(4)
C(19)-C(20)-C(21)-C(22)	180.0(2)	O(22)-S(2)-C(34)-F(23B)	-57.0(4)
C(23)-N(8)-C(22)-O(5)	2.1(4)	O(23)-S(2)-C(34)-F(21B)	-69.3(5)
C(23)-N(8)-C(22)-C(21)	-179.2(2)	O(21)-S(2)-C(34)-F(21B)	170.5(5)

N(7)-C(21)-C(22)-O(5)	-179.9(2)	O(22)-S(2)-C(34)-F(21B)	50.9(5)
C(20)-C(21)-C(22)-O(5)	0.4(4)	O(23)-S(2)-C(34)-F(22A)	76.9(6)
N(7)-C(21)-C(22)-N(8)	1.4(3)	O(21)-S(2)-C(34)-F(22A)	-43.3(6)
C(20)-C(21)-C(22)-N(8)	-178.3(2)	O(22)-S(2)-C(34)-F(22A)	-162.9(5)
O(6)-N(9)-C(23)-N(8)	3.2(4)	O(23)-S(2)-C(34)-F(22B)	51.8(5)
C(22)-N(8)-C(23)-N(9)	-164.0(2)	O(21)-S(2)-C(34)-F(22B)	-68.4(5)
N(9)-O(6)-C(24)-C(25)	-174.44(19)	O(22)-S(2)-C(34)-F(22B)	172.0(5)
C(29)-N(10)-C(25)-C(26)	-0.4(3)	O(23)-S(2)-C(34)-F(21A)	-48.2(4)
C(29)-N(10)-C(25)-C(24)	179.5(2)	O(21)-S(2)-C(34)-F(21A)	-168.4(4)
O(6)-C(24)-C(25)-N(10)	-51.9(3)	O(22)-S(2)-C(34)-F(21A)	72.1(4)
O(6)-C(24)-C(25)-C(26)	128.0(2)	O(23)-S(2)-C(34)-F(23A)	-177.3(3)
N(10)-C(25)-C(26)-C(27)	-0.6(4)	O(21)-S(2)-C(34)-F(23A)	62.5(3)
C(24)-C(25)-C(26)-C(27)	179.5(2)	O(22)-S(2)-C(34)-F(23A)	-57.0(3)

**Table B1.7.** Hydrogen bonds for ap16 [Å and °].

D-H...A	d(D-H)	d(H...A)	d(D...A)	∠(DHA)
N(8)-H(8C)...O(1W)	0.88	2.06	2.873(3)	153.1
N(12)-H(12B)...O(1W)	0.88	2.11	2.920(3)	151.9
O(1W)-H(1WB)...N(4)	0.80(4)	2.11(4)	2.893(3)	166(3)
O(1W)-H(1WA)...N(10)	0.79(4)	2.19(4)	2.976(3)	174(3)
N(13A)-H(13B)...O(5)#1	0.92	1.85	2.759(4)	169.0
N(13A)-H(13A)...O(11A)#2	0.92	1.98	2.844(5)	156.0
N(13B)-H(13C)...O(11B)#2	0.92	2.40	2.991(13)	122.1
N(13B)-H(13C)...N(11)#3	0.92	2.66	3.334(10)	130.3
N(13B)-H(13D)...O(21)	0.92	2.07	2.953(12)	159.7
N(14)-H(14C)...O(22)#4	0.92	2.04	2.871(3)	149.6
N(14)-H(14D)...O(12B)#5	0.92	2.09	2.813(7)	134.7
N(14)-H(14D)...O(8)	0.92	2.31	2.889(3)	120.3
N(14)-H(14D)...O(12A)#5	0.92	2.35	3.093(5)	138.3

Symmetry transformations used to generate equivalent atoms:

#1 -x+1,-y,-z+1    #2 -x,-y,-z+1    #3 -x,-y+1,-z+1  
#4 -x+1,-y+1,-z+1    #5 x,y+1,z

## 2) Macrocycle M2-MeOH adduct

A crystal of the compound (colorless, block-shaped, size 0.20 x 0.15 x 0.12 mm) was mounted on a glass fiber with grease and cooled to -93 °C in a stream of nitrogen gas controlled with Cryostream Controller 700. Data collection was performed on a Bruker SMART APEX II X-ray diffractometer with graphite-monochromated Mo K $\alpha$  radiation ( $\lambda = 0.71073 \text{ \AA}$ ), operating at 50 kV and 30 mA over 2 $\theta$  ranges of 3.76 ~ 52.00°. No significant decay was observed during the data collection.

Data were processed on a PC using the Bruker AXS Crystal Structure Analysis Package:<sup>[1]</sup> Data collection: APEX2 (Bruker, 2006); cell refinement: SAINT (Bruker, 2005); data reduction: SAINT (Bruker, 2005); structure solution: XPREP (Bruker, 2005) and SHELXTL (Bruker, 2000); structure refinement: SHELXTL; molecular graphics: SHELXTL; publication materials: SHELXTL. Neutral atom scattering factors were taken from Cromer and Waber.<sup>[2]</sup> The crystal is monoclinic space group  $P2_1/n$ , based on the systematic absences, *E* statistics and successful refinement of the structure. The structure was solved by direct methods. Full-matrix least-square refinements minimizing the function  $\sum w (F_o^2 - F_c^2)^2$  were applied to the compound. All non-hydrogen atoms were refined anisotropically. The H atom of OH from MeOH was located from difference Fourier maps. All of the other H atoms were placed in geometrically calculated positions, with C-H = 0.95 (aromatic), 0.99(CH<sub>2</sub>), and 0.88(N-H) Å, and refined as riding atoms, with Uiso(H) = 1.2 Ueq(C or N). The methyl group of MeOH was refined with AFIX 137, which allowed the rotation of the methyl group whilst keeping the C-H distances and X-C-H angles fixed.

Convergence to final  $R_1 = 0.0405$  and  $wR_2 = 0.0933$  for 2336 ( $I > 2\sigma(I)$ ) independent reflections, and  $R_1 = 0.0681$  and  $wR_2 = 0.1084$  for all 3451 ( $R(\text{int}) = 0.0357$ ) independent reflections, with 259 parameters and 0 restraints, were achieved.<sup>[3]</sup> The largest residual peak and hole to be 0.157 and -0.146 e/Å<sup>3</sup>, respectively. Crystallographic data, atomic coordinates and equivalent isotropic displacement parameters, bond lengths and angles, anisotropic displacement parameters, hydrogen coordinates and isotropic displacement parameters, torsion angles and H-bonding information are given in Table B2.1 to B2.7. The

molecular structure and the cell packing are shown in Figure B2.1 and B2.2.

[1] Bruker AXS Crystal Structure Analysis Package: Bruker (2000). SHELXTL. Version 6.14. Bruker AXS Inc., Madison, Wisconsin, USA; Bruker (2005). XPREP. Version 2005/2. Bruker AXS Inc., Madison, Wisconsin, USA; Bruker (2005). SAINT. Version 7.23A. Bruker AXS Inc., Madison, Wisconsin, USA; Bruker (2006). APEX2. Version 2.0-2. Bruker AXS Inc., Madison, Wisconsin, USA.

[2] Cromer, D. T.; Waber, J. T. *International Tables for X-ray Crystallography*; Kynoch Press: Birmingham, UK, 1974; Vol. 4, Table 2.2 A.

$$[3] R_1 = \sum | |F_O| - |F_C| | / \sum |F_O|$$

$$wR_2 = \{ \sum [w(F_O^2 - F_C^2)^2] / \sum [w(F_O^2)^2] \}^{1/2}$$

$$(w = 1 / [\sigma^2(F_O^2) + (0.0625P)^2 + 3.25P], \text{ where } P = [\text{Max}(F_O^2, 0) + 2F_C^2] / 3)$$

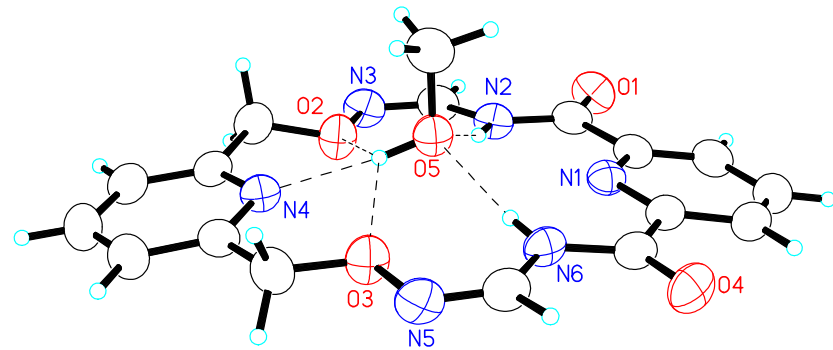


**Figure B2.1.** Molecular Structure (displacement ellipsoids for non-H atoms are shown at the 50% probability level and H atoms are represented by circles of arbitrary size

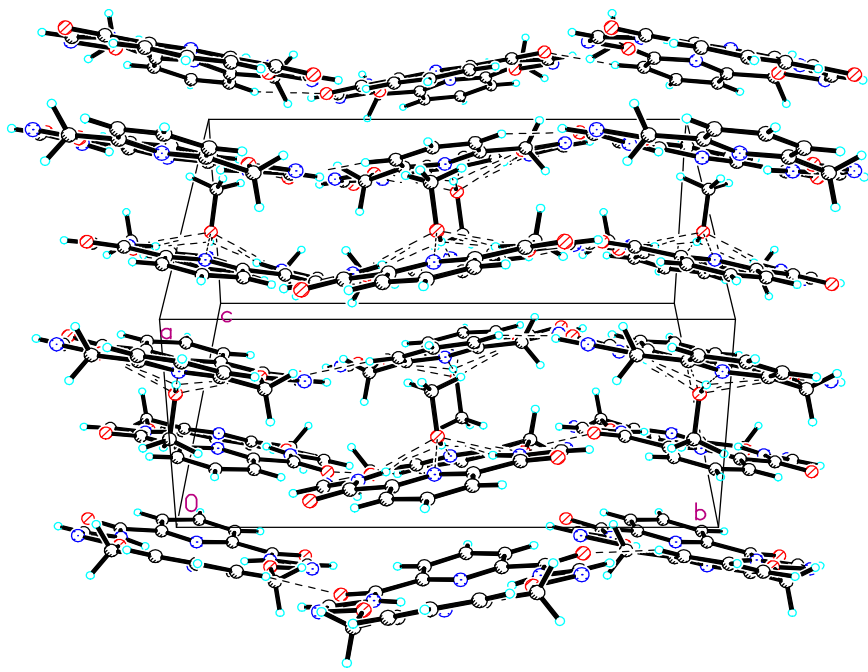


**Figure B2.2** Unit cell packing

**Table B2.1.** Crystal data and structure refinement for ap19

Identification code	ap19		
Empirical formula	C <sub>17</sub> H <sub>18</sub> N <sub>6</sub> O <sub>5</sub>		
Formula weight	386.37		
Temperature	180(2) K		
Wavelength	0.71073 Å		
Crystal system	Monoclinic		
Space group	P2(1)/n		
Unit cell dimensions	$a = 7.5319(8)$ Å	$\alpha = 90^\circ$ .	
	$b = 15.1775(19)$ Å	$\beta = 98.919(3)^\circ$ .	
	$c = 15.610(2)$ Å	$\gamma = 90^\circ$ .	
Volume	$1762.8(4)$ Å <sup>3</sup>		
Z	4		
Density (calculated)	1.456 Mg/m <sup>3</sup>		
Absorption coefficient	0.110 mm <sup>-1</sup>		
F(000)	808		
Crystal size	$0.20 \times 0.15 \times 0.12$ mm <sup>3</sup>		
	125		

Theta range for data collection	1.88 to 26.00°.
Index ranges	-9<=h<=8, -18<=k<=14, -17<=l<=19
Reflections collected	9428
Independent reflections	3451 [R(int) = 0.0357]
Completeness to theta = 26.00°	99.5 %
Absorption correction	Multi-scan
Max. and min. transmission	0.9869 and 0.9782
Refinement method	Full-matrix least-squares on F <sup>2</sup>
Data / restraints / parameters	3451 / 0 / 259
Goodness-of-fit on F <sup>2</sup>	1.038
Final R indices [I>2sigma(I)]	R1 = 0.0405, wR2 = 0.0933
R indices (all data)	R1 = 0.0681, wR2 = 0.1084
Extinction coefficient	0.0046(8)
Largest diff. peak and hole	0.157 and -0.146 e.Å <sup>-3</sup>
<b>Table B2.2.</b> Atomic coordinates ( x 10 <sup>4</sup> ) and equivalent isotropic displacement parameters (Å <sup>2</sup> x 10 <sup>3</sup> ) for ap19. U(eq) is defined as one third of the trace of the orthogonalized U <sup>ij</sup> tensor.	

	x	y	z	U(eq)
O(1)	3292(2)	6998(1)	157(1)	49(1)
O(2)	446(2)	6474(1)	2615(1)	44(1)
O(3)	-690(2)	3508(1)	2582(1)	44(1)
O(4)	1296(2)	2481(1)	30(1)	50(1)
O(5)	1716(2)	4809(1)	2243(1)	40(1)
N(1)	2134(2)	4759(1)	408(1)	35(1)
N(2)	2023(2)	6349(1)	1228(1)	37(1)
N(3)	1023(2)	7281(1)	2291(1)	43(1)
N(4)	-758(2)	5054(1)	3411(1)	36(1)
N(5)	-745(2)	2644(1)	2226(1)	44(1)
N(6)	807(2)	3322(1)	1174(1)	37(1)
C(1)	2082(2)	3990(1)	-19(1)	36(1)
C(2)	2544(2)	3909(1)	-840(1)	44(1)
C(3)	3085(3)	4644(1)	-1245(1)	47(1)
		126		

C(4)	3169(2)	5442(1)	-811(1)	43(1)
C(5)	2693(2)	5468(1)	9(1)	36(1)
C(6)	2718(2)	6336(1)	473(1)	37(1)
C(7)	1753(2)	7141(1)	1623(1)	41(1)
C(8)	50(3)	6625(1)	3455(1)	45(1)
C(9)	-918(2)	5854(1)	3771(1)	36(1)
C(10)	-1893(3)	5992(1)	4434(1)	42(1)
C(11)	-2759(3)	5288(1)	4748(1)	48(1)
C(12)	-2637(3)	4470(1)	4378(1)	44(1)
C(13)	-1635(2)	4378(1)	3719(1)	36(1)
C(14)	-1488(3)	3470(1)	3345(1)	43(1)
C(15)	14(3)	2638(1)	1552(1)	42(1)
C(16)	1385(2)	3198(1)	396(1)	38(1)
C(17)	3408(3)	4695(1)	2763(1)	55(1)

---

**Table B2.3** Bond lengths [ $\text{\AA}$ ] and angles [ $^\circ$ ] for ap19.

O(1)-C(6)	1.227(2)	N(5)-C(15)	1.272(2)	C(8)-H(8B)	0.9900
O(2)-C(8)	1.409(2)	N(6)-C(16)	1.365(2)	C(9)-C(10)	1.374(2)
O(2)-N(3)	1.4189(18)	N(6)-C(15)	1.375(2)	C(10)-C(11)	1.380(3)
O(3)-C(14)	1.417(2)	N(6)-H(6A)	0.8800	C(10)-H(10A)	0.9500
O(3)-N(5)	1.4221(18)	C(1)-C(2)	1.385(3)	C(11)-C(12)	1.379(3)
O(4)-C(16)	1.227(2)	C(1)-C(16)	1.498(3)	C(11)-H(11A)	0.9500
O(5)-C(17)	1.411(2)	C(2)-C(3)	1.375(3)	C(12)-C(13)	1.375(2)
O(5)-H(5H)	0.90(3)	C(2)-H(2A)	0.9500	C(12)-H(12A)	0.9500
N(1)-C(1)	1.342(2)	C(3)-C(4)	1.385(3)	C(13)-C(14)	1.507(2)
N(1)-C(5)	1.344(2)	C(3)-H(3A)	0.9500	C(14)-H(14A)	0.9900
N(2)-C(6)	1.363(2)	C(4)-C(5)	1.382(3)	C(14)-H(14B)	0.9900
N(2)-C(7)	1.380(2)	C(4)-H(4A)	0.9500	C(15)-H(15A)	0.9500
N(2)-H(2B)	0.8800	C(5)-C(6)	1.502(2)	C(17)-H(17A)	0.9800
N(3)-C(7)	1.270(2)	C(7)-H(7A)	0.9500	C(17)-H(17B)	0.9800
N(4)-C(13)	1.349(2)	C(8)-C(9)	1.503(2)	C(17)-H(17C)	0.9800
N(4)-C(9)	1.350(2)	C(8)-H(8A)	0.9900		

C(8)-O(2)-N(3)	108.15(12)	O(2)-C(8)-H(8B)	109.4
C(14)-O(3)-N(5)	107.49(12)	C(9)-C(8)-H(8B)	109.4
C(17)-O(5)-H(5H)	109.9(16)	H(8A)-C(8)-H(8B)	108.0
C(1)-N(1)-C(5)	116.93(16)	N(4)-C(9)-C(10)	122.88(16)
C(6)-N(2)-C(7)	120.12(15)	N(4)-C(9)-C(8)	118.99(16)
C(6)-N(2)-H(2B)	119.9	C(10)-C(9)-C(8)	118.11(16)
C(7)-N(2)-H(2B)	119.9	C(9)-C(10)-C(11)	119.15(18)
C(7)-N(3)-O(2)	110.15(14)	C(9)-C(10)-H(10A)	120.4
C(13)-N(4)-C(9)	117.11(16)	C(11)-C(10)-H(10A)	120.4
C(15)-N(5)-O(3)	109.86(14)	C(12)-C(11)-C(10)	118.78(19)
C(16)-N(6)-C(15)	119.85(15)	C(12)-C(11)-H(11A)	120.6
C(16)-N(6)-H(6A)	120.1	C(10)-C(11)-H(11A)	120.6
C(15)-N(6)-H(6A)	120.1	C(13)-C(12)-C(11)	119.06(17)
N(1)-C(1)-C(2)	123.05(17)	C(13)-C(12)-H(12A)	120.5
N(1)-C(1)-C(16)	117.87(16)	C(11)-C(12)-H(12A)	120.5
C(2)-C(1)-C(16)	118.97(16)	N(4)-C(13)-C(12)	123.01(17)
C(3)-C(2)-C(1)	119.19(18)	N(4)-C(13)-C(14)	119.28(16)
C(3)-C(2)-H(2A)	120.4	C(12)-C(13)-C(14)	117.70(16)
C(1)-C(2)-H(2A)	120.4	O(3)-C(14)-C(13)	110.74(14)
C(2)-C(3)-C(4)	118.69(19)	O(3)-C(14)-H(14A)	109.5
C(2)-C(3)-H(3A)	120.7	C(13)-C(14)-H(14A)	109.5
C(4)-C(3)-H(3A)	120.7	O(3)-C(14)-H(14B)	109.5
C(5)-C(4)-C(3)	118.57(18)	C(13)-C(14)-H(14B)	109.5
C(5)-C(4)-H(4A)	120.7	H(14A)-C(14)-H(14B)	108.1
C(3)-C(4)-H(4A)	120.7	N(5)-C(15)-N(6)	129.08(17)
N(1)-C(5)-C(4)	123.54(17)	N(5)-C(15)-H(15A)	115.5
N(1)-C(5)-C(6)	117.41(16)	N(6)-C(15)-H(15A)	115.5
C(4)-C(5)-C(6)	119.00(16)	O(4)-C(16)-N(6)	122.33(17)
O(1)-C(6)-N(2)	122.83(17)	O(4)-C(16)-C(1)	120.50(17)
O(1)-C(6)-C(5)	120.25(17)	N(6)-C(16)-C(1)	117.14(15)
N(2)-C(6)-C(5)	116.88(15)	O(5)-C(17)-H(17A)	109.5
N(3)-C(7)-N(2)	128.60(17)	O(5)-C(17)-H(17B)	109.5
N(3)-C(7)-H(7A)	115.7	H(17A)-C(17)-H(17B)	109.5
N(2)-C(7)-H(7A)	115.7	O(5)-C(17)-H(17C)	109.5
O(2)-C(8)-C(9)	111.20(14)	H(17A)-C(17)-H(17C)	109.5

O(2)-C(8)-H(8A)	109.4	H(17B)-C(17)-H(17C)	109.5
C(9)-C(8)-H(8A)	109.4		

**Table B2.4.** Anisotropic displacement parameters ( $\text{\AA}^2 \times 10^3$ ) for ap19. The anisotropic displacement factor exponent takes the form:  $-2\pi^2 [ h^2 a^* a^* U^{11} + \dots + 2 h k a^* b^* U^{12} ]$

	U <sup>11</sup>	U <sup>22</sup>	U <sup>33</sup>	U <sup>23</sup>	U <sup>13</sup>	U <sup>12</sup>
O(1)	54(1)	38(1)	58(1)	12(1)	14(1)	-4(1)
O(2)	64(1)	26(1)	47(1)	-2(1)	19(1)	-9(1)
O(3)	60(1)	24(1)	50(1)	-2(1)	15(1)	-5(1)
O(4)	62(1)	33(1)	54(1)	-10(1)	5(1)	5(1)
O(5)	46(1)	32(1)	43(1)	-2(1)	10(1)	-3(1)
N(1)	32(1)	34(1)	38(1)	2(1)	2(1)	4(1)
N(2)	39(1)	28(1)	43(1)	6(1)	5(1)	-2(1)
N(3)	50(1)	26(1)	54(1)	2(1)	8(1)	-7(1)
N(4)	38(1)	30(1)	40(1)	0(1)	4(1)	0(1)
N(5)	50(1)	25(1)	57(1)	-4(1)	8(1)	-4(1)
N(6)	41(1)	26(1)	42(1)	-4(1)	3(1)	0(1)
C(1)	31(1)	38(1)	39(1)	-3(1)	-1(1)	7(1)
C(2)	40(1)	46(1)	44(1)	-8(1)	1(1)	6(1)
C(3)	42(1)	60(1)	39(1)	2(1)	5(1)	6(1)
C(4)	37(1)	48(1)	44(1)	10(1)	5(1)	4(1)
C(5)	30(1)	37(1)	41(1)	8(1)	2(1)	5(1)
C(6)	32(1)	35(1)	43(1)	9(1)	1(1)	1(1)
C(7)	43(1)	27(1)	53(1)	4(1)	6(1)	-5(1)
C(8)	55(1)	36(1)	46(1)	-7(1)	11(1)	-7(1)
C(9)	38(1)	33(1)	36(1)	-2(1)	0(1)	1(1)
C(10)	48(1)	38(1)	41(1)	-4(1)	4(1)	4(1)
C(11)	54(1)	49(1)	42(1)	1(1)	15(1)	3(1)

C(12)	48(1)	41(1)	44(1)	7(1)	12(1)	-1(1)
C(13)	34(1)	33(1)	38(1)	6(1)	2(1)	1(1)
C(14)	49(1)	32(1)	50(1)	4(1)	15(1)	-2(1)
C(15)	46(1)	27(1)	51(1)	-4(1)	4(1)	-2(1)
C(16)	34(1)	34(1)	43(1)	-4(1)	-3(1)	8(1)
C(17)	49(1)	61(1)	53(1)	8(1)	6(1)	3(1)

**Table B2.5** Hydrogen coordinates ( $\times 10^4$ ) and isotropic displacement parameters ( $\text{\AA}^2 \times 10^3$ ) for ap19.

	x	y	z	U(eq)
H(5H)	860(40)	4881(16)	2582(17)	84(9)
H(2B)	1747	5852	1465	44
H(6A)	942	3838	1433	44
H(2A)	2488	3352	-1121	53
H(3A)	3395	4605	-1811	57
H(4A)	3546	5962	-1071	52
H(7A)	2168	7650	1360	50
H(8A)	-707	7159	3451	54
H(8B)	1181	6731	3858	54
H(10A)	-1970	6564	4672	51
H(11A)	-3427	5367	5211	57
H(12A)	-3237	3977	4576	52
H(14A)	-753	3090	3779	52
H(14B)	-2700	3205	3210	52
H(15A)	37	2084	1272	50
H(17A)	3788	5252	3053	82
H(17B)	4291	4515	2398	82
H(17C)	3319	4240	3199	82

**Table B2.6** Torsion angles [°] for ap19.

C(8)-O(2)-N(3)-C(7)	166.09(16)	C(13)-N(4)-C(9)-C(8)	179.40(16)
C(14)-O(3)-N(5)-C(15)	-177.77(15)	O(2)-C(8)-C(9)-N(4)	22.2(2)
C(5)-N(1)-C(1)-C(2)	-1.1(2)	O(2)-C(8)-C(9)-C(10)	-159.54(16)
C(5)-N(1)-C(1)-C(16)	-177.33(15)	N(4)-C(9)-C(10)-C(11)	-0.3(3)
N(1)-C(1)-C(2)-C(3)	0.0(3)	C(8)-C(9)-C(10)-C(11)	-178.50(18)
C(16)-C(1)-C(2)-C(3)	176.25(16)	C(9)-C(10)-C(11)-C(12)	-0.9(3)
C(1)-C(2)-C(3)-C(4)	0.7(3)	C(10)-C(11)-C(12)-C(13)	1.1(3)
C(2)-C(3)-C(4)-C(5)	-0.5(3)	C(9)-N(4)-C(13)-C(12)	-1.0(2)
C(1)-N(1)-C(5)-C(4)	1.4(3)	C(9)-N(4)-C(13)-C(14)	-179.49(16)
C(1)-N(1)-C(5)-C(6)	178.68(15)	C(11)-C(12)-C(13)-N(4)	-0.1(3)
C(3)-C(4)-C(5)-N(1)	-0.6(3)	C(11)-C(12)-C(13)-C(14)	178.38(18)
C(3)-C(4)-C(5)-C(6)	-177.90(16)	N(5)-O(3)-C(14)-C(13)	-174.88(14)
C(7)-N(2)-C(6)-O(1)	7.3(3)	N(4)-C(13)-C(14)-O(3)	-11.7(2)
C(7)-N(2)-C(6)-C(5)	-170.31(15)	C(12)-C(13)-C(14)-O(3)	169.74(15)
N(1)-C(5)-C(6)-O(1)	176.77(16)	O(3)-N(5)-C(15)-N(6)	0.1(3)
C(4)-C(5)-C(6)-O(1)	-5.8(3)	C(16)-N(6)-C(15)-N(5)	-173.08(18)
N(1)-C(5)-C(6)-N(2)	-5.5(2)	C(15)-N(6)-C(16)-O(4)	-3.2(3)
C(4)-C(5)-C(6)-N(2)	171.88(16)	C(15)-N(6)-C(16)-C(1)	174.56(15)
O(2)-N(3)-C(7)-N(2)	-0.7(3)	N(1)-C(1)-C(16)-O(4)	179.44(16)
C(6)-N(2)-C(7)-N(3)	175.14(18)	C(2)-C(1)-C(16)-O(4)	3.0(3)
N(3)-O(2)-C(8)-C(9)	168.52(14)	N(1)-C(1)-C(16)-N(6)	1.6(2)
C(13)-N(4)-C(9)-C(10)	1.2(3)	C(2)-C(1)-C(16)-N(6)	-174.80(15)

**Table B2.7.** Hydrogen bonds for ap19 [ $\text{\AA}$  and °].

D-H...A	d(D-H)	d(H...A)	d(D...A)	$\angle$ (DHA)
O(5)-H(5H)...N(4)	0.90(3)	1.93(3)	2.827(2)	174(2)
O(5)-H(5H)...O(2)	0.90(3)	2.44(2)	2.7935(17)	103.7(18)
O(5)-H(5H)...O(3)	0.90(3)	2.39(2)	2.7864(17)	106.8(18)
N(2)-H(2B)...O(5)	0.88	2.00	2.8523(19)	164.0
N(6)-H(6A)...O(5)	0.88	1.97	2.8273(18)	164.2

### 3) Maxi-M2

A crystal of the compound (colorless, block-shaped, size 0.10 x 0.15 x 0.20 mm) was mounted on a glass fiber with grease and cooled to -93 °C in a stream of nitrogen gas controlled with Cryostream Controller 700. Data collection was performed on a Bruker SMART APEX II X-ray diffractometer with graphite-monochromated Mo K $\alpha$  radiation ( $\lambda = 0.71073 \text{ \AA}$ ), operating at 50 kV and 30 mA over 2 $\theta$  ranges of 3.24 ~ 52.00°. No significant decay was observed during the data collection.

Data were processed on a PC using the Bruker AXS Crystal Structure Analysis Package:<sup>[1]</sup> Data collection: APEX2 (Bruker, 2006); cell refinement: SAINT (Bruker, 2005); data reduction: SAINT (Bruker, 2005); structure solution: XPREP (Bruker, 2005) and SHELXTL (Bruker, 2000); structure refinement: SHELXTL; molecular graphics: SHELXTL; publication materials: SHELXTL. Neutral atom scattering factors were taken from Cromer and Waber.<sup>[2]</sup> The crystal is monoclinic space group Cc, based on the systematic absences, E statistics and successful refinement of the structure. The structure was solved by direct methods. Full-matrix least-square refinements minimizing the function  $\sum w (F_o^2 - F_c^2)^2$  were applied to the compound. All non-hydrogen atoms were refined anisotropically. All H atoms were placed in geometrically calculated positions, with C-H = 0.95 (aromatic), 0.99(CH<sub>2</sub>), 0.88(N-H) Å, and refined as riding atoms, with Uiso(H) = 1.5UeqC(CH<sub>3</sub>) or 1.2 UeqC(N or other C). Convergence to final  $R_1 = 0.0443$  and  $wR_2 = 0.0898$  for 7115 ( $I > 2\sigma(I)$ ) independent reflections, and  $R_1 = 0.0742$  and  $wR_2 = 0.1869$  for all 9760 (R(int) = 0.0581) independent reflections, with 718 parameters and 4 restraints, were achieved.<sup>[3]</sup> The largest residual peak and hole to be 0.234 and -0.165 e/Å<sup>3</sup>, respectively. Crystallographic data, atomic coordinates and equivalent isotropic displacement parameters, bond lengths and angles, anisotropic displacement parameters, hydrogen coordinates and isotropic displacement parameters, torsion angles and hydrogen bonding information are given in Table B3.1 to B3.7. The molecular structure and the cell packing are shown in Figures B3.1 and B3.2.

**Figure B3.1.** Molecular Structure (Displacement ellipsoids for non-H atoms are shown at the 50% probability level and H atoms are omitted for clarity.)

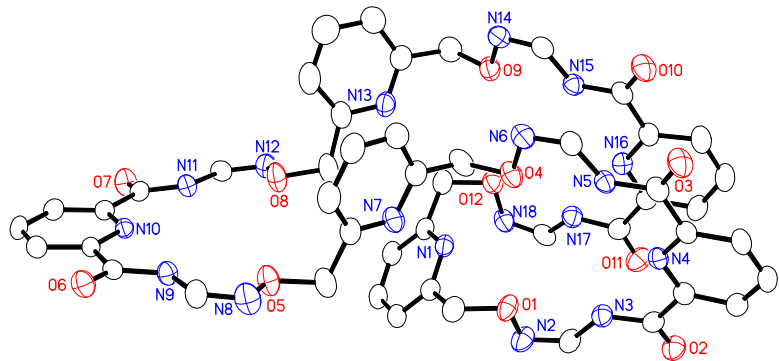
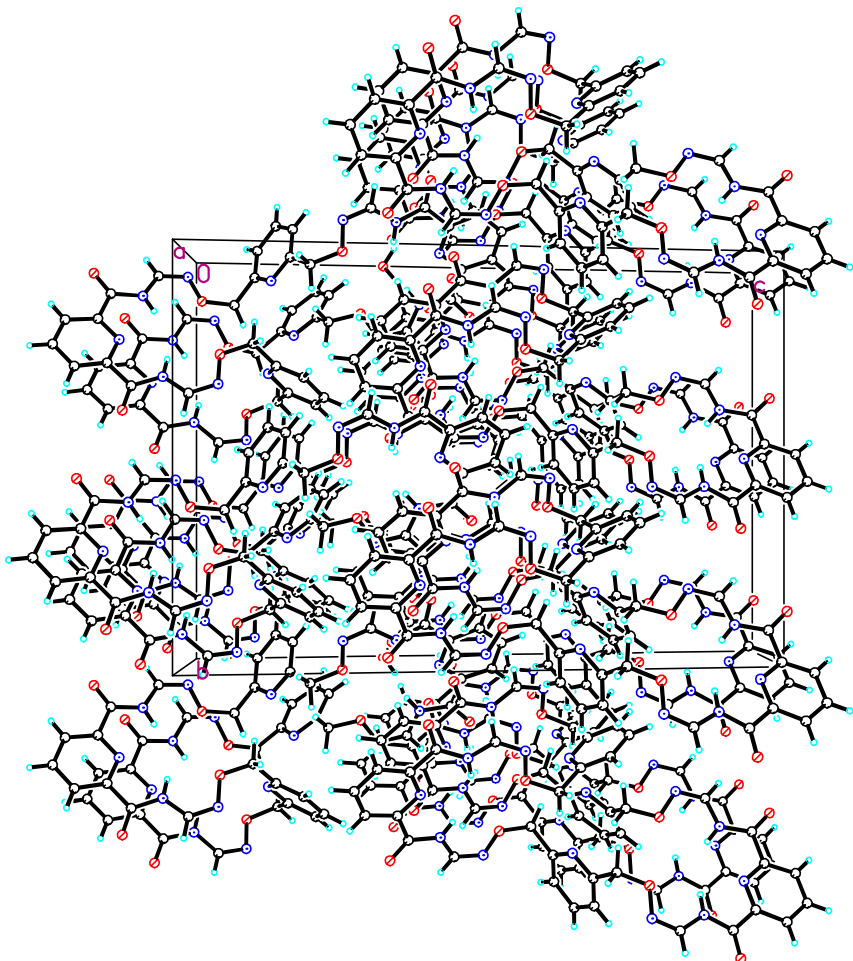


**Figure B3.2.** Unit cell packing



[1] Bruker AXS Crystal Structure Analysis Package:

Bruker (2000). SHELXTL. Version 6.14. Bruker AXS Inc., Madison, Wisconsin, USA.

Bruker (2005). XPREP. Version 2005/2. Bruker AXS Inc., Madison, Wisconsin, USA.

Bruker (2005). SAINT. Version 7.23A. Bruker AXS Inc., Madison, Wisconsin, USA.

Bruker (2006). APEX2. Version 2.0-2. Bruker AXS Inc., Madison, Wisconsin, USA.

[2] Cromer, D. T.; Waber, J. T. *International Tables for X-ray Crystallography*; Kynoch Press: Birmingham, UK, 1974; Vol. 4, Table 2.2 A.

$$[3] R_1 = \sum |Fo| - |Fc| / \sum |Fo|$$

$$wR_2 = \{ \sum [w(Fo^2 - Fc^2)^2] / \sum [w(Fo^2)^2] \}^{1/2}$$

$$(w = 1 / [\sigma^2(Fo^2) + (0.0457P)^2 + 0.1746P], \text{ where } P = [\text{Max}(Fo^2, 0) + 2Fc^2] / 3)$$

**Table B3.1.** Crystal data and structure refinement for ap17

Identification code	ap17	
Empirical formula	C48 H44 N18 O13	
Formula weight	1081.01	
Temperature	180(2) K	
Wavelength	0.71073 Å	
Crystal system	Monoclinic	
Space group	Cc	
Unit cell dimensions	a = 11.3994(2) Å b = 17.3955(4) Å c = 25.7476(5) Å	α = 90°. β = 102.6120(10)°. γ = 90°.
Volume	4982.51(17) Å³	
Z	4	
Density (calculated)	1.441 Mg/m³	
Absorption coefficient	0.109 mm⁻¹	
F(000)	2248	
Crystal size	0.20 x 0.15 x 0.10 mm³	
Theta range for data collection	1.62 to 26.00°.	
Index ranges	-14<=h<=14, -21<=k<=21, -31<=l<=31	
Reflections collected	35628	
Independent reflections	9760 [R(int) = 0.0581]	
Completeness to theta = 26.00°	100.0 %	
Absorption correction	Multi-scan	
Max. and min. transmission	0.9892 and 0.9786	

Refinement method	Full-matrix least-squares on F <sup>2</sup>
Data / restraints / parameters	9760 / 4 / 718
Goodness-of-fit on F <sup>2</sup>	1.014
Final R indices [I>2sigma(I)]	R1 = 0.0443, wR2 = 0.0898
R indices (all data)	R1 = 0.0742, wR2 = 0.1042
Absolute structure parameter	N/A
Largest diff. peak and hole	0.234 and -0.165 e. $\text{\AA}^{-3}$

**Table B3.2.** Atomic coordinates ( $x \times 10^4$ ) and equivalent isotropic displacement parameters ( $\text{\AA}^2 \times 10^3$ ) for ap17. U(eq) is defined as one third of the trace of the orthogonalized  $U^{ij}$  tensor.

	x	y	z	U(eq)
O(1)	11600(2)	2480(1)	5627(1)	40(1)
O(2)	11839(2)	1137(1)	4065(1)	43(1)
O(3)	8459(2)	4518(1)	3432(1)	45(1)
O(4)	8798(2)	3861(1)	5232(1)	41(1)
O(5)	12116(2)	4959(1)	7636(1)	46(1)
O(6)	13011(2)	6641(1)	9101(1)	38(1)
O(7)	9705(2)	3533(1)	9767(1)	43(1)
O(8)	9252(2)	3592(1)	7905(1)	47(1)
O(9)	5834(2)	2844(1)	5575(1)	41(1)
O(10)	5913(2)	3540(1)	3818(1)	44(1)
O(11)	9504(2)	256(1)	4477(1)	48(1)
O(12)	8110(2)	1132(1)	5956(1)	41(1)
N(1)	10135(2)	2073(1)	6375(1)	35(1)
N(2)	12174(2)	1764(2)	5614(1)	45(1)
N(3)	11421(2)	1943(1)	4695(1)	36(1)
N(4)	10146(2)	2858(1)	3931(1)	29(1)
N(5)	8826(2)	3971(1)	4256(1)	31(1)
N(6)	8111(2)	4481(1)	4971(1)	39(1)
N(7)	10247(2)	4316(1)	6420(1)	38(1)
N(8)	12727(3)	5668(2)	7655(1)	50(1)

N(9)	12360(2)	5664(1)	8526(1)	32(1)
N(10)	11262(2)	5004(1)	9248(1)	27(1)
N(11)	9735(2)	3821(1)	8908(1)	30(1)
N(12)	8800(2)	3018(1)	8201(1)	40(1)
N(13)	7024(2)	3120(2)	6727(1)	42(1)
N(14)	5335(2)	3529(2)	5320(1)	41(1)
N(15)	6174(2)	2997(1)	4641(1)	34(1)
N(16)	7622(2)	1898(1)	4344(1)	32(1)
N(17)	8751(2)	908(2)	5098(1)	38(1)
N(18)	8881(2)	482(2)	5972(1)	42(1)
C(1)	9626(3)	1624(2)	6688(1)	35(1)
C(2)	10267(3)	1327(2)	7165(1)	40(1)
C(3)	11463(3)	1477(2)	7323(1)	43(1)
C(4)	11997(3)	1943(2)	7000(1)	42(1)
C(5)	11306(3)	2228(2)	6530(1)	33(1)
C(6)	11833(3)	2741(2)	6172(1)	43(1)
C(7)	12036(3)	1542(2)	5132(1)	41(1)
C(8)	11385(3)	1725(2)	4184(1)	34(1)
C(9)	10760(3)	2281(2)	3768(1)	32(1)
C(10)	10871(3)	2191(2)	3248(1)	38(1)
C(11)	10342(3)	2725(2)	2871(1)	41(1)
C(12)	9720(3)	3332(2)	3036(1)	37(1)
C(13)	9630(2)	3372(2)	3561(1)	30(1)
C(14)	8913(3)	4010(2)	3735(1)	34(1)
C(15)	8195(3)	4494(2)	4486(1)	34(1)
C(16)	8585(3)	3790(2)	5764(1)	46(1)
C(17)	9150(3)	4442(2)	6122(1)	40(1)
C(18)	8557(3)	5130(2)	6148(1)	57(1)
C(19)	9135(4)	5713(2)	6474(1)	64(1)
C(20)	10250(4)	5575(2)	6781(1)	57(1)
C(21)	10769(3)	4873(2)	6752(1)	38(1)
C(22)	11953(3)	4644(2)	7104(1)	49(1)
C(23)	12811(3)	5965(2)	8112(1)	40(1)
C(24)	12495(2)	6033(2)	9004(1)	28(1)
C(25)	11940(2)	5629(2)	9406(1)	26(1)

C(26)	12143(3)	5918(2)	9922(1)	34(1)
C(27)	11645(3)	5541(2)	10293(1)	34(1)
C(28)	10952(3)	4891(2)	10138(1)	33(1)
C(29)	10779(2)	4647(2)	9616(1)	30(1)
C(30)	10026(3)	3947(2)	9446(1)	31(1)
C(31)	9085(3)	3186(2)	8694(1)	33(1)
C(32)	8863(3)	3400(3)	7353(1)	58(1)
C(33)	7551(3)	3567(2)	7134(1)	43(1)
C(34)	6926(4)	4149(2)	7326(1)	55(1)
C(35)	5743(4)	4275(2)	7086(2)	65(1)
C(36)	5213(4)	3824(2)	6653(1)	55(1)
C(37)	5873(3)	3260(2)	6489(1)	41(1)
C(38)	5339(3)	2723(2)	6034(1)	47(1)
C(39)	5559(3)	3553(2)	4856(1)	38(1)
C(40)	6321(3)	3022(2)	4130(1)	34(1)
C(41)	7025(3)	2375(2)	3969(1)	32(1)
C(42)	7030(3)	2293(2)	3434(1)	40(1)
C(43)	7698(3)	1710(2)	3281(1)	43(1)
C(44)	8345(3)	1228(2)	3657(1)	38(1)
C(45)	8263(3)	1337(2)	4185(1)	33(1)
C(46)	8914(3)	784(2)	4596(1)	38(1)
C(47)	9143(3)	413(2)	5518(1)	41(1)
C(48)	8317(3)	1449(2)	6483(1)	45(1)
O(1W)	5444(2)	5022(2)	3259(1)	63(1)

---

**Table B3.3.** Bond lengths [ $\text{\AA}$ ] and angles [ $^\circ$ ] for ap17.

O(1)-N(2)	1.409(3)	N(13)-C(33)	1.337(4)	C(18)-H(18A)	0.9500
O(1)-C(6)	1.444(4)	N(13)-C(37)	1.344(4)	C(19)-C(20)	1.362(5)
O(2)-C(8)	1.216(3)	N(14)-C(39)	1.276(4)	C(19)-H(19A)	0.9500
O(3)-C(14)	1.217(3)	N(15)-C(40)	1.363(4)	C(20)-C(21)	1.367(4)
O(4)-N(6)	1.414(3)	N(15)-C(39)	1.378(4)	C(23)-H(23A)	0.9500
O(4)-C(16)	1.450(4)	N(15)-H(15B)	0.8800	C(24)-C(25)	1.501(4)
O(5)-N(8)	1.413(3)	N(16)-C(45)	1.335(4)	C(25)-C(26)	1.390(4)

O(5)-C(22)	1.449(4)	N(16)-C(41)	1.339(4)	C(26)-C(27)	1.378(4)
O(6)-C(24)	1.209(3)	N(17)-C(46)	1.363(4)	C(26)-H(26A)	0.9500
O(7)-C(30)	1.212(3)	N(17)-C(47)	1.380(4)	C(27)-C(28)	1.387(4)
O(8)-N(12)	1.418(3)	N(17)-H(17A)	0.8800	C(27)-H(27A)	0.9500
O(8)-C(32)	1.432(3)	N(18)-C(47)	1.272(4)	C(28)-C(29)	1.383(4)
O(9)-N(14)	1.419(3)	C(1)-C(2)	1.386(4)	C(28)-H(28A)	0.9500
O(9)-C(38)	1.431(4)	C(1)-C(48)	1.502(4)	C(29)-C(30)	1.499(4)
O(10)-C(40)	1.229(3)	C(2)-C(3)	1.359(4)	C(31)-H(31A)	0.9500
O(11)-C(46)	1.216(3)	C(2)-H(2A)	0.9500	C(32)-C(33)	1.508(5)
O(12)-N(18)	1.428(3)	C(3)-C(4)	1.392(5)	C(32)-H(32A)	0.9900
O(12)-C(48)	1.436(3)	C(3)-H(3A)	0.9500	C(32)-H(32B)	0.9900
N(1)-C(5)	1.335(4)	C(20)-H(20A)	0.9500	C(33)-C(34)	1.390(5)
N(1)-C(1)	1.342(4)	C(21)-C(22)	1.506(4)	C(34)-C(35)	1.373(5)
N(2)-C(7)	1.279(4)	C(22)-H(22A)	0.9900	C(34)-H(34A)	0.9500
N(3)-C(8)	1.361(4)	C(22)-H(22B)	0.9900	C(35)-C(36)	1.389(5)
N(3)-C(7)	1.378(4)	C(4)-C(5)	1.384(4)	C(35)-H(35A)	0.9500
N(3)-H(3B)	0.8800	C(4)-H(4A)	0.9500	C(36)-C(37)	1.360(5)
N(4)-C(9)	1.342(4)	C(5)-C(6)	1.500(4)	C(36)-H(36A)	0.9500
N(4)-C(13)	1.345(4)	C(6)-H(6A)	0.9900	C(37)-C(38)	1.517(4)
N(5)-C(14)	1.369(4)	C(6)-H(6B)	0.9900	C(38)-H(38A)	0.9900
N(5)-C(15)	1.371(4)	C(7)-H(7A)	0.9500	C(38)-H(38B)	0.9900
N(5)-H(5A)	0.8800	C(8)-C(9)	1.503(4)	C(39)-H(39A)	0.9500
N(6)-C(15)	1.274(4)	C(9)-C(10)	1.381(4)	C(40)-C(41)	1.494(4)
N(7)-C(17)	1.335(4)	C(10)-C(11)	1.383(4)	C(41)-C(42)	1.387(4)
N(7)-C(21)	1.342(4)	C(10)-H(10A)	0.9500	C(42)-C(43)	1.377(5)
N(8)-C(23)	1.270(4)	C(11)-C(12)	1.388(4)	C(42)-H(42A)	0.9500
N(9)-C(24)	1.366(3)	C(11)-H(11A)	0.9500	C(43)-C(44)	1.367(4)
N(9)-C(23)	1.384(4)	C(12)-C(13)	1.382(4)	C(43)-H(43A)	0.9500
N(9)-H(9A)	0.8800	C(12)-H(12A)	0.9500	C(44)-C(45)	1.397(4)
N(10)-C(25)	1.345(3)	C(13)-C(14)	1.503(4)	C(44)-H(44A)	0.9500
N(10)-C(29)	1.348(4)	C(15)-H(15A)	0.9500	C(45)-C(46)	1.501(4)
N(11)-C(30)	1.370(3)	C(16)-C(17)	1.513(4)	C(47)-H(47A)	0.9500
N(11)-C(31)	1.376(4)	C(16)-H(16A)	0.9900	C(48)-H(48A)	0.9900
N(11)-H(11B)	0.8800	C(16)-H(16B)	0.9900	C(48)-H(48B)	0.9900
N(12)-C(31)	1.275(3)	C(17)-C(18)	1.384(5)	O(1W)-H(1WB)	0.95(2)

C(18)-C(19) 1.388(5) O(1W)-H(1WA) 0.97(3)

N(2)-O(1)-C(6)	108.2(2)	C(19)-C(20)-H(20A)	120.5
N(6)-O(4)-C(16)	108.9(2)	C(21)-C(20)-H(20A)	120.5
N(8)-O(5)-C(22)	108.8(2)	N(7)-C(21)-C(20)	122.9(3)
N(12)-O(8)-C(32)	107.3(2)	N(7)-C(21)-C(22)	114.0(3)
N(14)-O(9)-C(38)	108.4(2)	C(20)-C(21)-C(22)	123.1(3)
N(18)-O(12)-C(48)	107.7(2)	O(5)-C(22)-C(21)	112.5(3)
C(5)-N(1)-C(1)	118.2(2)	O(5)-C(22)-H(22A)	109.1
C(7)-N(2)-O(1)	109.2(2)	C(21)-C(22)-H(22A)	109.1
C(8)-N(3)-C(7)	123.3(3)	O(5)-C(22)-H(22B)	109.1
C(8)-N(3)-H(3B)	118.3	C(21)-C(22)-H(22B)	109.1
C(7)-N(3)-H(3B)	118.3	H(22A)-C(22)-H(22B)	107.8
C(9)-N(4)-C(13)	117.0(2)	N(8)-C(23)-N(9)	126.5(3)
C(14)-N(5)-C(15)	123.1(3)	N(8)-C(23)-H(23A)	116.7
C(14)-N(5)-H(5A)	118.4	N(9)-C(23)-H(23A)	116.7
C(15)-N(5)-H(5A)	118.4	O(6)-C(24)-N(9)	123.4(3)
C(15)-N(6)-O(4)	109.0(2)	O(6)-C(24)-C(25)	121.7(2)
C(17)-N(7)-C(21)	118.5(3)	N(9)-C(24)-C(25)	114.9(2)
C(23)-N(8)-O(5)	108.8(3)	N(10)-C(25)-C(26)	123.1(3)
C(24)-N(9)-C(23)	121.9(2)	N(10)-C(25)-C(24)	118.0(2)
C(24)-N(9)-H(9A)	119.1	C(26)-C(25)-C(24)	118.9(2)
C(23)-N(9)-H(9A)	119.1	C(27)-C(26)-C(25)	118.9(3)
C(25)-N(10)-C(29)	117.1(2)	C(27)-C(26)-H(26A)	120.6
C(30)-N(11)-C(31)	121.5(2)	C(25)-C(26)-H(26A)	120.6
C(30)-N(11)-H(11B)	119.2	C(26)-C(27)-C(28)	118.9(3)
C(31)-N(11)-H(11B)	119.2	C(26)-C(27)-H(27A)	120.5
C(31)-N(12)-O(8)	109.3(2)	C(28)-C(27)-H(27A)	120.5
C(33)-N(13)-C(37)	118.6(3)	C(29)-C(28)-C(27)	118.7(3)
C(39)-N(14)-O(9)	108.6(2)	C(29)-C(28)-H(28A)	120.6
C(40)-N(15)-C(39)	123.0(3)	C(27)-C(28)-H(28A)	120.6
C(40)-N(15)-H(15B)	118.5	N(10)-C(29)-C(28)	123.3(3)
C(39)-N(15)-H(15B)	118.5	N(10)-C(29)-C(30)	117.7(2)
C(45)-N(16)-C(41)	117.3(2)	C(28)-C(29)-C(30)	119.0(3)
C(46)-N(17)-C(47)	123.9(3)	O(7)-C(30)-N(11)	123.6(3)

C(46)-N(17)-H(17A)	118.1	O(7)-C(30)-C(29)	121.5(3)
C(47)-N(17)-H(17A)	118.1	N(11)-C(30)-C(29)	115.0(2)
C(47)-N(18)-O(12)	108.4(2)	N(12)-C(31)-N(11)	125.5(3)
N(1)-C(1)-C(2)	122.4(3)	N(12)-C(31)-H(31A)	117.3
N(1)-C(1)-C(48)	115.8(3)	N(11)-C(31)-H(31A)	117.3
C(2)-C(1)-C(48)	121.8(3)	O(8)-C(32)-C(33)	113.2(3)
C(3)-C(2)-C(1)	119.6(3)	O(8)-C(32)-H(32A)	108.9
C(3)-C(2)-H(2A)	120.2	C(33)-C(32)-H(32A)	108.9
C(1)-C(2)-H(2A)	120.2	O(8)-C(32)-H(32B)	108.9
C(2)-C(3)-C(4)	118.4(3)	C(33)-C(32)-H(32B)	108.9
C(2)-C(3)-H(3A)	120.8	H(32A)-C(32)-H(32B)	107.7
C(4)-C(3)-H(3A)	120.8	N(13)-C(33)-C(34)	121.7(3)
C(5)-C(4)-C(3)	119.3(3)	N(13)-C(33)-C(32)	114.9(3)
C(5)-C(4)-H(4A)	120.3	C(34)-C(33)-C(32)	123.4(3)
C(3)-C(4)-H(4A)	120.3	C(35)-C(34)-C(33)	119.1(3)
N(1)-C(5)-C(4)	122.1(3)	C(35)-C(34)-H(34A)	120.5
N(1)-C(5)-C(6)	116.3(3)	C(33)-C(34)-H(34A)	120.5
C(4)-C(5)-C(6)	121.6(3)	C(34)-C(35)-C(36)	118.9(3)
O(1)-C(6)-C(5)	113.4(2)	C(34)-C(35)-H(35A)	120.5
O(1)-C(6)-H(6A)	108.9	C(36)-C(35)-H(35A)	120.5
C(5)-C(6)-H(6A)	108.9	C(37)-C(36)-C(35)	119.0(4)
O(1)-C(6)-H(6B)	108.9	C(37)-C(36)-H(36A)	120.5
C(5)-C(6)-H(6B)	108.9	C(35)-C(36)-H(36A)	120.5
H(6A)-C(6)-H(6B)	107.7	N(13)-C(37)-C(36)	122.7(3)
N(2)-C(7)-N(3)	124.9(3)	N(13)-C(37)-C(38)	115.4(3)
N(2)-C(7)-H(7A)	117.5	C(36)-C(37)-C(38)	121.9(3)
N(3)-C(7)-H(7A)	117.5	O(9)-C(38)-C(37)	112.5(3)
O(2)-C(8)-N(3)	123.7(3)	O(9)-C(38)-H(38A)	109.1
O(2)-C(8)-C(9)	121.5(3)	C(37)-C(38)-H(38A)	109.1
N(3)-C(8)-C(9)	114.8(3)	O(9)-C(38)-H(38B)	109.1
N(4)-C(9)-C(10)	123.5(3)	C(37)-C(38)-H(38B)	109.1
N(4)-C(9)-C(8)	117.2(2)	H(38A)-C(38)-H(38B)	107.8
C(10)-C(9)-C(8)	119.3(3)	N(14)-C(39)-N(15)	125.2(3)
C(9)-C(10)-C(11)	119.1(3)	N(14)-C(39)-H(39A)	117.4
C(9)-C(10)-H(10A)	120.5	N(15)-C(39)-H(39A)	117.4

C(11)-C(10)-H(10A)	120.5	O(10)-C(40)-N(15)	123.2(3)
C(10)-C(11)-C(12)	118.1(3)	O(10)-C(40)-C(41)	121.3(3)
C(10)-C(11)-H(11A)	121.0	N(15)-C(40)-C(41)	115.5(3)
C(12)-C(11)-H(11A)	121.0	N(16)-C(41)-C(42)	122.7(3)
C(13)-C(12)-C(11)	119.3(3)	N(16)-C(41)-C(40)	119.1(2)
C(13)-C(12)-H(12A)	120.4	C(42)-C(41)-C(40)	118.2(3)
C(11)-C(12)-H(12A)	120.4	C(43)-C(42)-C(41)	118.8(3)
N(4)-C(13)-C(12)	123.1(3)	C(43)-C(42)-H(42A)	120.6
N(4)-C(13)-C(14)	117.6(2)	C(41)-C(42)-H(42A)	120.6
C(12)-C(13)-C(14)	119.3(3)	C(44)-C(43)-C(42)	119.7(3)
O(3)-C(14)-N(5)	123.5(3)	C(44)-C(43)-H(43A)	120.2
O(3)-C(14)-C(13)	121.9(3)	C(42)-C(43)-H(43A)	120.2
N(5)-C(14)-C(13)	114.6(3)	C(43)-C(44)-C(45)	117.8(3)
N(6)-C(15)-N(5)	124.8(3)	C(43)-C(44)-H(44A)	121.1
N(6)-C(15)-H(15A)	117.6	C(45)-C(44)-H(44A)	121.1
N(5)-C(15)-H(15A)	117.6	N(16)-C(45)-C(44)	123.7(3)
O(4)-C(16)-C(17)	112.1(2)	N(16)-C(45)-C(46)	118.3(3)
O(4)-C(16)-H(16A)	109.2	C(44)-C(45)-C(46)	118.0(3)
C(17)-C(16)-H(16A)	109.2	O(11)-C(46)-N(17)	123.7(3)
O(4)-C(16)-H(16B)	109.2	O(11)-C(46)-C(45)	121.6(3)
C(17)-C(16)-H(16B)	109.2	N(17)-C(46)-C(45)	114.6(3)
H(16A)-C(16)-H(16B)	107.9	N(18)-C(47)-N(17)	124.1(3)
N(7)-C(17)-C(18)	121.3(3)	N(18)-C(47)-H(47A)	118.0
N(7)-C(17)-C(16)	116.6(3)	N(17)-C(47)-H(47A)	118.0
C(18)-C(17)-C(16)	122.0(3)	O(12)-C(48)-C(1)	110.8(2)
C(17)-C(18)-C(19)	119.3(3)	O(12)-C(48)-H(48A)	109.5
C(17)-C(18)-H(18A)	120.4	C(1)-C(48)-H(48A)	109.5
C(19)-C(18)-H(18A)	120.4	O(12)-C(48)-H(48B)	109.5
C(20)-C(19)-C(18)	118.8(3)	C(1)-C(48)-H(48B)	109.5
C(20)-C(19)-H(19A)	120.6	H(48A)-C(48)-H(48B)	108.1
C(18)-C(19)-H(19A)	120.6	H(1WB)-O(1W)-H(1WA)	113(3)
C(19)-C(20)-C(21)	119.1(3)		

**Table B3.4.** Anisotropic displacement parameters ( $\text{\AA}^2 \times 10^3$ ) for ap17. The anisotropic

displacement factor exponent takes the form:  $-2\pi^2 [ h^2 a^* U^{11} + \dots + 2 h k a^* b^* U^{12} ]$

	$U^{11}$	$U^{22}$	$U^{33}$	$U^{23}$	$U^{13}$	$U^{12}$
O(1)	58(1)	35(1)	32(1)	6(1)	17(1)	11(1)
O(2)	50(1)	37(1)	43(1)	-1(1)	12(1)	9(1)
O(3)	58(2)	35(1)	37(1)	4(1)	2(1)	10(1)
O(4)	47(1)	39(1)	31(1)	5(1)	-1(1)	2(1)
O(5)	59(2)	44(1)	31(1)	1(1)	4(1)	-9(1)
O(6)	42(1)	33(1)	39(1)	0(1)	7(1)	-9(1)
O(7)	59(2)	38(1)	32(1)	8(1)	11(1)	-10(1)
O(8)	58(2)	56(2)	28(1)	-4(1)	10(1)	-24(1)
O(9)	46(1)	44(1)	32(1)	0(1)	5(1)	3(1)
O(10)	54(2)	38(1)	38(1)	10(1)	3(1)	6(1)
O(11)	54(1)	40(1)	55(2)	-1(1)	20(1)	8(1)
O(12)	44(1)	43(1)	34(1)	1(1)	3(1)	5(1)
N(1)	42(2)	36(1)	27(1)	-1(1)	8(1)	5(1)
N(2)	56(2)	42(2)	40(2)	7(1)	17(1)	19(1)
N(3)	40(2)	34(1)	33(1)	0(1)	8(1)	6(1)
N(4)	31(1)	27(1)	29(1)	-4(1)	4(1)	-5(1)
N(5)	34(1)	29(1)	29(1)	-2(1)	2(1)	2(1)
N(6)	40(2)	36(2)	37(2)	0(1)	2(1)	1(1)
N(7)	44(2)	38(2)	29(1)	5(1)	3(1)	0(1)
N(8)	59(2)	48(2)	43(2)	1(1)	11(1)	-18(1)
N(9)	36(1)	31(1)	28(1)	0(1)	6(1)	-5(1)
N(10)	29(1)	26(1)	25(1)	-1(1)	3(1)	2(1)
N(11)	35(1)	29(1)	26(1)	2(1)	6(1)	-7(1)
N(12)	44(2)	39(2)	37(2)	-4(1)	12(1)	-10(1)
N(13)	45(2)	51(2)	31(1)	-6(1)	12(1)	-7(1)
N(14)	37(2)	45(2)	38(2)	-3(1)	1(1)	6(1)
N(15)	35(1)	32(1)	32(1)	2(1)	4(1)	3(1)
N(16)	36(1)	30(1)	31(1)	1(1)	8(1)	-4(1)
N(17)	41(2)	36(2)	34(2)	2(1)	6(1)	5(1)
N(18)	47(2)	38(2)	35(2)	-1(1)	0(1)	3(1)

C(1)	42(2)	35(2)	28(2)	-1(1)	11(1)	2(1)
C(2)	53(2)	38(2)	30(2)	1(1)	11(2)	3(2)
C(3)	54(2)	47(2)	26(2)	0(1)	6(2)	9(2)
C(4)	45(2)	45(2)	33(2)	-11(2)	3(1)	7(2)
C(5)	39(2)	29(2)	31(2)	-2(1)	9(1)	5(1)
C(6)	50(2)	39(2)	42(2)	-6(2)	14(2)	-2(2)
C(7)	49(2)	40(2)	34(2)	5(2)	12(2)	17(2)
C(8)	31(2)	35(2)	36(2)	-1(1)	10(1)	-4(1)
C(9)	34(2)	27(2)	34(2)	-2(1)	6(1)	-3(1)
C(10)	36(2)	40(2)	36(2)	-10(1)	7(1)	-1(2)
C(11)	43(2)	53(2)	26(2)	-6(2)	7(1)	-7(2)
C(12)	41(2)	42(2)	25(2)	0(1)	2(1)	-3(2)
C(13)	30(2)	31(2)	29(2)	-2(1)	3(1)	-6(1)
C(14)	38(2)	28(2)	34(2)	-3(1)	1(1)	-4(1)
C(15)	38(2)	29(2)	33(2)	-4(1)	2(1)	0(1)
C(16)	46(2)	55(2)	34(2)	13(2)	-2(2)	-9(2)
C(17)	46(2)	48(2)	26(2)	7(1)	11(1)	5(2)
C(18)	53(2)	79(3)	35(2)	-4(2)	2(2)	24(2)
C(19)	79(3)	65(3)	42(2)	-9(2)	2(2)	40(2)
C(20)	74(3)	52(2)	40(2)	-10(2)	2(2)	20(2)
C(21)	51(2)	34(2)	30(2)	0(1)	7(1)	4(2)
C(22)	59(2)	43(2)	38(2)	-10(2)	-5(2)	6(2)
C(23)	49(2)	44(2)	30(2)	-1(2)	10(1)	-10(2)
C(24)	26(2)	30(2)	26(2)	0(1)	1(1)	4(1)
C(25)	28(2)	26(2)	23(1)	0(1)	2(1)	4(1)
C(26)	34(2)	32(2)	35(2)	-4(1)	3(1)	2(1)
C(27)	43(2)	38(2)	22(2)	-5(1)	8(1)	4(2)
C(28)	38(2)	34(2)	28(2)	2(1)	10(1)	3(1)
C(29)	32(2)	29(2)	29(2)	1(1)	4(1)	5(1)
C(30)	34(2)	28(2)	31(2)	0(1)	8(1)	4(1)
C(31)	33(2)	33(2)	35(2)	5(1)	8(1)	-5(1)
C(32)	60(2)	88(3)	26(2)	-8(2)	10(2)	-18(2)
C(33)	53(2)	47(2)	28(2)	3(2)	9(2)	-6(2)
C(34)	80(3)	43(2)	39(2)	-7(2)	7(2)	-1(2)
C(35)	80(3)	47(2)	64(3)	-5(2)	8(2)	19(2)

C(36)	64(2)	50(2)	47(2)	1(2)	3(2)	13(2)
C(37)	47(2)	45(2)	32(2)	6(2)	15(2)	-2(2)
C(38)	44(2)	55(2)	44(2)	-1(2)	10(2)	-10(2)
C(39)	35(2)	39(2)	36(2)	-2(1)	-1(1)	4(1)
C(40)	32(2)	36(2)	32(2)	-2(1)	0(1)	-7(1)
C(41)	36(2)	28(2)	31(2)	-2(1)	6(1)	-9(1)
C(42)	51(2)	38(2)	30(2)	2(1)	7(2)	-10(2)
C(43)	55(2)	46(2)	30(2)	-4(2)	12(2)	-13(2)
C(44)	48(2)	32(2)	39(2)	-9(1)	17(2)	-12(2)
C(45)	34(2)	29(2)	36(2)	-3(1)	10(1)	-7(1)
C(46)	37(2)	35(2)	42(2)	0(1)	12(1)	-4(2)
C(47)	38(2)	35(2)	44(2)	-1(2)	-3(2)	1(2)
C(48)	50(2)	54(2)	33(2)	-3(2)	14(2)	-4(2)
O(1W)	74(2)	58(2)	53(2)	4(1)	2(1)	-4(1)

---

**Table B3.5.** Hydrogen coordinates ( $\times 10^4$ ) and isotropic displacement parameters ( $\text{\AA}^2 \times 10^3$ ) for ap17.

	x	y	z	U(eq)
H(3B)	11031	2362	4749	43
H(5A)	9194	3592	4454	38
H(9A)	11974	5222	8480	38
H(11B)	9970	4154	8694	36
H(15B)	6487	2609	4844	40
H(17A)	8372	1329	5157	45
H(2A)	9874	1022	7382	48
H(3A)	11922	1268	7644	51
H(4A)	12829	2064	7102	50
H(6A)	11497	3264	6181	52

H(6B)	12713	2774	6310	52
H(7A)	12385	1064	5069	49
H(10A)	11304	1768	3151	45
H(11A)	10404	2679	2511	49
H(12A)	9361	3716	2789	44
H(15A)	7791	4894	4267	41
H(16A)	8919	3295	5920	56
H(16B)	7708	3785	5745	56
H(18A)	7763	5203	5945	68
H(19A)	8761	6199	6484	76
H(20A)	10661	5963	7011	68
H(22A)	11998	4076	7127	59
H(22B)	12615	4824	6942	59
H(23A)	13226	6441	8176	49
H(26A)	12616	6366	10017	41
H(27A)	11775	5724	10649	41
H(28A)	10602	4619	10387	40
H(31A)	8827	2845	8934	40
H(32A)	9012	2846	7306	70
H(32B)	9349	3693	7147	70
H(34A)	7312	4456	7619	66
H(35A)	5295	4665	7214	78
H(36A)	4401	3908	6475	66
H(38A)	5488	2185	6155	57
H(38B)	4458	2802	5935	57
H(39A)	5279	3987	4641	46
H(42A)	6579	2633	3177	48
H(43A)	7710	1642	2916	52
H(44A)	8833	833	3562	46
H(47A)	9641	-6	5466	49
H(48A)	8047	1078	6724	54
H(48B)	7841	1926	6478	54
H(1WB)	5360(30)	4567(17)	3448(14)	76
H(1WA)	5990(30)	5390(20)	3468(14)	76

**Table B3.6.** Torsion angles [°] for ap17.

C(6)-O(1)-N(2)-C(7)	-176.4(3)	C(29)-N(10)-C(25)-C(24)	179.5(2)
C(16)-O(4)-N(6)-C(15)	-173.1(2)	O(6)-C(24)-C(25)-N(10)	172.3(3)
C(22)-O(5)-N(8)-C(23)	176.4(3)	N(9)-C(24)-C(25)-N(10)	-7.2(3)
C(32)-O(8)-N(12)-C(31)	-177.3(3)	O(6)-C(24)-C(25)-C(26)	-7.5(4)
C(38)-O(9)-N(14)-C(39)	-166.0(2)	N(9)-C(24)-C(25)-C(26)	173.1(2)
C(48)-O(12)-N(18)-C(47)	-150.3(3)	N(10)-C(25)-C(26)-C(27)	1.1(4)
C(5)-N(1)-C(1)-C(2)	0.8(4)	C(24)-C(25)-C(26)-C(27)	-179.2(3)
C(5)-N(1)-C(1)-C(48)	-178.1(3)	C(25)-C(26)-C(27)-C(28)	-0.5(4)
N(1)-C(1)-C(2)-C(3)	-1.5(5)	C(26)-C(27)-C(28)-C(29)	-0.4(4)
C(48)-C(1)-C(2)-C(3)	177.2(3)	C(25)-N(10)-C(29)-C(28)	-0.2(4)
C(1)-C(2)-C(3)-C(4)	1.6(5)	C(25)-N(10)-C(29)-C(30)	-179.7(2)
C(2)-C(3)-C(4)-C(5)	-0.9(4)	C(27)-C(28)-C(29)-N(10)	0.7(4)
C(1)-N(1)-C(5)-C(4)	-0.1(4)	C(27)-C(28)-C(29)-C(30)	-179.7(3)
C(1)-N(1)-C(5)-C(6)	-179.2(2)	C(31)-N(11)-C(30)-O(7)	-2.6(4)
C(3)-C(4)-C(5)-N(1)	0.2(4)	C(31)-N(11)-C(30)-C(29)	177.7(2)
C(3)-C(4)-C(5)-C(6)	179.2(3)	N(10)-C(29)-C(30)-O(7)	169.3(3)
N(2)-O(1)-C(6)-C(5)	-63.7(3)	C(28)-C(29)-C(30)-O(7)	-10.3(4)
N(1)-C(5)-C(6)-O(1)	-53.3(4)	N(10)-C(29)-C(30)-N(11)	-11.0(4)
C(4)-C(5)-C(6)-O(1)	127.6(3)	C(28)-C(29)-C(30)-N(11)	169.5(3)
O(1)-N(2)-C(7)-N(3)	-0.1(4)	O(8)-N(12)-C(31)-N(11)	-0.4(4)
C(8)-N(3)-C(7)-N(2)	173.8(3)	C(30)-N(11)-C(31)-N(12)	-178.4(3)
C(7)-N(3)-C(8)-O(2)	3.9(5)	N(12)-O(8)-C(32)-C(33)	75.0(4)
C(7)-N(3)-C(8)-C(9)	-174.6(3)	C(37)-N(13)-C(33)-C(34)	2.4(5)
C(13)-N(4)-C(9)-C(10)	-0.7(4)	C(37)-N(13)-C(33)-C(32)	-176.4(3)
C(13)-N(4)-C(9)-C(8)	177.3(2)	O(8)-C(32)-C(33)-N(13)	-151.9(3)
O(2)-C(8)-C(9)-N(4)	171.1(3)	O(8)-C(32)-C(33)-C(34)	29.3(5)
N(3)-C(8)-C(9)-N(4)	-10.4(4)	N(13)-C(33)-C(34)-C(35)	-1.1(5)
O(2)-C(8)-C(9)-C(10)	-10.8(4)	C(32)-C(33)-C(34)-C(35)	177.6(3)
N(3)-C(8)-C(9)-C(10)	167.7(3)	C(33)-C(34)-C(35)-C(36)	-0.9(5)
N(4)-C(9)-C(10)-C(11)	1.1(4)	C(34)-C(35)-C(36)-C(37)	1.5(6)
C(8)-C(9)-C(10)-C(11)	-176.9(3)	C(33)-N(13)-C(37)-C(36)	-1.8(5)
C(9)-C(10)-C(11)-C(12)	0.0(4)	C(33)-N(13)-C(37)-C(38)	-179.5(3)

C(10)-C(11)-C(12)-C(13)	-1.3(4)	C(35)-C(36)-C(37)-N(13)	-0.1(5)
C(9)-N(4)-C(13)-C(12)	-0.8(4)	C(35)-C(36)-C(37)-C(38)	177.4(3)
C(9)-N(4)-C(13)-C(14)	178.5(2)	N(14)-O(9)-C(38)-C(37)	-74.9(3)
C(11)-C(12)-C(13)-N(4)	1.8(4)	N(13)-C(37)-C(38)-O(9)	-70.2(4)
C(11)-C(12)-C(13)-C(14)	-177.5(3)	C(36)-C(37)-C(38)-O(9)	112.0(4)
C(15)-N(5)-C(14)-O(3)	1.5(4)	O(9)-N(14)-C(39)-N(15)	0.6(4)
C(15)-N(5)-C(14)-C(13)	-179.0(2)	C(40)-N(15)-C(39)-N(14)	175.4(3)
N(4)-C(13)-C(14)-O(3)	176.8(3)	C(39)-N(15)-C(40)-O(10)	-0.3(4)
C(12)-C(13)-C(14)-O(3)	-3.9(4)	C(39)-N(15)-C(40)-C(41)	179.3(2)
N(4)-C(13)-C(14)-N(5)	-2.7(4)	C(45)-N(16)-C(41)-C(42)	1.6(4)
C(12)-C(13)-C(14)-N(5)	176.6(2)	C(45)-N(16)-C(41)-C(40)	-178.5(2)
O(4)-N(6)-C(15)-N(5)	1.7(4)	O(10)-C(40)-C(41)-N(16)	168.7(3)
C(14)-N(5)-C(15)-N(6)	-178.9(3)	N(15)-C(40)-C(41)-N(16)	-10.9(4)
N(6)-O(4)-C(16)-C(17)	-70.9(3)	O(10)-C(40)-C(41)-C(42)	-11.4(4)
C(21)-N(7)-C(17)-C(18)	0.4(4)	N(15)-C(40)-C(41)-C(42)	169.0(3)
C(21)-N(7)-C(17)-C(16)	-178.5(3)	N(16)-C(41)-C(42)-C(43)	-1.6(4)
O(4)-C(16)-C(17)-N(7)	-94.2(3)	C(40)-C(41)-C(42)-C(43)	178.5(3)
O(4)-C(16)-C(17)-C(18)	86.9(4)	C(41)-C(42)-C(43)-C(44)	-0.3(5)
N(7)-C(17)-C(18)-C(19)	2.8(5)	C(42)-C(43)-C(44)-C(45)	2.1(5)
C(16)-C(17)-C(18)-C(19)	-178.4(3)	C(41)-N(16)-C(45)-C(44)	0.4(4)
C(17)-C(18)-C(19)-C(20)	-3.3(6)	C(41)-N(16)-C(45)-C(46)	-178.4(2)
C(18)-C(19)-C(20)-C(21)	0.8(6)	C(43)-C(44)-C(45)-N(16)	-2.2(4)
C(17)-N(7)-C(21)-C(20)	-3.0(5)	C(43)-C(44)-C(45)-C(46)	176.6(3)
C(17)-N(7)-C(21)-C(22)	174.8(3)	C(47)-N(17)-C(46)-O(11)	-6.1(5)
C(19)-C(20)-C(21)-N(7)	2.4(5)	C(47)-N(17)-C(46)-C(45)	171.7(3)
C(19)-C(20)-C(21)-C(22)	-175.2(3)	N(16)-C(45)-C(46)-O(11)	179.4(3)
N(8)-O(5)-C(22)-C(21)	-92.4(3)	C(44)-C(45)-C(46)-O(11)	0.5(4)
N(7)-C(21)-C(22)-O(5)	-142.2(3)	N(16)-C(45)-C(46)-N(17)	1.5(4)
C(20)-C(21)-C(22)-O(5)	35.6(5)	C(44)-C(45)-C(46)-N(17)	-177.4(3)
O(5)-N(8)-C(23)-N(9)	-1.6(5)	O(12)-N(18)-C(47)-N(17)	1.4(4)
C(24)-N(9)-C(23)-N(8)	-179.7(3)	C(46)-N(17)-C(47)-N(18)	-172.0(3)
C(23)-N(9)-C(24)-O(6)	0.0(4)	N(18)-O(12)-C(48)-C(1)	54.7(3)
C(23)-N(9)-C(24)-C(25)	179.4(2)	N(1)-C(1)-C(48)-O(12)	53.9(3)
C(29)-N(10)-C(25)-C(26)	-0.7(4)	C(2)-C(1)-C(48)-O(12)	-124.9(3)

**Table B3.7.** Hydrogen bonds for ap17 [Å and °].

D-H...A	d(D-H)	d(H...A)	d(D...A)	∠(DHA)
O(1W)-H(1WB)...O(10)	0.95(2)	2.06(3)	2.943(3)	155(3)
O(1W)-H(1WA)...O(2)#1	0.97(3)	2.09(3)	3.026(4)	163(3)

Symmetry transformations used to generate equivalent atoms:  
#1 x-1/2,y+1/2,z

#### 4) Macrocycle M1

A crystal of the compound (colorless, needle-shaped, size 0.30 x 0.08 x 0.06 mm) was mounted on a glass fiber with grease and cooled to -93 °C in a stream of nitrogen gas controlled with Cryostream Controller 700. Data collection was performed on a Bruker SMART APEX II X-ray diffractometer with graphite-monochromated Mo K<sub>α</sub> radiation ( $\lambda = 0.71073 \text{ \AA}$ ), operating at 50 kV and 30 mA over 2θ ranges of 3.94 ~ 52.00°. No significant decay was observed during the data collection.

Data were processed on a PC using the Bruker AXS Crystal Structure Analysis Package:<sup>[1]</sup> Data collection: APEX2 (Bruker, 2006); cell refinement: SAINT (Bruker, 2005); data reduction: SAINT (Bruker, 2005); structure solution: XPREP (Bruker, 2005) and SHELXTL (Bruker, 2000); structure refinement: SHELXTL; molecular graphics: SHELXTL; publication materials: SHELXTL. Neutral atom scattering factors were taken from Cromer and Waber.<sup>[2]</sup> The crystal is triclinic space group *P*-1, based on the systematic absences, *E* statistics and successful refinement of the structure. The structure was solved by direct methods. Full-matrix least-square refinements minimizing the function  $\sum w (F_o^2 - F_c^2)^2$  were applied to the compound. All non-hydrogen atoms were refined anisotropically. All H atoms were placed in geometrically calculated positions, with C-H = 0.95 (aromatic), 0.99(CH<sub>2</sub>) and 0.88 (N-H) Å, and refined as riding atoms, with Uiso(H) = 1.2 Ueq(C or N).

Convergence to final  $R_1 = 0.0698$  and  $wR_2 = 0.1564$  for 1408 ( $I > 2\sigma(I)$ ) independent

reflections, and  $R_1 = 0.1623$  and  $wR_2 = 0.2054$  for all 3145 ( $R(\text{int}) = 0.0618$ ) independent reflections, with 218 parameters and 0 restraints, were achieved.<sup>[3]</sup> The largest residual peak and hole to be 0.289 and  $-0.267 \text{ e}/\text{\AA}^3$ , respectively. Crystallographic data, atomic coordinates and equivalent isotropic displacement parameters, bond lengths and angles, anisotropic displacement parameters, hydrogen coordinates and isotropic displacement parameters, torsion angles and H-bonding information are given in Table B4.1 to B4.7. The molecular structure and the cell packing are shown in Figures B4.1 and B4.2.

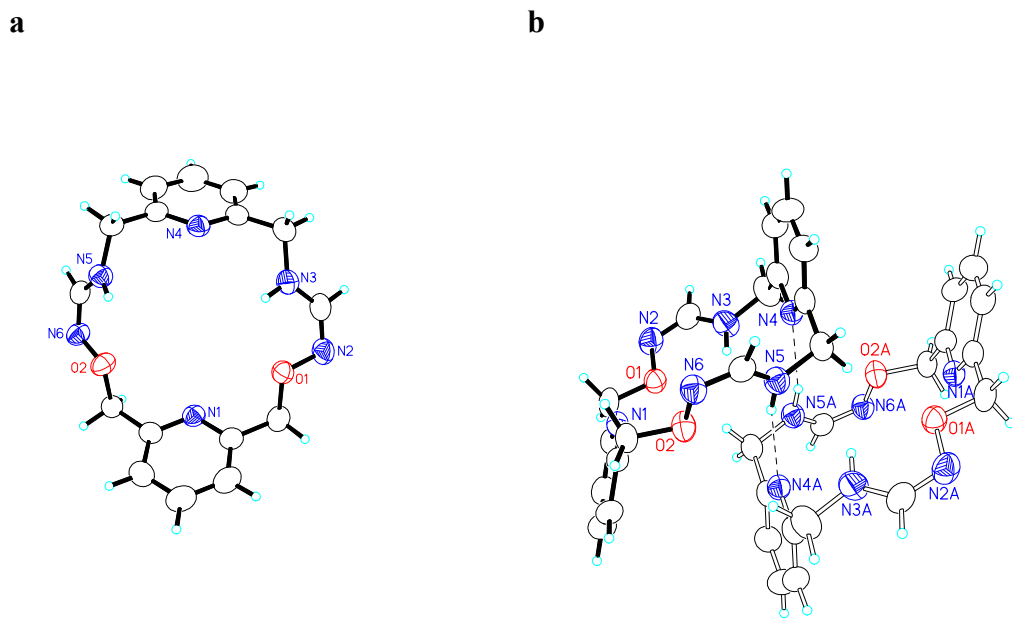


**Figure B4.1 a)** Molecular Structure (displacement ellipsoids for non-H atoms are shown at the 50% probability level and H atoms are represented by circles of arbitrary size. b) The structure of the hydrogen-bonding dimer

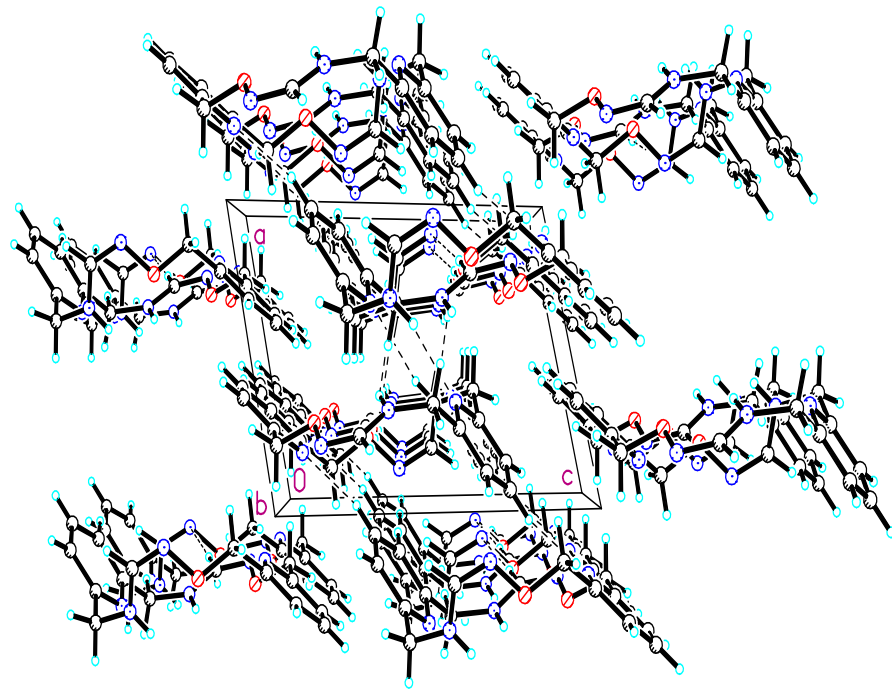


**Figure B4.2** Unit cell packing

[1] Bruker AXS Crystal Structure Analysis Package:

Bruker (2000). SHELXTL. Version 6.14. Bruker AXS Inc., Madison, Wisconsin, USA.

Bruker (2005). XPREP. Version 2005/2. Bruker AXS Inc., Madison, Wisconsin, USA.

Bruker (2005). SAINT. Version 7.23A. Bruker AXS Inc., Madison, Wisconsin, USA.

Bruker (2006). APEX2. Version 2.0-2. Bruker AXS Inc., Madison, Wisconsin, USA.

[2] Cromer, D. T.; Waber, J. T. *International Tables for X-ray Crystallography*; Kynoch Press:

Birmingham, UK, 1974; Vol. 4, Table 2.2 A.

$$R_1 = \sum | |F_o| - |F_c| | / \sum |F_o|$$

$$wR_2 = \{ \sum [w(F_o^2 - F_c^2)^2] / \sum [w(F_o^2)^2] \}^{1/2}$$

$$(w = 1 / [\sigma^2(F_o^2) + (0.0476P)^2 + 0.134P], \text{ where } P = [\text{Max}(F_o^2, 0) + 2F_c^2] / 3)$$

**Table B4.1.** Crystal data and structure refinement for ap14

Identification code	ap14
Empirical formula	C16 H18 N6 O2
Formula weight	326.36
Temperature	180(2) K
	150

Wavelength	0.71073 Å
Crystal system	Triclinic
Space group	P-1
Unit cell dimensions	a = 8.583(4) Å b = 9.964(5) Å c = 11.384(9) Å
	α= 111.097(8)°. β= 93.118(8)°. γ = 113.238(5)°.
Volume	812.4(9) Å <sup>3</sup>
Z	2
Density (calculated)	1.334 Mg/m <sup>3</sup>
Absorption coefficient	0.093 mm <sup>-1</sup>
F(000)	344
Crystal size	0.30 x 0.08 x 0.06 mm <sup>3</sup>
Theta range for data collection	1.97 to 26.00°.
Index ranges	-10<=h<=10, -12<=k<=12, -14<=l<=14
Reflections collected	6113
Independent reflections	3145 [R(int) = 0.0618]
Completeness to theta = 26.00°	98.5 %
Absorption correction	Multi-scan
Max. and min. transmission	0.9944 and 0.9726
Refinement method	Full-matrix least-squares on F <sup>2</sup>
Data / restraints / parameters	3145 / 0 / 218
Goodness-of-fit on F <sup>2</sup>	0.945
Final R indices [I>2sigma(I)]	R1 = 0.0698, wR2 = 0.1564
R indices (all data)	R1 = 0.1623, wR2 = 0.2054
Extinction coefficient	0.027(6)
Largest diff. peak and hole	0.289 and -0.267 e.Å <sup>-3</sup>

**Table B4.2.** Atomic coordinates ( x 10<sup>4</sup>) and equivalent isotropic displacement parameters (Å<sup>2</sup> x 10<sup>3</sup>) for ap14. U(eq) is defined as one third of the trace of the orthogonalized U<sup>ij</sup> tensor.

	x	y	z	U(eq)
O(1)	2856(3)	10593(3)	1605(2)	44(1)
O(2)	2270(3)	6145(3)	3018(2)	47(1)

N(1)	1840(4)	7253(3)	967(3)	41(1)
N(2)	2203(4)	11768(4)	1747(3)	53(1)
N(3)	3284(5)	12489(4)	3924(3)	55(1)
N(4)	3495(4)	11416(3)	6002(3)	41(1)
N(5)	3406(4)	8134(3)	5402(3)	44(1)
N(6)	1219(4)	5636(4)	3866(3)	45(1)
C(1)	2142(5)	6007(4)	893(3)	40(1)
C(2)	3145(5)	5493(5)	107(4)	51(1)
C(3)	3900(5)	6318(6)	-624(4)	59(1)
C(4)	3616(5)	7606(5)	-550(4)	52(1)
C(5)	2581(5)	8041(4)	242(3)	41(1)
C(6)	2149(5)	9396(4)	325(3)	49(1)
C(7)	2504(5)	12613(5)	2957(4)	49(1)
C(8)	3469(6)	13417(5)	5299(4)	61(1)
C(9)	2708(5)	12333(4)	5966(3)	46(1)
C(10)	1320(6)	12311(5)	6549(4)	59(1)
C(11)	737(6)	11347(6)	7190(4)	67(1)
C(12)	1551(6)	10419(5)	7238(4)	55(1)
C(13)	2917(5)	10476(4)	6633(3)	41(1)
C(14)	3837(5)	9469(4)	6640(3)	48(1)
C(15)	1932(5)	6752(4)	5013(4)	42(1)
C(16)	1273(5)	5163(4)	1715(3)	44(1)

**Table**

**B4.3.** Bond lengths [ $\text{\AA}$ ] and angles [ $^\circ$ ] for ap14.

O(1)-C(6)	1.412(4)	N(6)-C(15)	1.283(4)	C(8)-H(8B)	0.9900
O(1)-N(2)	1.451(4)	C(1)-C(2)	1.381(5)	C(9)-C(10)	1.391(6)
O(2)-C(16)	1.430(4)	C(1)-C(16)	1.512(5)	C(10)-C(11)	1.368(6)
O(2)-N(6)	1.445(4)	C(2)-C(3)	1.385(5)	C(10)-H(10A)	0.9500
N(1)-C(1)	1.340(4)	C(2)-H(2B)	0.9500	C(11)-C(12)	1.374(6)
N(1)-C(5)	1.353(4)	C(3)-C(4)	1.373(5)	C(11)-H(11A)	0.9500
N(2)-C(7)	1.276(5)	C(3)-H(3B)	0.9500	C(12)-C(13)	1.384(5)
N(3)-C(7)	1.326(5)	C(4)-C(5)	1.378(5)	C(12)-H(12A)	0.9500
N(3)-C(8)	1.466(5)	C(4)-H(4B)	0.9500	C(13)-C(14)	1.504(5)
N(3)-H(3A)	0.8800	C(5)-C(6)	1.509(5)	C(14)-H(14A)	0.9900

N(4)-C(13)	1.340(4)	C(6)-H(6B)	0.9900	C(14)-H(14B)	0.9900
N(4)-C(9)	1.343(4)	C(6)-H(6C)	0.9900	C(15)-H(15A)	0.9500
N(5)-C(15)	1.348(4)	C(7)-H(7A)	0.9500	C(16)-H(16A)	0.9900
N(5)-C(14)	1.449(4)	C(8)-C(9)	1.503(5)	C(16)-H(16B)	0.9900
N(5)-H(5A)	0.8800	C(8)-H(8A)	0.9900		
C(6)-O(1)-N(2)		107.9(2)		N(3)-C(8)-C(9)	111.2(3)
C(16)-O(2)-N(6)		108.1(3)		N(3)-C(8)-H(8A)	109.4
C(1)-N(1)-C(5)		117.6(3)		C(9)-C(8)-H(8A)	109.4
C(7)-N(2)-O(1)		107.0(3)		N(3)-C(8)-H(8B)	109.4
C(7)-N(3)-C(8)		125.0(4)		C(9)-C(8)-H(8B)	109.4
C(7)-N(3)-H(3A)		117.5		H(8A)-C(8)-H(8B)	108.0
C(8)-N(3)-H(3A)		117.5		N(4)-C(9)-C(10)	121.8(4)
C(13)-N(4)-C(9)		117.9(3)		N(4)-C(9)-C(8)	115.4(4)
C(15)-N(5)-C(14)		122.2(3)		C(10)-C(9)-C(8)	122.7(4)
C(15)-N(5)-H(5A)		118.9		C(11)-C(10)-C(9)	119.8(4)
C(14)-N(5)-H(5A)		118.9		C(11)-C(10)-H(10A)	120.1
C(15)-N(6)-O(2)		107.1(3)		C(9)-C(10)-H(10A)	120.1
N(1)-C(1)-C(2)		123.0(3)		C(10)-C(11)-C(12)	118.4(4)
N(1)-C(1)-C(16)		115.4(3)		C(10)-C(11)-H(11A)	120.8
C(2)-C(1)-C(16)		121.5(4)		C(12)-C(11)-H(11A)	120.8
C(1)-C(2)-C(3)		118.6(4)		C(11)-C(12)-C(13)	119.4(4)
C(1)-C(2)-H(2B)		120.7		C(11)-C(12)-H(12A)	120.3
C(3)-C(2)-H(2B)		120.7		C(13)-C(12)-H(12A)	120.3
C(4)-C(3)-C(2)		119.1(4)		N(4)-C(13)-C(12)	122.6(4)
C(4)-C(3)-H(3B)		120.5		N(4)-C(13)-C(14)	115.9(3)
C(2)-C(3)-H(3B)		120.5		C(12)-C(13)-C(14)	121.6(3)
C(3)-C(4)-C(5)		119.3(4)		N(5)-C(14)-C(13)	113.1(3)
C(3)-C(4)-H(4B)		120.3		N(5)-C(14)-H(14A)	109.0
C(5)-C(4)-H(4B)		120.3		C(13)-C(14)-H(14A)	109.0
N(1)-C(5)-C(4)		122.4(4)		N(5)-C(14)-H(14B)	109.0
N(1)-C(5)-C(6)		115.4(4)		C(13)-C(14)-H(14B)	109.0
C(4)-C(5)-C(6)		122.1(3)		H(14A)-C(14)-H(14B)	107.8
O(1)-C(6)-C(5)		107.8(3)		N(6)-C(15)-N(5)	128.1(4)
O(1)-C(6)-H(6B)		110.1		N(6)-C(15)-H(15A)	115.9

C(5)-C(6)-H(6B)	110.1	N(5)-C(15)-H(15A)	115.9
O(1)-C(6)-H(6C)	110.1	O(2)-C(16)-C(1)	107.1(3)
C(5)-C(6)-H(6C)	110.1	O(2)-C(16)-H(16A)	110.3
H(6B)-C(6)-H(6C)	108.5	C(1)-C(16)-H(16A)	110.3
N(2)-C(7)-N(3)	127.8(4)	O(2)-C(16)-H(16B)	110.3
N(2)-C(7)-H(7A)	116.1	C(1)-C(16)-H(16B)	110.3
N(3)-C(7)-H(7A)	116.1	H(16A)-C(16)-H(16B)	108.6

**Table B4.4.** Anisotropic displacement parameters ( $\text{\AA}^2 \times 10^3$ ) for ap14. The anisotropic displacement factor exponent takes the form:  $-2\pi^2 [ h^2 a^*{}^2 U^{11} + \dots + 2 h k a^* b^* U^{12} ]$

	U <sup>11</sup>	U <sup>22</sup>	U <sup>33</sup>	U <sup>23</sup>	U <sup>13</sup>	U <sup>12</sup>
O(1)	48(2)	42(2)	42(2)	17(1)	5(1)	22(1)
O(2)	45(2)	47(2)	37(1)	18(1)	5(1)	11(1)
N(1)	40(2)	42(2)	36(2)	14(2)	4(1)	15(2)
N(2)	59(2)	49(2)	54(2)	24(2)	3(2)	27(2)
N(3)	79(3)	53(2)	49(2)	22(2)	12(2)	44(2)
N(4)	41(2)	39(2)	38(2)	13(2)	5(1)	16(2)
N(5)	43(2)	40(2)	44(2)	15(2)	7(2)	15(2)
N(6)	44(2)	47(2)	40(2)	20(2)	10(2)	15(2)
C(1)	35(2)	40(2)	38(2)	11(2)	4(2)	15(2)
C(2)	50(3)	59(3)	53(3)	21(2)	10(2)	34(2)
C(3)	51(3)	80(3)	53(3)	30(3)	19(2)	34(3)
C(4)	39(2)	62(3)	46(2)	25(2)	6(2)	13(2)
C(5)	36(2)	41(2)	34(2)	11(2)	0(2)	12(2)
C(6)	48(3)	46(2)	43(2)	18(2)	-6(2)	13(2)
C(7)	47(3)	44(2)	59(3)	26(2)	5(2)	19(2)
C(8)	91(4)	44(2)	50(3)	16(2)	10(2)	34(2)
C(9)	57(3)	40(2)	36(2)	9(2)	2(2)	23(2)
C(10)	61(3)	71(3)	52(3)	18(2)	7(2)	44(3)
C(11)	49(3)	88(4)	67(3)	29(3)	26(2)	35(3)
C(12)	53(3)	66(3)	49(3)	25(2)	19(2)	26(2)

C(13)	42(2)	38(2)	31(2)	9(2)	0(2)	12(2)
C(14)	57(3)	49(2)	36(2)	13(2)	2(2)	26(2)
C(15)	43(2)	48(2)	44(2)	25(2)	11(2)	24(2)
C(16)	47(2)	38(2)	37(2)	12(2)	-2(2)	16(2)

---

**Table B4.5** Hydrogen coordinates ( $\times 10^4$ ) and isotropic displacement parameters ( $\text{\AA}^2 \times 10^3$ ) for ap14.

	x	y	z	U(eq)
H(3A)	3724	11795	3724	66
H(5A)	4131	8229	4886	53
H(2B)	3315	4593	69	62
H(3B)	4604	5997	-1169	71
H(4B)	4127	8191	-1040	62
H(6B)	2655	9842	-290	59
H(6C)	871	9001	104	59
H(7A)	2124	13430	3194	59
H(8A)	2872	14108	5390	73
H(8B)	4719	14123	5718	73
H(10A)	779	12963	6501	71
H(11A)	-208	11321	7594	80
H(12A)	1179	9744	7681	66
H(14A)	5110	10157	6887	58
H(14B)	3525	9048	7304	58
H(15A)	1349	6584	5669	50
H(16A)	60	5026	1657	53
H(16B)	1249	4089	1416	53

---

**Table B4.6.** Torsion angles [°] for ap14.

C(6)-O(1)-N(2)-C(7)      165.0(3)      C(13)-N(4)-C(9)-C(8)      177.2(3)

C(16)-O(2)-N(6)-C(15)	-164.3(3)	N(3)-C(8)-C(9)-N(4)	64.0(4)
C(5)-N(1)-C(1)-C(2)	-0.8(5)	N(3)-C(8)-C(9)-C(10)	-118.1(4)
C(5)-N(1)-C(1)-C(16)	-179.6(3)	N(4)-C(9)-C(10)-C(11)	0.7(6)
N(1)-C(1)-C(2)-C(3)	1.1(5)	C(8)-C(9)-C(10)-C(11)	-177.1(4)
C(16)-C(1)-C(2)-C(3)	179.8(3)	C(9)-C(10)-C(11)-C(12)	-0.1(6)
C(1)-C(2)-C(3)-C(4)	-0.5(6)	C(10)-C(11)-C(12)-C(13)	-0.4(6)
C(2)-C(3)-C(4)-C(5)	-0.4(6)	C(9)-N(4)-C(13)-C(12)	0.2(5)
C(1)-N(1)-C(5)-C(4)	-0.1(5)	C(9)-N(4)-C(13)-C(14)	179.8(3)
C(1)-N(1)-C(5)-C(6)	178.0(3)	C(11)-C(12)-C(13)-N(4)	0.4(6)
C(3)-C(4)-C(5)-N(1)	0.7(5)	C(11)-C(12)-C(13)-C(14)	-179.2(3)
C(3)-C(4)-C(5)-C(6)	-177.2(3)	C(15)-N(5)-C(14)-C(13)	-80.8(4)
N(2)-O(1)-C(6)-C(5)	-170.7(3)	N(4)-C(13)-C(14)-N(5)	-73.0(4)
N(1)-C(5)-C(6)-O(1)	64.8(4)	C(12)-C(13)-C(14)-N(5)	106.6(4)
C(4)-C(5)-C(6)-O(1)	-117.1(4)	O(2)-N(6)-C(15)-N(5)	-1.7(5)
O(1)-N(2)-C(7)-N(3)	0.9(5)	C(14)-N(5)-C(15)-N(6)	163.8(3)
C(8)-N(3)-C(7)-N(2)	-175.0(4)	N(6)-O(2)-C(16)-C(1)	163.4(3)
C(7)-N(3)-C(8)-C(9)	123.7(4)	N(1)-C(1)-C(16)-O(2)	-77.3(4)
C(13)-N(4)-C(9)-C(10)	-0.7(5)	C(2)-C(1)-C(16)-O(2)	103.9(4)

**Table B4.7** Hydrogen bonds for ap14 [Å and °].

D-H...A	d(D-H)	d(H...A)	d(D...A)	∠(DHA)
N(5)-H(5A)...N(4)#1	0.88	2.28	3.141(5)	165.1

Symmetry transformations used to generate equivalent atoms:

#1 -x+1,-y+2,-z+1

## 5) 4.2 ZE

A crystal of the compound (colorless, plate-shaped, size  $0.30 \times 0.15 \times 0.08$  mm) was mounted on a glass fiber with grease and cooled to -93 °C in a stream of nitrogen gas controlled with Cryostream Controller 700. Data collection was performed on a Bruker

SMART APEX II X-ray diffractometer with graphite-monochromated Mo K<sub>α</sub> radiation ( $\lambda = 0.71073 \text{ \AA}$ ), operating at 50 kV and 30 mA over  $2\theta$  ranges of  $3.58 \sim 52.00^\circ$ . No significant decay was observed during the data collection. Data were processed on a PC using the Bruker AXS Crystal Structure Analysis Package:<sup>[1]</sup> Data collection: APEX2 (Bruker, 2006); cell refinement: SAINT (Bruker, 2005); data reduction: SAINT (Bruker, 2005); structure solution: XPREP (Bruker, 2005) and SHELXTL (Bruker, 2000); structure refinement: SHELXTL; molecular graphics: SHELXTL; publication materials: SHELXTL. Neutral atom scattering factors were taken from Cromer and Waber.<sup>[2]</sup> The crystal is monoclinic space group  $Pn$ , based on the systematic absences,  $E$  statistics and successful refinement of the structure. The structure was solved by direct methods. Full-matrix least-square refinements minimizing the function  $\sum w(F_o^2 - F_c^2)^2$  were applied to the compound. All non-hydrogen atoms were refined anisotropically. All of the H atoms were placed in geometrically calculated positions, with C-H = 0.95 (aromatic), 0.99(CH<sub>2</sub>), and 0.88(N-H) Å, and refined as riding atoms, with  $U_{iso}(\text{H}) = 1.2 \text{ Ueq(C or N)}$ . The phenyl- groups on each arm are disordered. SHLEX commands, SADI, EXYZ, EADP and SAME were used to resolve the disorder. CheckCIF issues one Level B alert on the low precision of the C-C bond. We believe it is due to the low quality of the crystal. Convergence to final  $R_1 = 0.1025$  and  $wR_2 = 0.2564$  for 5019 ( $I > 2\sigma(I)$ ) independent reflections, and  $R_1 = 0.1545$  and  $wR_2 = 0.2911$  for all 8327 ( $R(\text{int}) = 0.0937$ ) independent reflections, with 428 parameters and 58 restraints, were achieved.<sup>[3]</sup> The largest residual peak and hole to be 0.650 and  $-0.368 \text{ e/}\text{\AA}^3$ , respectively. Crystallographic data, atomic coordinates and equivalent isotropic displacement parameters, bond lengths and angles, anisotropic displacement parameters, hydrogen coordinates and isotropic displacement parameters, and torsion angles are given in Tables B5.1 to B5.6. The molecular structure and the cell packing are shown in Figures B5.1 and B5.2.

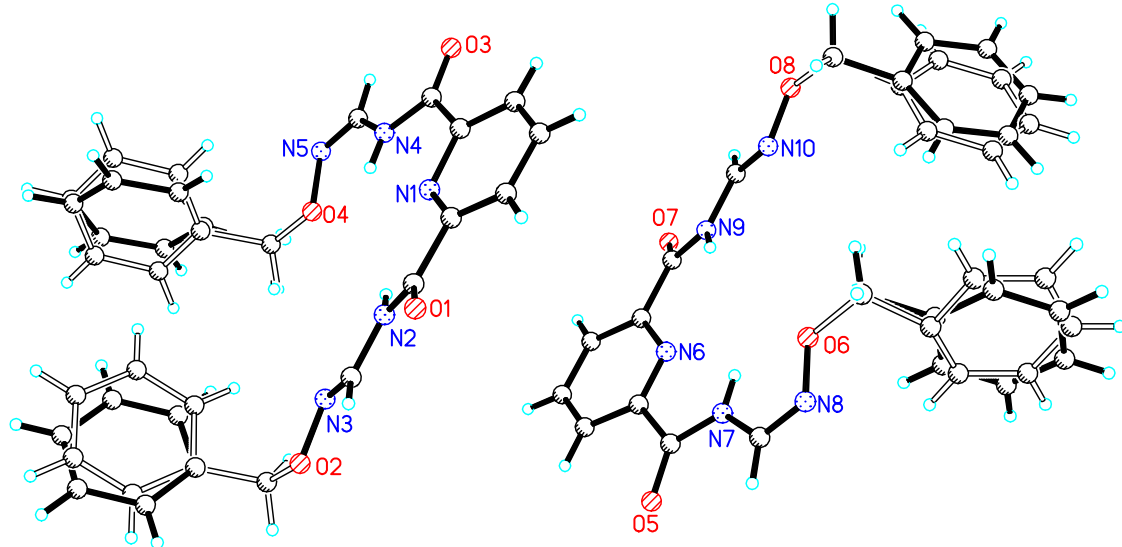
[1] Bruker AXS Crystal Structure Analysis Package: Bruker (2000). SHELXTL. Version 6.14. Bruker AXS Inc., Madison, Wisconsin, USA; Bruker (2005). XPREP. Version 2005/2. Bruker AXS Inc., Madison, Wisconsin, USA; Bruker (2005). SAINT. Version 7.23A. Bruker AXS Inc., Madison, Wisconsin, USA; Bruker (2006). APEX2. Version 2.0-2. Bruker AXS Inc., Madison, Wisconsin, USA.

[2] Cromer, D. T.; Waber, J. T. *International Tables for X-ray Crystallography*; Kynoch Press: Birmingham, UK, 1974; Vol. 4, Table 2.2 A.

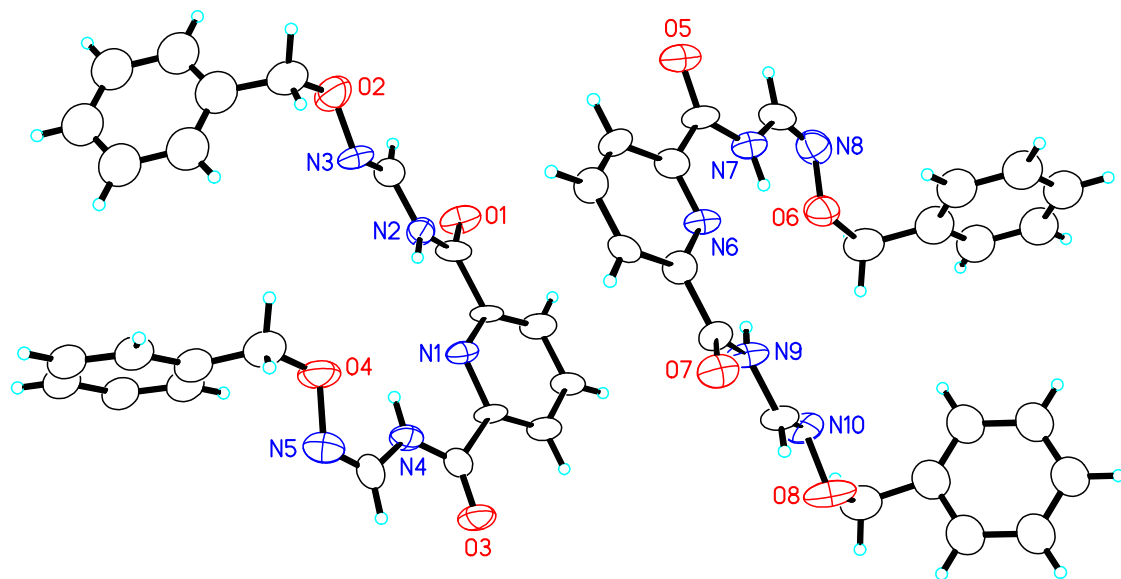
$$[3] \quad R_1 = \sum | |F_o| - |F_c| | / \sum |F_o|$$

$$wR_2 = \{ \sum [w(Fo^2 - Fc^2)^2] / \sum [w(Fo^2)^2] \}^{1/2}$$

$$(w = 1 / [\sigma^2(Fo^2) + (0.101P)^2 + 5.46P], \text{ where } P = [\text{Max}(Fo^2, 0) + 2Fc^2] / 3)$$



**Figure B5.1.** (top) Molecular structure showing the disorder of the phenyl groups (bottom)  
 Molecular Structure (one component was shown; the displacement ellipsoids for non-H atoms are shown at the 50% probability level and H atoms are represented by circles of arbitrary size)



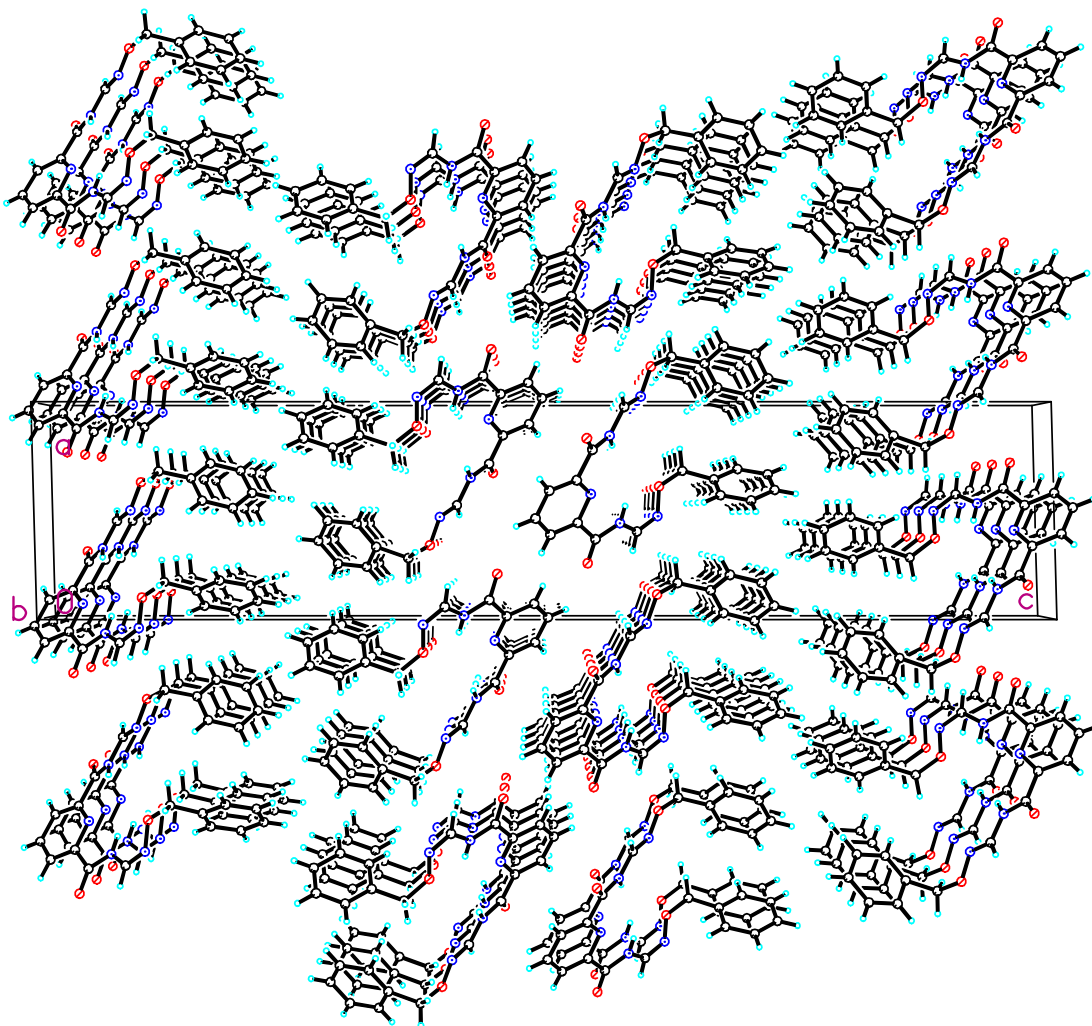


**Figure B5.2** Unit cell packing

**Table B5.1.** Crystal data and structure refinement for ap20a

Identification code	ap20a		
Empirical formula	C <sub>23</sub> H <sub>21</sub> N <sub>5</sub> O <sub>4</sub>		
Formula weight	431.45		
Temperature	180(2) K		
Wavelength	0.71073 Å		
Crystal system	Monoclinic		
Space group	Pn		
Unit cell dimensions	$a = 9.764(3)$ Å	$\alpha = 90^\circ$ .	
	$b = 4.8363(15)$ Å	$\beta = 91.567(5)^\circ$ .	
	$c = 45.628(14)$ Å	$\gamma = 90^\circ$ .	

Volume	2153.8(11) Å <sup>3</sup>
Z	4
Density (calculated)	1.331 Mg/m <sup>3</sup>
Absorption coefficient	0.094 mm <sup>-1</sup>
F(000)	904
Crystal size	0.30 x 0.15 x 0.08 mm <sup>3</sup>
Theta range for data collection	1.79 to 26.00°.
Index ranges	-12<=h<=12, -5<=k<=5, -56<=l<=56
Reflections collected	27188
Independent reflections	8327 [R(int) = 0.0937]
Completeness to theta = 26.00°	99.7 %
Absorption correction	Multi-scan
Max. and min. transmission	0.9925 and 0.9724
Refinement method	Full-matrix least-squares on F <sup>2</sup>
Data / restraints / parameters	8327 / 58 / 428
Goodness-of-fit on F <sup>2</sup>	1.055
Final R indices [I>2sigma(I)]	R1 = 0.1025, wR2 = 0.2564
R indices (all data)	R1 = 0.1545, wR2 = 0.2911
Absolute structure parameter	?
Extinction coefficient	0.0130(18)
Largest diff. peak and hole	0.650 and -0.368 e.Å <sup>-3</sup>

Table B5.2. Atomic coordinates ( $\times 10^4$ ) and equivalent isotropic displacement parameters ( $\text{Å}^2 \times 10^3$ ) for ap20a. U(eq) is defined as one third of the trace of the orthogonalized  $U^{ij}$  tensor.

	x	y	z	U(eq)
O(1)	8092(6)	16261(9)	5408(2)	46(2)
O(2)	11312(8)	11384(15)	6036(2)	66(2)
O(3)	2643(6)	6774(12)	5402(2)	50(2)
O(4)	6085(7)	4908(14)	6113(2)	62(2)
O(5)	12174(6)	7658(12)	4538(2)	52(2)
O(6)	8727(7)	9645(15)	3820(2)	58(2)
O(7)	6729(6)	-1671(10)	4509(1)	46(2)

O(8)	3427(6)	3171(12)	3886(2)	63(2)
N(1)	5717(6)	10778(12)	5442(2)	34(2)
N(2)	8261(7)	12034(13)	5630(2)	40(2)
N(3)	10014(8)	10602(19)	5936(2)	59(2)
N(4)	4434(7)	6770(12)	5721(2)	38(2)
N(5)	4743(8)	3557(15)	6095(2)	52(2)
N(6)	9124(6)	3750(10)	4490(2)	31(2)
N(7)	10325(7)	7765(12)	4211(2)	40(2)
N(8)	9980(9)	11111(15)	3835(2)	53(2)
N(9)	6492(6)	2576(11)	4296(2)	38(2)
N(10)	4709(7)	4110(16)	3992(2)	50(2)
C(1)	6311(7)	12896(12)	5310(2)	31(2)
C(2)	5851(8)	14120(15)	5051(2)	41(2)
C(3)	4645(8)	13077(13)	4917(2)	35(2)
C(4)	3939(8)	10898(13)	5053(2)	36(2)
C(5)	4449(8)	9949(13)	5313(2)	33(2)
C(6)	7631(8)	13845(14)	5461(2)	38(2)
C(7)	9521(9)	12488(17)	5773(2)	42(2)
C(8A)	11796(10)	9340(20)	6243(2)	67(1)
C(9A)	11482(12)	9960(30)	6550(2)	78(2)
C(10A)	10449(11)	8380(20)	6673(2)	78(2)
C(11A)	10112(11)	8780(20)	6965(2)	78(2)
C(12A)	10808(13)	10760(20)	7135(2)	78(2)
C(13A)	11841(12)	12340(20)	7012(2)	78(2)
C(14A)	12178(11)	11940(30)	6719(2)	78(2)
C(8B)	11796(10)	9340(20)	6243(2)	67(1)
C(9B)	11470(20)	9880(70)	6563(3)	78(2)
C(10B)	10230(30)	8500(60)	6592(4)	78(2)
C(11B)	9480(30)	8850(60)	6846(4)	78(2)
C(12B)	9970(30)	10570(60)	7071(4)	78(2)
C(13B)	11220(30)	11950(60)	7042(4)	78(2)
C(14B)	11970(30)	11600(70)	6788(4)	78(2)
C(15)	3722(9)	7688(16)	5480(2)	41(2)
C(16)	4056(10)	4597(19)	5890(2)	49(2)
C(17A)	6794(10)	3670(20)	6346(2)	67(1)

C(18A)	6404(12)	4500(30)	6645(2)	61(2)
C(19A)	5685(13)	6950(30)	6687(2)	61(2)
C(20A)	5439(14)	7870(30)	6969(3)	61(2)
C(21A)	5913(13)	6350(30)	7210(2)	61(2)
C(22A)	6632(14)	3900(30)	7169(2)	61(2)
C(23A)	6878(13)	2980(20)	6886(2)	61(2)
C(17B)	6794(10)	3670(20)	6346(2)	67(1)
C(18B)	6499(10)	4870(30)	6650(2)	61(2)
C(19B)	5276(12)	6270(30)	6706(2)	61(2)
C(20B)	4937(14)	6890(40)	6996(3)	61(2)
C(21B)	5820(11)	6100(30)	7229(3)	61(2)
C(22B)	7043(12)	4700(40)	7172(2)	61(2)
C(23B)	7383(13)	4090(40)	6883(3)	61(2)
C(24)	10248(8)	4641(14)	4614(2)	37(2)
C(25)	10781(8)	3527(15)	4880(2)	39(2)
C(26)	10132(8)	1383(16)	5010(2)	40(2)
C(27)	8962(7)	399(15)	4878(2)	34(2)
C(28)	8428(8)	1657(13)	4620(2)	35(2)
C(29)	11002(8)	6840(15)	4454(2)	39(2)
C(30)	10746(9)	9981(15)	4038(2)	42(2)
C(31A)	7843(10)	10780(20)	3584(2)	67(1)
C(32A)	8311(12)	10020(30)	3276(2)	69(2)
C(33A)	7747(10)	11320(20)	3033(2)	69(2)
C(34A)	8168(12)	10610(20)	2757(2)	69(2)
C(35A)	9151(12)	8600(20)	2725(2)	69(2)
C(36A)	9715(11)	7300(20)	2968(2)	69(2)
C(37A)	9294(12)	8010(30)	3244(2)	69(2)
C(31B)	7843(10)	10780(20)	3584(2)	67(1)
C(32B)	8490(30)	10090(90)	3296(4)	69(2)
C(33B)	7520(30)	11370(80)	3114(5)	69(2)
C(34B)	7520(30)	10900(70)	2814(6)	69(2)
C(35B)	8490(30)	9150(80)	2696(6)	69(2)
C(36B)	9460(40)	7880(80)	2878(6)	69(2)
C(37B)	9460(30)	8350(90)	3178(5)	69(2)
C(38)	7138(8)	668(12)	4476(2)	29(2)

C(39)	5245(7)	1968(16)	4155(2)	38(2)
C(40A)	2866(10)	5290(20)	3685(2)	67(1)
C(41A)	3367(18)	4960(40)	3377(3)	63(2)
C(42A)	2453(16)	2960(40)	3268(3)	63(2)
C(43A)	2582(16)	1950(30)	2982(3)	63(2)
C(44A)	3626(17)	2950(40)	2806(3)	63(2)
C(45A)	4540(17)	4950(40)	2916(3)	63(2)
C(46A)	4410(18)	5960(40)	3201(3)	63(2)
C(40B)	2866(10)	5290(20)	3685(2)	67(1)
C(41B)	3458(11)	4800(30)	3386(2)	63(2)
C(42B)	2850(12)	2810(30)	3208(2)	63(2)
C(43B)	3260(13)	2490(30)	2923(3)	63(2)
C(44B)	4278(11)	4160(30)	2815(3)	63(2)
C(45B)	4886(13)	6150(30)	2993(3)	63(2)
C(46B)	4475(13)	6470(30)	3278(3)	63(2)

---

**Table B5.3.** Bond lengths [ $\text{\AA}$ ] and angles [ $^\circ$ ] for ap20a.

O(1)-C(6)	1.277(9)	C(12A)-C(13A)	1.396(6)	C(30)-H(30A)	0.9500
O(2)-N(3)	1.387(10)	C(12A)-H(12A)	0.9500	C(31A)-C(32A)	1.531(10)
O(2)-C(8A)	1.438(12)	C(13A)-C(14A)	1.396(6)	C(31A)-H(31A)	0.9900
O(3)-C(15)	1.189(10)	C(13A)-H(13A)	0.9500	C(31A)-H(31B)	0.9900
O(4)-C(17A)	1.390(12)	C(14A)-H(14A)	0.9500	C(32A)-C(33A)	1.378(6)
O(4)-N(5)	1.464(10)	C(9B)-C(10B)	1.398(7)	C(32A)-C(37A)	1.379(6)
O(5)-C(29)	1.261(10)	C(9B)-C(14B)	1.398(7)	C(33A)-C(34A)	1.379(6)
O(6)-N(8)	1.415(10)	C(10B)-C(11B)	1.398(7)	C(33A)-H(33A)	0.9500
O(6)-C(31A)	1.469(12)	C(10B)-H(10B)	0.9500	C(34A)-C(35A)	1.378(6)
O(7)-C(38)	1.210(8)	C(11B)-C(12B)	1.398(7)	C(34A)-H(34A)	0.9500
O(8)-N(10)	1.406(10)	C(11B)-H(11B)	0.9500	C(35A)-C(36A)	1.379(6)
O(8)-C(40A)	1.472(13)	C(12B)-C(13B)	1.398(7)	C(35A)-H(35A)	0.9500
N(1)-C(1)	1.328(10)	C(12B)-H(12B)	0.9500	C(36A)-C(37A)	1.378(6)
N(1)-C(5)	1.413(9)	C(13B)-C(14B)	1.398(7)	C(36A)-H(36A)	0.9500
N(2)-C(6)	1.309(10)	C(13B)-H(13B)	0.9500	C(37A)-H(37A)	0.9500
N(2)-C(7)	1.395(11)	C(14B)-H(14B)	0.9500	C(32B)-C(37B)	1.388(17)

N(2)-H(2B)	0.8800	C(16)-H(16A)	0.9500	C(32B)-C(33B)	1.388(17)
N(3)-C(7)	1.264(12)	C(17A)-C(18A)	1.482(11)	C(33B)-C(34B)	1.388(17)
N(4)-C(15)	1.358(11)	C(17A)-H(17A)	0.9900	C(33B)-H(33B)	0.9500
N(4)-C(16)	1.361(11)	C(17A)-H(17B)	0.9900	C(34B)-C(35B)	1.388(17)
N(4)-H(4B)	0.8800	C(18A)-C(23A)	1.392(6)	C(34B)-H(34B)	0.9500
N(5)-C(16)	1.245(12)	C(18A)-C(19A)	1.392(6)	C(35B)-C(36B)	1.388(18)
N(6)-C(24)	1.294(10)	C(19A)-C(20A)	1.392(6)	C(35B)-H(35B)	0.9500
N(6)-C(28)	1.365(10)	C(19A)-H(19A)	0.9500	C(36B)-C(37B)	1.388(17)
N(7)-C(29)	1.350(11)	C(20A)-C(21A)	1.391(6)	C(36B)-H(36B)	0.9500
N(7)-C(30)	1.398(11)	C(20A)-H(20A)	0.9500	C(37B)-H(37B)	0.9500
N(7)-H(7B)	0.8800	C(21A)-C(22A)	1.392(6)	C(39)-H(39A)	0.9500
N(8)-C(30)	1.297(12)	C(21A)-H(21A)	0.9500	C(40A)-C(41A)	1.506(12)
N(9)-C(38)	1.377(9)	C(22A)-C(23A)	1.392(6)	C(40A)-H(40A)	0.9900
N(9)-C(39)	1.394(10)	C(22A)-H(22A)	0.9500	C(40A)-H(40B)	0.9900
N(9)-H(9A)	0.8800	C(23A)-H(23A)	0.9500	C(41A)-C(42A)	1.400(10)
N(10)-C(39)	1.369(10)	C(18B)-C(19B)	1.403(6)	C(41A)-C(46A)	1.400(10)
C(1)-C(2)	1.385(12)	C(18B)-C(23B)	1.403(6)	C(42A)-C(43A)	1.402(10)
C(1)-C(6)	1.516(10)	C(19B)-C(20B)	1.403(6)	C(42A)-H(42A)	0.9500
C(2)-C(3)	1.406(11)	C(19B)-H(19B)	0.9500	C(43A)-C(44A)	1.401(10)
C(2)-H(2A)	0.9500	C(20B)-C(21B)	1.403(6)	C(43A)-H(43A)	0.9500
C(3)-C(4)	1.413(11)	C(20B)-H(20B)	0.9500	C(44A)-C(45A)	1.401(10)
C(3)-H(3A)	0.9500	C(21B)-C(22B)	1.403(6)	C(44A)-H(44A)	0.9500
C(4)-C(5)	1.355(12)	C(21B)-H(21B)	0.9500	C(45A)-C(46A)	1.401(10)
C(4)-H(4A)	0.9500	C(22B)-C(23B)	1.403(6)	C(45A)-H(45A)	0.9500
C(5)-C(15)	1.520(11)	C(22B)-H(22B)	0.9500	C(46A)-H(46A)	0.9500
C(7)-H(7A)	0.9500	C(23B)-H(23B)	0.9500	C(41B)-C(46B)	1.381(7)
C(8A)-C(9A)	1.474(10)	C(24)-C(25)	1.413(12)	C(41B)-C(42B)	1.381(7)
C(8A)-H(8AA)	0.9900	C(24)-C(29)	1.495(12)	C(42B)-C(43B)	1.381(7)
C(8A)-H(8AB)	0.9900	C(25)-C(26)	1.361(12)	C(42B)-H(42B)	0.9500
C(9A)-C(14A)	1.396(6)	C(25)-H(25A)	0.9500	C(43B)-C(44B)	1.381(7)
C(9A)-C(10A)	1.396(6)	C(26)-C(27)	1.363(11)	C(43B)-H(43B)	0.9500
C(10A)-C(11A)	1.395(6)	C(26)-H(26A)	0.9500	C(44B)-C(45B)	1.381(7)
C(10A)-H(10A)	0.9500	C(27)-C(28)	1.410(11)	C(44B)-H(44B)	0.9500
C(11A)-C(12A)	1.396(6)	C(27)-H(27A)	0.9500	C(45B)-C(46B)	1.381(7)
C(11A)-H(11A)	0.9500	C(28)-C(38)	1.484(11)	C(45B)-H(45B)	0.9500

C(46B)-H(46B) 0.9500

N(3)-O(2)-C(8A)	108.0(7)	C(21B)-C(20B)-C(19B)	120.0
C(17A)-O(4)-N(5)	106.0(7)	C(21B)-C(20B)-H(20B)	120.0
N(8)-O(6)-C(31A)	109.8(7)	C(20B)-C(21B)-C(22B)	120.0
N(10)-O(8)-C(40A)	107.6(7)	C(20B)-C(21B)-H(21B)	120.0
C(1)-N(1)-C(5)	114.9(7)	C(22B)-C(21B)-H(21B)	120.0
C(6)-N(2)-C(7)	124.4(7)	C(21B)-C(22B)-C(23B)	120.0
C(6)-N(2)-H(2B)	117.8	C(21B)-C(22B)-H(22B)	120.0
C(7)-N(2)-H(2B)	117.8	C(23B)-C(22B)-H(22B)	120.0
C(7)-N(3)-O(2)	109.0(8)	C(18B)-C(23B)-C(22B)	120.0
C(15)-N(4)-C(16)	124.7(7)	C(18B)-C(23B)-H(23B)	120.0
C(15)-N(4)-H(4B)	117.7	C(22B)-C(23B)-H(23B)	120.0
C(16)-N(4)-H(4B)	117.7	N(6)-C(24)-C(25)	122.4(7)
C(16)-N(5)-O(4)	108.9(8)	N(6)-C(24)-C(29)	116.5(7)
C(24)-N(6)-C(28)	118.8(7)	C(25)-C(24)-C(29)	121.0(7)
C(29)-N(7)-C(30)	124.9(7)	C(26)-C(25)-C(24)	120.1(7)
C(29)-N(7)-H(7B)	117.6	C(26)-C(25)-H(25A)	120.0
C(30)-N(7)-H(7B)	117.6	C(24)-C(25)-H(25A)	120.0
C(30)-N(8)-O(6)	107.6(7)	C(25)-C(26)-C(27)	117.8(8)
C(38)-N(9)-C(39)	121.0(6)	C(25)-C(26)-H(26A)	121.1
C(38)-N(9)-H(9A)	119.5	C(27)-C(26)-H(26A)	121.1
C(39)-N(9)-H(9A)	119.5	C(26)-C(27)-C(28)	120.3(8)
C(39)-N(10)-O(8)	105.4(7)	C(26)-C(27)-H(27A)	119.9
N(1)-C(1)-C(2)	125.4(7)	C(28)-C(27)-H(27A)	119.9
N(1)-C(1)-C(6)	113.8(7)	N(6)-C(28)-C(27)	120.4(7)
C(2)-C(1)-C(6)	120.7(7)	N(6)-C(28)-C(38)	118.2(7)
C(1)-C(2)-C(3)	117.8(7)	C(27)-C(28)-C(38)	121.3(7)
C(1)-C(2)-H(2A)	121.1	O(5)-C(29)-N(7)	124.4(8)
C(3)-C(2)-H(2A)	121.1	O(5)-C(29)-C(24)	122.0(8)
C(2)-C(3)-C(4)	119.3(8)	N(7)-C(29)-C(24)	113.6(7)
C(2)-C(3)-H(3A)	120.3	N(8)-C(30)-N(7)	123.7(8)
C(4)-C(3)-H(3A)	120.3	N(8)-C(30)-H(30A)	118.2
C(5)-C(4)-C(3)	117.8(7)	N(7)-C(30)-H(30A)	118.2
C(5)-C(4)-H(4A)	121.1	O(6)-C(31A)-C(32A)	113.6(8)

C(3)-C(4)-H(4A)	121.1	O(6)-C(31A)-H(31A)	108.9
C(4)-C(5)-N(1)	124.3(7)	C(32A)-C(31A)-H(31A)	108.9
C(4)-C(5)-C(15)	121.1(7)	O(6)-C(31A)-H(31B)	108.9
N(1)-C(5)-C(15)	114.4(7)	C(32A)-C(31A)-H(31B)	108.9
O(1)-C(6)-N(2)	124.1(7)	H(31A)-C(31A)-H(31B)	107.7
O(1)-C(6)-C(1)	119.4(7)	C(33A)-C(32A)-C(37A)	120.0
N(2)-C(6)-C(1)	116.4(6)	C(33A)-C(32A)-C(31A)	120.5(8)
N(3)-C(7)-N(2)	118.6(7)	C(37A)-C(32A)-C(31A)	119.5(8)
N(3)-C(7)-H(7A)	120.7	C(32A)-C(33A)-C(34A)	120.0
N(2)-C(7)-H(7A)	120.7	C(32A)-C(33A)-H(33A)	120.0
O(2)-C(8A)-C(9A)	114.3(9)	C(34A)-C(33A)-H(33A)	120.0
O(2)-C(8A)-H(8AA)	108.7	C(35A)-C(34A)-C(33A)	120.0
C(9A)-C(8A)-H(8AA)	108.7	C(35A)-C(34A)-H(34A)	120.0
O(2)-C(8A)-H(8AB)	108.7	C(33A)-C(34A)-H(34A)	120.0
C(9A)-C(8A)-H(8AB)	108.7	C(34A)-C(35A)-C(36A)	120.0
H(8AA)-C(8A)-H(8AB)	107.6	C(34A)-C(35A)-H(35A)	120.0
C(14A)-C(9A)-C(10A)	120.0	C(36A)-C(35A)-H(35A)	120.0
C(14A)-C(9A)-C(8A)	123.7(8)	C(37A)-C(36A)-C(35A)	120.0
C(10A)-C(9A)-C(8A)	116.2(8)	C(37A)-C(36A)-H(36A)	120.0
C(11A)-C(10A)-C(9A)	120.0	C(35A)-C(36A)-H(36A)	120.0
C(11A)-C(10A)-H(10A)	120.0	C(36A)-C(37A)-C(32A)	120.0
C(9A)-C(10A)-H(10A)	120.0	C(36A)-C(37A)-H(37A)	120.0
C(10A)-C(11A)-C(12A)	120.0	C(32A)-C(37A)-H(37A)	120.0
C(10A)-C(11A)-H(11A)	120.0	C(37B)-C(32B)-C(33B)	120.0
C(12A)-C(11A)-H(11A)	120.0	C(34B)-C(33B)-C(32B)	120.0
C(11A)-C(12A)-C(13A)	120.0	C(34B)-C(33B)-H(33B)	120.0
C(11A)-C(12A)-H(12A)	120.0	C(32B)-C(33B)-H(33B)	120.0
C(13A)-C(12A)-H(12A)	120.0	C(33B)-C(34B)-C(35B)	120.0
C(14A)-C(13A)-C(12A)	120.0	C(33B)-C(34B)-H(34B)	120.0
C(14A)-C(13A)-H(13A)	120.0	C(35B)-C(34B)-H(34B)	120.0
C(12A)-C(13A)-H(13A)	120.0	C(34B)-C(35B)-C(36B)	120.0
C(9A)-C(14A)-C(13A)	120.0	C(34B)-C(35B)-H(35B)	120.0
C(9A)-C(14A)-H(14A)	120.0	C(36B)-C(35B)-H(35B)	120.0
C(13A)-C(14A)-H(14A)	120.0	C(37B)-C(36B)-C(35B)	120.0
C(10B)-C(9B)-C(14B)	120.0	C(37B)-C(36B)-H(36B)	120.0

C(9B)-C(10B)-C(11B)	120.0	C(35B)-C(36B)-H(36B)	120.0
C(9B)-C(10B)-H(10B)	120.0	C(36B)-C(37B)-C(32B)	120.0
C(11B)-C(10B)-H(10B)	120.0	C(36B)-C(37B)-H(37B)	120.0
C(12B)-C(11B)-C(10B)	119.99(9)	C(32B)-C(37B)-H(37B)	120.0
C(12B)-C(11B)-H(11B)	120.0	O(7)-C(38)-N(9)	123.6(7)
C(10B)-C(11B)-H(11B)	120.0	O(7)-C(38)-C(28)	121.6(6)
C(11B)-C(12B)-C(13B)	120.0	N(9)-C(38)-C(28)	114.7(6)
C(11B)-C(12B)-H(12B)	120.0	N(10)-C(39)-N(9)	114.0(7)
C(13B)-C(12B)-H(12B)	120.0	N(10)-C(39)-H(39A)	123.0
C(14B)-C(13B)-C(12B)	120.01(7)	N(9)-C(39)-H(39A)	123.0
C(14B)-C(13B)-H(13B)	120.0	O(8)-C(40A)-C(41A)	112.5(11)
C(12B)-C(13B)-H(13B)	120.0	O(8)-C(40A)-H(40A)	109.1
C(13B)-C(14B)-C(9B)	119.99(11)	C(41A)-C(40A)-H(40A)	109.1
C(13B)-C(14B)-H(14B)	120.0	O(8)-C(40A)-H(40B)	109.1
C(9B)-C(14B)-H(14B)	120.0	C(41A)-C(40A)-H(40B)	109.1
O(3)-C(15)-N(4)	123.5(8)	H(40A)-C(40A)-H(40B)	107.8
O(3)-C(15)-C(5)	122.6(8)	C(42A)-C(41A)-C(46A)	120.1
N(4)-C(15)-C(5)	113.8(7)	C(42A)-C(41A)-C(40A)	100.7(12)
N(5)-C(16)-N(4)	126.1(9)	C(46A)-C(41A)-C(40A)	139.2(12)
N(5)-C(16)-H(16A)	116.9	C(41A)-C(42A)-C(43A)	120.0
N(4)-C(16)-H(16A)	116.9	C(41A)-C(42A)-H(42A)	120.0
O(4)-C(17A)-C(18A)	117.0(9)	C(43A)-C(42A)-H(42A)	120.0
O(4)-C(17A)-H(17A)	108.0	C(44A)-C(43A)-C(42A)	120.0
C(18A)-C(17A)-H(17A)	108.0	C(44A)-C(43A)-H(43A)	120.0
O(4)-C(17A)-H(17B)	108.0	C(42A)-C(43A)-H(43A)	120.0
C(18A)-C(17A)-H(17B)	108.0	C(43A)-C(44A)-C(45A)	120.0
H(17A)-C(17A)-H(17B)	107.3	C(43A)-C(44A)-H(44A)	120.0
C(23A)-C(18A)-C(19A)	120.0	C(45A)-C(44A)-H(44A)	120.0
C(23A)-C(18A)-C(17A)	119.8(9)	C(46A)-C(45A)-C(44A)	120.0
C(19A)-C(18A)-C(17A)	119.9(9)	C(46A)-C(45A)-H(45A)	120.0
C(18A)-C(19A)-C(20A)	120.0	C(44A)-C(45A)-H(45A)	120.0
C(18A)-C(19A)-H(19A)	120.0	C(41A)-C(46A)-C(45A)	120.0
C(20A)-C(19A)-H(19A)	120.0	C(41A)-C(46A)-H(46A)	120.0
C(21A)-C(20A)-C(19A)	120.0	C(45A)-C(46A)-H(46A)	120.0
C(21A)-C(20A)-H(20A)	120.0	C(46B)-C(41B)-C(42B)	120.0

C(19A)-C(20A)-H(20A)	120.0	C(43B)-C(42B)-C(41B)	120.0
C(20A)-C(21A)-C(22A)	120.0	C(43B)-C(42B)-H(42B)	120.0
C(20A)-C(21A)-H(21A)	120.0	C(41B)-C(42B)-H(42B)	120.0
C(22A)-C(21A)-H(21A)	120.0	C(42B)-C(43B)-C(44B)	120.0
C(23A)-C(22A)-C(21A)	120.0	C(42B)-C(43B)-H(43B)	120.0
C(23A)-C(22A)-H(22A)	120.0	C(44B)-C(43B)-H(43B)	120.0
C(21A)-C(22A)-H(22A)	120.0	C(43B)-C(44B)-C(45B)	120.0
C(22A)-C(23A)-C(18A)	120.0	C(43B)-C(44B)-H(44B)	120.0
C(22A)-C(23A)-H(23A)	120.0	C(45B)-C(44B)-H(44B)	120.0
C(18A)-C(23A)-H(23A)	120.0	C(46B)-C(45B)-C(44B)	120.0
C(19B)-C(18B)-C(23B)	120.0	C(46B)-C(45B)-H(45B)	120.0
C(19B)-C(20B)-H(20B)	120.0	C(44B)-C(45B)-H(45B)	120.0
C(20B)-C(19B)-C(18B)	120.0	C(45B)-C(46B)-C(41B)	120.0
C(20B)-C(19B)-H(19B)	120.0	C(45B)-C(46B)-H(46B)	120.0
C(18B)-C(19B)-H(19B)	120.0	C(41B)-C(46B)-H(46B)	120.0

**Table B5.4.** Anisotropic displacement parameters ( $\text{\AA}^2 \times 10^3$ ) for ap20a. The anisotropic displacement factor exponent takes the form:  $-2\pi^2 [ h^2 a^{*2} U^{11} + \dots + 2 h k a^{*} b^{*} U^{12} ]$

	U <sup>11</sup>	U <sup>22</sup>	U <sup>33</sup>	U <sup>23</sup>	U <sup>13</sup>	U <sup>12</sup>
O(1)	42(3)	15(2)	81(5)	3(2)	-10(3)	-6(2)
O(2)	60(4)	81(4)	57(4)	16(4)	-15(3)	-26(4)
O(3)	38(3)	47(3)	63(4)	1(3)	-4(3)	-19(3)
O(4)	40(4)	73(4)	74(5)	16(4)	-6(3)	-25(3)
O(5)	31(3)	52(3)	73(5)	-4(3)	-2(3)	-2(3)
O(6)	38(3)	85(4)	53(4)	8(3)	-1(3)	7(3)
O(7)	38(3)	31(3)	67(4)	-5(3)	-2(3)	6(2)
O(8)	30(3)	42(3)	114(6)	9(3)	-16(4)	-4(3)
N(1)	22(3)	30(3)	51(4)	-11(3)	-2(3)	1(2)
N(2)	41(4)	44(3)	34(4)	8(3)	-4(3)	-16(3)
N(3)	28(4)	92(6)	56(6)	-2(5)	-9(4)	-21(4)
N(4)	35(4)	29(3)	50(5)	-1(3)	3(3)	-13(3)
N(5)	41(4)	47(4)	69(6)	4(4)	5(4)	-6(3)
N(6)	22(3)	15(2)	54(4)	-2(2)	-2(3)	4(2)
N(7)	32(3)	34(3)	54(5)	1(3)	-4(3)	-2(3)
N(8)	58(5)	44(4)	59(6)	0(4)	10(4)	-11(4)
N(9)	20(3)	17(2)	78(6)	-1(3)	-8(3)	9(2)
N(10)	26(4)	60(4)	64(6)	-3(4)	-15(4)	20(3)
C(1)	17(3)	20(3)	55(5)	-6(3)	2(3)	-9(3)
C(2)	33(4)	24(3)	67(6)	2(3)	-3(4)	-3(3)
C(3)	27(4)	18(3)	59(5)	0(3)	3(4)	-5(3)
C(4)	24(3)	24(3)	59(6)	-6(3)	0(4)	2(3)
C(5)	22(4)	24(3)	53(5)	-6(3)	-2(3)	-13(3)
C(6)	21(4)	30(4)	64(6)	-8(4)	5(4)	-2(3)
C(7)	41(5)	41(4)	43(5)	-2(3)	2(4)	-12(4)
C(8A)	46(2)	82(3)	71(2)	10(2)	-9(2)	5(2)
C(9A)	71(4)	87(4)	75(4)	11(3)	-6(3)	9(3)
C(10A)	71(4)	87(4)	75(4)	11(3)	-6(3)	9(3)
C(11A)	71(4)	87(4)	75(4)	11(3)	-6(3)	9(3)
C(12A)	71(4)	87(4)	75(4)	11(3)	-6(3)	9(3)

C(13A)	71(4)	87(4)	75(4)	11(3)	-6(3)	9(3)
C(14A)	71(4)	87(4)	75(4)	11(3)	-6(3)	9(3)
C(8B)	46(2)	82(3)	71(2)	10(2)	-9(2)	5(2)
C(9B)	71(4)	87(4)	75(4)	11(3)	-6(3)	9(3)
C(10B)	71(4)	87(4)	75(4)	11(3)	-6(3)	9(3)
C(11B)	71(4)	87(4)	75(4)	11(3)	-6(3)	9(3)
C(12B)	71(4)	87(4)	75(4)	11(3)	-6(3)	9(3)
C(13B)	71(4)	87(4)	75(4)	11(3)	-6(3)	9(3)
C(14B)	71(4)	87(4)	75(4)	11(3)	-6(3)	9(3)
C(15)	44(5)	41(4)	38(5)	-7(3)	10(4)	-13(4)
C(16)	52(5)	62(5)	34(5)	-4(4)	10(4)	-5(4)
C(17A)	46(2)	82(3)	71(2)	10(2)	-9(2)	5(2)
C(18A)	45(3)	80(4)	59(3)	3(3)	-6(2)	-8(3)
C(19A)	45(3)	80(4)	59(3)	3(3)	-6(2)	-8(3)
C(20A)	45(3)	80(4)	59(3)	3(3)	-6(2)	-8(3)
C(21A)	45(3)	80(4)	59(3)	3(3)	-6(2)	-8(3)
C(22A)	45(3)	80(4)	59(3)	3(3)	-6(2)	-8(3)
C(23A)	45(3)	80(4)	59(3)	3(3)	-6(2)	-8(3)
C(17B)	46(2)	82(3)	71(2)	10(2)	-9(2)	5(2)
C(18B)	45(3)	80(4)	59(3)	3(3)	-6(2)	-8(3)
C(19B)	45(3)	80(4)	59(3)	3(3)	-6(2)	-8(3)
C(20B)	45(3)	80(4)	59(3)	3(3)	-6(2)	-8(3)
C(21B)	45(3)	80(4)	59(3)	3(3)	-6(2)	-8(3)
C(22B)	45(3)	80(4)	59(3)	3(3)	-6(2)	-8(3)
C(23B)	45(3)	80(4)	59(3)	3(3)	-6(2)	-8(3)
C(24)	30(4)	28(3)	52(6)	-5(3)	2(4)	12(3)
C(25)	29(4)	41(4)	47(5)	-12(4)	-9(4)	-2(3)
C(26)	40(4)	35(4)	45(5)	-4(3)	-4(4)	22(3)
C(27)	22(4)	39(4)	42(5)	-1(3)	9(3)	14(3)
C(28)	36(4)	22(3)	47(5)	2(3)	-2(4)	16(3)
C(29)	22(4)	31(4)	65(6)	-9(3)	-5(4)	-1(3)
C(30)	33(4)	28(4)	66(7)	-2(4)	10(4)	-4(3)
C(31A)	46(2)	82(3)	71(2)	10(2)	-9(2)	5(2)
C(32A)	60(3)	80(3)	66(4)	4(3)	-8(3)	12(3)
C(33A)	60(3)	80(3)	66(4)	4(3)	-8(3)	12(3)

C(34A)	60(3)	80(3)	66(4)	4(3)	-8(3)	12(3)
C(35A)	60(3)	80(3)	66(4)	4(3)	-8(3)	12(3)
C(36A)	60(3)	80(3)	66(4)	4(3)	-8(3)	12(3)
C(37A)	60(3)	80(3)	66(4)	4(3)	-8(3)	12(3)
C(31B)	46(2)	82(3)	71(2)	10(2)	-9(2)	5(2)
C(32B)	60(3)	80(3)	66(4)	4(3)	-8(3)	12(3)
C(33B)	60(3)	80(3)	66(4)	4(3)	-8(3)	12(3)
C(34B)	60(3)	80(3)	66(4)	4(3)	-8(3)	12(3)
C(35B)	60(3)	80(3)	66(4)	4(3)	-8(3)	12(3)
C(36B)	60(3)	80(3)	66(4)	4(3)	-8(3)	12(3)
C(37B)	60(3)	80(3)	66(4)	4(3)	-8(3)	12(3)
C(38)	29(4)	12(3)	45(5)	0(3)	-6(3)	8(3)
C(39)	16(3)	39(4)	59(6)	2(3)	-8(4)	11(3)
C(40A)	46(2)	82(3)	71(2)	10(2)	-9(2)	5(2)
C(41A)	57(3)	71(4)	63(4)	2(3)	3(3)	17(3)
C(42A)	57(3)	71(4)	63(4)	2(3)	3(3)	17(3)
C(43A)	57(3)	71(4)	63(4)	2(3)	3(3)	17(3)
C(44A)	57(3)	71(4)	63(4)	2(3)	3(3)	17(3)
C(45A)	57(3)	71(4)	63(4)	2(3)	3(3)	17(3)
C(46A)	57(3)	71(4)	63(4)	2(3)	3(3)	17(3)
C(40B)	46(2)	82(3)	71(2)	10(2)	-9(2)	5(2)
C(41B)	57(3)	71(4)	63(4)	2(3)	3(3)	17(3)
C(42B)	57(3)	71(4)	63(4)	2(3)	3(3)	17(3)
C(43B)	57(3)	71(4)	63(4)	2(3)	3(3)	17(3)
C(44B)	57(3)	71(4)	63(4)	2(3)	3(3)	17(3)
C(45B)	57(3)	71(4)	63(4)	2(3)	3(3)	17(3)
C(46B)	57(3)	71(4)	63(4)	2(3)	3(3)	17(3)

---

**Table B5.5.** Hydrogen coordinates ( $\times 10^4$ ) and isotropic displacement parameters ( $\text{\AA}^2 \times 10^3$ ) for ap20a.

	x	y	z	U(eq)
H(2B)	7863	10421	5655	48
H(4B)	5196	7644	5771	46

H(7B)	9563	6910	4157	48
H(9A)	6873	4203	4270	46
H(2A)	6335	15614	4967	50
H(3A)	4308	13830	4737	42
H(4A)	3133	10124	4965	43
H(7A)	10000	14179	5748	50
H(8AA)	12801	9161	6227	80
H(8AB)	11382	7534	6189	80
H(10A)	9975	7032	6558	93
H(11A)	9408	7705	7049	93
H(12A)	10578	11034	7334	93
H(13A)	12315	13691	7127	93
H(14A)	12881	13018	6636	93
H(8BA)	12802	9185	6227	80
H(8BB)	11396	7532	6186	80
H(10B)	9887	7332	6439	93
H(11B)	8627	7913	6866	93
H(12B)	9463	10807	7243	93
H(13B)	11559	13118	7194	93
H(14B)	12819	12536	6768	93
H(16A)	3184	3797	5847	59
H(17A)	7781	4067	6326	80
H(17B)	6675	1643	6329	80
H(19A)	5362	7985	6522	74
H(20A)	4948	9543	6998	74
H(21A)	5745	6984	7403	74
H(22A)	6956	2867	7333	74
H(23A)	7369	1308	6858	74
H(17C)	7788	3836	6313	80
H(17D)	6566	1675	6347	80
H(19B)	4678	6805	6549	74
H(20B)	4109	7837	7034	74
H(21B)	5590	6520	7425	74
H(22B)	7641	4171	7330	74
H(23B)	8211	3139	6844	74

H(25A)	11593	4276	4967	47
H(26A)	10483	598	5188	48
H(27A)	8504	-1141	4959	41
H(30A)	11642	10698	4072	50
H(31A)	7820	12815	3602	80
H(31B)	6898	10083	3608	80
H(33A)	7069	12710	3055	83
H(34A)	7780	11505	2589	83
H(35A)	9441	8104	2534	83
H(36A)	10393	5908	2946	83
H(37A)	9683	7112	3412	83
H(31C)	7755	12804	3606	80
H(31D)	6917	9946	3591	80
H(33B)	6860	12568	3195	83
H(34B)	6856	11774	2689	83
H(35B)	8487	8831	2491	83
H(36B)	10122	6680	2797	83
H(37B)	10127	7474	3303	83
H(39A)	4806	223	4170	46
H(40A)	3131	7145	3759	80
H(40B)	1853	5182	3681	80
H(42A)	1745	2280	3388	76
H(43A)	1962	592	2908	76
H(44A)	3714	2267	2612	76
H(45A)	5247	5631	2796	76
H(46A)	5030	7320	3276	76
H(40C)	3120	7161	3757	80
H(40D)	1854	5163	3673	80
H(42B)	2150	1662	3282	76
H(43B)	2842	1120	2801	76
H(44B)	4560	3936	2619	76
H(45B)	5586	7294	2919	76
H(46B)	4893	7836	3400	76

**Table B5.6.** Torsion angles [°] for ap20a.

C(8A)-O(2)-N(3)-C(7)	<b>174.5(8)</b>	C(19B)-C(18B)-C(23B)-C(22B)	<b>0.0</b>
C(17A)-O(4)-N(5)-C(16)	<b>179.7(8)</b>	C(21B)-C(22B)-C(23B)-C(18B)	<b>0.0</b>
C(31A)-O(6)-N(8)-C(30)	<b>-177.7(7)</b>	C(28)-N(6)-C(24)-C(25)	<b>0.0(11)</b>
C(40A)-O(8)-N(10)-C(39)	<b>-174.3(7)</b>	C(28)-N(6)-C(24)-C(29)	<b>177.1(6)</b>
C(5)-N(1)-C(1)-C(2)	<b>-6.2(11)</b>	N(6)-C(24)-C(25)-C(26)	<b>2.0(12)</b>
C(5)-N(1)-C(1)-C(6)	<b>176.9(6)</b>	C(29)-C(24)-C(25)-C(26)	<b>-175.0(7)</b>
N(1)-C(1)-C(2)-C(3)	<b>1.1(12)</b>	C(24)-C(25)-C(26)-C(27)	<b>-0.7(11)</b>
C(6)-C(1)-C(2)-C(3)	<b>177.8(7)</b>	C(25)-C(26)-C(27)-C(28)	<b>-2.4(11)</b>
C(1)-C(2)-C(3)-C(4)	<b>1.5(11)</b>	C(24)-N(6)-C(28)-C(27)	<b>-3.1(10)</b>
C(2)-C(3)-C(4)-C(5)	<b>1.5(11)</b>	C(24)-N(6)-C(28)-C(38)	<b>179.7(6)</b>
C(3)-C(4)-C(5)-N(1)	<b>-7.3(11)</b>	C(26)-C(27)-C(28)-N(6)	<b>4.4(11)</b>
C(3)-C(4)-C(5)-C(15)	<b>177.6(7)</b>	C(26)-C(27)-C(28)-C(38)	<b>-178.5(7)</b>
C(1)-N(1)-C(5)-C(4)	<b>9.5(10)</b>	C(30)-N(7)-C(29)-O(5)	<b>-8.1(13)</b>
C(1)-N(1)-C(5)-C(15)	<b>-175.1(7)</b>	C(30)-N(7)-C(29)-C(24)	<b>173.8(7)</b>
C(7)-N(2)-C(6)-O(1)	<b>-0.4(14)</b>	N(6)-C(24)-C(29)-O(5)	<b>-172.5(8)</b>
C(7)-N(2)-C(6)-C(1)	<b>176.3(7)</b>	C(25)-C(24)-C(29)-O(5)	<b>4.7(12)</b>
N(1)-C(1)-C(6)-O(1)	<b>-160.7(7)</b>	N(6)-C(24)-C(29)-N(7)	<b>5.6(10)</b>
C(2)-C(1)-C(6)-O(1)	<b>22.1(11)</b>	C(25)-C(24)-C(29)-N(7)	<b>-177.2(7)</b>

N(1)-C(1)-C(6)-N(2)	<b>22.3(10)</b>	O(6)-N(8)-C(30)-N(7)	<b>-1.8(12)</b>
C(2)-C(1)-C(6)-N(2)	<b>-154.8(8)</b>	C(29)-N(7)-C(30)-N(8)	<b>-168.7(9)</b>
O(2)-N(3)-C(7)-N(2)	<b>175.1(8)</b>	N(8)-O(6)-C(31A)-C(32A)	<b>73.0(11)</b>
C(6)-N(2)-C(7)-N(3)	<b>178.3(9)</b>	O(6)-C(31A)-C(32A)-C(33A)	<b>-168.1(8)</b>
N(3)-O(2)-C(8A)-C(9A)	<b>-91.9(11)</b>	O(6)-C(31A)-C(32A)-C(37A)	<b>12.5(12)</b>
O(2)-C(8A)-C(9A)-C(14A)	<b>-75.4(11)</b>	C(37A)-C(32A)-C(33A)-C(34A)	<b>0.0</b>
O(2)-C(8A)-C(9A)-C(10A)	<b>106.4(10)</b>	C(31A)-C(32A)-C(33A)-C(34A)	<b>-179.4(12)</b>
C(14A)-C(9A)-C(10A)-C(11A)	<b>0.0</b>	C(32A)-C(33A)-C(34A)-C(35A)	<b>0.0</b>
C(8A)-C(9A)-C(10A)-C(11A)	<b>178.3(11)</b>	C(33A)-C(34A)-C(35A)-C(36A)	<b>0.0</b>
C(9A)-C(10A)-C(11A)-C(12A)	<b>0.0</b>	C(34A)-C(35A)-C(36A)-C(37A)	<b>0.0</b>
C(10A)-C(11A)-C(12A)-C(13A)	<b>0.0</b>	C(35A)-C(36A)-C(37A)-C(32A)	<b>0.0</b>
C(11A)-C(12A)-C(13A)-C(14A)	<b>0.0</b>	C(33A)-C(32A)-C(37A)-C(36A)	<b>0.0</b>
C(10A)-C(9A)-C(14A)-C(13A)	<b>0.0</b>	C(31A)-C(32A)-C(37A)-C(36A)	<b>179.4(12)</b>
C(8A)-C(9A)-C(14A)-C(13A)	<b>-178.1(12)</b>	C(37B)-C(32B)-C(33B)-C(34B)	<b>0.0</b>
C(12A)-C(13A)-C(14A)-C(9A)	<b>0.0</b>	C(32B)-C(33B)-C(34B)-C(35B)	<b>0.0</b>
C(14B)-C(9B)-C(10B)-C(11B)	<b>0.0</b>	C(33B)-C(34B)-C(35B)-C(36B)	<b>0.0</b>
C(9B)-C(10B)-C(11B)-C(12B)	<b>0.0</b>	C(34B)-C(35B)-C(36B)-C(37B)	<b>0.0</b>
C(10B)-C(11B)-C(12B)-C(13B)	<b>0.0</b>	C(35B)-C(36B)-C(37B)-C(32B)	<b>0.0</b>
C(11B)-C(12B)-C(13B)-C(14B)	<b>0.0</b>	C(33B)-C(32B)-C(37B)-C(36B)	<b>0.0</b>

C(12B)-C(13B)-C(14B)-C(9B)	<b>0.0</b>	C(39)-N(9)-C(38)-O(7)	<b>4.9(12)</b>
C(10B)-C(9B)-C(14B)-C(13B)	<b>0.0</b>	C(39)-N(9)-C(38)-C(28)	<b>-177.7(7)</b>
C(16)-N(4)-C(15)-O(3)	<b>4.4(14)</b>	N(6)-C(28)-C(38)-O(7)	<b>153.1(7)</b>
C(16)-N(4)-C(15)-C(5)	<b>-173.8(7)</b>	C(27)-C(28)-C(38)-O(7)	<b>-24.0(12)</b>
C(4)-C(5)-C(15)-O(3)	<b>-4.7(12)</b>	N(6)-C(28)-C(38)-N(9)	<b>-24.4(10)</b>
N(1)-C(5)-C(15)-O(3)	<b>179.7(8)</b>	C(27)-C(28)-C(38)-N(9)	<b>158.5(7)</b>
C(4)-C(5)-C(15)-N(4)	<b>173.5(7)</b>	O(8)-N(10)-C(39)-N(9)	<b>-176.0(7)</b>
N(1)-C(5)-C(15)-N(4)	<b>-2.1(10)</b>	C(38)-N(9)-C(39)-N(10)	<b>177.7(8)</b>
O(4)-N(5)-C(16)-N(4)	<b>-4.5(13)</b>	N(10)-O(8)-C(40A)-C(41A)	<b>85.5(12)</b>
C(15)-N(4)-C(16)-N(5)	<b>173.3(9)</b>	O(8)-C(40A)-C(41A)-C(42A)	<b>83.1(10)</b>
N(5)-O(4)-C(17A)-C(18A)	<b>-76.1(11)</b>	O(8)-C(40A)-C(41A)-C(46A)	<b>-94.3(17)</b>
O(4)-C(17A)-C(18A)-C(23A)	<b>167.7(8)</b>	C(46A)-C(41A)-C(42A)-C(43A)	<b>0.0</b>
O(4)-C(17A)-C(18A)-C(19A)	<b>-18.8(14)</b>	C(40A)-C(41A)-C(42A)-C(43A)	<b>-178.1(13)</b>
C(23A)-C(18A)-C(19A)-C(20A)	<b>0.0</b>	C(41A)-C(42A)-C(43A)-C(44A)	<b>0.0</b>
C(17A)-C(18A)-C(19A)-C(20A)	<b>-173.5(11)</b>	C(42A)-C(43A)-C(44A)-C(45A)	<b>0.0</b>
C(18A)-C(19A)-C(20A)-C(21A)	<b>0.0</b>	C(43A)-C(44A)-C(45A)-C(46A)	<b>0.0</b>
C(19A)-C(20A)-C(21A)-C(22A)	<b>0.0</b>	C(42A)-C(41A)-C(46A)-C(45A)	<b>0.0</b>
C(20A)-C(21A)-C(22A)-C(23A)	<b>0.0</b>	C(40A)-C(41A)-C(46A)-C(45A)	<b>177(2)</b>
C(21A)-C(22A)-C(23A)-C(18A)	<b>0.0</b>	C(44A)-C(45A)-C(46A)-C(41A)	<b>0.0</b>

C(19A)-C(18A)-C(23A)-C(22A)	0.0	C(46B)-C(41B)-C(42B)-C(43B)	0.0
C(17A)-C(18A)-C(23A)-C(22A)	173.5(11)	C(41B)-C(42B)-C(43B)-C(44B)	0.0
C(23B)-C(18B)-C(19B)-C(20B)	0.0	C(42B)-C(43B)-C(44B)-C(45B)	0.0
C(18B)-C(19B)-C(20B)-C(21B)	0.0	C(43B)-C(44B)-C(45B)-C(46B)	0.0
C(19B)-C(20B)-C(21B)-C(22B)	0.0	C(44B)-C(45B)-C(46B)-C(41B)	0.0
C(20B)-C(21B)-C(22B)-C(23B)	0.0	C(42B)-C(41B)-C(46B)-C(45B)	0.0

## 6) 4.4Z

A crystal of the compound (colorless, plate-shaped, size 0.30 x 0.20 x 0.04 mm) was mounted on a glass fiber with grease and cooled to -93 °C in a stream of nitrogen gas controlled with Cryostream Controller 700. Data collection was performed on a Bruker SMART APEX II X-ray diffractometer with graphite-monochromated Mo K<sub>α</sub> radiation ( $\lambda = 0.71073 \text{ \AA}$ ), operating at 50 kV and 30 mA over 2θ ranges of 4.22 ~ 52.00°. No significant decay was observed during the data collection.

Data were processed on a PC using the Bruker AXS Crystal Structure Analysis Package:<sup>[1]</sup> Data collection: APEX2 (Bruker, 2006); cell refinement: SAINT (Bruker, 2005); data reduction: SAINT (Bruker, 2005); structure solution: XPREP (Bruker, 2005) and SHELXTL (Bruker, 2000); structure refinement: SHELXTL; molecular graphics: SHELXTL; publication materials: SHELXTL. Neutral atom scattering factors were taken from Cromer and Waber.<sup>[2]</sup> The crystal is monoclinic space group  $P2_1/c$ , based on the systematic absences, *E* statistics and successful refinement of the structure. The structure was solved by direct methods. Full-matrix least-square refinements minimizing the function  $\sum w (F_o^2 - F_c^2)^2$  were applied to the compound. All non-hydrogen atoms were refined anisotropically. All of the H atoms were placed in geometrically calculated positions, with C-H = 0.95 (aromatic), 0.99(CH<sub>2</sub>), and 0.88(N-H) Å, and refined as riding

atoms, with  $U_{\text{iso}}(\text{H}) = 1.2 \text{ U}_{\text{eq}}(\text{C or N})$ .

Convergence to final  $R_1 = 0.0441$  and  $wR_2 = 0.1017$  for 1731 ( $I > 2\sigma(I)$ ) independent reflections, and  $R_1 = 0.0717$  and  $wR_2 = 0.1172$  for all 2469 ( $\text{R(int)} = 0.0217$ ) independent reflections, with 162 parameters and 0 restraints, were achieved.<sup>[3]</sup> The largest residual peak and hole to be 0.280 and  $-0.292 \text{ e}/\text{\AA}^3$ , respectively. Crystallographic data, atomic coordinates and equivalent isotropic displacement parameters, bond lengths and angles, anisotropic displacement parameters, hydrogen coordinates and isotropic displacement parameters, and torsion angles are given in Table B6.1 to B6.6. The molecular structure and the cell packing are shown in Figures B6.1 and B6.2.

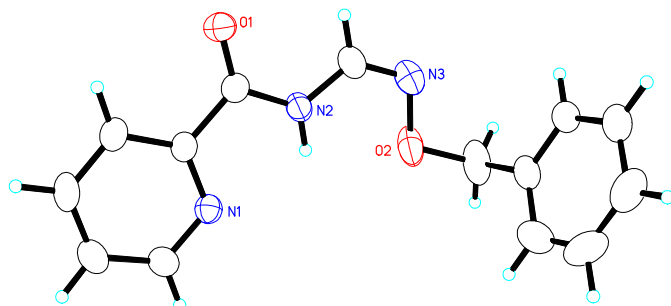


**Figure B6.1.** a) Molecular Structure (displacement ellipsoids for non-H atoms are shown at the 50% probability level and H atoms are represented by circles of arbitrary size

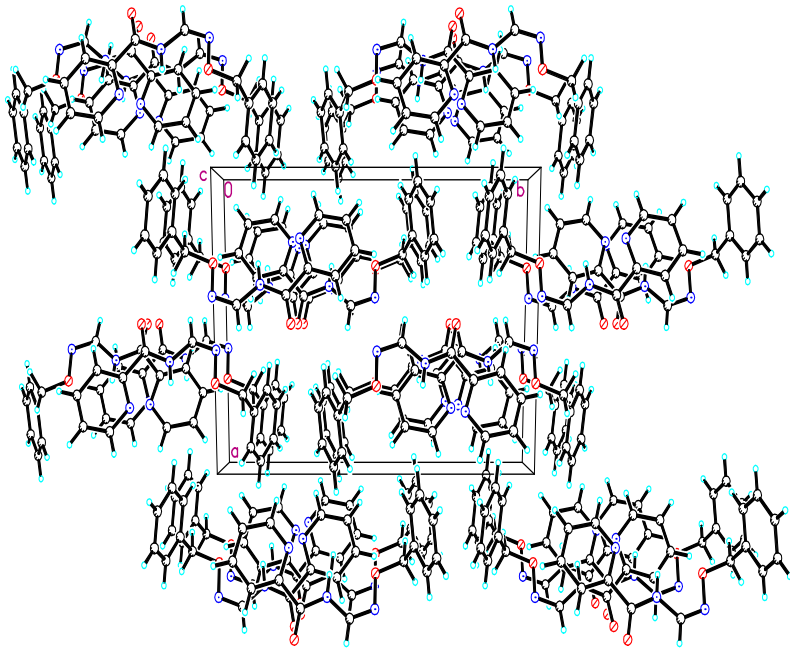


**Figure B6.2** Unit cell packing

[1] Bruker AXS Crystal Structure Analysis Package:

Bruker (2000). SHELXTL. Version 6.14. Bruker AXS Inc., Madison, Wisconsin, USA.

Bruker (2005). XPREP. Version 2005/2. Bruker AXS Inc., Madison, Wisconsin, USA.

Bruker (2005). SAINT. Version 7.23A. Bruker AXS Inc., Madison, Wisconsin, USA.

Bruker (2006). APEX2. Version 2.0-2. Bruker AXS Inc., Madison, Wisconsin, USA.

[2] Cromer, D. T.; Waber, J. T. *International Tables for X-ray Crystallography*; Kynoch Press: Birmingham, UK, 1974; Vol. 4, Table 2.2 A.

$$[3] R_1 = \sum | |F_O| - |F_C| | / \sum |F_O|$$

$$wR_2 = \{ \sum [w(F_O^2 - F_C^2)^2] / \sum [w(F_O^2)^2] \}^{1/2}$$

$$(w = 1 / [\sigma^2(F_O^2) + (0.0457P)^2 + 0.1746P], \text{ where } P = [\text{Max}(F_O^2, 0) + 2F_C^2] / 3)$$

**Table B6.1** Crystal data and structure refinement for ap21

Identification code	ap21
Empirical formula	C14 H13 N3 O2
Formula weight	255.27
Temperature	180(2) K

Wavelength	0.71073 Å		
Crystal system	Monoclinic		
Space group	P2(1)/c		
Unit cell dimensions	$a = 11.7004(12)$ Å	$\alpha = 90^\circ$ .	
	$b = 15.9776(13)$ Å	$\beta = 107.250(5)^\circ$ .	
	$c = 7.1602(6)$ Å	$\gamma = 90^\circ$ .	
Volume	$1278.3(2)$ Å <sup>3</sup>		
Z	4		
Density (calculated)	1.326 Mg/m <sup>3</sup>		
Absorption coefficient	0.092 mm <sup>-1</sup>		
F(000)	536		
Crystal size	0.30 x 0.20 x 0.04 mm <sup>3</sup>		
Theta range for data collection	2.22 to 26.00°.		
Index ranges	-14≤h≤14, -17≤k≤19, -7≤l≤8		
Reflections collected	5323		
Independent reflections	2469 [R(int) = 0.0217]		
Completeness to theta = 26.00°	98.1 %		
Absorption correction	Multi-scan		
Max. and min. transmission	0.9963 and 0.9730		
Refinement method	Full-matrix least-squares on F <sup>2</sup>		
Data / restraints / parameters	2469 / 0 / 162		
Goodness-of-fit on F <sup>2</sup>	1.035		
Final R indices [I>2sigma(I)]	R1 = 0.0441, wR2 = 0.1017		
R indices (all data)	R1 = 0.0717, wR2 = 0.1172		
Extinction coefficient	0.0067(16)		
Largest diff. peak and hole	0.280 and -0.292 e.Å <sup>-3</sup>		

**Table B6.2.** Atomic coordinates ( x 10<sup>4</sup>) and equivalent isotropic displacement parameters (Å<sup>2</sup> x 10<sup>3</sup>) for ap21. U(eq) is defined as one third of the trace of the orthogonalized U<sup>ij</sup> tensor.

	x	y	z	U(eq)
N(1)	2236(1)	2666(1)	-395(2)	31(1)

N(2)	3740(1)	1484(1)	1424(2)	32(1)
O(1)	4991(1)	2446(1)	3320(2)	40(1)
C(1)	1466(2)	3248(1)	-1339(3)	37(1)
C(2)	1629(2)	4095(1)	-961(3)	41(1)
C(3)	2634(2)	4360(1)	443(3)	40(1)
C(4)	3459(2)	3772(1)	1441(3)	34(1)
C(5)	3216(2)	2937(1)	973(2)	28(1)
C(6)	4077(2)	2281(1)	2021(3)	30(1)
C(7)	4395(2)	790(1)	2236(3)	39(1)
N(3)	4120(2)	33(1)	1742(3)	44(1)
O(2)	3045(1)	12(1)	183(2)	51(1)
C(8)	2657(2)	-851(1)	-134(3)	57(1)
C(9)	2071(1)	-1148(1)	1379(2)	38(1)
C(10)	2770(1)	-1522(1)	3069(2)	35(1)
C(11)	2259(1)	-1785(1)	4474(2)	43(1)
C(12)	1050(1)	-1674(1)	4190(2)	56(1)
C(13)	352(1)	-1300(1)	2499(3)	64(1)
C(14)	863(1)	-1037(1)	1094(2)	56(1)

**Table B6.3** Bond lengths [ $\text{\AA}$ ] and angles [ $^\circ$ ] for ap21.

N(1)-C(1)	1.331(2)	N(3)-O(2)	1.412(2)
N(1)-C(5)	1.340(2)	O(2)-C(8)	1.448(2)
N(2)-C(6)	1.364(2)	C(8)-C(9)	1.519(3)
N(2)-C(7)	1.374(2)	C(8)-H(8A)	0.9900
N(2)-H(2B)	0.8800	C(8)-H(8B)	0.9900
O(1)-C(6)	1.220(2)	C(9)-C(14)	1.3792
C(1)-C(2)	1.381(3)	C(9)-C(10)	1.3793
C(1)-H(1A)	0.9500	C(10)-C(11)	1.3792
C(2)-C(3)	1.368(3)	C(10)-H(10A)	0.9500
C(2)-H(2A)	0.9500	C(11)-C(12)	1.3793
C(3)-C(4)	1.384(3)	C(11)-H(11A)	0.9500
C(3)-H(3A)	0.9500	C(12)-C(13)	1.3793
C(4)-C(5)	1.385(2)	C(12)-H(12A)	0.9500
C(4)-H(4A)	0.9500	C(13)-C(14)	1.3792

C(5)-C(6)	1.493(2)	C(13)-H(13A)	0.9500
C(7)-N(3)	1.275(2)	C(14)-H(14A)	0.9500
C(7)-H(7A)	0.9500		
C(1)-N(1)-C(5)	116.69(16)	N(2)-C(7)-H(7A)	117.1
C(6)-N(2)-C(7)	123.14(16)	C(7)-N(3)-O(2)	109.59(16)
C(6)-N(2)-H(2B)	118.4	N(3)-O(2)-C(8)	108.16(15)
C(7)-N(2)-H(2B)	118.4	O(2)-C(8)-C(9)	111.89(16)
N(1)-C(1)-C(2)	123.46(18)	O(2)-C(8)-H(8A)	109.2
N(1)-C(1)-H(1A)	118.3	C(9)-C(8)-H(8A)	109.2
C(2)-C(1)-H(1A)	118.3	O(2)-C(8)-H(8B)	109.2
C(3)-C(2)-C(1)	119.10(18)	C(9)-C(8)-H(8B)	109.2
C(3)-C(2)-H(2A)	120.5	C(14)-C(9)-C(8)	120.92(13)
C(1)-C(2)-H(2A)	120.5	C(10)-C(9)-C(8)	119.07(13)
C(2)-C(3)-C(4)	118.96(18)	C(11)-C(10)-C(9)	120.0
C(2)-C(3)-H(3A)	120.5	C(11)-C(10)-H(10A)	120.0
C(4)-C(3)-H(3A)	120.5	C(9)-C(10)-H(10A)	120.0
C(3)-C(4)-C(5)	117.88(18)	C(10)-C(11)-C(12)	120.0
C(3)-C(4)-H(4A)	121.1	C(10)-C(11)-H(11A)	120.0
C(5)-C(4)-H(4A)	121.1	C(12)-C(11)-H(11A)	120.0
N(1)-C(5)-C(4)	123.91(17)	C(11)-C(12)-C(13)	120.0
N(1)-C(5)-C(6)	116.37(15)	C(11)-C(12)-H(12A)	120.0
C(4)-C(5)-C(6)	119.72(16)	C(13)-C(12)-H(12A)	120.0
O(1)-C(6)-N(2)	123.25(17)	C(14)-C(13)-C(12)	120.0
O(1)-C(6)-C(5)	122.61(16)	C(14)-C(13)-H(13A)	120.0
N(2)-C(6)-C(5)	114.13(15)	C(12)-C(13)-H(13A)	120.0
N(3)-C(7)-N(2)	125.74(19)	C(13)-C(14)-C(9)	120.0
N(3)-C(7)-H(7A)	117.1	C(13)-C(14)-H(14A)	120.0
H(8A)-C(8)-H(8B)	107.9	C(9)-C(14)-H(14A)	120.0
C(14)-C(9)-C(10)	120.0		

**Table B6.4.** Anisotropic displacement parameters ( $\text{\AA}^2 \times 10^3$ ) for ap21. The anisotropic displacement factor exponent takes the form:  $-2\pi^2 [ h^2 a^*{}^2 U^{11} + \dots + 2 h k a^* b^* U^{12} ]$

	U <sup>11</sup>	U <sup>22</sup>	U <sup>33</sup>	U <sup>23</sup>	U <sup>13</sup>	U <sup>12</sup>
N(1)	33(1)	29(1)	31(1)	1(1)	10(1)	-1(1)
N(2)	37(1)	27(1)	32(1)	3(1)	8(1)	2(1)
O(1)	34(1)	43(1)	40(1)	4(1)	4(1)	-3(1)
C(1)	38(1)	36(1)	35(1)	2(1)	7(1)	3(1)
C(2)	47(1)	35(1)	40(1)	8(1)	11(1)	8(1)
C(3)	57(1)	24(1)	44(1)	1(1)	20(1)	-1(1)
C(4)	42(1)	30(1)	33(1)	-1(1)	12(1)	-5(1)
C(5)	33(1)	28(1)	25(1)	2(1)	12(1)	-2(1)
C(6)	32(1)	32(1)	28(1)	2(1)	12(1)	-2(1)
C(7)	42(1)	32(1)	44(1)	6(1)	15(1)	7(1)
N(3)	54(1)	35(1)	45(1)	6(1)	15(1)	7(1)
O(2)	83(1)	29(1)	36(1)	5(1)	9(1)	-5(1)
C(8)	104(2)	31(1)	34(1)	-4(1)	16(1)	-8(1)
C(9)	56(1)	19(1)	35(1)	-7(1)	4(1)	0(1)
C(10)	40(1)	26(1)	39(1)	-2(1)	9(1)	1(1)
C(11)	54(1)	31(1)	45(1)	1(1)	15(1)	-3(1)
C(12)	57(1)	45(1)	74(2)	-11(1)	30(1)	-12(1)
C(13)	36(1)	50(2)	102(2)	-24(2)	13(1)	-5(1)
C(14)	57(1)	32(1)	59(2)	-11(1)	-15(1)	5(1)

**Table B6.5.** Hydrogen coordinates ( $\times 10^4$ ) and isotropic displacement parameters ( $\text{\AA}^2 \times 10^3$ ) for ap21.

	x	y	z	U(eq)
H(2B)	3071	1410	472	39
H(1A)	768	3072	-2324	45
H(2A)	1051	4487	-1666	50
H(3A)	2764	4940	728	49
H(4A)	4169	3937	2416	41
H(7A)	5117	884	3255	46

H(8A)	3355	-1211	-76	69
H(8B)	2080	-907	-1455	69
H(10A)	3602	-1598	3265	42
H(11A)	2740	-2042	5639	52
H(12A)	699	-1855	5158	68
H(13A)	-480	-1224	2303	77
H(14A)	382	-780	-70	68

---

**Table B6.6.** Torsion angles [°] for ap21.

C(5)-N(1)-C(1)-C(2)	-0.6(3)	C(6)-N(2)-C(7)-N(3)	179.61(18)
N(1)-C(1)-C(2)-C(3)	0.5(3)	N(2)-C(7)-N(3)-O(2)	1.6(3)
C(1)-C(2)-C(3)-C(4)	0.1(3)	C(7)-N(3)-O(2)-C(8)	-171.00(17)
C(2)-C(3)-C(4)-C(5)	-0.5(3)	N(3)-O(2)-C(8)-C(9)	77.7(2)
C(1)-N(1)-C(5)-C(4)	0.1(2)	O(2)-C(8)-C(9)-C(14)	87.83(19)
C(1)-N(1)-C(5)-C(6)	-179.85(15)	O(2)-C(8)-C(9)-C(10)	-91.17(19)
C(3)-C(4)-C(5)-N(1)	0.5(3)	C(14)-C(9)-C(10)-C(11)	0.0
C(3)-C(4)-C(5)-C(6)	-179.60(15)	C(8)-C(9)-C(10)-C(11)	179.01(13)
C(7)-N(2)-C(6)-O(1)	0.4(3)	C(9)-C(10)-C(11)-C(12)	0.0
C(7)-N(2)-C(6)-C(5)	-178.47(15)	C(10)-C(11)-C(12)-C(13)	0.0
N(1)-C(5)-C(6)-O(1)	-178.68(15)	C(11)-C(12)-C(13)-C(14)	0.0
C(4)-C(5)-C(6)-O(1)	1.4(2)	C(12)-C(13)-C(14)-C(9)	0.0
N(1)-C(5)-C(6)-N(2)	0.2(2)	C(10)-C(9)-C(14)-C(13)	0.0
C(4)-C(5)-C(6)-N(2)	-179.72(15)	C(8)-C(9)-C(14)-C(13)	-178.99(14)

## 7) 4.7E

A crystal of the compound (colorless, needle-shaped, size 0.35 x 0.06 x 0.04 mm) was mounted on a glass fiber with grease and cooled to -93 °C in a stream of nitrogen gas controlled with Cryostream Controller 700. Data collection was performed on a Bruker SMART APEX II X-ray diffractometer with graphite-monochromated Mo K<sub>α</sub> radiation ( $\lambda$  = 0.71073 Å), operating at 50 kV and 30 mA over 2θ ranges of 6.40 ~ 51.98°. No significant decay was observed during the data collection.

Data were processed on a PC using the Bruker AXS Crystal Structure Analysis Package:<sup>[1]</sup> Data collection: APEX2 (Bruker, 2006); cell refinement: SAINT (Bruker, 2005); data reduction: SAINT (Bruker, 2005); structure solution: XPREP (Bruker, 2005) and SHELXTL (Bruker, 2000); structure refinement: SHELXTL; molecular graphics: SHELXTL; publication materials: SHELXTL. Neutral atom scattering factors were taken from Cromer and Waber.<sup>[2]</sup> The crystal is monoclinic space group  $P2_1/c$ , based on the systematic absences,  $E$  statistics and successful refinement of the structure. The structure was solved by direct methods. Full-matrix least-square refinements minimizing the function  $\sum w (F_o^2 - F_c^2)^2$  were applied to the compound. All non-hydrogen atoms were refined anisotropically. All of the H atoms were placed in geometrically calculated positions, with C-H = 0.95 (aromatic), 0.99(CH<sub>2</sub>), 0.98(CH<sub>3</sub>) and 0.88(N-H) Å, and refined as riding atoms, with Uiso(H) = 1.2 Ueq(C or N) or 1.5Ueq (CH<sub>3</sub>).

Convergence to final  $R_1 = 0.0481$  and  $wR_2 = 0.1157$  for 1518 ( $I > 2\sigma(I)$ ) independent reflections, and  $R_1 = 0.0649$  and  $wR_2 = 0.1274$  for all 2002 ( $R(\text{int}) = 0.0250$ ) independent reflections, with 128 parameters and 0 restraints, were achieved.<sup>[3]</sup> The largest residual peak and hole to be 0.198 and -0.188 e/Å<sup>3</sup>, respectively. Crystallographic data, atomic coordinates and equivalent isotropic displacement parameters, bond lengths and angles, anisotropic displacement parameters, hydrogen coordinates and isotropic displacement parameters, torsion angles and hydrogen bonding information are given in Table B7.1 to B7.7. The molecular structure and the cell packing are shown in Figures B7.1 and B7.2.

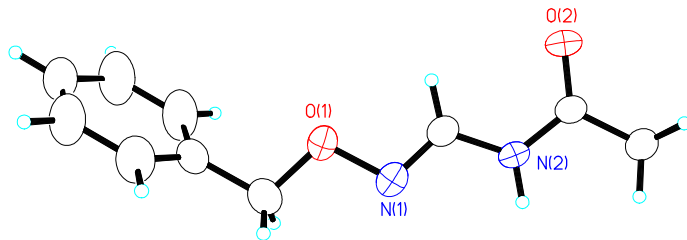


**Figure B7.1.** Molecular Structure (displacement ellipsoids for non-H atoms are shown at the 50% probability level and H atoms are represented by circles of arbitrary size).

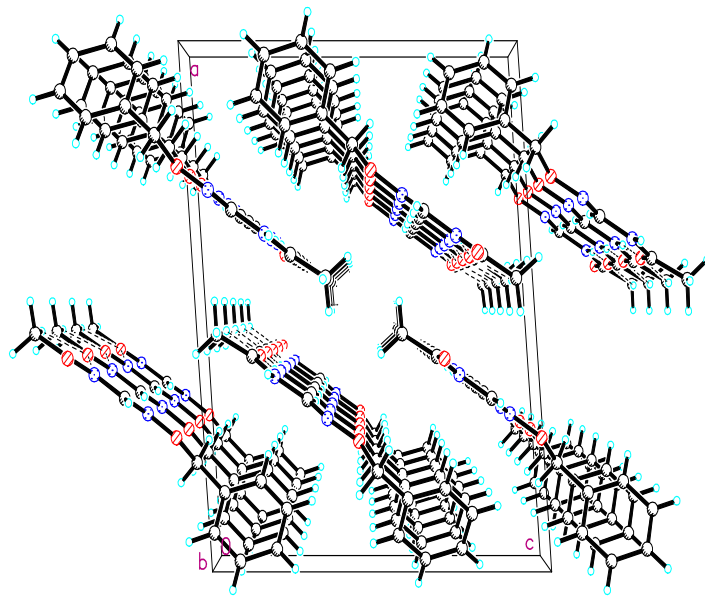


**Figure B7.2** Unit cell packing

[1] Bruker AXS Crystal Structure Analysis Package:

Bruker (2000). SHELXTL. Version 6.14. Bruker AXS Inc., Madison, Wisconsin, USA.

Bruker (2005). XPREP. Version 2005/2. Bruker AXS Inc., Madison, Wisconsin, USA.

Bruker (2005). SAINT. Version 7.23A. Bruker AXS Inc., Madison, Wisconsin, USA.

Bruker (2006). APEX2. Version 2.0-2. Bruker AXS Inc., Madison, Wisconsin, USA.

[2] Cromer, D. T.; Waber, J. T. *International Tables for X-ray Crystallography*; Kynoch Press:

Birmingham, UK, 1974; Vol. 4, Table 2.2 A.

$$[3] \quad R_1 = \sum | |F_o| - |F_c| | / \sum |F_o|$$

$$wR_2 = \{ \sum [w(F_o^2 - F_c^2)^2] / \sum [w(F_o^2)^2] \}^{1/2}$$

$$(w = 1 / [\sigma^2(F_o^2) + (0.0457P)^2 + 0.1746P], \text{ where } P = [\text{Max } (F_o^2, 0) + 2F_c^2] / 3)$$

**Table B7.1.** Crystal data and structure refinement for ap27

Identification code	ap27
Empirical formula	C10 H12 N2 O2
Formula weight	192.22
Temperature	180(2) K
	186

Wavelength	0.71073 Å		
Crystal system	Monoclinic		
Space group	P2(1)/c		
Unit cell dimensions	$a = 16.0446(14)$ Å	$\alpha = 90^\circ$ .	
	$b = 4.7640(4)$ Å	$\beta = 94.887(7)^\circ$ .	
	$c = 13.4292(15)$ Å	$\gamma = 90^\circ$ .	
Volume	$1022.75(17)$ Å <sup>3</sup>		
Z	4		
Density (calculated)	1.248 Mg/m <sup>3</sup>		
Absorption coefficient	0.089 mm <sup>-1</sup>		
F(000)	408		
Crystal size	0.35 x 0.06 x 0.04 mm <sup>3</sup>		
Theta range for data collection	3.20 to 25.99°.		
Index ranges	-16<=h<=19, -5<=k<=5, -16<=l<=11		
Reflections collected	5263		
Independent reflections	2002 [R(int) = 0.0250]		
Completeness to theta = 25.99°	99.5 %		
Absorption correction	Multi-scan		
Max. and min. transmission	0.9965 and 0.9696		
Refinement method	Full-matrix least-squares on F <sup>2</sup>		
Data / restraints / parameters	2002 / 0 / 128		
Goodness-of-fit on F <sup>2</sup>	1.035		
Final R indices [I>2sigma(I)]	R1 = 0.0481, wR2 = 0.1157		
R indices (all data)	R1 = 0.0649, wR2 = 0.1274		
Largest diff. peak and hole	0.198 and -0.188 e.Å <sup>-3</sup>		

**Table B7.2.** Atomic coordinates ( $\times 10^4$ ) and equivalent isotropic displacement parameters ( $\text{\AA}^2 \times 10^3$ ) for ap27. U(eq) is defined as one third of the trace of the orthogonalized  $U^{ij}$  tensor.

	x	y	z	U(eq)
O(1)	2700(1)	812(3)	9612(1)	47(1)
O(2)	4114(1)	5230(3)	7024(1)	53(1)
		187		

N(1)	3102(1)	-416(3)	8817(1)	44(1)
N(2)	3804(1)	812(3)	7470(1)	38(1)
C(1)	1726(1)	61(4)	10812(1)	46(1)
C(2)	1062(2)	1798(6)	10512(2)	70(1)
C(3)	612(2)	3125(6)	11204(2)	79(1)
C(4)	813(2)	2741(5)	12206(2)	60(1)
C(5)	1456(1)	1033(5)	12511(2)	62(1)
C(6)	1912(1)	-302(5)	11821(2)	56(1)
C(7)	2226(2)	-1329(5)	10059(2)	62(1)
C(8)	3399(1)	1546(4)	8298(1)	38(1)
C(9)	4136(1)	2704(3)	6858(1)	37(1)
C(10)	4522(1)	1536(4)	5970(1)	46(1)

---

**Table B7.3.** Bond lengths [ $\text{\AA}$ ] and angles [ $^\circ$ ] for ap27.

O(1)-N(1)	1.4204(18)	C(1)-C(7)	1.497(3)	C(6)-H(6A)	0.9500
O(1)-C(7)	1.434(2)	C(2)-C(3)	1.378(3)	C(7)-H(7A)	0.9900
O(2)-C(9)	1.225(2)	C(2)-H(2A)	0.9500	C(7)-H(7B)	0.9900
N(1)-C(8)	1.281(2)	C(3)-C(4)	1.369(3)	C(8)-H(8A)	0.9500
N(2)-C(9)	1.358(2)	C(3)-H(3A)	0.9500	C(9)-C(10)	1.497(2)
N(2)-C(8)	1.380(2)	C(4)-C(5)	1.350(3)	C(10)-H(10A)	0.9800
N(2)-H(2B)	0.8800	C(4)-H(4A)	0.9500	C(10)-H(10B)	0.9800
C(1)-C(6)	1.374(3)	C(5)-C(6)	1.384(3)	C(10)-H(10C)	0.9800
C(1)-C(2)	1.382(3)	C(5)-H(5A)	0.9500		
N(1)-O(1)-C(7)	108.24(13)	C(1)-C(6)-H(6A)		119.3	
C(8)-N(1)-O(1)	108.81(14)	C(5)-C(6)-H(6A)		119.3	
C(9)-N(2)-C(8)	123.72(14)	O(1)-C(7)-C(1)		107.54(16)	
C(9)-N(2)-H(2B)	118.1	O(1)-C(7)-H(7A)		110.2	
C(8)-N(2)-H(2B)	118.1	C(1)-C(7)-H(7A)		110.2	
C(6)-C(1)-C(2)	117.39(19)	O(1)-C(7)-H(7B)		110.2	
C(6)-C(1)-C(7)	121.8(2)	C(1)-C(7)-H(7B)		110.2	
C(2)-C(1)-C(7)	120.79(19)	H(7A)-C(7)-H(7B)		108.5	
C(3)-C(2)-C(1)	120.9(2)	N(1)-C(8)-N(2)		118.42(15)	

C(3)-C(2)-H(2A)	119.5	N(1)-C(8)-H(8A)	120.8
C(1)-C(2)-H(2A)	119.5	N(2)-C(8)-H(8A)	120.8
C(4)-C(3)-C(2)	120.6(2)	O(2)-C(9)-N(2)	121.59(15)
C(4)-C(3)-H(3A)	119.7	O(2)-C(9)-C(10)	121.99(16)
C(2)-C(3)-H(3A)	119.7	N(2)-C(9)-C(10)	116.42(14)
C(5)-C(4)-C(3)	119.2(2)	C(9)-C(10)-H(10A)	109.5
C(5)-C(4)-H(4A)	120.4	C(9)-C(10)-H(10B)	109.5
C(3)-C(4)-H(4A)	120.4	H(10A)-C(10)-H(10B)	109.5
C(4)-C(5)-C(6)	120.5(2)	C(9)-C(10)-H(10C)	109.5
C(4)-C(5)-H(5A)	119.7	H(10A)-C(10)-H(10C)	109.5
C(6)-C(5)-H(5A)	119.7	H(10B)-C(10)-H(10C)	109.5
C(1)-C(6)-C(5)	121.3(2)		

**Table B7.4.** Anisotropic displacement parameters ( $\text{\AA}^2 \times 10^3$ ) for ap27. The anisotropic displacement factor exponent takes the form:  $-2\pi^2 [ h^2 a^*{}^2 U^{11} + \dots + 2 h k a^* b^* U^{12} ]$

	U <sup>11</sup>	U <sup>22</sup>	U <sup>33</sup>	U <sup>23</sup>	U <sup>13</sup>	U <sup>12</sup>
O(1)	57(1)	43(1)	45(1)	-8(1)	23(1)	-4(1)
O(2)	68(1)	25(1)	68(1)	-7(1)	25(1)	-1(1)
N(1)	49(1)	42(1)	43(1)	-6(1)	15(1)	2(1)
N(2)	48(1)	25(1)	43(1)	-5(1)	15(1)	1(1)
C(1)	48(1)	42(1)	48(1)	2(1)	16(1)	-8(1)
C(2)	77(2)	92(2)	44(1)	19(1)	14(1)	19(1)
C(3)	75(2)	98(2)	69(2)	30(1)	28(1)	39(2)
C(4)	60(1)	65(1)	59(1)	1(1)	26(1)	3(1)
C(5)	55(1)	87(2)	43(1)	1(1)	8(1)	-2(1)
C(6)	44(1)	71(1)	54(1)	7(1)	6(1)	7(1)
C(7)	80(2)	46(1)	66(1)	-1(1)	34(1)	-12(1)
C(8)	41(1)	33(1)	42(1)	-5(1)	10(1)	2(1)
C(9)	41(1)	28(1)	44(1)	-4(1)	10(1)	1(1)
C(10)	59(1)	37(1)	44(1)	-2(1)	18(1)	3(1)

**Table B7.5.** Hydrogen coordinates ( $\times 10^4$ ) and isotropic displacement parameters ( $\text{\AA}^2 \times 10^3$ ) for ap27.

	x	y	z	U(eq)
H(2B)	3851	-983	7330	46
H(2A)	914	2083	9819	85
H(3A)	159	4317	10984	95
H(4A)	503	3666	12681	72
H(5A)	1596	745	13205	74
H(6A)	2364	-1492	12050	68
H(7A)	2605	-2751	10389	75
H(7B)	1849	-2277	9542	75
H(8A)	3341	3459	8479	46
H(10A)	5085	2317	5944	69
H(10B)	4177	2038	5359	69
H(10C)	4558	-512	6027	69

**Table B7.6.** Torsion angles [°] for ap27.

C(7)-O(1)-N(1)-C(8)	168.19(17)	C(4)-C(5)-C(6)-C(1)	-0.1(4)
C(6)-C(1)-C(2)-C(3)	0.5(4)	N(1)-O(1)-C(7)-C(1)	-173.37(16)
C(7)-C(1)-C(2)-C(3)	-178.7(2)	C(6)-C(1)-C(7)-O(1)	-109.1(2)
C(1)-C(2)-C(3)-C(4)	-0.2(4)	C(2)-C(1)-C(7)-O(1)	70.1(3)
C(2)-C(3)-C(4)-C(5)	-0.3(4)	O(1)-N(1)-C(8)-N(2)	-178.77(14)
C(3)-C(4)-C(5)-C(6)	0.5(4)	C(9)-N(2)-C(8)-N(1)	179.30(17)
C(2)-C(1)-C(6)-C(5)	-0.3(3)	C(8)-N(2)-C(9)-O(2)	2.0(3)



**Table B7.7.** Hydrogen bonds for ap27 [Å and °].

D-H...A	d(D-H)	d(H...A)	d(D...A)	∠(DHA)
N(2)-H(2B)...O(2)#1	0.88	1.91	2.7803(18)	172.0

Symmetry transformations used to generate equivalent atoms:  
#1 x,y-1,z

### 8) 4.5E-room temperature-monoclinic

A crystal of the compound (colorless, block-shaped, size 0.25 x 0.25 x 0.20 mm) was mounted on a glass fiber with epoxy. Data collection was performed at room temperature on a Bruker SMART APEX II X-ray diffractometer with graphite-monochromated Mo K $\alpha$  radiation ( $\lambda = 0.71073 \text{ \AA}$ ), operating at 50 kV and 30 mA over 2 $\theta$  ranges of 4.58 ~ 51.98°. No significant decay was observed during the data collection.

Data were processed on a PC using the Bruker AXS Crystal Structure Analysis Package:<sup>[1]</sup> Data collection: APEX2 (Bruker, 2006); cell refinement: SAINT (Bruker, 2005); data reduction: SAINT (Bruker, 2005); structure solution: XPREP (Bruker, 2005) and SHELXTL (Bruker, 2000); structure refinement: SHELXTL; molecular graphics: SHELXTL; publication materials: SHELXTL. Neutral atom scattering factors were taken from Cromer and Waber.<sup>[2]</sup> The crystal is monoclinic space group  $P2_1/c$ , based on the systematic absences,  $E$  statistics and successful refinement of the structure. The structure

was solved by direct methods. Full-matrix least-square refinements minimizing the function  $\sum w (F_o^2 - F_c^2)^2$  were applied to the compound. All non-hydrogen atoms were refined anisotropically. All of the H atoms were placed in geometrically calculated positions, with C-H = 0.93 (aromatic), 0.96(CH<sub>3</sub>), and 0.86(N-H) Å, and refined as riding atoms, with Uiso(H) = 1.2 Ueq(C or N).

Convergence to final  $R_1 = 0.0431$  and  $wR_2 = 0.1040$  for 1347 ( $I > 2\sigma(I)$ ) independent reflections, and  $R_1 = 0.0549$  and  $wR_2 = 0.1124$  for all 1715 ( $R(\text{int}) = 0.0183$ ) independent reflections, with 119 parameters and 0 restraints, were achieved.<sup>[3]</sup> The largest residual peak and hole to be 0.161 and  $-0.184 \text{ e}/\text{\AA}^3$ , respectively. Crystallographic data, atomic coordinates and equivalent isotropic displacement parameters, bond lengths and angles, anisotropic displacement parameters, hydrogen coordinates and isotropic displacement parameters, and torsion angles are given in Table B8.1 to B8.6. The molecular structure and the cell packing are shown in Figures B8.1 and B8.2.

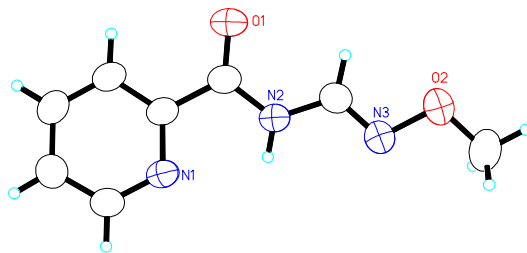


**Figure B8.1.** Molecular Structure (displacement ellipsoids for non-H atoms are shown at the 50% probability level and H atoms are represented by circles of arbitrary size).

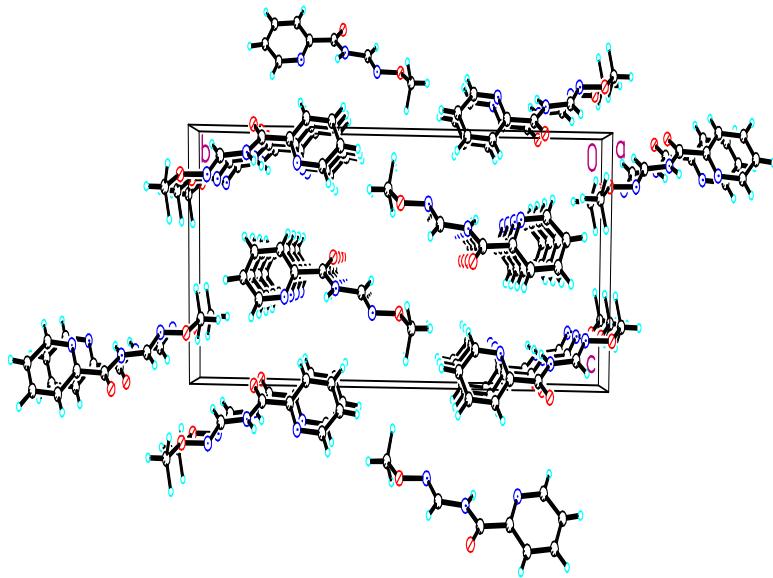


**Figure B8.2** Unit cell packing

[1] Bruker AXS Crystal Structure Analysis Package:

Bruker (2000). SHELXTL. Version 6.14. Bruker AXS Inc., Madison, Wisconsin, USA.

Bruker (2005). XPREP. Version 2005/2. Bruker AXS Inc., Madison, Wisconsin, USA.

Bruker (2005). SAINT. Version 7.23A. Bruker AXS Inc., Madison, Wisconsin, USA.

Bruker (2006). APEX2. Version 2.0-2. Bruker AXS Inc., Madison, Wisconsin, USA.

[2] Cromer, D. T.; Waber, J. T. *International Tables for X-ray Crystallography*; Kynoch Press: Birmingham, UK, 1974; Vol. 4, Table 2.2 A.

$$[3] \quad R_1 = \sum |F_O| - |F_C| / \sum |F_O|$$

$$wR_2 = \{ \sum [w(F_O^2 - F_C^2)^2] / \sum [w(F_O^2)^2] \}^{1/2}$$

$$(w = 1 / [\sigma^2(F_O^2) + (0.0457P)^2 + 0.1746P], \text{ where } P = [\text{Max}(F_O^2, 0) + 2F_C^2] / 3)$$

**Table B8.1.** Crystal data and structure refinement for ap25

Identification code	ap25
Empirical formula	C8 H9 N3 O2
Formula weight	179.18
Temperature	296(2) K

Wavelength	0.71073 Å
Crystal system	Monoclinic
Space group	P2(1)/c
Unit cell dimensions	a = 5.2034(12) Å b = 22.755(5) Å c = 7.5244(18) Å
	α= 90°. β= 99.349(3)°. γ = 90°.
Volume	879.1(4) Å <sup>3</sup>
Z	4
Density (calculated)	1.354 Mg/m <sup>3</sup>
Absorption coefficient	0.101 mm <sup>-1</sup>
F(000)	376
Crystal size	0.25 x 0.20 x 0.15 mm <sup>3</sup>
Theta range for data collection	2.89 to 25.99°.
Index ranges	-6<=h<=6, -27<=k<=27, -5<=l<=9
Reflections collected	4038
Independent reflections	1715 [R(int) = 0.0183]
Completeness to theta = 25.99°	98.8 %
Absorption correction	Multi-scan
Max. and min. transmission	0.9850 and 0.9753
Refinement method	Full-matrix least-squares on F <sup>2</sup>
Data / restraints / parameters	1715 / 0 / 119
Goodness-of-fit on F <sup>2</sup>	1.068
Final R indices [I>2sigma(I)]	R1 = 0.0431, wR2 = 0.1040
R indices (all data)	R1 = 0.0549, wR2 = 0.1124
Largest diff. peak and hole	0.161 and -0.184 e.Å <sup>-3</sup>

**Table B8.2.** Atomic coordinates ( $\times 10^4$ ) and equivalent isotropic displacement parameters ( $\text{Å}^2 \times 10^3$ ) for ap25. U(eq) is defined as one third of the trace of the orthogonalized  $U^{ij}$  tensor.

	x	y	z	U(eq)
O(1)	1653(2)	8435(1)	-29(2)	76(1)
O(2)	7620(3)	9988(1)	2020(2)	89(1)
		194		

N(1)	6335(2)	7354(1)	1492(2)	51(1)
N(2)	5913(3)	8519(1)	1137(2)	55(1)
N(3)	8001(3)	9376(1)	2013(2)	64(1)
C(1)	6624(3)	6774(1)	1600(2)	58(1)
C(2)	4779(3)	6382(1)	795(3)	62(1)
C(3)	2506(3)	6597(1)	-176(2)	61(1)
C(4)	2138(3)	7196(1)	-280(2)	52(1)
C(5)	4094(3)	7555(1)	566(2)	43(1)
C(6)	3740(3)	8206(1)	510(2)	50(1)
C(7)	5964(3)	9121(1)	1277(2)	60(1)
C(8)	10048(4)	10269(1)	2531(3)	81(1)

---

**Table B8.3.** Bond lengths [ $\text{\AA}$ ] and angles [ $^\circ$ ] for ap25.

O(1)-C(6)	1.2127(18)	N(3)-C(7)	1.254(2)	C(4)-H(4A)	0.9300
O(2)-N(3)	1.4088(18)	C(1)-C(2)	1.377(2)	C(5)-C(6)	1.493(2)
O(2)-C(8)	1.412(2)	C(1)-H(1A)	0.9300	C(7)-H(7A)	0.9300
N(1)-C(1)	1.330(2)	C(2)-C(3)	1.375(2)	C(8)-H(8A)	0.9600
N(1)-C(5)	1.3383(18)	C(2)-H(2A)	0.9300	C(8)-H(8B)	0.9600
N(2)-C(6)	1.354(2)	C(3)-C(4)	1.376(2)	C(8)-H(8C)	0.9600
N(2)-C(7)	1.375(2)	C(3)-H(3A)	0.9300		
N(2)-H(2B)	0.8600	C(4)-C(5)	1.378(2)		
N(3)-O(2)-C(8)		109.22(14)	C(5)-C(4)-H(4A)	120.8	
C(1)-N(1)-C(5)		116.79(13)	N(1)-C(5)-C(4)	123.63(15)	
C(6)-N(2)-C(7)		123.72(14)	N(1)-C(5)-C(6)	116.51(13)	
C(6)-N(2)-H(2B)		118.1	C(4)-C(5)-C(6)	119.84(13)	
C(7)-N(2)-H(2B)		118.1	O(1)-C(6)-N(2)	122.90(15)	
C(7)-N(3)-O(2)		110.43(14)	O(1)-C(6)-C(5)	122.30(14)	
N(1)-C(1)-C(2)		123.58(15)	N(2)-C(6)-C(5)	114.79(13)	
N(1)-C(1)-H(1A)		118.2	N(3)-C(7)-N(2)	119.87(15)	
C(2)-C(1)-H(1A)		118.2	N(3)-C(7)-H(7A)	120.1	
C(3)-C(2)-C(1)		118.69(16)	N(2)-C(7)-H(7A)	120.1	
C(3)-C(2)-H(2A)		120.7	O(2)-C(8)-H(8A)	109.5	

C(1)-C(2)-H(2A)	120.7	O(2)-C(8)-H(8B)	109.5
C(2)-C(3)-C(4)	118.89(15)	H(8A)-C(8)-H(8B)	109.5
C(2)-C(3)-H(3A)	120.6	O(2)-C(8)-H(8C)	109.5
C(4)-C(3)-H(3A)	120.6	H(8A)-C(8)-H(8C)	109.5
C(3)-C(4)-C(5)	118.40(15)	H(8B)-C(8)-H(8C)	109.5
C(3)-C(4)-H(4A)	120.8		

**Table B8.4.** Anisotropic displacement parameters ( $\text{\AA}^2 \times 10^3$ ) for ap25. The anisotropic displacement factor exponent takes the form:  $-2\pi^2 [ h^2 a^*{}^2 U^{11} + \dots + 2 h k a^* b^* U^{12} ]$

	U <sup>11</sup>	U <sup>22</sup>	U <sup>33</sup>	U <sup>23</sup>	U <sup>13</sup>	U <sup>12</sup>
O(1)	48(1)	61(1)	110(1)	-2(1)	-17(1)	11(1)
O(2)	76(1)	42(1)	138(1)	-7(1)	-16(1)	1(1)
N(1)	40(1)	51(1)	57(1)	-2(1)	-5(1)	3(1)
N(2)	45(1)	45(1)	68(1)	-3(1)	-8(1)	4(1)
N(3)	62(1)	43(1)	80(1)	-3(1)	-8(1)	2(1)
C(1)	46(1)	54(1)	70(1)	3(1)	-5(1)	5(1)
C(2)	59(1)	48(1)	77(1)	0(1)	2(1)	0(1)
C(3)	52(1)	57(1)	68(1)	-4(1)	-4(1)	-11(1)
C(4)	41(1)	59(1)	53(1)	1(1)	-4(1)	-2(1)
C(5)	37(1)	51(1)	41(1)	0(1)	2(1)	1(1)
C(6)	43(1)	53(1)	51(1)	-1(1)	-2(1)	4(1)
C(7)	54(1)	49(1)	72(1)	0(1)	-7(1)	6(1)
C(8)	88(2)	56(1)	95(2)	-4(1)	-3(1)	-17(1)

**Table B8.5.** Hydrogen coordinates ( $\times 10^4$ ) and isotropic displacement parameters ( $\text{\AA}^2 \times 10^3$ ) for ap25.

	x	y	z	U(eq)
H(2B)	7342	8330	1467	66
H(1A)	8156	6625 196	2254	70

H(2A)	5064	5979	906	75
H(3A)	1240	6343	-752	73
H(4A)	606	7354	-906	63
H(7A)	4492	9340	827	72
H(8A)	9799	10688	2521	122
H(8B)	11190	10167	1698	122
H(8C)	10804	10145	3721	122

---

**Table B8.6.** Torsion angles [°] for ap25.

C(8)-O(2)-N(3)-C(7)	-168.83(17)	C(7)-N(2)-C(6)-O(1)	2.0(3)
C(5)-N(1)-C(1)-C(2)	1.0(3)	C(7)-N(2)-C(6)-C(5)	-176.87(15)
N(1)-C(1)-C(2)-C(3)	0.0(3)	N(1)-C(5)-C(6)-O(1)	-167.79(16)
C(1)-C(2)-C(3)-C(4)	-1.2(3)	C(4)-C(5)-C(6)-O(1)	10.8(2)
C(2)-C(3)-C(4)-C(5)	1.3(3)	N(1)-C(5)-C(6)-N(2)	11.1(2)
C(1)-N(1)-C(5)-C(4)	-0.9(2)	C(4)-C(5)-C(6)-N(2)	-170.28(14)
C(1)-N(1)-C(5)-C(6)	177.70(15)	O(2)-N(3)-C(7)-N(2)	-179.66(15)
C(3)-C(4)-C(5)-N(1)	-0.3(2)	C(6)-N(2)-C(7)-N(3)	173.93(17)
C(3)-C(4)-C(5)-C(6)	-178.83(15)		

### 9) 4.5E-low temperature, non-merohedrally twinned triclinic

A crystal of the compound (colorless, block-shaped, size 0.25 x 0.25 x 0.20mm) was mounted on a glass fiber with grease and cooled to -93 °C in a stream of nitrogen gas controlled with Cryostream Controller 700. Data collection was performed on a Bruker SMART APEX II X-ray diffractometer with graphite-monochromated Mo K  $\alpha$  radiation ( $\lambda = 0.71073 \text{ \AA}$ ), operating at 50 kV and 30 mA over 2 ranges of  $3.60 \sim 52.00^\circ$ . No significant decay was observed during the data collection. The crystal is monoclinic at room temperature (see ap25), but undergoes a phase transformation when cooled to 180K to a non-merohedrally twinned triclinic with a  $180^\circ$  rotation about the reciprocal axis (0,0,1). This was determined with the program CELL\_NOW (Sheldrick, 2005). Integration of the raw intensity data for the two twin components was accomplished with SAINT as

controlled by the two-component orientation matrix generated by CELL\_NOW and the data were further corrected for absorption and decay effects with TWINABS. Solution of the structure was accomplished with rough intensities derived from the major twin component using HKL4 format and final refinement (including refinement of the twin ratio) was performed with the full reflection file using HKL5 format, which included contributions from both twin components. Merging of equivalent reflections other than Friedel pairs could not be performed before refinement, because of the overlap of twin components.

Data were processed on a PC using the Bruker AXS Crystal Structure Analysis Package:<sup>[1]</sup> data collection: APEX2 (Bruker, 2006); cell refinement: SAINT (Bruker, 2005); data reduction: SAINT (Bruker, 2005); structure solution: XPREP (Bruker, 2005) and SHELXTL (Bruker, 2000); structure refinement: SHELXTL; molecular graphics: SHELXTL; publication materials: SHELXTL. Neutral atom scattering factors were taken from Cromer and Waber.<sup>[2]</sup> The crystal is triclinic space group P-1, based on the systematic absences, E statistics and successful refinement of the structure. The structure was solved by direct methods. Full-matrix least-square refinements minimizing the function  $\sum w (F_o^2 - F_c^2)^2$  were applied to the compound. All non-hydrogen atoms were refined anisotropically. The positions for all hydrogen atoms were calculated and their contributions were included in the structure factor calculations.

Convergence to final  $R_1 = 0.0550$  and  $wR_2 = 0.1325$  for 5174 ( $I > 2\sigma(I)$ ) independent reflections, and  $R_1 = 0.0578$  and  $wR_2 = 0.1337$  for all 5467 independent reflections, with 238 parameters, were achieved.<sup>[3]</sup> The largest residual peak and hole to be 0.177 and –0.231 e/Å<sup>3</sup>, respectively. Crystallographic data, atomic coordinates and equivalent isotropic displacement parameters, bond lengths and angles, anisotropic displacement parameters, hydrogen coordinates and isotropic displacement parameters, and torsion angles are given in Table B9.1 to B9.6. The molecular structure and the cell packing are shown in Figures B9.1 and B9.2.

[1] Bruker AXS Crystal Structure Analysis Package:

Bruker (2000). SHELXTL. Version 6.14. Bruker AXS Inc., Madison, Wisconsin, USA.

Bruker (2005). XPREP. Version 2005/2. Bruker AXS Inc., Madison, Wisconsin, USA.

Bruker (2005). SAINT. Version 7.23A. Bruker AXS Inc., Madison, Wisconsin, USA.

- Bruker (2006). APEX2. Version 2.0-2. Bruker AXS Inc., Madison, Wisconsin, USA.
- Sheldrick (2005). *TWINABS* and *CELL\_NOW*. University of Göttingen, Germany.
- [2] Cromer, D. T.; Waber, J. T. *International Tables for X-ray Crystallography*; Kynoch Press: Birmingham, UK, 1974; Vol. 4, Table 2.2 A.
- [3]  $R_1 = \sum |F_o| - |F_c| / \sum |F_o|$   
 $wR_2 = \{ \sum [w(F_o^2 - F_c^2)^2] / \sum [w(F_o^2)^2] \}^{1/2}$   
 $(w = 1 / [\sigma^2(F_o^2) + (0.0226P)^2 + 0.6583P], \text{ where } P = [\text{Max}(F_o^2, 0) + 2F_c^2] / 3)$

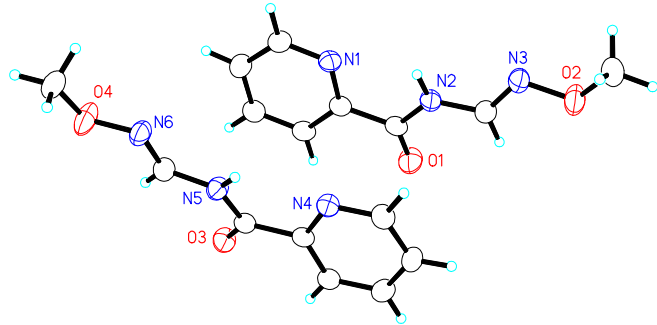


**Figure B9.1.** Molecular Structure (displacement ellipsoids for non-H atoms are shown at the 50% probability level and H atoms are represented by circles of arbitrary size)

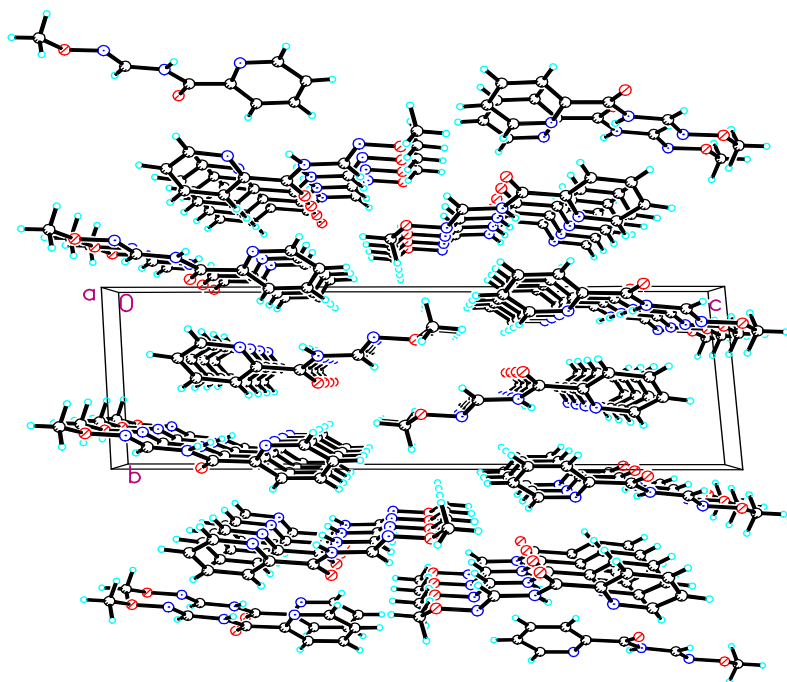


**Figure B9.2** Unit cell packing

**Table B9.1.** Crystal data and structure refinement for ap23e

Identification code	ap23e		
Empirical formula	C <sub>8</sub> H <sub>9</sub> N <sub>3</sub> O <sub>2</sub>		
Formula weight	179.18		
Temperature	180(2) K		
Wavelength	0.71073 Å		
Crystal system	Triclinic		
Space group	P-1		
Unit cell dimensions	a = 5.1780(2) Å	α= 85.6807(19)°.	
	b = 7.4431(3) Å	β= 87.5095(19)°.	
	c = 22.6665(9) Å	γ = 80.988(2)°.	
Volume	859.90(6) Å <sup>3</sup>		
Z	4		
Density (calculated)	1.384 Mg/m <sup>3</sup>		
Absorption coefficient	0.103 mm <sup>-1</sup>		

F(000)	376
Crystal size	0.25 x 0.25 x 0.20 mm <sup>3</sup>
Theta range for data collection	1.80 to 26.00°.
Index ranges	-6<=h<=6, -9<=k<=9, 0<=l<=27
Reflections collected	5467
Independent reflections	5467 [R(int) = 0.0000]
Completeness to theta = 26.00°	99.9 %
Absorption correction	Multi-scan
Max. and min. transmission	0.9797 and 0.9747
Refinement method	Full-matrix least-squares on F <sup>2</sup>
Data / restraints / parameters	5467 / 0 / 238
Goodness-of-fit on F <sup>2</sup>	1.250
Final R indices [I>2sigma(I)]	R1 = 0.0550, wR2 = 0.1325
R indices (all data)	R1 = 0.0578, wR2 = 0.1337
Largest diff. peak and hole	0.177 and -0.231 e.Å <sup>-3</sup>

**Table B9.2.** Atomic coordinates ( $\times 10^4$ ) and equivalent isotropic displacement parameters ( $\text{\AA}^2 \times 10^3$ ) for ap23e. U(eq) is defined as one third of the trace of the orthogonalized  $U_{ij}$  tensor.

	x	y	z	U(eq)
O(1)	6754(3)	5288(3)	3453(1)	45(1)
O(2)	12734(4)	3073(3)	5001(1)	49(1)
O(3)	6441(3)	9760(2)	1576(1)	36(1)
O(4)	12536(4)	7846(3)	2(1)	49(1)
N(1)	11271(4)	3438(3)	2363(1)	30(1)
N(2)	10949(4)	3887(3)	3519(1)	32(1)
N(3)	13049(4)	2953(3)	4382(1)	38(1)
N(4)	11256(3)	8470(3)	2651(1)	28(1)
N(5)	10802(4)	8756(3)	1472(1)	30(1)
N(6)	12945(4)	7943(3)	611(1)	35(1)
C(1)	11511(5)	3226(3)	1784(1)	34(1)
C(2)	9618(5)	3988(3)	1382(1)	35(1)
		201		

C(3)	7357(5)	5024(3)	1596(1)	35(1)
C(4)	7056(4)	5239(3)	2198(1)	31(1)
C(5)	9059(4)	4432(3)	2561(1)	27(1)
C(6)	8776(4)	4596(3)	3214(1)	30(1)
C(7)	11057(5)	3836(3)	4126(1)	34(1)
C(8)	15191(5)	2460(4)	5264(1)	45(1)
C(9)	11573(4)	8441(3)	3233(1)	33(1)
C(10)	9738(5)	9304(3)	3624(1)	34(1)
C(11)	7423(5)	10244(3)	3400(1)	35(1)
C(12)	7031(4)	10269(3)	2800(1)	29(1)
C(13)	8978(4)	9363(3)	2446(1)	26(1)
C(14)	8575(4)	9321(3)	1796(1)	29(1)
C(15)	10826(4)	8570(3)	873(1)	32(1)
C(16)	15028(5)	7478(4)	-294(1)	43(1)

---

**Table B9.3.** Bond lengths [ $\text{\AA}$ ] and angles [ $^\circ$ ] for ap23e.

O(1)-C(6)	1.216(3)	N(5)-C(15)	1.374(3)	C(8)-H(8C)	0.9800
O(2)-N(3)	1.414(3)	N(5)-H(5A)	0.8800	C(9)-C(10)	1.386(3)
O(2)-C(8)	1.423(3)	N(6)-C(15)	1.265(3)	C(9)-H(9A)	0.9500
O(3)-C(14)	1.219(3)	C(1)-C(2)	1.392(3)	C(10)-C(11)	1.387(3)
O(4)-N(6)	1.415(3)	C(1)-H(1A)	0.9500	C(10)-H(10A)	0.9500
O(4)-C(16)	1.425(3)	C(2)-C(3)	1.387(3)	C(11)-C(12)	1.381(3)
N(1)-C(1)	1.331(3)	C(2)-H(2A)	0.9500	C(11)-H(11A)	0.9500
N(1)-C(5)	1.342(3)	C(3)-C(4)	1.385(3)	C(12)-C(13)	1.383(3)
N(2)-C(6)	1.360(3)	C(3)-H(3A)	0.9500	C(12)-H(12A)	0.9500
N(2)-C(7)	1.376(3)	C(4)-C(5)	1.385(3)	C(13)-C(14)	1.501(3)
N(2)-H(2B)	0.8800	C(4)-H(4A)	0.9500	C(15)-H(15A)	0.9500
N(3)-C(7)	1.271(3)	C(5)-C(6)	1.494(3)	C(16)-H(16A)	0.9800
N(4)-C(9)	1.335(3)	C(7)-H(7A)	0.9500	C(16)-H(16B)	0.9800
N(4)-C(13)	1.343(3)	C(8)-H(8A)	0.9800	C(16)-H(16C)	0.9800
N(5)-C(14)	1.366(3)	C(8)-H(8B)	0.9800		

N(3)-O(2)-C(8)                    108.75(19)                    O(2)-C(8)-H(8A)                    109.5

N(6)-O(4)-C(16)	108.09(19)	O(2)-C(8)-H(8B)	109.5
C(1)-N(1)-C(5)	117.19(19)	H(8A)-C(8)-H(8B)	109.5
C(6)-N(2)-C(7)	123.6(2)	O(2)-C(8)-H(8C)	109.5
C(6)-N(2)-H(2B)	118.2	H(8A)-C(8)-H(8C)	109.5
C(7)-N(2)-H(2B)	118.2	H(8B)-C(8)-H(8C)	109.5
C(7)-N(3)-O(2)	109.96(19)	N(4)-C(9)-C(10)	124.0(2)
C(9)-N(4)-C(13)	116.60(19)	N(4)-C(9)-H(9A)	118.0
C(14)-N(5)-C(15)	123.13(19)	C(10)-C(9)-H(9A)	118.0
C(14)-N(5)-H(5A)	118.4	C(9)-C(10)-C(11)	118.2(2)
C(15)-N(5)-H(5A)	118.4	C(9)-C(10)-H(10A)	120.9
C(15)-N(6)-O(4)	110.14(19)	C(11)-C(10)-H(10A)	120.9
N(1)-C(1)-C(2)	123.6(2)	C(12)-C(11)-C(10)	118.9(2)
N(1)-C(1)-H(1A)	118.2	C(12)-C(11)-H(11A)	120.5
C(2)-C(1)-H(1A)	118.2	C(10)-C(11)-H(11A)	120.5
C(3)-C(2)-C(1)	118.2(2)	C(11)-C(12)-C(13)	118.5(2)
C(3)-C(2)-H(2A)	120.9	C(11)-C(12)-H(12A)	120.7
C(1)-C(2)-H(2A)	120.9	C(13)-C(12)-H(12A)	120.7
C(4)-C(3)-C(2)	119.0(2)	N(4)-C(13)-C(12)	123.7(2)
C(4)-C(3)-H(3A)	120.5	N(4)-C(13)-C(14)	116.52(19)
C(2)-C(3)-H(3A)	120.5	C(12)-C(13)-C(14)	119.73(19)
C(3)-C(4)-C(5)	118.3(2)	O(3)-C(14)-N(5)	122.9(2)
C(3)-C(4)-H(4A)	120.8	O(3)-C(14)-C(13)	122.7(2)
C(5)-C(4)-H(4A)	120.8	N(5)-C(14)-C(13)	114.34(19)
N(1)-C(5)-C(4)	123.7(2)	N(6)-C(15)-N(5)	119.2(2)
N(1)-C(5)-C(6)	116.49(19)	N(6)-C(15)-H(15A)	120.4
C(4)-C(5)-C(6)	119.8(2)	N(5)-C(15)-H(15A)	120.4
O(1)-C(6)-N(2)	122.9(2)	O(4)-C(16)-H(16A)	109.5
O(1)-C(6)-C(5)	122.5(2)	O(4)-C(16)-H(16B)	109.5
N(2)-C(6)-C(5)	114.53(19)	H(16A)-C(16)-H(16B)	109.5
N(3)-C(7)-N(2)	119.6(2)	O(4)-C(16)-H(16C)	109.5
N(3)-C(7)-H(7A)	120.2	H(16A)-C(16)-H(16C)	109.5
N(2)-C(7)-H(7A)	120.2	H(16B)-C(16)-H(16C)	109.5

**Table B9.4.** Anisotropic displacement parameters ( $\text{\AA}^2 \times 10^3$ ) for ap23e. The anisotropic

displacement factor exponent takes the form:  $-2\pi^2 [ h^2 a^*{}^2 U^{11} + \dots + 2 h k a^* b^* U^{12} ]$

	U <sup>11</sup>	U <sup>22</sup>	U <sup>33</sup>	U <sup>23</sup>	U <sup>13</sup>	U <sup>12</sup>
O(1)	32(1)	60(1)	37(1)	-4(1)	4(1)	10(1)
O(2)	43(1)	74(1)	25(1)	-4(1)	-3(1)	10(1)
O(3)	26(1)	45(1)	33(1)	-2(1)	-5(1)	2(1)
O(4)	41(1)	80(1)	24(1)	-11(1)	-1(1)	4(1)
N(1)	23(1)	32(1)	33(1)	-2(1)	0(1)	-1(1)
N(2)	28(1)	37(1)	28(1)	-1(1)	0(1)	6(1)
N(3)	41(1)	43(1)	26(1)	-2(1)	0(1)	3(1)
N(4)	22(1)	32(1)	30(1)	-2(1)	-2(1)	-2(1)
N(5)	26(1)	37(1)	26(1)	-5(1)	-4(1)	1(1)
N(6)	38(1)	42(1)	23(1)	-6(1)	-3(1)	1(1)
C(1)	28(1)	36(1)	36(1)	-4(1)	3(1)	2(1)
C(2)	35(1)	40(1)	31(1)	-5(1)	-1(1)	-5(1)
C(3)	33(1)	36(1)	36(1)	-3(1)	-8(1)	0(1)
C(4)	23(1)	30(1)	39(1)	-3(1)	-2(1)	-1(1)
C(5)	23(1)	25(1)	34(1)	-2(1)	-1(1)	-6(1)
C(6)	27(1)	26(1)	34(1)	0(1)	1(1)	0(1)
C(7)	33(1)	37(1)	30(1)	-2(1)	2(1)	2(1)
C(8)	47(2)	53(2)	34(1)	-2(1)	-12(1)	1(1)
C(9)	28(1)	36(1)	34(1)	0(1)	-6(1)	-2(1)
C(10)	38(1)	39(1)	26(1)	-5(1)	-2(1)	-4(1)
C(11)	31(1)	38(1)	34(1)	-6(1)	4(1)	2(1)
C(12)	24(1)	28(1)	34(1)	-2(1)	-2(1)	-1(1)
C(13)	23(1)	22(1)	32(1)	-1(1)	-1(1)	-3(1)
C(14)	29(1)	26(1)	30(1)	-2(1)	-2(1)	0(1)
C(15)	32(1)	36(1)	27(1)	-2(1)	-7(1)	1(1)
C(16)	49(2)	49(2)	30(1)	-9(1)	9(1)	-5(1)

**Table B9.5.** Hydrogen coordinates ( $\times 10^4$ ) and isotropic displacement parameters ( $\text{\AA}^2 \times 10^3$ ) for ap23e.

	x	y	z	U(eq)
H(2B)	12363	3436	3318	38
H(5A)	12292	8499	1655	36
H(1A)	13059	2517	1638	41
H(2A)	9869	3803	972	42
H(3A)	6035	5578	1333	43
H(4A)	5515	5922	2358	37
H(7A)	9652	4456	4352	41
H(8A)	15012	2585	5692	68
H(8B)	16484	3195	5092	68
H(8C)	15767	1177	5190	68
H(9A)	13151	7790	3389	39
H(10A)	10059	9252	4035	41
H(11A)	6127	10860	3654	42
H(12A)	5459	10896	2634	34
H(15A)	9269	8908	659	39
H(16A)	14791	7417	-718	65
H(16B)	15966	6310	-132	65
H(16C)	16041	8453	-234	65

**Table B9.6.** Torsion angles [°] for ap23e.

C(8)-O(2)-N(3)-C(7)	-166.4(2)	C(6)-N(2)-C(7)-N(3)	171.4(2)
C(16)-O(4)-N(6)-C(15)	168.9(2)	C(13)-N(4)-C(9)-C(10)	-1.6(4)
C(5)-N(1)-C(1)-C(2)	0.6(4)	N(4)-C(9)-C(10)-C(11)	0.5(4)
N(1)-C(1)-C(2)-C(3)	0.0(4)	C(9)-C(10)-C(11)-C(12)	0.5(4)
C(1)-C(2)-C(3)-C(4)	-0.9(4)	C(10)-C(11)-C(12)-C(13)	-0.4(4)
C(2)-C(3)-C(4)-C(5)	1.2(3)	C(9)-N(4)-C(13)-C(12)	1.8(3)
C(1)-N(1)-C(5)-C(4)	-0.3(3)	C(9)-N(4)-C(13)-C(14)	-177.3(2)
C(1)-N(1)-C(5)-C(6)	177.7(2)	C(11)-C(12)-C(13)-N(4)	-0.8(3)
C(3)-C(4)-C(5)-N(1)	-0.6(3)	C(11)-C(12)-C(13)-C(14)	178.2(2)

C(3)-C(4)-C(5)-C(6)	-178.5(2)	C(15)-N(5)-C(14)-O(3)	-2.4(4)
C(7)-N(2)-C(6)-O(1)	1.8(4)	C(15)-N(5)-C(14)-C(13)	177.9(2)
C(7)-N(2)-C(6)-C(5)	-177.3(2)	N(4)-C(13)-C(14)-O(3)	165.4(2)
N(1)-C(5)-C(6)-O(1)	-171.8(2)	C(12)-C(13)-C(14)-O(3)	-13.7(4)
C(4)-C(5)-C(6)-O(1)	6.3(4)	N(4)-C(13)-C(14)-N(5)	-14.9(3)
N(1)-C(5)-C(6)-N(2)	7.4(3)	C(12)-C(13)-C(14)-N(5)	166.1(2)
C(4)-C(5)-C(6)-N(2)	-174.6(2)	O(4)-N(6)-C(15)-N(5)	179.4(2)
O(2)-N(3)-C(7)-N(2)	-179.5(2)	C(14)-N(5)-C(15)-N(6)	-176.1(2)